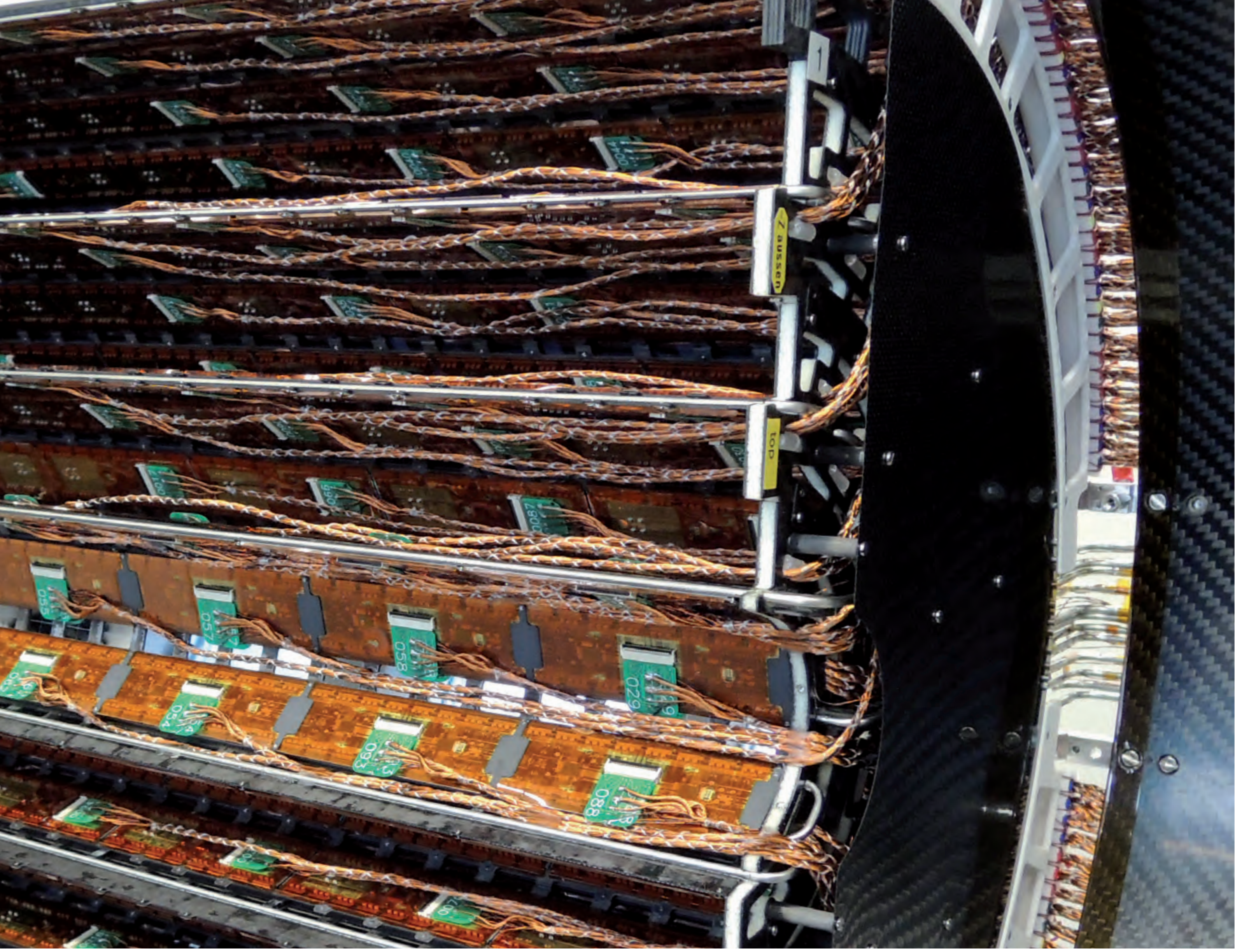

PARTICLE PHYSICS 2016.

Highlights and Annual Report

Accelerators | Photon Science | Particle Physics

Deutsches Elektronen-Synchrotron
A Research Centre of the Helmholtz Association

Cover

Fully assembled half-barrel of the new CMS pixel detector

PARTICLE PHYSICS 2016.

Highlights and
Annual Report

Contents.

The year 2016 at DESY.

Chairman's foreword

The year 2016 has – again – seen tremendous progress and extremely intense work in all the divisions and departments at DESY – in photon science, accelerator development and particle and astroparticle physics.

During the past years, photon science at DESY has developed into a powerhouse that attracts the best scientists from all over the world. The additional research opportunities offered by the modern beamlines in the second experimental hall at the FLASH soft X-ray free-electron laser and in the two extension halls at the PETRA III synchrotron radiation source strengthen DESY immensely. And the construction of the European X-ray free-electron laser XFEL – currently drawing to a close – is already a remarkable success story: The world's most advanced electron linear accelerator was assembled with no major delays and no major budget adjustments. We are all looking forward to the start of European XFEL operation for users in 2017.

A very different accelerator project at DESY also reached a major milestone in 2016. In collaboration with the University of Hamburg, the first electron beam was produced by means of plasma wakefield acceleration. The electrons in the first test run were accelerated to energies of around 400 MeV, using a plasma cell just a few millimetres in length. This corresponds very nearly to the energy achieved by DESY's linear pre-accelerator LINAC II – on a length of 70 m!

Figure 1

The European XFEL will start operation for users in 2017.

Particle and astroparticle physics also advanced in great steps. DESY is strongly involved in the ATLAS and CMS experiments at the Large Hadron Collider (LHC) at CERN near Geneva, Switzerland, and in the Belle II experiment at the SuperKEKB collider at KEK in Japan – the two major accelerators currently driving experimental particle physics. Both passed important milestones. Funding from the German Federal Ministry of Education and Research (BMBF) and from the Helmholtz Association amounting to a total of about 120 million euros was obtained for the upgrades of the LHC experiments for the high-luminosity phase (HL-LHC), with 15.7 million euros of that sum earmarked for the DESY ATLAS and CMS groups. In Japan, commissioning of the SuperKEKB collider has begun. Both endeavours will keep particle physicists not only at DESY busy for many years to come.

In astroparticle physics, the two biggest accomplishments for DESY in 2016 were probably the finalisation of the camera upgrade at the H.E.S.S. gamma-ray telescopes in Namibia and the siting decision regarding the Cherenkov Telescope Array (CTA), the next-generation gamma-ray observatory. Its two telescope arrays will be located in Chile and on the Canary Islands, with the Science Data Management Centre to be based at DESY in Zeuthen, turning the Zeuthen site into a major hub for astroparticle physics in Germany and internationally.

The progress in particle and astroparticle physics also strengthened DESY's personnel "underpinning", attracting, for example, Beate Heinemann, formerly a professor at the University of California, Berkeley, USA, and deputy spokesperson of the ATLAS experiment, in a common appointment to a position of leading scientist at DESY and professor at the University of Freiburg, Germany. Furthermore, Kerstin Tackmann obtained a prestigious starting grant of the European Research Council (ERC), and three new Helmholtz Young Investigator Groups were granted in 2016, to Sarah Heim, Elisa Pueschel and Anna Franckowiak.

What challenges will DESY face in the coming years?

Photon science at DESY critically hinges on the successful operation of PETRA III and FLASH for users. To maintain the world-leading positions of these facilities, DESY has set up project teams to devise the next generation of storage-ring-based X-ray sources (PETRA IV) and of linear-accelerator-based X-ray lasers (FLASH2020). In addition, as initiator of the League of European Accelerator-based Photon Sources (LEAPS) initiative, DESY is working on a roadmap for the better integration of all European synchrotron radiation and X-ray laser facilities, aiming to influence the upcoming Framework Programme FP9 of the European Commission.

Future accelerators are not only one of the topic of the LEAPS initiative, they are also a building block of the future strategy of DESY's Accelerator Division. Increasing efforts and resources are being devoted to this field of research, which will hopefully one day give rise to novel particle accelerators that are much smaller and more powerful than the ones in operation around the world today.

While the LHC experiments and Belle II will produce unsurpassed amounts of data that might well reveal exciting new physics beyond the Standard Model of particle physics, and while the HL-LHC upgrades will be a backbone of activities at DESY for some years to come, particle physics is facing challenging strategic decisions. First of all, a number of large-scale projects are contending for an entry in the next update of the European Strategy for Particle Physics, to be released in 2020, and DESY clearly intends to play a major role in the definition and realisation of future global projects. At the same time, DESY particle physicists are contemplating strengthening their efforts in the searches for hypothetical new lightweight particles called axions, maybe with new on-site successor experiments to ALPS II, or embarking on accelerator-based neutrino physics experiments as a new research direction. Particle physicists at DESY are thus looking towards a bright and exciting future.

Astroparticle physicists too are looking forward to the coming years. The industrial pre-production of the mid-sized telescopes for CTA will start in 2017, with many major contributions from DESY. And the international collaboration

Figure 2

Inauguration of the two new experimental halls at PETRA III in September 2016

operating the IceCube neutrino observatory at the South Pole, in which DESY is strongly involved, is currently discussing a major upgrade programme that would further extend IceCube's already impressively broad science programme and, by the same token, DESY's key role in the experiment.

One additional future challenge will be to unlock the innovation potential of the research centre's advancements. Consequently, in 2016, DESY initiated important steps to foster further partnerships and cooperation with industry. In particular, a new DESY Innovation and Technology Transfer unit was established under the direction of Arik Willner, DESY's newly appointed first Chief Technology Officer (CTO).

All in all, DESY is well prepared to tackle the future challenges. My thanks go to all our staff members and external collaborators, whose excellent work and continued commitment have been instrumental in building up the major role that DESY plays today in so many scientific fields.

Helmut Dosch
Chairman of the DESY Board of Directors

Particle and astroparticle physics at DESY.

Introduction

In 2016, the international flagship project of particle physics, the Large Hadron Collider (LHC) at CERN near Geneva, Switzerland, made a big step forward. Thanks to its record integrated luminosity at the highest energy, particle physicists are now able to scrutinise the Higgs boson, discovered in 2012, in great detail, trying to find answers to some of the most pressing questions: What is the origin of mass? What comes beyond the Standard model of particle physics? What is dark matter?

To tackle these questions in the most effective way possible, experiments require continuous improvements. Consequently, DESY has taken on a key role in the design, construction and upgrade of detectors at forefront accelerator facilities, such as the ATLAS and CMS experiments at the LHC, or the Belle II experiment at the SuperKEKB collider at KEK in Japan. The DESY CMS group finalised the production of 300 silicon pixel modules for the fourth layer of the new CMS pixel detector, while the DESY ATLAS group played a crucial role in writing, editing and publishing the technical design report of the inner tracking system for the high-luminosity LHC (HL-LHC) upgrade. A very successful test of the Belle II vertex detector system was carried out at the DESY test beam facility, and the DESY Belle II group published one of the highlight physics analyses of the year: an angular analysis of the decay $B \rightarrow Kll$ that could confirm the significant deviation in the muon channel first seen at the LHC experiment LHCb. The ALPS II experiment at DESY, which aims to probe for hypothetical very weakly interacting ultralight particles (WISPs), also saw significant progress. The University of Florida, Gainsville, USA, joined the collaboration as a new partner institute, and first long-term stable operation of a 20 m long optical resonator at high power was achieved.

Figure 1

Belle II components are put to the test at the DESY test beam facility.

Detector development and construction activities at DESY in the coming years will clearly focus on the upgrades of ATLAS and CMS. Here, DESY can prove its strength as a national laboratory and an architect of large-scale projects, with expertise in handling the full life cycle of particle physics experiments. Together with its partners from universities in Germany and abroad, DESY has started to design and construct silicon tracker end-caps for both ATLAS and CMS – two truly challenging projects, which are to be completed in the mid-2020s. In 2016, DESY successfully obtained funding of 15.7 million euros for these big endeavours from the Helmholtz Association. Together with the funding provided by the German Federal Ministry of Education and Research (BMBF) for the universities, Germany thus contributes about 120 million euros to the investment costs for the HL-LHC detector upgrades, underlining the country's leading role at the LHC and demonstrating the pivotal role that DESY plays in both the German and international community of particle physics.

Projects such as the ATLAS and CMS tracker end-caps require first-class facilities – workshops, cleanrooms and equipment. To this end, DESY started to set up a dedicated Detector Assembly Facility (DAF) in 2016. The DAF is a cornerstone of the research centre's plans for the LHC and beyond, and it will become an asset for DESY's future attractiveness for particle physicists from all over the world.

Figure 2
Plasma-based accelerators hold great promise for the future.

In astroparticle physics, DESY is involved in the running gamma-ray experiments Fermi, VERITAS, MAGIC and H.E.S.S., which continue to deliver key results. Highlights in 2016 included the H.E.S.S. detection of a cosmic peta-electronvolt particle accelerator – dubbed a PeVatron – in the galactic centre of the Milky Way and the camera upgrade for the H.E.S.S. telescopes under the leadership of DESY.

The main focus in astroparticle physics at DESY is currently on the two major large-scale projects in neutrino and gamma-ray physics: IceCube and the Cherenkov Telescope Array (CTA). IceCube, a neutrino observatory at the South Pole, is constantly increasing its data set and science scope. Improved spectral measurements and neutrino oscillation studies are increasingly constraining neutrino sources and properties. DESY is also a driver of the IceCube upgrade schemes that are currently being developed. The plans for IceCube-Gen2 will turn IceCube into a multicomponent observatory, with additional air shower detectors at the surface, a tenfold increase in neutrino detection volume, a subsurface radio detector, a low-energy extension dubbed PINGU and the dense DeepCore instrumentation. Currently, funding is sought for these far-reaching plans.

For CTA, 2016 was a decisive year. First of all, the negotiations regarding the sites of the observatory were successfully concluded. The southern observatory is to be constructed at the Paranal site of the European Southern Observatory (ESO) in Chile. The smaller northern part of CTA will be located on the Canary Island of La Palma, Spain. DESY in Zeuthen was chosen to host the Science Data Management Centre for CTA, further strengthening the Zeuthen site as an international centre for astroparticle physics. Most importantly, the funding agencies started to commit funding at a level enabling the imminent realisation of CTA.

Given the long lead times of large-scale projects, now – with the HL-LHC upgrades organised and funded and the Belle II and ALPS II experiments well on their way towards completion – is the right time to carefully consider the next generation of particle physics experiments DESY wants to engage in, and to drive the corresponding strategy and decision processes on the national, European and international level.

Nationally, the German Committee for Elementary Particle Physics (KET) is organising a series of workshops on the various directions of particle physics, with the aim to derive a consensus in the German community. DESY, as the national hub for particle physics and a facilitator of large-scale projects, has a well-heard voice in these discussions. They will also impact on the European and global particle physics strategy process. The next update of the European Strategy for Particle Physics, scheduled to be released in 2020, will have a long-term effect: There are numerous contenders for the realisation of the next large-scale project after the LHC, and a decision for any of them will determine the future of a large fraction of the next generations of particle physicists.

However, before exerting its influence on the national or international level, DESY needs to define what future directions it actually wants to take, and which possibilities it has. For this reason, as well as for defining the future portfolio of DESY and its strategy for the next period of programme-oriented funding (POF) of the Helmholtz Association, we have started a strategy process within DESY. In many discussions, we are currently developing our picture of DESY in 10 or 15 years from now, taking our ambitions, our possibilities and the global landscapes of our scientific fields into account. This process will conclude sometime in 2017, and I am very much looking forward to everybody's input and creativity in helping to shape DESY's future!

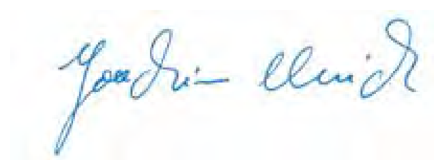

Joachim Mnich
Director in charge of Particle Physics
and Astroparticle Physics

News and events.

A busy year 2016

January

PhD thesis prize of BTU for Ihar Marfin

Ihar Marfin, until recently PhD student in the CMS group at DESY in Zeuthen, was awarded the prize for the best PhD thesis 2015 by the Brandenburg University of Technology (BTU) in Germany. His thesis “Search for additional Higgs bosons with multi *b*-quark final states at the LHC” caught the attention of the international CMS science community because it sets new limits for theoretically possible additional Higgs particles using new procedures in statistical data analysis. The award ceremony took place on 27 January in the main auditorium of BTU in Cottbus.

Ihar Marfin

Helmholtz grant for Janna Katharina Behr

Janna Katharina Behr was awarded a postdoc grant by the Helmholtz Association. Over the next three years, her team will receive funding as part of the Helmholtz Postdoc Programme, with DESY and the Helmholtz Association each contributing half of the funds. As a member of the DESY ATLAS group, Behr intends to search for previously unknown particles decaying into the heaviest of the six quarks, the top quark. Behr has developed a method that considerably increases the chances of spotting such processes in the ATLAS detector.

Janna Katharina Behr

ALPS II on the track of lightweights

Setting up the ALPS optics

Using the ALPS II experiment at DESY – a joint effort of DESY, the Albert Einstein Institute in Hannover, the Universities of Hamburg and Mainz in Germany as well as the University of Florida in Gainesville, USA – physicists will look for undetected lightweight particles at low energies. These so-called WISPs (for weakly interacting sub-eV particles) are promising candidates for the mysterious dark matter in our universe. Funding for the experiment has been largely secured, in part thanks to grants amounting to 740 000 US dollars from the US Heising–Simons Foundation and the National Science Foundation for the University of Florida. With ALPS II, an extended version of its predecessor ALPS, the physicists aim to further pin down the features of these hypothetical particles.

February

Youth science competition “Jugend forscht” 2016 at DESY

Eleven-year-old Felix Eberle presented investigations using a home-made parabolic mirror. He won the first place in physics in the “Schüler experimentieren” competition.

For the fourth time, DESY hosted the regional “Jugend forscht” youth science competition in Hamburg-Bahrenfeld, one of four regional competitions in Hamburg. On 25 and 26 February, 74 participants met at the DESY school lab to present a total of 40 projects to a group of expert jurors. Half of the projects were part of the “Schüler experimentieren” competition for pupils from fourth grade on, the other half were part of “Jugend forscht” for youths aged 15 to 21. The science competition encourages special achievements and talents in mathematics, natural sciences and technology with the aim to inspire lasting enthusiasm for these topics among young people.

Poster of
“Jugend forscht 2016”

March

Third DESY–KEK Workshop at DESY

DESY and the Japanese high-energy accelerator research organisation KEK have been collaborating for over 40 years, especially in the field of particle physics. DESY is participating in the Belle II experiment at KEK, both institutes are closely involved in the ATLAS experiment at the LHC and in the future International Linear Collider (ILC), and both are operating radiation sources for photon science.

To bolster this cooperation, regular workshops are taking place once every eighteen months, alternating between Hamburg and Tsukuba, to provide an opportunity to discuss existing and future projects, develop new ideas and move projects ahead. The third such DESY–KEK Workshop was held in Hamburg on 7 and 8 March. In view of the success of the collaboration, KEK Director General Masanori Yamauchi and DESY Director Helmut Dosch decided to extend their cooperation agreement by another five years.

Participants of the DESY–KEK workshop

DIS 2016 conference at DESY

More than 320 participants met at DESY in Hamburg from 11 to 15 April for the 24th Workshop on Deep-Inelastic Scattering (DIS 2016), one of the largest spring conferences in particle physics. The workshop was established in 1993 on the occasion of the first results at DESY's former HERA electron–proton collider. It brings together experts from around the world who explore the inner structure of protons or complex nuclei and the forces acting inside them, using the technique of deep-inelastic scattering.

At the 24th edition of the conference, which took place at DESY in Hamburg for the first time, scientists from more than 30 countries discussed recent results from a wide range of experiments, focusing on the physics of nucleon spin, progress of the theory and results at the LHC, which ran at an energy of 13 TeV for the first time in 2015. The conference also spanned plans for future collider experiments, such as the EIC project, an electron–ion collider in the USA offering highest beam intensities, or studies of the LHeC, in which protons from the LHC would collide with electrons from a new ring to be built.

Participants of DIS 2016

Reinhard Brinkmann elected EPS fellow

Reinhard Brinkmann, DESY Director in charge of the Accelerator Division, was appointed fellow of the European Physical Society (EPS). The EPS elected him in recognition of his outstanding leadership and achievements in accelerator physics and technology, including ground-breaking solutions for modern free-electron lasers and linear colliders based on superconducting accelerator technology and the success of longitudinally polarised electron beams in the HERA collider.

Reinhard Brinkmann

Reinhard Brinkmann started working at DESY in 1984. As the machine coordinator of the HERA electron ring accelerator from the late 1980s to the mid-1990s, he contributed decisively to the successful and swift commissioning of this highly complex facility. In 1995, he was appointed leading scientist for accelerator physics at DESY. He was instrumental in designing the TESLA superconducting linear accelerator and in drawing up the technical design report for the project, which was published in 2001. In 2003, he became the project leader for the preparation of the European XFEL project at DESY. In 2007, he took over as Director of the Accelerator Division.

May

Green light for industrial alliance MicroTCA.4 Tech Lab

Together with private enterprises, DESY set up the MicroTCA.4 Technology Lab, a cooperative venture aiming to further develop the MicroTCA.4 electronics standard and establish it for a large market. Over the next three years, the project will be funded as a Helmholtz Innovation Lab, with the Helmholtz Association providing almost 2.5 million euros. Together with the funds contributed by DESY and private-sector companies, the budget of the innovation lab will amount to 5.07 million euros.

The Micro Telecommunications Computing Architecture (MicroTCA.4) electronics standard combines ultrafast digital electronics with the option to integrate analogue components within extremely small spaces. Its outstanding stability and scalability make it ideal for controlling particle accelerators and detectors, but also for a range of potential industrial uses, including in telecommunications, online inspection, aviation, medical engineering and high-precision measurements. MicroTCA.4 was developed by a consortium of research institutions and industrial enterprises led by DESY, up to the point where it was ready for use in the superconducting linear accelerator of the European XFEL X-ray free-electron laser, which is currently under construction in the Hamburg region. The new MicroTCA.4 Tech Lab aims to open up novel areas of application for this universally deployable technology.

MicroTCA.4 printed circuit boards

IAXO meeting at DESY

The German community interested in the International Axion Observatory (IAXO) gathered at DESY in Hamburg on 24 May. IAXO is a fourth-generation helioscope proposed by a large fraction of the axion physics community. The participants of the meeting discussed the physics cases that can be investigated with IAXO as well as the status of the project and the next steps. In addition, the current involvement of German groups was presented, and potential future collaborations were considered.

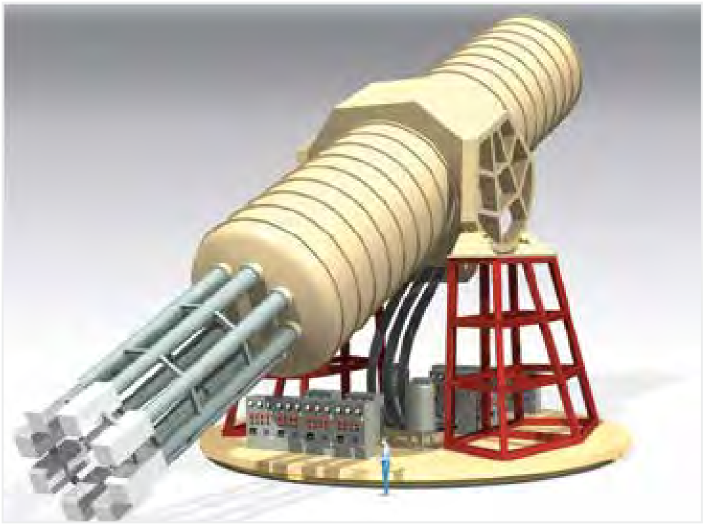

Conceptual design of the International Axion Observatory (IAXO)

June

DESY prepares for HL-LHC upgrade

The high-luminosity upgrade of the LHC (HL-LHC), which is due to take place in the mid-2020s, will also require the replacement of major detector components. Together with German and international partners, DESY will build one of the large end-caps for each of the new ATLAS and CMS tracker detectors. Preparations at DESY started with activities to set up a Detector Assembly Facility (DAF) for this purpose in two existing buildings.

Günter Eckerlin, coordinator of the LHC upgrade activities at DESY

In June, workers began to construct an ISO-6 cleanroom, laboratories and other infrastructure in a former experimental hall next to the DORIS storage ring. The modules for the end-caps of the trackers will be produced in this building. In 2017, conversion work and cleanroom installation will go on in another building, where the complete end-caps – of about 2.5 m radius and 2 m length – will be assembled. The German universities involved in ATLAS and CMS will contribute to integration and testing at the DAF.

DESY mourns Helen Edwards

On 21 June, Helen T. Edwards passed away at the age of 80 at her home in Illinois, USA. Helen Edwards was the chief scientist in charge of building and operating the Tevatron proton–antiproton collider at Fermilab, and from the early 1990s on she played a key role in developing the TESLA superconducting accelerator technology. She maintained close ties with DESY for over three decades, and together with her husband Don, she was an essential driving force behind years of fruitful collaboration of Fermilab and DESY.

During the early stages of the HERA electron–proton collider project, DESY profited enormously from her experience at the Tevatron, and in the course of numerous visits to DESY, she contributed to getting the HERA proton ring accelerator up and running. Within the TESLA collaboration, she organised crucial contributions of Fermilab towards the design of the linear collider as well as the design and construction of the TESLA test facility, which was later converted into the FLASH free-electron laser. Numerous colleagues at DESY remember and value Helen Edwards from many years of collaboration, and were extremely fond of her.

Helen Edwards

Scientific centre of CTA observatory comes to DESY

The Cherenkov Telescope Array (CTA), the next-generation gamma-ray observatory, took another important step towards becoming a reality. On 14 June, the shareholders' meeting of the company CTAO GmbH decided that the Science Data Management Centre and the seat of the CTA Scientific Director was to be located at DESY in Zeuthen. The administrative headquarters of the CTA organisation will be in Bologna, Italy.

Architectural rendering of the building for the scientific centre of CTA on the DESY campus in Zeuthen

The CTA gamma-ray observatory will consist of more than 100 individual telescopes located at a site in the southern hemisphere and another site in the northern hemisphere. Over 1000 scientists and engineers from more than 30 countries have joined forces to set up the facility over the next five years and operate it for at least 20 years. The project, which will cost around 400 million euros, is part of the roadmap for future research infrastructures of the German Federal Ministry of Education and Research (BMBF), as well as of its European counterpart, the roadmap of the European Strategy Forum on Research Infrastructure (ESFRI).

Felix Sefkow appointed coordinator of AIDA-2020

DESY particle physicist Felix Sefkow became the new coordinator of the project AIDA-2020, which receives funding of 10 million euros from the European Union. AIDA – short for Advanced European Infrastructures for Detectors at Accelerators – brings together physicists and engineers from 38 institutions in 19 countries and from CERN to develop and optimise research facilities, testing tools and installations that are fundamental for developing future detectors and new technologies. Sefkow took over from Laurent Serin of LAL/IN2P3 in France. His first official appearance as project coordinator was at the first annual meeting of AIDA-2020, which took place at DESY from 13 to 17 June.

Felix Sefkow

July

Christian Harringa becomes new Administrative Director

DESY's Foundation Council appointed Christian Harringa as the new Administrative Director and, by the same token, the deputy chairman of DESY's Board of Directors. The jurist joined DESY in April 2015 as head of administration and temporarily took over the office of Administrative Director from Christian Scherf in November 2015, when Scherf moved to EMBL in Heidelberg, Germany.

Christian Harringa

Before joining DESY, Harringa worked for the City of Hamburg, among other things in the capacity of head of the Division for University Medicine and Life Sciences as well as head of the senator's office in the Departmental Authority for Science and Research. For four years, he served the European Commission as a seconded national expert in the Directorate-General for Competition.

DESY welcomes 104 summer students from 33 countries

DESY summer students in Hamburg …

For seven weeks, 104 young scientists from 33 countries were given the opportunity to gain practical insight into research at DESY in Hamburg and Zeuthen as part of the DESY summer student programme, which is one of the largest and most international summer schools in Germany. The DESY summer student programme is extremely popular among students, both because of the practical experience it provides in genuine research projects and because of its internationality.

The 86 students from 28 countries at the Hamburg site and 18 students from 14 countries at the Zeuthen site were integrated into various DESY groups in the fields of particle and astroparticle physics, accelerator physics and photon science, where they experienced everyday life in science at first hand. A series of lectures providing the necessary theoretical background complemented the practical experience.

… and Zeuthen

August

Beate Heinemann leading scientist at DESY and professor at the University of Freiburg

Particle physicist Beate Heinemann accepted a common appointment by DESY and the University of Freiburg, Germany, and joined the DESY ATLAS Group on 1 August as leading scientist. Beate Heinemann, who completed both her master and PhD theses at DESY, was most recently a professor at the University of California, Berkeley, USA. Since 2007, she has been a member of the ATLAS collaboration, becoming its deputy spokesperson in 2013, a position she will hold until February 2017. Her appointment is part of the recruitment initiative of the Helmholtz Association.

Beate Heinemann in the main ATLAS control room at CERN

CMS pixel detector production completed

DESY and the University of Hamburg successfully completed the production of modules for the pixel detector for the CMS upgrade Phase 1, with all the 286 modules passing the specifications defined by the CMS collaboration. On 14 August, the modules were transported from DESY to PSI in Switzerland, tested again and mounted on a carbon fibre frame with integrated cooling pipes. The integration of the pixel detector into the CMS experiment is scheduled for March 2017.

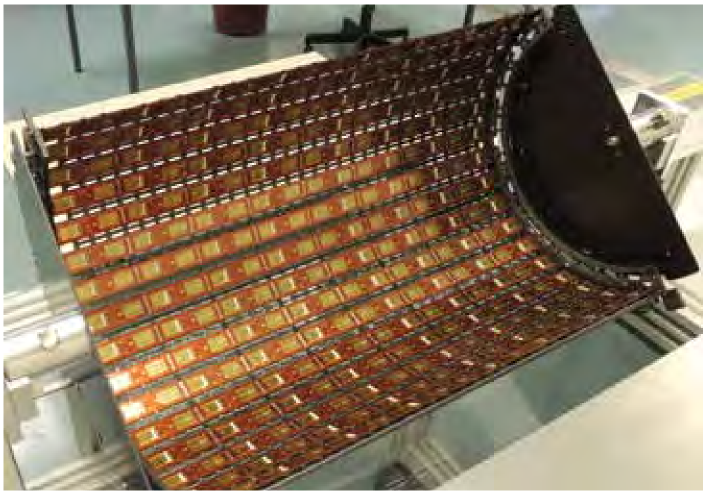

Fourth barrel layer of the CMS pixel detector with half of the mounted modules

September

Helmholtz PhD prize for Wolfgang Hollik

Wolfgang Hollik

Wolfgang Hollik, a physicist in the DESY theory group, was awarded the Helmholtz PhD prize at the annual meeting of the Helmholtz Association in September. As one of six award winners, he received 5000 euros and a monthly allowance of up to 2000 euros for travel and material costs for a stay abroad of up to six months at an international research institute. In his PhD thesis at the Karlsruhe Institute of Technology (KIT), Germany, Hollik explored the stability of the vacuum state in an extension of the Standard Model.

H.E.S.S. camera upgrade finished

Camera upgrade work at the H.E.S.S. gamma-ray telescopes in Namibia

The renewal of four cameras in the H.E.S.S. gamma-ray telescopes in Namibia was completed in September. The DESY team from Zeuthen led by Stefan Klepser needed only four weeks to connect and install the detectors. The complete electronics of the highly sensitive H.E.S.S cameras had to be updated. After the modernisation of the first telescope (CT1) in June 2015, the telescopes CT2 to CT4 followed in September 2016. Routine operation of the observatory is due to start in early 2017. The H.E.S.S. telescopes record the faint blue glow that cosmic gamma rays produce in the Earth's atmosphere, enabling scientists to search for gamma rays from natural cosmic particle accelerators, such as supernova remnants and active galactic nuclei.

Open campus at DESY in Zeuthen

On 11 September, nearly 900 visitors came to DESY in Zeuthen for the open day. They visited the laboratories and workshops, attended lectures and movies about the Zeuthen research projects and discussed them with DESY staff members. The visitors also had the opportunity to explore everyday phenomena with hands-on experiments.

Hands-on experiments on the open day at DESY in Zeuthen

October

Superconducting part of the European XFEL accelerator ready

An important milestone in the construction of the European XFEL X-ray free-electron laser was reached with the end of the installation of the 1.7 km long superconducting accelerator in the tunnel. The linear accelerator will bring bunches of electrons to an energy of 17.5 GeV in superconducting cavities operated at -271°C. In the subsequent part of the facility, the electron bunches will be used to generate brilliant X-ray flashes that will allow scientists new insights into the nanocosmos.

As the main shareholder of European XFEL, DESY is responsible for the construction and operation of the linear accelerator, which will be the largest and most powerful of its kind in the world. On 6 October, commissioning of the X-ray laser including the accelerator officially started. User operation at the European XFEL is due to begin in mid-2017.

Superconducting accelerator modules (yellow) in the European XFEL tunnel

October

Two Helmholtz Young Investigator Groups at DESY

The Helmholtz Association awarded funding for two Young Investigator Groups at DESY. Elisa Pueschel and Anna Franckowiak will set up their own research groups at DESY in Zeuthen, drawing on an annual grant of 300 000 euros each over the next five years. Half of these funds will come from DESY, the other half from the Helmholtz Association.

Elisa Pueschel

Elisa Pueschel's group will search for signs of new particles produced in astrophysical processes, using the Cherenkov Telescope Array (CTA), a next-generation gamma-ray observatory. CTA will be sensitive to extremely energetic gamma rays, which could provide information about the decay or annihilation of new, as yet undetected heavy elementary particles.

Anna Franckowiak

Anna Franckowiak's group will investigate the origins of high-energy cosmic neutrinos. In 2013, the IceCube neutrino telescope at the South Pole discovered the first high-energy neutrinos, which must originate outside our solar system. The question where they come from is as yet unresolved, but Franckowiak's group is hoping to answer it using multimessenger observations.

Starting signal for innovation centre

The innovation centre jointly planned by DESY, the University of Hamburg and the City of Hamburg got under way in October, with the three partners setting up the operating company for the centre. The innovation centre, which is to be established on the DESY campus in Hamburg-Bahrenfeld, is aimed at research spin-offs, technology start-ups and small companies that want to settle near DESY. To this end, a new building is to be erected on a 5000 m^2 plot of land on the edge of the campus. Construction work is to begin in 2017 and should be completed in 2018.

Architectural concept of the new innovation centre

November

DESY Golden Pin of Honour for Erich Lohrmann

Experimental physicist Erich Lohrmann was awarded the DESY Golden Pin of Honour in recognition of his outstanding scientific contributions in the field of particle physics and towards the development of DESY. For more than five decades, Erich Lohrmann has played a key role in shaping research at DESY in many different capacities. He joined DESY in 1961, assuming responsibility as leading scientist and Director of Research. As a professor at the University of Hamburg, Lohrmann also trained many generations of young scientists. His textbooks on high-energy physics and on statistical and numerical methods of data analysis have become definitive standards.

DESY Director Helmut Dosch (left) presented the DESY Golden Pin of Honour to Erich Lohrmann on 2 November.

25 years of DESY in Brandenburg

The treaty integrating the former Zeuthen Institute of High-Energy Physics into DESY

Twenty-five years ago, on 11 November 1991, the Federal Republic of Germany signed a treaty with the states of Hamburg and Brandenburg for the Zeuthen Institute of High-Energy Physics, which was part of the former Academy of Sciences of the German Democratic Republic, to be integrated into DESY. The treaty came into force on 1 January 1992, and since that day, DESY has been operating at two sites.

In the past 25 years, DESY has become a major player in the scientific environment of the Berlin-Brandenburg region, jointly appointing staff with both the University of Potsdam and the Humboldt University in Berlin. Scientists at DESY in Zeuthen are participating in major international projects, such as the neutrino telescope IceCube at the South Pole, the next-generation gamma-ray observatory CTA and the LHC experiment ATLAS.

“Science on Tap”

On 17 November, DESY and the University of Hamburg organised the public outreach event “Science on Tap” (“Wissen vom Fass”) for the second time. Initiator Jan Louis, a professor at the University of Hamburg, brought back the idea from Tel Aviv in Israel, where “Science on tap” has been a resounding success for many years. The goal of the event is to inspire people for the natural sciences in an unconventional, relaxed atmosphere – while at the same time showing how fascinating, but also how important research is for culture and society. The scientists’ presentations were very well received in about 50 bars throughout the city, and the event obtained wide media attention.

December

John von Neumann Excellence project for muon magnetic moment

The research project “Hadronic contributions to electroweak observables“ of Karl Jansen from DESY in Zeuthen was selected as John von Neumann Excellence project 2016 and thus granted extra computing time on the JURECA supercomputer. The distinction is awarded by the John von Neumann Institute for Computing (NIC), a joint venture of the three Helmholtz research centres Forschungszentrum Jülich, DESY and GSI. The project was selected owing to the excellent preparatory work, its outstanding importance and the high quality of the methods used.

Jansen is the second DESY scientist to lead a John von Neumann Excellence project in 2016. Half a year earlier, a simulation project of Alberto Martinez de la Ossa from DESY’s FLASHForward group was similarly distinguished and granted extra time on the NIC supercomputers.

Karl Jansen

DAF house warming

In December, a first milestone was reached in the construction of the Detector Assembly Facility (DAF), which DESY is setting up to build the large end-caps for the new ATLAS and CMS tracker detector. The infrastructure in the first building was completed, and the hall is now ready to host the cleanroom, which will be delivered in February 2017.

Assembly in the DAF on 16 December

Physics with protons.

Physics with protons has been at the heart of DESY's particle physics activities since the start-up of its electron–proton collider HERA in 1992. Today, the cornerstones of DESY's proton physics programme are its ATLAS and CMS groups, which are involved in a large variety of developments at the Large Hadron Collider (LHC) at CERN, from hardware design to data analysis.

One activity paving the way to the discovery of new phenomena is the re-establishment of Standard Model measurements at the LHC. These include a precise determination of the *W*-boson mass (p. 20) and evidence for light-by-light scattering (p. 21) as observed by ATLAS. Enhanced accuracy has been achieved by CMS in the description of the proton using parton distribution functions (p. 22) and by both experiments in the determination of the production cross section of top quark–antiquark pairs (p. 32). At the same time, jet data from the H1 experiment at DESY's former HERA collider is still being analysed and confronted with the most recent theoretical predictions of the strong coupling constant (p. 38).

Another focus of the DESY LHC groups is the properties of the recently discovered Higgs boson, including studies by ATLAS and CMS of the Higgs coupling to the top quark (p. 24) and of Higgs decays into four leptons (p. 26). Several new DESY research groups funded by third parties are centred around the Higgs properties as well, investigating the Higgs boson as a messenger to the dark-matter sector (p. 27 and 28) and top quark–antiquark production in association with a Higgs boson (p. 29). These new activities connect well with the expertise in new physics searches already present at DESY (p. 30).

At the same time, the DESY LHC groups are preparing for the future LHC upgrades – in particular, the high-luminosity upgrade foreseen for the years after LHC Run 2. The DESY ATLAS group contributes to the development of the new inner tracking detector (p. 31), while the DESY CMS group is instrumental in the current upgrade of the CMS pixel detector modules (p. 34). A joined effort is the set-up of a dedicated Detector Assembly Facility (DAF) at DESY, which will provide the infrastructure required for further tracker R&D (p. 36).

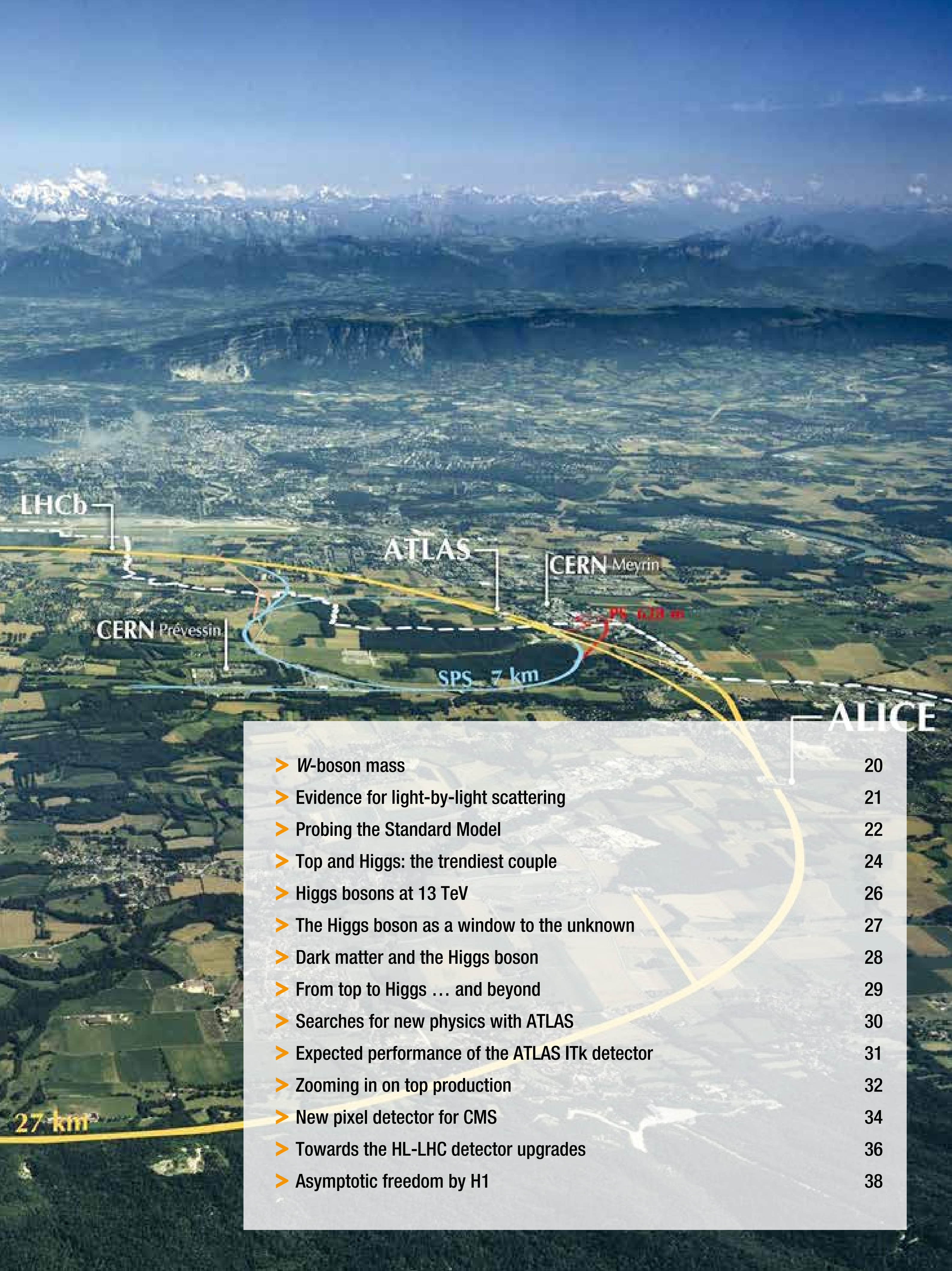
LHCb
ATLAS
CERN Meyrin
CERN Prévessin
SPS 7 km
ALICE
27 km

W-boson mass.

ATLAS releases first precision measurement

The carrier of the weak interactions, the *W* boson, is an important ingredient of the Standard Model. Previous measurements of the *W*-boson mass gave strong indirect evidence for particles such as the top quark and the Higgs boson before they were directly observed. Further, more accurate results may reveal a need for new physics. In December 2016, the ATLAS collaboration released the first, and astoundingly precise, measurement of the *W*-boson mass at the LHC [1].

In the Standard Model, the *W*-boson mass (m_W) is determined by a few well-measured parameters plus radiative corrections from heavy virtual particles. In the past, precision measurements of m_W provided indirect evidence and gave a range for the top-quark and Higgs-boson masses, confirmed later by the direct discoveries. In the same manner, m_W may be affected by heavy new particles, which may lead to deviations from the Standard Model expectations.

The current world average value of m_W is 80 385 ± 15 MeV. The large samples of *W* bosons collected by ATLAS offer a chance to improve the precision of this value. However, a measurement at ~0.02% precision is challenging, as it requires painstaking calibration of the detector. Moreover, the measurement relies on a precise theoretical modelling of *W*-boson production, which poses a challenge. The measurement becomes possible only when accompanied by auxiliary measurements of *Z*-boson production, as well as measurements of *W*- and *Z*-boson rapidity distributions. *Z*-boson measurements are used to constrain the detector calibration as well as the *W*-boson transverse momentum [2] and polarisation. The rapidity distribution measurements probe the quark flavour decomposition of the initial-state protons. In December 2016, ATLAS published a precision measurement of the latter [3], confirming a relatively large contribution from strange quarks, as ATLAS had previously determined, with improved precision.

The measured value of the *W*-boson mass, m_W = 80 370 ± 19 MeV, is compatible with the world average, and its precision is similar to the single most accurate previous measurement from the Tevatron collider. The ATLAS measurements of the *W*-boson, top-quark and Higgs-boson masses are in excellent agreement with the expectations of the Standard Model, as shown in Fig. 1, providing another triumph of this theory.

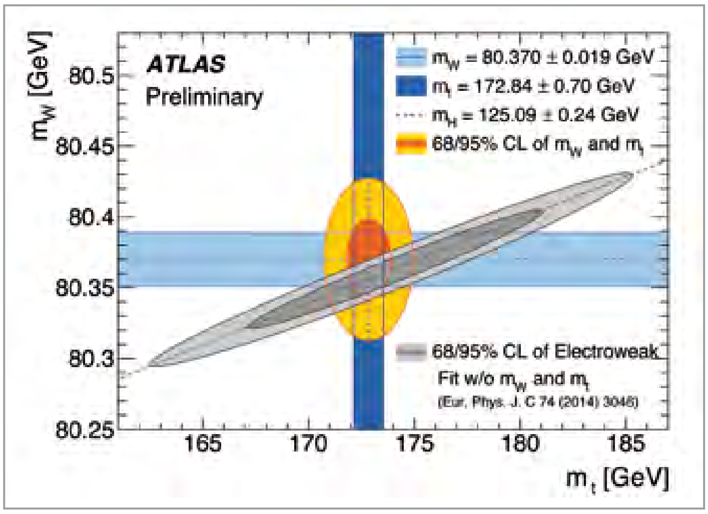

Figure 1

ATLAS measurements of the top-quark and *W*-boson mass (light and dark blue bands) compared to predictions of the Standard Model (grey ellipses), which are based on the LHC measurement of the Higgs-boson mass.

Contact:

James Ferrando, james.ferrando@desy.de
Sasha Glazov, alexander.glazov@desy.de
Beate Heinemann, beate.heinemann@desy.de

References:

[1] ATLAS Collaboration, ATLAS-CONF-2016-113.
[2] ATLAS Collaboration, JHEP 1409 (2014) 145.
[3] ATLAS Collaboration, arXiv:1612.03016.

Evidence for light-by-light scattering.

ATLAS observes $\gamma\gamma \rightarrow \gamma\gamma$ interactions

Light-by-light scattering ($\gamma\gamma \rightarrow \gamma\gamma$) is a quantum-mechanical process that is forbidden in the classical theory of electrodynamics. This reaction is accessible at the LHC thanks to the strong electromagnetic fields generated in the collisions of ultrarelativistic ions. The ATLAS collaboration reports evidence for the $\gamma\gamma \rightarrow \gamma\gamma$ reaction, using data recorded at a centre-of-mass energy of 5.02 TeV [1].

During the very first days of quantum electrodynamics (QED), in 1936, Hans Heinrich Euler and Werner Heisenberg realised that photons may scatter off each other through a quantum-loop process involving virtual pairs. This phenomenon of light-by-light scattering, albeit very rare, breaks the linearity of the Maxwell equations and belongs to the oldest predictions of QED. To date, light-by-light scattering via an electron–positron loop has been tested precisely, however indirectly, in measurements of the electron and muon anomalous magnetic moments. Closely related are the observations of the Delbrück process and photon splitting, both of which involve the scattering of a photon in the nuclear Coulomb field.

Recently, a novel approach to detect quasi-elastic photon–photon scattering was suggested, namely, that light-by-light scattering can be studied using electromagnetic fields produced in relativistic hadron–hadron collisions at the LHC. In such collisions, beams of nearly real photons interact, allowing for the process $\gamma\gamma \rightarrow \gamma\gamma$ to occur directly. The colliding hadrons generally stay intact, which makes the phenomenon easy to detect. Light-by-light scattering is thus characterised by the presence of two low-energy photons, back-to-back in the transverse plane, and no additional activity measured in the detector.

An ATLAS group led by a DESY scientist has performed a search for light-by-light scattering using 480 μb^{-1} of lead–lead collision data recorded at a nucleon–nucleon centre-of-mass energy of 5.02 TeV. A total of 13 candidate events were observed with an expected background of 2.6 ± 0.7 events (Fig. 1). This Standard Model background arises from misidentified electrons from the QED process $\gamma\gamma \rightarrow e^+e^-$, as well as from the central exclusive production of two photons from the fusion of two gluons (CEP $gg \rightarrow \gamma\gamma$). The probability for the background to fluctuate and give an excess of events as large as or larger than that observed in the data is found to be very small, about five per million.

With the additional integrated luminosity expected in the upcoming runs, further studies of the $\gamma\gamma \rightarrow \gamma\gamma$ process should be possible. Such studies will allow tests to be performed on many of the proposed extensions of the Standard Model in which new particles can be exchanged, thus providing an additional window into new physics at the LHC.

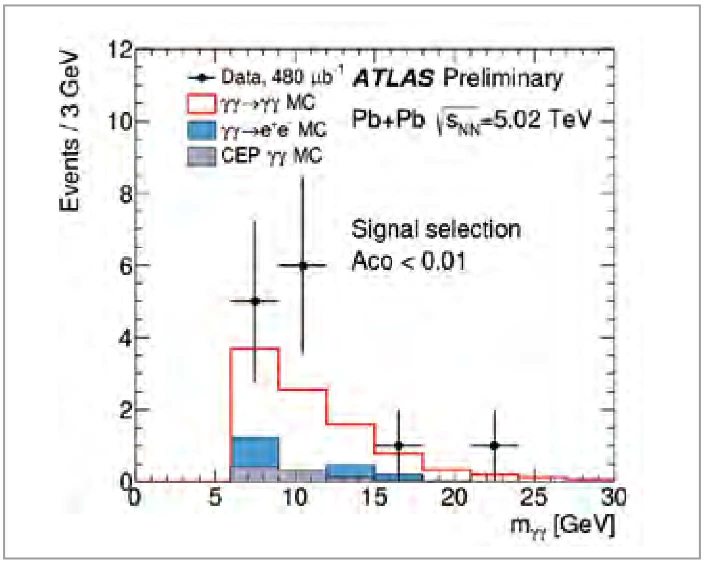

Figure 1

Diphoton invariant-mass distribution for $\gamma\gamma \rightarrow \gamma\gamma$ event candidates. Data (points) are compared to Monte Carlo (MC) predictions (histograms). The statistical uncertainties on the data are shown as vertical bars.

Contact:

Mateusz Dyndal, mateusz.dyndal@desy.de

References:

[1] ATLAS Collaboration, ATLAS-CONF-2016-111.

Probing the Standard Model.

CMS provides new insights into QCD

The interactions between the colliding hadrons at the LHC are explained in terms of the Standard Model of particle physics, which covers strong interactions, described by quantum chromodynamics (QCD), and electroweak interactions. Precise measurements of jets, heavy quarks or electroweak boson production at the LHC give insights into the very structure of colliding hadrons. The DESY CMS group uses these measurements to verify the peculiarities of theoretical expectations for the rates of all possible processes in hadron–hadron collisions within or beyond the Standard Model. The findings about hadron structure can be utilised for a vast number of applications in particle and astroparticle physics.

CMS legacy in QCD and proton structure

The precise description of the proton structure and of fundamental QCD parameters is of key importance for interpreting the observations in proton–proton collisions at the LHC. The key measurements of the Standard Model processes, including production of electroweak bosons, hadronic jets or charm, beauty and top quarks, have been performed, providing crucial input for the further understanding of QCD. The CMS collaboration is now completing the analyses of data collected in proton–proton collisions at centre-of-mass energies of 7 and 8 TeV.

Measurements of the lepton charge asymmetry in *W*-boson production [1] and of inclusive jet production cross sections [2] at 8 TeV with the CMS detector represent the most precise data of this kind to date. Used in a QCD analysis, these data significantly improve the precision of the valence quark (Fig.1) and gluon distributions in the proton. In addition, they enable the simultaneous determination of the gluon distribution and the strong coupling.

By measuring the cross section of the top-quark pair production as a function of the process kinematics multidifferentially, disentangling the kinematics of the interacting partons from two colliding protons becomes possible. Such a measurement, performed by the CMS experiment at 8 TeV, was used for the first time to constrain the gluon distribution (Fig. 2).

Members of the DESY CMS group are participating in the PROSA [4] effort, initiated at DESY, which brings together theory and experiment experts in the field of proton structure. One of the recent highlights of this activity is the first-time use of charm- and beauty-flavoured hadron production at very forward rapidities at the LHC to determine the gluon distribution at yet unprobed low fractions *x* of the proton momenta. The resulting parton distributions were used to predict the fluxes

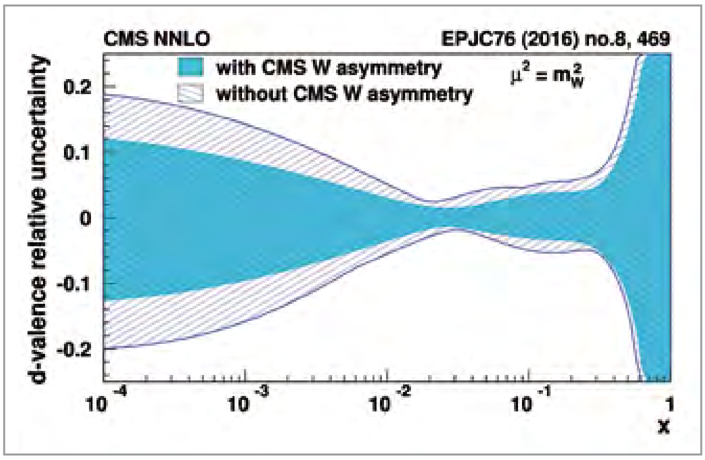

Figure 1

Decrease of the uncertainty in the *d*-quark valence distribution thanks to constraints provided by the measurement of *W*-boson cross sections at CMS

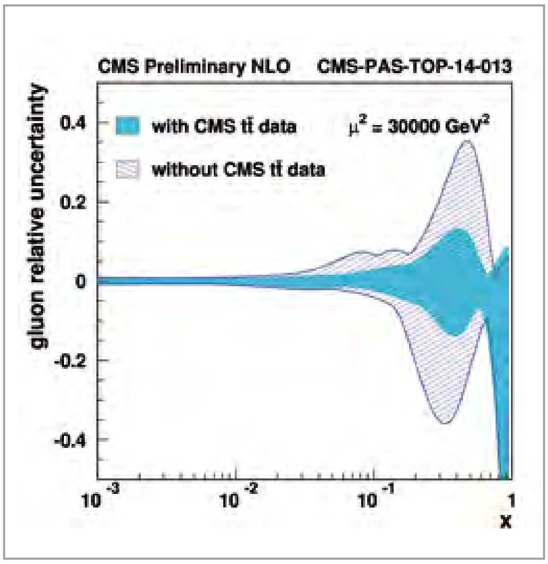

Figure 2

Impact of double-differential top-quark pair production measurements at CMS on the gluon uncertainty

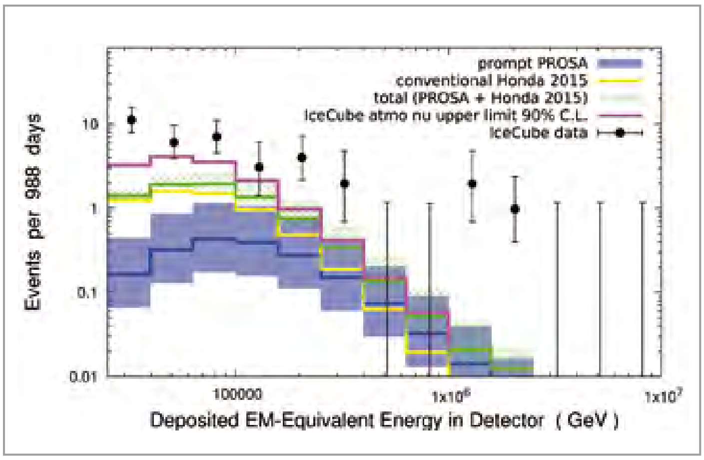

Figure 3

Predictions of the number of atmospheric neutrino events for the IceCube 988-day analysis compared to data, using the PROSA gluon distribution

of prompt atmospheric neutrinos [5] with the most realistic uncertainty related to the description of the proton structure (Fig. 3).

QCD and multijets

Upon completing the physics analyses from the LHC, the CMS collaboration started to perform measurements with multijets to directly investigate the contribution from hard double parton scattering (DPS). A direct observation of DPS is not possible, but the CMS measurement [6] of two jets containing a bottom quark, together with two other jets, provides a scenario that is very sensitive to DPS: the two bottom-quark jets can originate from one partonic interaction, the other two jets from the second interaction (both interactions come from the same vertex and happen at the same time, in contrast to pile-up interactions). Since these two interactions are not directly correlated, an angular correlation ΔS between the two pairs of jets could indicate a contribution of DPS. Small ΔS values indicate no correlation between the jet pairs, and this is the region in which theoretical predictions without DPS fail to describe the measurements (Fig. 4).

Parton distributions revisited

The parton densities as a function of x and of the scale Q^2 describe the probability to find a parton with momentum fraction x in a proton. These densities don't provide any information about the transverse momentum distributions of those partons inside the proton, however. These are described by new distributions, called transverse momentum dependent (TMD) parton distributions.

For the first time, a complete set of TMD parton distributions (quarks and gluons) was obtained recently [7] using the xFitter framework, from a fit to structure function measurements performed at DESY's former HERA electron–proton collider (Fig. 5). With a new tool developed at DESY, called TMDplotter [8,9], these TMDs – as well as any other parton distribution function – can be visualised online and compared to any other available distribution.

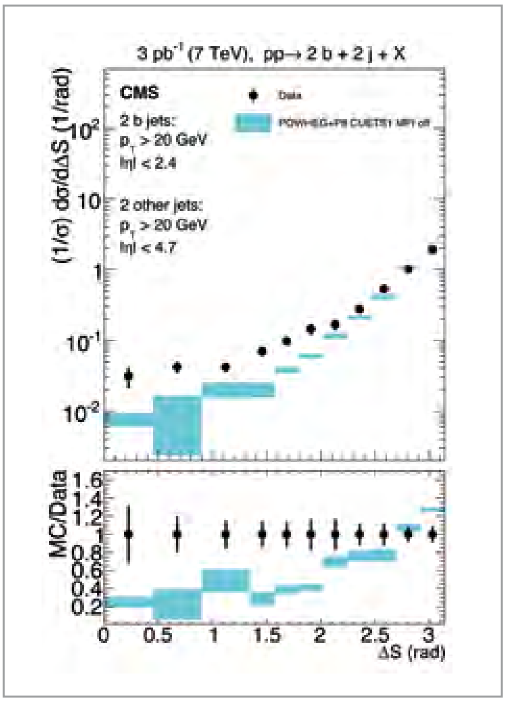

Figure 4

Distribution of the angular correlation between the two bottom-quark jets and the two other jets compared to theoretical predictions without DPS [6]

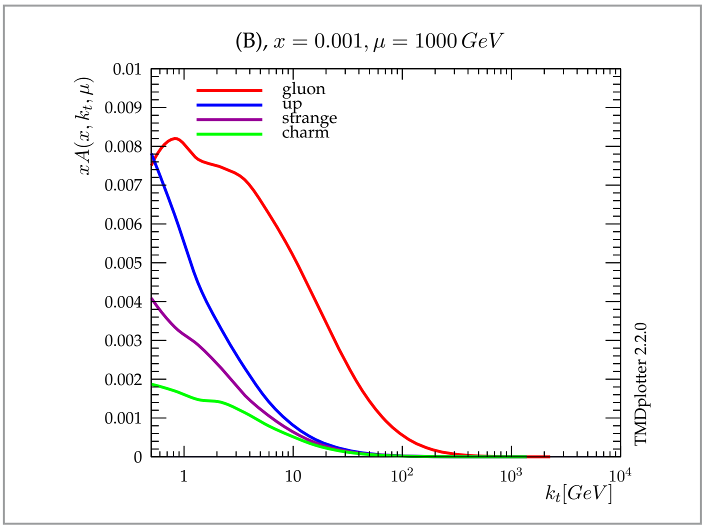

Figure 5

Transverse momentum distribution as obtained from a QCD fit to HERA structure function measurements for different parton species [7–9]

Contact:

Katerina Lipka, katerina.lipka@desy.de
Hannes Jung, hannes.jung@desy.de

References:

[1] CMS Collaboration, Eur. Phys. J. C76 (2016) no. 8, 469.
[2] CMS Collaboration, submitted to Eur. Phys. J. C., arXiv:1609.05331.
[3] CMS Collaboration, CMS-PAS-TOP-14-013.
[4] PROSA Collaboration, www.prosa.desy.de.
[5] PROSA Collaboration, arXiv: 1611.03815.
[6] CMS Collaboration, Phys. Rev. D94 (2016) no. 11, 112005.
[7] F. Hautmann, H. Jung, A. Lelek, DESY-16-174.
[8] F. Hautmann et al., Eur. Phys. J. C 74 (2014) 3220.
[9] P. Connor et al., tmdplotter.desy.de.

Top and Higgs: the trendiest couple.

Towards measuring the top–Higgs coupling

The DESY CMS and ATLAS groups have performed searches for the associated production of a Higgs boson with a top quark–antiquark pair using proton–proton collision data taken at LHC Run 2. This process allows the direct measurement of the top–Higgs coupling, a crucial test of the Higgs mechanism, which aims to explain the generation of particle masses.

Introduction

Since the discovery of the Higgs boson at the LHC in 2012, the study of its properties has been a major research target for particle physicists. Up to now, all measurements of the properties of the Higgs boson are in agreement with the expectations from the Standard Model (SM).

One important property of the Higgs boson is that its coupling to elementary particles causes them to obtain mass. The top quark is the heaviest elementary particle and therefore provides the best possibility to directly measure this coupling. A direct measurement of the top-quark coupling to the Higgs boson is a missing vital element to verify the SM nature of its associated Higgs field. A deviation from the expected coupling could reveal the first signs of new physics beyond the SM.

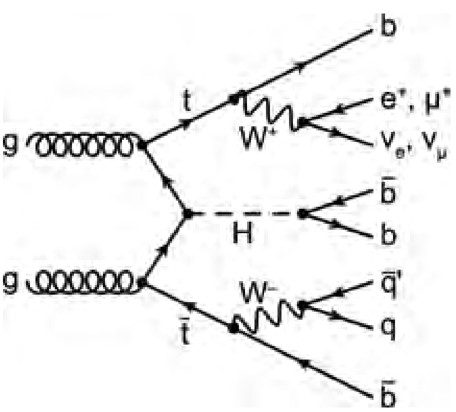

Figure 1

Example of a leading-order Feynman diagram for $t\bar{t}H$ production, where the Higgs boson decays into a bottom quark–antiquark pair

A complex analysis strategy for a complex final state

The ATLAS and CMS groups at DESY play a leading role in the first searches for the production of a top-quark pair and a Higgs boson ($t\bar{t}H$) at a centre-of-mass-energy of 13 TeV.

Both DESY groups searched for events where the Higgs boson decays to two bottom (*b*) quarks, which is the most likely decay channel (Fig. 1). Since the top quark decays almost always to a *W* boson and a *b* quark, the decay of the $t\bar{t}H$ leads

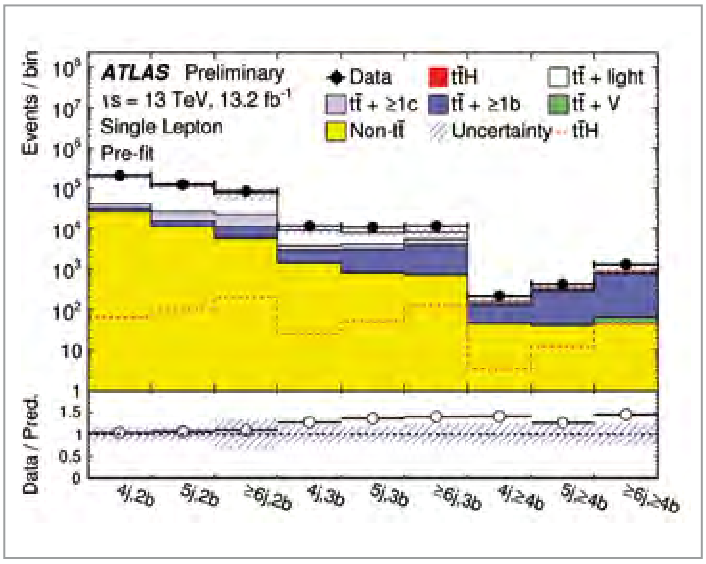

Figure 2

Comparison of the predicted and observed number of events in different categories of jet and *b*-quark jet multiplicity. The $t\bar{t}H$ signal is normalised to the SM prediction.

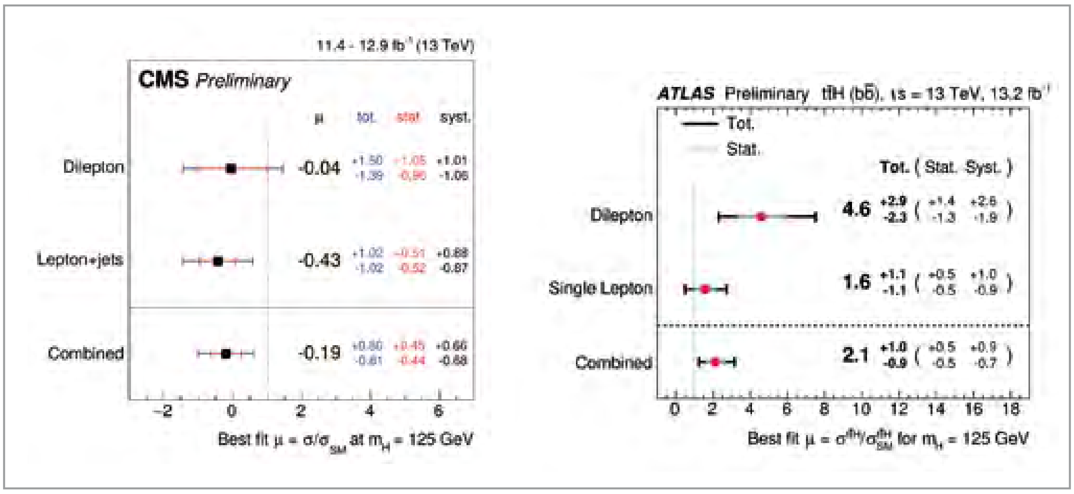

Figure 3

Summary of the signal strength measurements (the ratio of the measured $t\bar{t}H$ signal cross section to the SM expectation) in the individual channels and for the combination for CMS (left) and ATLAS (right)

to very complex final states with multiple *b*-quark jets, which experimentally cannot be easily assigned to the top quarks and Higgs boson they originate from. The DESY groups focus on the cases where both *W* bosons decay into a lepton and the corresponding neutrino (the so-called dilepton channel), or one *W* boson decays into quark jets and the other leptonically (the so-called single-lepton or lepton+jets channel).

Furthermore, these events are very rare and are hidden under a huge amount of background. The dominant background process is the production of top-quark pairs, which has a production rate 2000 times larger than the $t\bar{t}H$ signal. Especially, top-quark pair events with additional *b*-quark jets produced from e.g. a gluon instead of Higgs-boson decay are almost indistinguishable from $t\bar{t}H$ events. This complex final state with large background requires the analysis to be split in regions of jet and *b*-quark jet multiplicity (Fig. 2 and Ref. [1]) with different sensitivity to signal and background processes. Even in the most sensitive region with at least six jets and four *b*-quark jets, the signal-to-background ratio is only 6%. To further disentangle signal from background events, machine learning techniques and advanced statistic tools are used in the analyses. These techniques allow optimal exploitation of the full information of the final-state particles.

Results

The ATLAS [1] and CMS [2] results are shown in Fig. 3 for the considered decay channels of the top-quark pair and their combination. The measurements use a partial set of the data collected in 2016 corresponding to an integrated luminosity of about 13 fb^{-1}. The vertical line in the figures represents the SM prediction assuming a Higgs-boson mass of 125 GeV. The signal strength μ indicates the measured production rate in comparison to the value predicted in the SM.

The ratio of the measured $t\bar{t}H$ signal cross section to the SM expectation is found to be $\mu = 2.1^{+1.0}_{-0.9}$ in the ATLAS experiment, which disfavours the background-only hypothesis by 2 standard deviations. The result from the CMS experiment yields $\mu = -0.2^{+0.8}_{-0.8}$, which is compatible with the background-only hypothesis but still consistent with the ATLAS measurement. In the light of these results, it is still too early to claim an observation of the process.

The coming measurements with the full 2016 data set, corresponding to an integrated luminosity of more than 36 fb^{-1}, could allow the observation of the elusive $t\bar{t}H$ process. This would be one of the most important results of the current Run 2 of the LHC.

Contact:

Maria Aldaya Martin, maria.aldaya@desy.de
Carmen Diez Pardos, carmen.diez@desy.de
Judith Katzy, judith.katzy@desy.de

References:

[1] ATLAS Collaboration, ATLAS-CONF-16-080.
[2] CMS Collaboration, CMS-PAS-HIG-16-038.

Higgs bosons at 13 TeV.

First results from ATLAS and CMS at LHC Run 2

In 2015 and 2016, LHC Run 2 delivered approximately 40 fb^{-1} of integrated luminosity useful for physics to each of the ATLAS and CMS experiments, at a record centre-of-mass energy of 13 TeV. The increased centre-of-mass energy and amount of data open new exciting prospects for Higgs-boson physics – a topic in which the DESY ATLAS and CMS groups play a major role. By summer 2016, the two experiments had already analysed one third of the 2016 data.

LHC Run 1 brought the discovery of the Higgs boson and first precise measurements of its properties with the data taken in 2011 and 2012. From the combination of the ATLAS and CMS data, the Higgs-boson mass, which is one of the fundamental parameters in the Standard Model (SM), was measured already with a precision of 2 per mille (m_H = 125.09 ± 0.24 GeV). The global signal strength, that is, the ratio of the measured production cross section to the SM prediction, was determined from Run 1 to a precision of 10%. In Run 2, at a centre-of-mass energy of 13 TeV, the production rate in the main channel (gluon–gluon fusion) is a factor of 2.3 higher compared to Run 1 at 8 TeV. For this reason, and given the successful data taking in 2016, the Higgs boson physics programme is expected to be even more exciting than before. By summer 2016, the experiments had re-established the existence of the Higgs-boson signal and performed initial measurements of its production processes and differential cross sections with the data taken up till then. The DESY ATLAS group contributed to measurements of the Higgs decays into two photons and to their combination with results obtained from Higgs decays into four leptons. The measured production cross sections of the gluon–gluon fusion and the vector boson fusion processes are shown in Fig. 1.

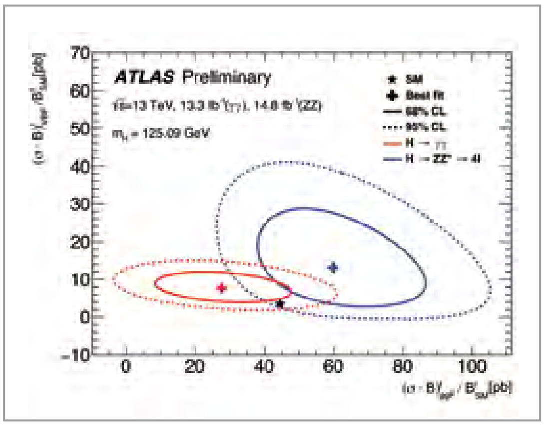

Figure 1
Measurement of the gluon–gluon fusion and vector boson fusion production cross sections in Higgs boson decays to two photons and to four leptons

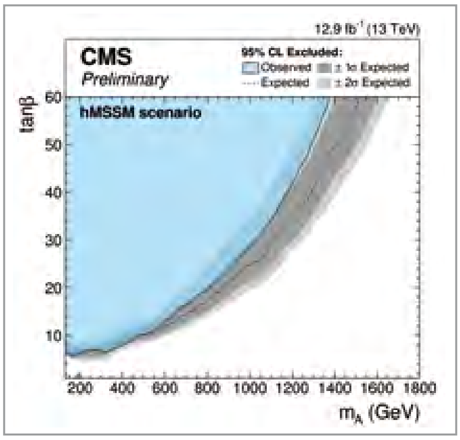

Figure 2
Region of MSSM parameter space (in tanβ and mass of an additional heavy neutral Higgs m_A) excluded by the CMS collaboration with the first 2016 data. The hMSSM is a particular scenario where the Higgs boson found is assumed to be the lightest state.

The observed Higgs boson could be the lightest of a richer spectrum of Higgs states, such as those predicted by supersymmetry (SUSY), the most popular extension of the SM. In the Minimal Supersymmetric Standard Model (MSSM), additional heavier neutral Higgs bosons could be produced at the LHC and be strongly coupled especially to third-generation fermions. The DESY CMS group searched for a heavy Higgs decaying into tau leptons, covering a large mass region. However, no signal was found, allowing strong constraints to be set in the parameter space, as shown by the blue region in Fig. 2. New physics still has to be detected at the LHC, and the Higgs sector is one of the most promising channels.

Contact:
Elisabetta Gallo, elisabetta.gallo@desy.de
Alexei Raspereza, alexei.raspereza@desy.de
Kerstin Tackmann, kerstin.tackmann@desy.de

References:

[1] CMS Collaboration, CMS-PAS-HIG-16-037.
[2] ATLAS Collaboration, ATLAS-CONF-2016-067.
[3] ATLAS Collaboration, ATLAS-CONF-2016-081.

The Higgs boson as a window to the unknown.

Using precision studies of the Higgs boson to search for new physics

The Standard Model (SM) of particle physics very successfully describes a large range of experimental observations, but provides no explanation for cosmological observations such as the matter–antimatter asymmetry or the existence of dark matter in the universe. A DESY group funded by a European Research Council (ERC) Starting Grant will use Higgs-boson decays to two photons and to four leptons to carry out precision studies and search for signs of physics beyond the SM in the Higgs sector.

The discovery of a Higgs boson by the ATLAS and CMS experiments at the LHC in summer 2012 opened a new window to test our understanding of the physics of elementary particles and search for physics beyond the SM of particle physics. The SM makes testable predictions about how the Higgs boson interacts with other particles, how it is produced and how it decays. Confronting measurements with theoretical predictions is therefore a sensitive test of the SM. The ongoing LHC Run 2 at a centre-of-mass energy of 13 TeV is expected to produce more than 20 times the number of Higgs bosons generated in 2011 and 2012 at 7 and 8 TeV, offering the chance for much more precise measurements.

The ERC group contributed to the initial measurements at 13 TeV at the ATLAS experiment, carried out using the data taken in 2015 and up to summer 2016. Figure 1 shows the Higgs transverse momentum spectrum measured from Higgs decays into two photons with the 13 TeV data. The measurements and the theoretical predictions agree within the present uncertainties.

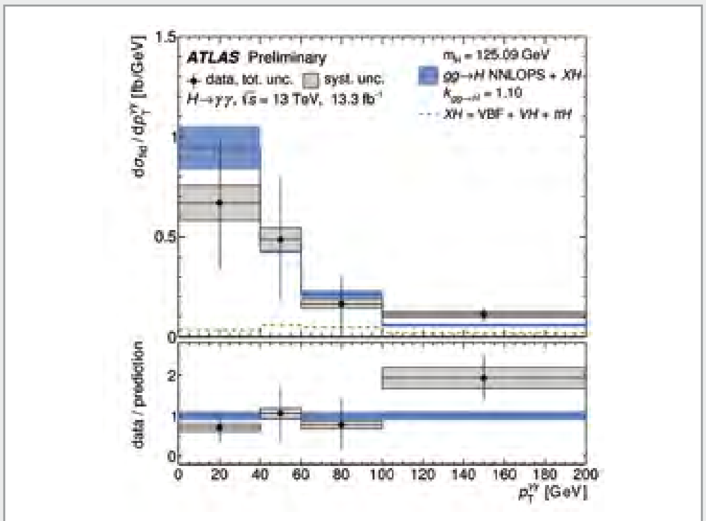

Figure 1

Higgs transverse momentum spectrum measured in 13 TeV data and compared to theoretical predictions

In the future, the ERC group will participate in the measurements of Higgs kinematic distributions, such as the Higgs transverse momentum spectrum, using the 13 TeV data recorded by the ATLAS experiment. Since these measurements will be limited by the size of the available data set in the next few years, the group will use and combine Higgs-boson decays to two photons and to four leptons. Both decay channels allow the reconstruction of a clear signal peak and therefore a robust subtraction of the background.

To support these measurements, the group is working on the reconstruction and identification of photons in the ATLAS detector to cope with the challenges of the increasing instantaneous luminosity. Making use of precise theoretical predictions, the kinematic distributions will then be used to constrain the couplings of the Higgs boson to the SM particles – an approach that is complementary to the studies of Higgs-boson production processes and decay branching ratios – and to search for signs of yet unknown physics beyond the SM.

ERC Starting Grant

“HiggspT: Differential Higgs distributions as a unique window to New Physics at the LHC”

Contact:

Kerstin Tackmann, kerstin.tackmann@desy.de

References:

[1] ATLAS Collaboration, ATLAS-CONF-2016-067.
[2] ATLAS Collaboration, ATLAS-CONF-2016-081.

Dark matter and the Higgs boson.

Using the Higgs boson to find dark matter and other new physics

The Standard Model (SM) of particle physics is a very successful theory describing the fundamental particles of matter and their interactions. However, there are many cosmological observations that the SM cannot explain, for example the existence of dark matter in the universe. A Helmholtz Young Investigator Group (YIG) at DESY uses Higgs events from the ATLAS detector to investigate some of these unsolved cosmological puzzles.

The $H \rightarrow ZZ^* \rightarrow 4l$ decay channel is one of the best final states to study the properties of the Higgs boson. It is often termed the "golden channel" because the four leptons in the final state cause the background contamination be very low (Fig. 1). Measurements of the cross sections of Higgs-boson production are particularly interesting. Cross sections can be measured as a function of Higgs-boson kinematics, such as the transverse momentum of the Higgs boson, and as a function of the properties of hadronic jets produced in association with the Higgs boson. These distributions are used to test the calculations of SM Higgs production. Furthermore, deviations from SM predictions could indicate the presence of new physics. So far, the YIG has focused on estimating the very small but challenging backgrounds due to misidentified electrons and muons, including the differential distributions, and on investigating various unfolding methods to correct the reconstructed distributions for detector effects.

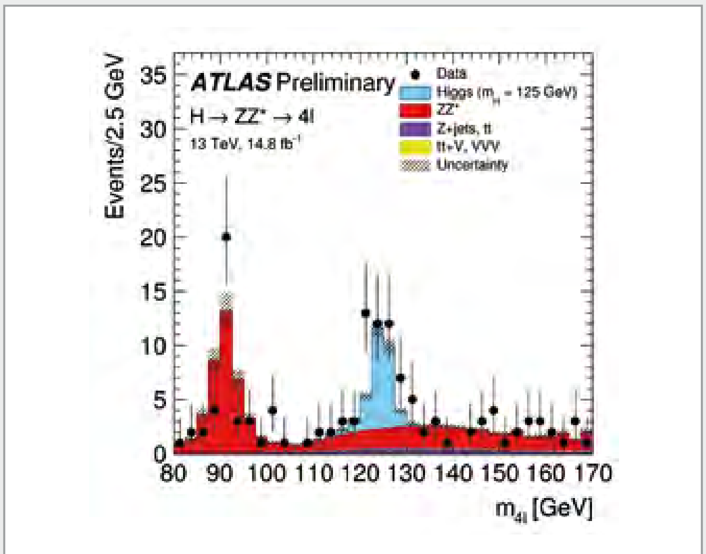

Figure 1

Four-lepton invariant-mass distribution of the events selected in the $H \rightarrow ZZ^* \rightarrow 4l$ analysis with 14.8 fb^{-1} of 13 TeV data, compared to the expected signal and background processes

It is possible to use Higgs-boson decays to invisible particles to directly search for physics beyond the SM, in particular dark-matter candidates coupling to the Higgs boson. Since the transverse momentum of all produced particles should add up to zero in a proton–proton collision, these particles can be detected by looking for missing transverse momentum. To reject background processes, the YIG is using a distinctive Higgs production channel in which the Higgs boson is produced in association with a *Z* boson. This final state can also be used to search for a new heavy Higgs boson and dark matter produced in association with a *Z* boson. To control the background due to "*Z* + jet" events, the YIG has concentrated on improving the missing transverse momentum reconstruction for cases in which an electron and a hadronic jet are close together.

The YIG is contributing to the work on the end-cap of the new ATLAS ITk strip detector that will be built at DESY. The plan is to help develop and implement the readout software and perform tests of detector modules of increasing sizes.

Helmholtz Young Investigator Group

"Search for dark matter and other new physics with the Higgs boson at the ATLAS experiment"

HELMHOLTZ ASSOCIATION

Contact:

Sarah Heim, sarah.heim@desy.de

References:

http://hgf.desy.de/ivf/projekte/e208842/

ATLAS Collaboration, ATLAS-CONF-2016-079.

From top to Higgs... and beyond.

Understanding the origin of mass and searching for new physics

Very precise knowledge of the top-quark properties is crucial to test the Standard Model (SM) of particle physics and provides a window to new physics phenomena beyond it. In particular, understanding the interplay between the top quark and the Higgs boson is essential to shed light on the mechanism expected to generate the mass of elementary particles. The Helmholtz Young Investigator Group (YIG) "Ultimate precision measurements and searches for new physics using top quarks at the CMS experiment at the LHC" is part of this exciting endeavour.

The top quark plays a very special role in the description of the structure of matter and interactions within the SM. It is by far the heaviest fundamental particle known to date and therefore believed to be key to the mechanism that lends mass to elementary particles through their couplings to the Higgs boson. Moreover, many models of novel physics phenomena beyond the SM expect the top quark to couple to yet unknown particles whose existence could hereby be revealed. So far, the measured Higgs-boson properties agree with the SM expectations; however, a direct measurement of the top–Higgs coupling is the crucial missing piece to ascertain its SM nature. Thus, it is of great importance to measure the properties of the top quark as precisely as possible and to investigate its interaction with the Higgs boson. The LHC at CERN, with its unprecedented energies, provides a unique environment for these studies.

The main focus of the YIG is the search for top quark–antiquark pair production in association with a Higgs boson ($t\bar{t}H$) and the direct measurement of the top–Higgs coupling. The YIG contributes to the first $t\bar{t}H$ production measurements at the CMS experiment at a centre-of-mass energy of 13 TeV. We search for events where the Higgs boson decays into two bottom quarks. The latest results, using a reduced set of data collected in 2016, are shown in Fig. 1. More data are needed to possibly claim an observation of the $t\bar{t}H$ process. The YIG is performing high-precision measurements of top-quark properties at CMS at centre-of-mass energies of 8 and 13 TeV. We explore $t\bar{t}$ production as a function of kinematic properties of the process. Results are confronted with state-of-the-art SM theoretical calculations and used to improve the models and constrain SM parameters. With the LHC luminosity upgrade planned for 2023, the CMS tracking system will have to be replaced by an enhanced one that is able to withstand the harsh radiation environment. The YIG is also participating in the development of designs for tracker sensor modules and optimising their assembly in an automated way.

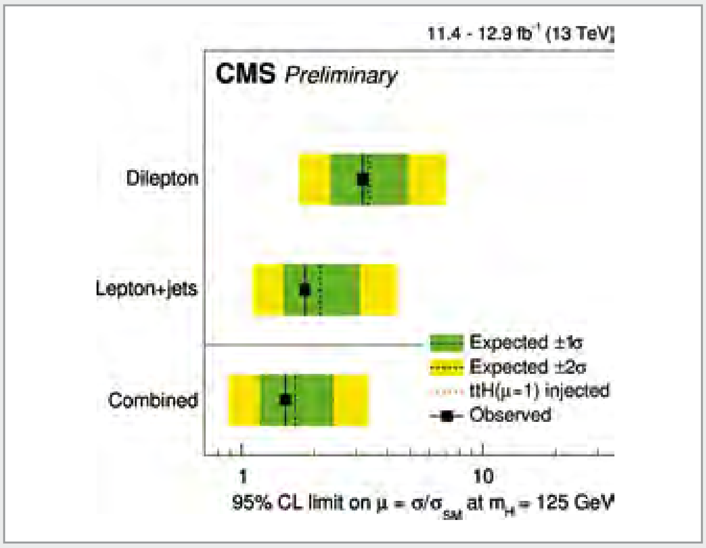

Figure 1

Expected and observed 95% confidence level limits on the signal strength μ (ratio of the measured $t\bar{t}H$ cross section to the SM expectation) for the individual $t\bar{t}H$ ($\rightarrow b\bar{b}$) channels and their combination. The combination results in an observed (expected) limit on the $t\bar{t}H$ production cross section of 1.5 (1.7) relative to the SM expectation.

Helmholtz Young Investigator Group

"Ultimate precision measurements and searches for new physics using top quarks at the CMS experiment at the LHC"

HELMHOLTZ ASSOCIATION

Contact:
Maria Aldaya Martin, maria.aldaya@desy.de

References:

http://hgf.desy.de/ivf/projekte/vh_ng_1004
CMS Collaboration, CMS-PAS HIG-16-038.

Searches for new physics with ATLAS.

Looking for particles and interactions beyond the Standard Model

The high centre-of-mass energies of LHC Run 2 offer unique opportunities to search for new phenomena. Thanks to an exceptionally well performing LHC, the ATLAS experiment collected the first large data set of 14 TeV collisions. The analysis of these high-energy collision events, in which the DESY ATLAS group is strongly involved, highly increases the sensitivity to beyond-the-Standard-Model (BSM) processes.

Beyond bump hunting

Additional heavy Higgs bosons decaying into a top quark–antiquark pair ($t\bar{t}$) are predicted in various extensions of the SM, most notably two-Higgs-doublet models (2HDMs), which are well motivated by supersymmetry and theories of dark matter. Traditional searches for $t\bar{t}$ resonances have a low sensitivity for these new bosons as they are designed based on the simplifying assumption that new resonances will appear as a localised excess or "bump" in the $t\bar{t}$ invariant-mass spectrum. In the case of new scalar and pseudoscalar states, however, which are predominantly produced via top-quark loops from gluon–gluon initial states, strong interference effects between the signal and the dominant background from SM $t\bar{t}$ production distort the signal shape from a simple Breit–Wigner peak to a peak–dip structure.

The DESY ATLAS group is the first to present a search for heavy scalar and pseudoscalar states decaying into $t\bar{t}$ in which these interference effects are taken into account [1]. In the absence of a signal, exclusion limits are obtained as a function of the ratio of the vacuum expectation values of the two Higgs fields, tan β, and the mass of the neutral (pseudo-)scalar state in a Type-II 2HDM. For a (pseudo-)scalar with a mass of 500 GeV, values of tan $\beta < 0.45$ (0.85) are excluded at 95% confidence level using 20.3 fb^{-1} of $\sqrt{s}$ = 8 TeV proton–proton collision data. These limits are the most stringent to date in the high-mass, low-tan β 2HDM parameter region.

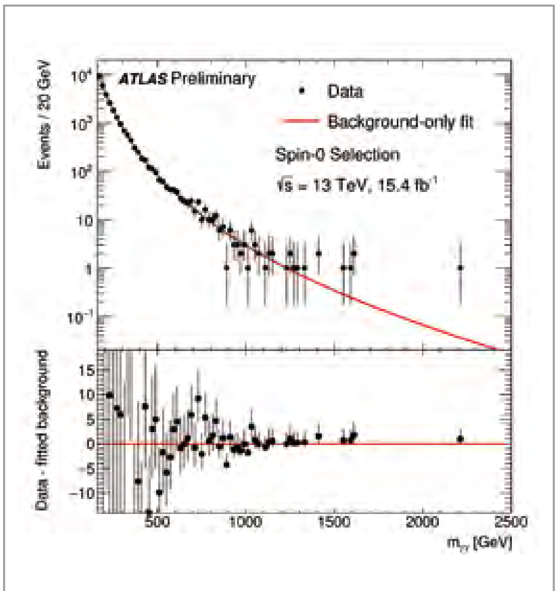

Figure 1
Di-photon invariant mass for the selected data events, compared to the background prediction (red line)

High-mass diphoton resonances

Many extensions of the SM predict the existence of new high-mass states, for example of additional heavy Higgs bosons. The DESY ATLAS group participated in searches for new high-mass states decaying into two photons or into a Z boson and a photon. Both final states have clean experimental signatures with an excellent energy resolution. A high-mass resonance, if it was narrow, would show up as an excess of events on top of a smoothly falling background. Figure 1 shows the observed diphoton invariant-mass spectrum using the first 15.4 fb^{-1} of 13 TeV data [2]. The data is compatible with no excess over the smooth background in the full invariant-mass range. An analogous result is obtained by the search in the $Z\gamma$ decay channel: the data is compatible with no excess from 250 GeV to 2.4 TeV, the full invariant-mass range studied [3].

Contact:
Krisztian Peters, krisztian.peters@desy.de
Katharina Behr, katharina.behr@desy.de
Kerstin Tackmann, kerstin.tackmann@desy.de

References:

[1] ATLAS-CONF-2016-073.
[2] ATLAS-CONF-2016-059.
[3] ATLAS-CONF-2016-044.

Expected performance of the ATLAS ITk detector.

Exploring inner tracker concepts for high-luminosity LHC operation

To cope with the challenging detector conditions at the high-luminosity LHC (HL-LHC), the inner detector of ATLAS will be completely replaced with a brand-new all-silicon tracking detector (ITk). Two layout concepts are currently under consideration for the innermost region of the detector, based on pixel sensor technologies, to complement the microstrip sensors used at larger radii. Both of these concepts provide tracking coverage in a significantly larger pseudorapidity range than the current inner detector. Detailed studies based on Monte Carlo detector simulations were performed to ensure that the layout concepts meet the stringent performance requirements that will allow the HL-LHC to reach its physics goals.

Layout concepts

Two concepts for extending tracking coverage of the ITk detector up to high pseudorapidity ($\eta < 4$) are under consideration: the extended and inclined layouts. In the extended layout, the innermost pixel layers extend up to large *z* along the beampipe direction. The inclined layout uses modules inclined at various angles to the beampipe to ensure close-to-perpendicular particle incidence angles. The strip system common to both designs comprises four barrel stave layers and six end-cap petals of double-sided silicon microstrips. The DESY ATLAS group simulated both layout concepts in detail using Geant4 and the ATLAS Athena software framework.

Performance studies

Monte Carlo samples of various physics processes, including the approximately 200 additional pile-up interactions per event expected at luminosities of 7.5×10^{34} $cm^{-2}s^{-1}$, were produced to study the performance of the candidate layout concepts. These studies demonstrated the excellent performance of the two concepts, which meet the requirements for reaching the goals of the ATLAS HL-LHC physics programme. Detailed investigations were performed not only for high-level performance metrics such as tracking efficiencies and track parameter resolutions, but also of low-level quantities that can be crucial for assessing the technical performance of the reconstruction. So-called “seeds”, which represent the first step in identifying tracks, are very important to understand (Fig. 1), and ways in which seeds that will not eventually lead to useful tracks can be rejected as early as possible may give large computational advantages.

In addition to excellent performance for isolated tracks, reconstruction of tracks within jets and other dense objects will be increasingly important. Dedicated methods for maintaining high efficiency for tracks in dense environments were developed and studied for the ITk layout concepts (Fig. 2).

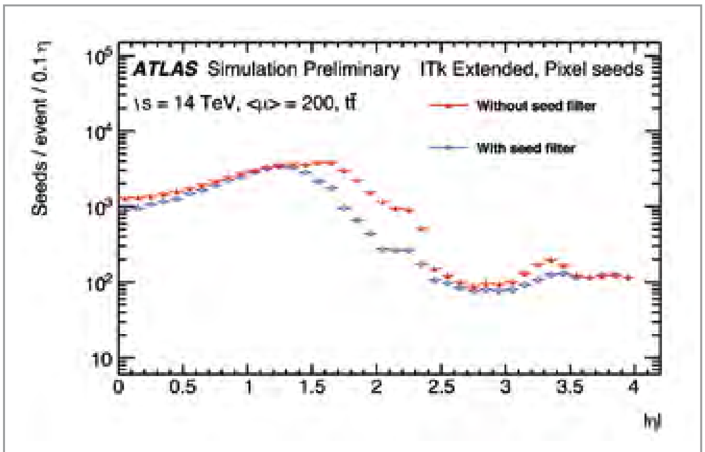

Figure 1

Number of seeds in a typical HL-LHC event before and after applying a filter based on properties of the pixel clusters used in the seeds

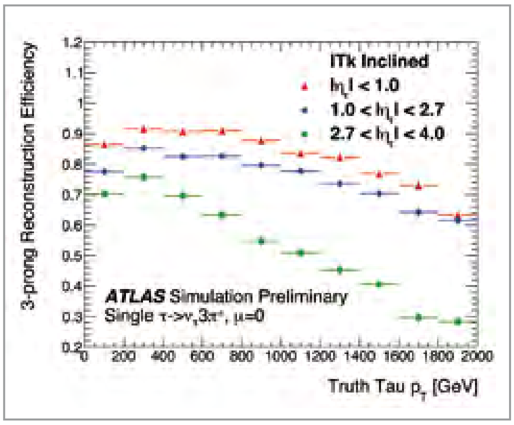

Figure 2

Efficiency for reconstructing all three tracks in a tau-lepton decay to three charged pions, shown as a function of the tau transverse momentum and for different pseudorapidity regions

Contact:

Nicholas Styles, nicholas.styles@desy.de

Zooming in on top production.

New differential measurements of top-quark production at the LHC

In 2015, the LHC produced a few million events containing a top quark–antiquark pair ($t\bar{t}$) at the new energy frontier of 13 TeV. The ATLAS and CMS groups at DESY explored these and previous 8 TeV data for differential $t\bar{t}$ production studies in unprecedented detail. The results are compared with state-of-the-art quantum chromodynamics (QCD) calculations.

Introduction

Ever since its discovery at the Tevatron in 1996, the top quark has been a major subject of particle physics research. One mystery is why the top quark is so much heavier than any other known fermionic elementary particle (quark or lepton). Its intriguing heaviness leads the top quark to play an important role in various scenarios of new physics beyond the well-established Standard Model (SM). However, all top-quark-related results so far from the Tevatron or the LHC show agreement with the SM predictions and no evidence for new physics.

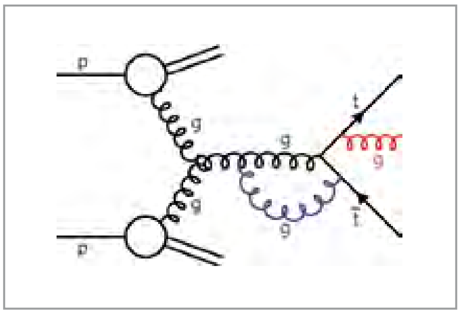

Figure 1

Exemplary diagram for $t\bar{t}$ production at the LHC

Top quarks are produced at the LHC predominantly together with a top antiquark ($t\bar{t}$, for short) through the strong force as mediated by gluons. The largest contributions are from processes initiated by gluons from the colliding protons, as shown in an exemplary process in Fig. 1.

Investigating $t\bar{t}$ production cross sections is interesting for the following reasons:

- The SM $t\bar{t}$ production can be calculated accurately in perturbative QCD (pQCD). Processes with more gluons (as in Fig. 1, where a real emission is shown in red and a virtual one in blue) contribute to the higher orders and are suppressed. Any significant deviation of the data from the accurate perturbative predictions could signal the presence of new physics.
- As evident from Fig. 1, the $t\bar{t}$ production is highly sensitive to the gluon density in the proton. This density is not calculable in pQCD, but it was accurately determined from deep-inelastic scattering data at DESY's former electron–proton collider HERA (see *DESY Particle Physics 2014*). However, assuming the validity of the SM, it is possible to further constrain the density with precise $t\bar{t}$ production measurements.
- In numerous scenarios of new physics, top-quark pairs would also be produced in the decay of new heavy resonances, leading to detectable distortions of differential kinematic spectra in the $t\bar{t}$ events.

This article presents selected new measurements of differential $t\bar{t}$ production carried out by the DESY ATLAS and CMS groups. As top quarks decay almost always into a bottom quark and a *W* boson, top-quark final states are classified according to the decay channel of the *W* bosons. The DESY groups focused on the case where both *W* bosons decay into a lepton (electron or muon) and the corresponding neutrino. The outgoing bottom quarks and any extra real hard gluon emission are observed as collimated sprays of particles in the detector, called jets.

Single-differential measurements

Figure 2 shows examples of new measurements by ATLAS and CMS obtained with the 2015 data. Results as a function of the invariant mass of the $t\bar{t}$ system (left panel) are compared to several modern pQCD calculations. Since most

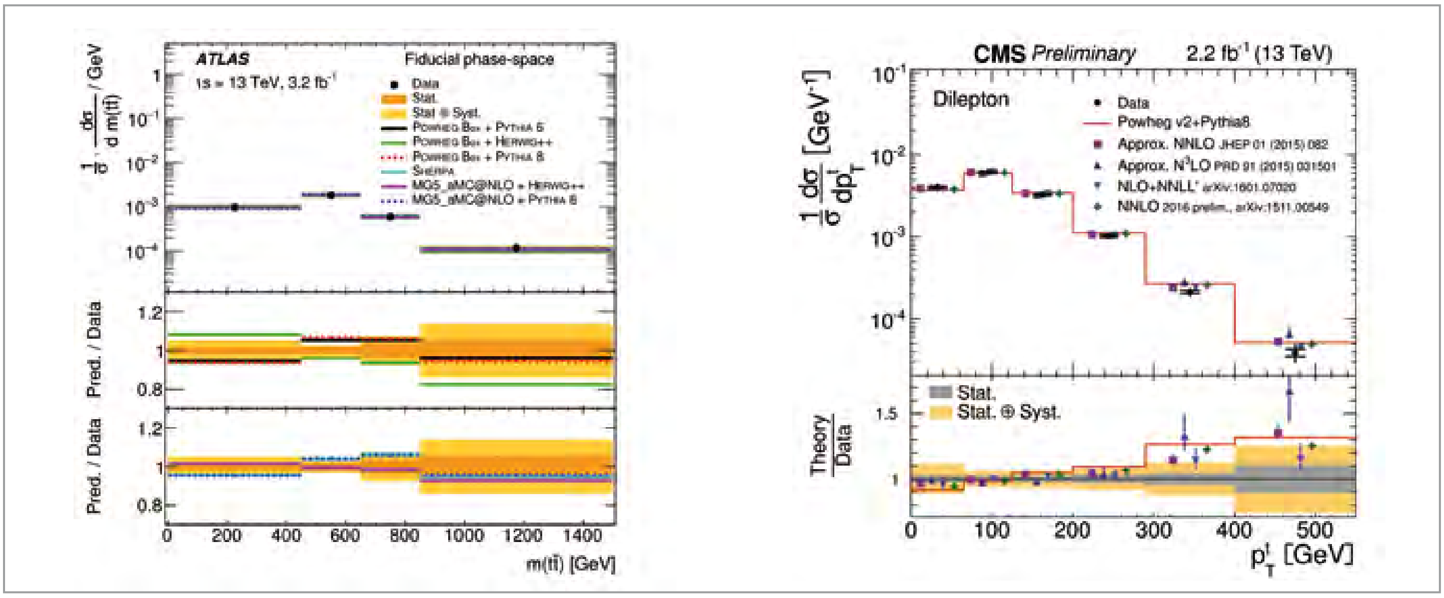

Figure 2

Differential $t\bar{t}$ production cross sections as a function of the invariant mass of the $t\bar{t}$ system (left) and of the top-quark transverse momentum (right)

models describe the data, there is no clear evidence for new physics. In the right panel, the measurements are presented as a function of the transverse momentum of the top quark. The best prediction is provided by the brand-new next-to-next-to-leading-order calculation (labelled "NNLO"). This is the first prediction that provides the exact perturbative result including processes with up to two extra gluons (as the one shown in Fig. 1), thus demonstrating the advances of the models.

Figure 3 shows a new ATLAS measurement of additional jet activity in the $t\bar{t}$ events. The study is probing real hard gluon emissions such as the red gluon in Fig. 1 and is thus directly sensitive to higher orders in pQCD. For larger numbers of additional jets in particular, obtaining accurate predictions is a challenge. However, it is possible to effectively tune the amount of gluon radiation in the models (as shown in the bottom panel for "Powheg+Pythia6") in order to describe the data.

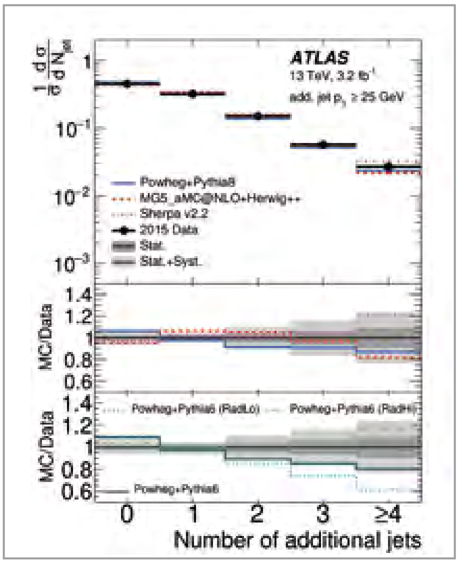

Figure 3

Spectrum of additional number of jets in $t\bar{t}$ events

Double-differential results

The DESY CMS group performed the first-ever double-differential $t\bar{t}$ production measurements using 8 TeV data recorded in 2012. Figure 4 shows exemplary results as a function of the rapidity of the $t\bar{t}$ system in different ranges of the $t\bar{t}$ mass. Using the "NLO QCD" predictions shown in Fig. 4, the group proved that these data can significantly improve the knowledge of the gluon density in the proton at large proton momentum fractions ~0.3. This may be useful to enhance the accuracy of predictions for any LHC processes initiated by highly energetic gluons.

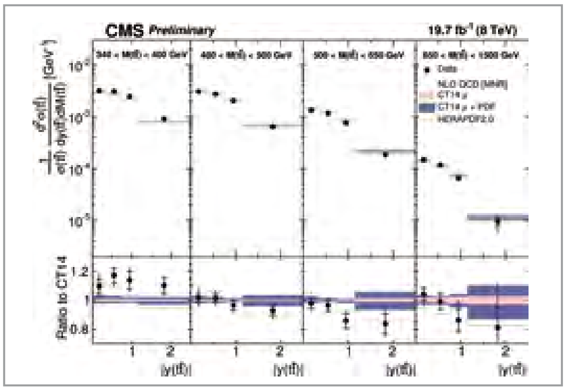

Figure 4

First-ever double-differential $t\bar{t}$ production cross sections

Contact:

Olaf Behnke, olaf.behnke@desy.de
Carmen Diez Pardos, carmen.diez@desy.de
Mahsana Haleem, mahsana.haleem@desy.de

References:

CMS Collaboration, CMS-PAS-TOP-16-011.
CMS Collaboration, CMS-PAS-TOP-14-013.
ATLAS Collaboration, arXiv:1612.0522.
ATLAS Collaboration, arXiv:1610.09978.

New pixel detector for CMS.

Producing 300 modules for the fourth barrel pixel layer

A new silicon pixel tracking detector system was built for the CMS experiment at the LHC for efficient operation at twice the design luminosity. Together with the University of Hamburg, DESY contributed 300 modules for half of the fourth barrel pixel layer.

In 2016, the peak luminosity of the LHC exceeded the design value by 50%. While this is beneficial for studying rare processes, the most common collision products tend to overwhelm the innermost detector regions: 40 simultaneous proton–proton collisions create on average 1000 charged particles leaving signals in 12 000 pixels every 25 ns. In the CMS detector, the signals have to be stored for 3.5 μs until a trigger decision arrives, meaning that the data from 140 bunch crossings are accumulated. In 2016, this exhausted the storage capacity of the innermost pixel layer, leading to a data loss of up to 5%. This loss would increase even further with higher luminosity, as is expected in the coming years. This effect was anticipated, prompting the CMS collaboration to develop new pixel readout chips with extended storage and higher data rate capability. DESY accompanied the process with test beam campaigns, providing essential feedback to the chip designers.

The CMS pixel detector is accessible and can be extracted without affecting the silicon strip tracking detector or the LHC beam pipe. The CMS collaboration decided to replace the entire pixel detector with a new system consisting of four instead of three barrel layers and six extended instead of four smaller end-cap disks, by making use of previously unoccupied regions. The extension was limited by the space available for electrical cables, optical fibres and cooling pipes.

The additional pixel units increase the efficiency and purity of the track reconstruction in a high pile-up environment. The fourth barrel pixel layer and the radially extended disks increase the lever arm for pixel tracks, which improves the momentum resolution and thereby also the impact parameter resolution. This information can be used in the high-level trigger, a processor farm that has to reduce the event rate from 100 kHz triggered to about 1 kHz written to tape, by selecting processes of interest using a fast partial event reconstruction.

The new pixel detector improves the assignment of tracks to a specific collision point and allows the identification of

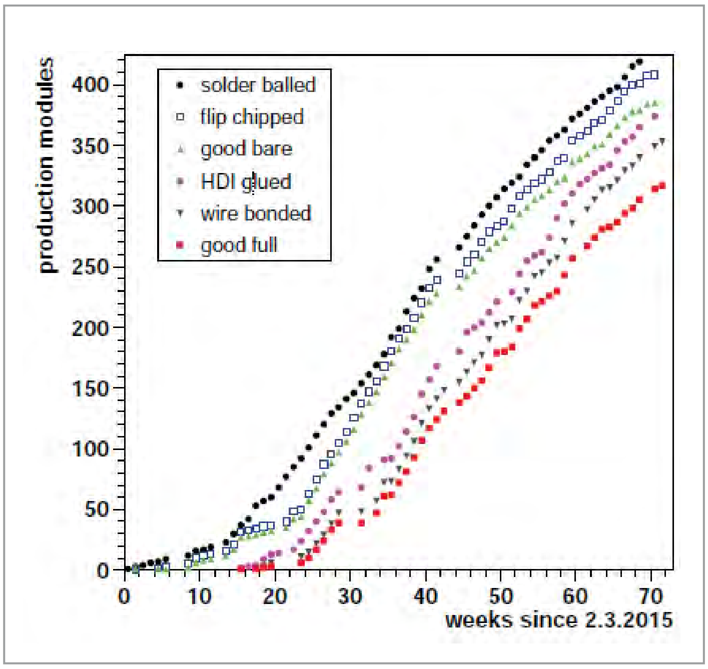

Figure 1

Production rate at DESY in Hamburg with quality control for bare and full modules

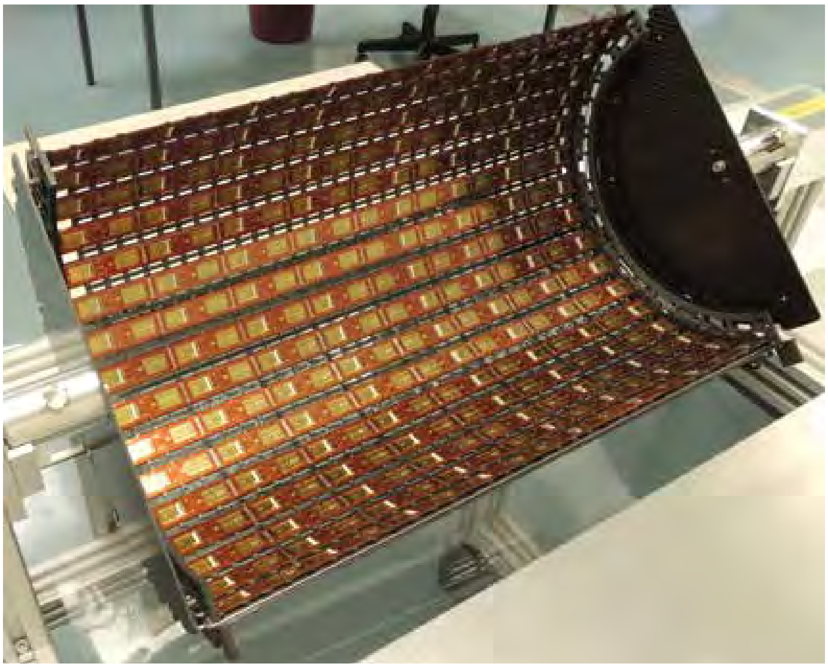

Figure 2

Modules mounted onto the fourth barrel layer carbon fibre frame

beauty, charm and tau decays at a transverse distance of 0.03 mm from the beam. This translates into a lifetime resolution of 50 fs or better, depending on the momentum boost. Pile-up events are distributed along the beam axis with a Gaussian spread of about 40 mm and can be separated thanks to the longitudinal pixel vertex resolution of 0.1 mm.

The new barrel pixel detector consists of 1184 modules, 256 of which come from DESY and the University of Hamburg. The production details were described in *DESY Particle Physics 2015*. Figure 1 shows the production rate, starting from a review of a few pre-series modules in March 2015 until completion in June 2016. Once all the components were available (silicon sensors, readout chips, controller chips and Kapton interconnects), an average rate of eight modules was sustained in all stages. The production stopped when all sensors were used up, yielding enough high-quality modules plus spares.

All modules were stress-tested and calibrated at the foreseen operating temperature of -20°C. In addition, they were tested at the expected LHC collision rate using hard X-ray illumination, leading to the rejection of a few modules where one readout chip developed problems in the data buffer section. In a final step, all modules were covered with a thin polyimide layer – glued to 55 miniature filtering capacitors – to protect the open wire bonds during transport, mounting and cabling.

The modules were transported by DESY to PSI in Switzerland, tested again (no losses) and mounted on a carbon fibre frame with integrated cooling pipes using six tiny screws for good thermal contact. The mechanical placement tolerance is about 0.2 mm (documented by digital photographs), which is sufficient to start the precision software alignment using cosmic rays and collision tracks once the detector is installed. The main mechanical requirement is stability at the micrometre scale on time scales of microseconds (vibrations) to hours (thermal drifts), which has to be fulfilled by the CO_2 cooling system.

Figure 2 shows a view of the inside of the fourth barrel layer with half of the mounted modules. The other half are mounted from the outside, thus covering the full azimuth. Three further half-shells are mounted inside this one, with modules produced in Germany, Italy and Switzerland. Two half barrels together with service cylinders carrying power cables, optical fibres and cooling pipes will then be transported to CERN in early 2017 and installed in CMS around the beryllium beam pipe. The detector is expected to be operated for at least seven years, until the high-luminosity upgrade of CMS and the LHC.

Contact:

Daniel Pitzl, daniel.pitzl@desy.de

References:

CMS Technical Design Report for the Pixel Detector Upgrade
https://cdsweb.cern.ch/record/1481838/files/CMS-TDR-011.pdf

Towards the HL-LHC detector upgrades.

Detector Assembly Facility and R&D for ATLAS and CMS upgrades

The ATLAS and CMS collaborations are preparing for the high-luminosity phase of the LHC (HL-LHC), which will start in 2026. Both collaborations will replace their current tracking detectors with more radiation-hard and more precise silicon tracking detectors. Together with German institutes in the ATLAS and CMS collaborations, DESY will deliver one end-cap detector each for the ATLAS inner tracker and the CMS outer tracker. The process will include module production, end-cap construction and integration at DESY. The necessary infrastructure is currently being prepared by building a dedicated Detector Assembly Facility (DAF) at DESY, and the DESY ATLAS and CMS groups are contributing substantially to the necessary R&D to get ready for production.

Detector Assembly Facility

The DESY ATLAS and CMS groups have committed to produce a substantial part of the silicon detector modules required for the two end-cap detectors, construct mechanical parts and carry out the full integration of the end-caps and the final system test. This process will need dedicated cleanroom space for the production of silicon sensor detector modules and larger areas to integrate the modules onto the big end-cap structures of about 2.5 m radius and 2 m length.

For this purpose, DESY is currently setting up the Detector Assembly facility (DAF) in two existing buildings. It will consist of a ~250 m^2 ISO-6 cleanroom for module production and a ~700 m^2 ISO-7 cleanroom for module assembly into bigger structures and integration into the full end-cap. The DESY ATLAS and CMS groups laid out a detailed plan for the necessary infrastructure and personnel, and a project proposal was submitted to the DESY Foundation Council. The project resources were granted, and the project was launched in June 2016 with the refurbishing of the first building. Cleanroom installation is expected to start as scheduled in February 2017. At about the same time, the second building will be available and refurbishment followed by cleanroom installation will begin. The first cleanroom will be ready in time for the prototype module production, which will start in the second half of 2017. The second cleanroom will be ready at the beginning of 2018 for module assembly and integration.

ATLAS detector upgrade activities at DESY

The DESY ATLAS detector upgrade activities focus on the design, prototyping and construction of one of the two inner tracker (ITk) strip end-caps. The mechanical and electrical support structures that make up the disks of the ITk strip end-caps are called petals. They are ultralow-mass, wedge-shaped structures with embedded cooling pipes, hosting silicon microstrip modules and associated readout and power electronics. There are six wheels per end-cap, each of them composed of 32 double-sided petals.

One major highlight of 2016 in the ATLAS instrumentation effort was the finalisation of the construction of the first thermomechanical petal prototype. Figure 1 (top) shows a picture of the prototype. Thermomechanical modules were built at the DESY site in Zeuthen, as planned for the production phase, with a first version of module-building mechanical precision tools. These modules consist of dummy silicon sensors, glass-patterned application-specific integrated circuits (ASICs) mimicking readout chips and commercial electronic power components. The mechanical core was designed with realistic materials and mechanical components, including 2.275 mm diameter titanium pipes and a custom multi-layered polyimide–copper bus tape with power and data traces.

Detailed characterisation evaluations were carried out: the surface of the petal was surveyed optically before the placement of the thermomechanical modules to check the surface flatness, and after the module placement to check the accuracy of the build and the glue thickness between modules and core structure. Results were found to be consistent with the current understanding of the future detector requirements.

Finally, detailed thermal characterisation is currently being performed on the thermomechanical petal by means of an

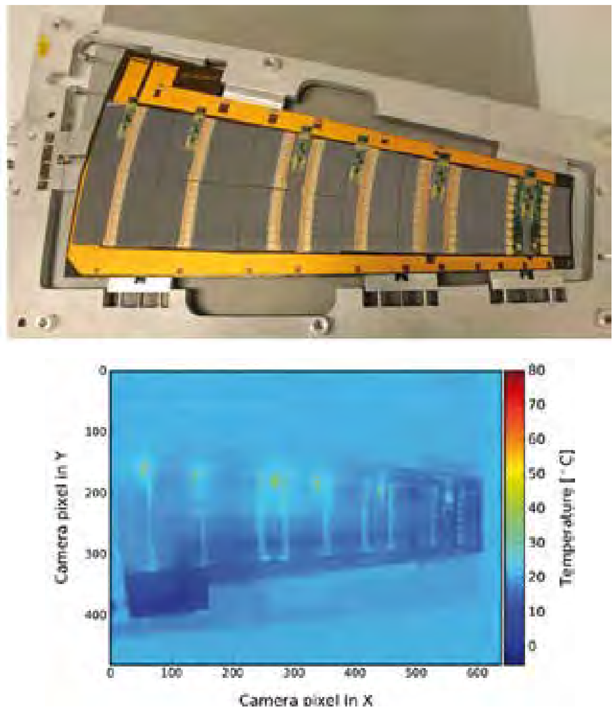

Figure 1

First thermomechanical petal prototype for ATLAS.
Top: Photograph of the prototype. Bottom: Infrared image with corrected emissivity values for the silicon surface.

Figure 2

Test of the image capture and pattern recognition. Left: Lab setup with camera mounted on motion stage. Right: Result of the image capture and pattern recognition.

infrared camera and a complex experimental setup developed in-house. The setup allows for emissivity corrections coming from differences in emissivity for the different surfaces of the petal. Figure 1 (bottom) shows an infrared image with corrected emissivity values for the silicon surface. Results agree qualitatively with the results obtained from thermal simulations. A future upgrade of the setup will permit the test under more realistic conditions and with CO_2 coolant.

These precision measurements will allow for detailed comparisons with simulations and help to build a high level of understanding of the future ATLAS ITk end-caps long before the detector is finalised.

Preparing for CMS module production at DESY

The CMS outer tracker for the HL-LHC will consist of detector modules that provide particle momentum information at the hit level, thereby crucially increasing the performance of the trigger. The momentum measurement is performed on the modules by correlating hit signals in two closely spaced silicon sensors. Precise relative alignment below 40 μm of the two sensors is a fundamental requirement for the momentum measurement. As corrections for sensor misalignment are not possible in the installed detector, this requirement must be satisfied at the module production stage.

The DESY CMS group has committed to build 1000 modules for the future CMS tracker and is currently investigating the possibility of an automated module assembly system providing precise sensor alignment with short production times and minimal manual intervention. The automation is provided by an integrated motion and vision system consisting of a precise motion stage and high-resolution cameras. A dedicated software application performs real-time pattern recognition on images to deduce the location of module components and controls the motion stage to achieve high-precision assembly.

Figure 2 shows a test of the system's image capture and pattern recognition. On the left, the lab setup is shown with a high-resolution camera mounted on the motion stage ready to acquire an image of the silicon sensor below. On the right, the results of the image capture and pattern recognition are shown, with a fiducial marker at the sensor's corner clearly visible. The white rectangle indicates the marker position deduced by the pattern recognition. The close match between this estimated position and the visible marker demonstrates the precision of the pattern recognition.

The motion and imaging procedures fundamental to the automated assembly system have thus been demonstrated. The next step is to produce an array of mechanical dummy modules in order to prove the viability of the system for fast and precise module production on a large scale.

Contact:
Ingo Bloch, ingo.bloch@desy.de
Sergio Diez Cornell, sergio.diez.cornell@desy.de
Günter Eckerlin, guenter.eckerlin@desy.de
James Keaveney, james.keaveney@desy.de
Andreas Mussgiller, andreas.mussgiller@desy.de

Asymptotic freedom by H1.

Precision predictions of strong interactions confronted with new measurements

In our universe, interactions between fundamental particles are mediated by the electroweak and strong forces. Using data recorded by the H1 experiment at DESY's former HERA electron–proton collider, the H1 collaboration performed a new analysis to study the dynamics of the strong interaction. The data were compared to recent significantly improved predictions of the theory of the strong force. Taken together, the experimental and theoretical advancements confirm the currently well-established theory and further deepen our understanding of strong interactions of elementary particles. The results may ultimately serve to improve the precision of measurements at the LHC.

At DESY's former HERA collider in Hamburg, electrons collided with protons at high energies. As both particles are electrically charged, the scattering process is mediated predominantly by the electromagnetic interaction. While the electron is a point-like fundamental particle, the proton is a compound particle consisting of quarks, antiquarks and gluons. The quarks and gluons interact through the strong force, which binds these particles together to form a proton. The electron does not interact through the strong force. Instead, in electron–proton collisions such as those recorded at HERA, the electron probes quarks inside the proton by means of the electroweak force. As a quark or antiquark is smashed out of the proton, the proton breaks up and the pieces interact through the strong force. This fortunate constellation of the two fundamental interactions, electroweak and strong, allows precise tests of the strong interaction, which is the focus of this article.

Until HERA was switched off in 2007, the H1 detector at HERA recorded a large number of electron–proton collisions, which were all stored. This data were analysed in great detail, for example regarding deep-inelastic scattering cross sections, proton structure, production of charm and bottom quarks, or searches for physics beyond the Standard Model. In the last years, members of the H1 collaboration transformed these data, as well as the required software needed to analyse them, into a format that allows a long-term use. This data preservation initiative turned out to be a key component of the analysis presented here, enabling the use of the original H1 software developed 30 years ago on modern computing infrastructure.

The H1 collaboration has now analysed the recorded electron–proton collision data with an emphasis on the most direct probes of the strong interaction [1]. This analysis significantly extends the reach of earlier studies, while also being of high precision. It was based on selected collision events featuring the scattered electron and two jets. A jet consists of many particles in close geometrical vicinity. A dedicated algorithm defines the jet's momentum and energy. Each jet corresponds to a single quark or a gluon. The two-jet requirement indicates the presence of a strong interaction between the two jets at a high energy scale. The quantitative results of these analysis efforts are probabilities of producing jets per electron–proton collision as a function of the jet's momentum and for different ranges of the quantity Q^2, which is the electroweak part of the reaction.

The well-established theory of quantum chromodynamics (QCD) provides a comprehensive description of interactions involving the strong force. Although the QCD equations have a very elegant and compact form, predictions are difficult to obtain because the mathematical calculations can be very complicated. First QCD predictions were made in the 1970s, but more precise calculations for jet production in electron–proton collisions could only be performed in the 1990s. These results for QCD jet observables were standard for many years until very recently.

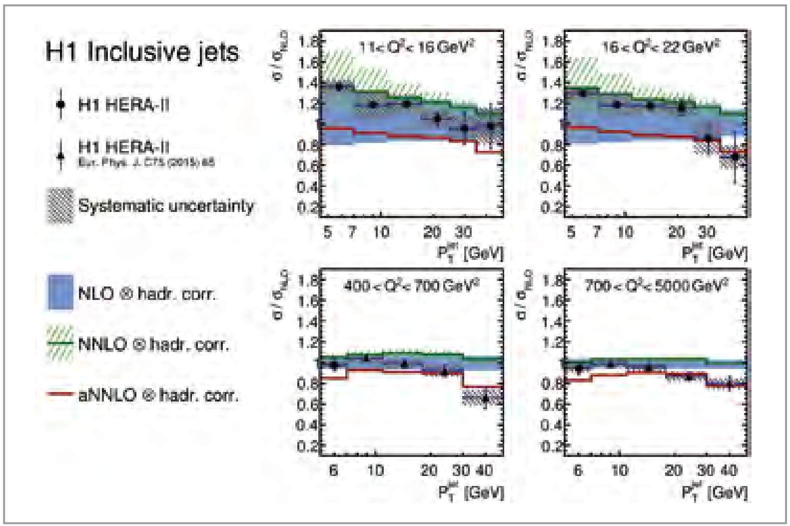

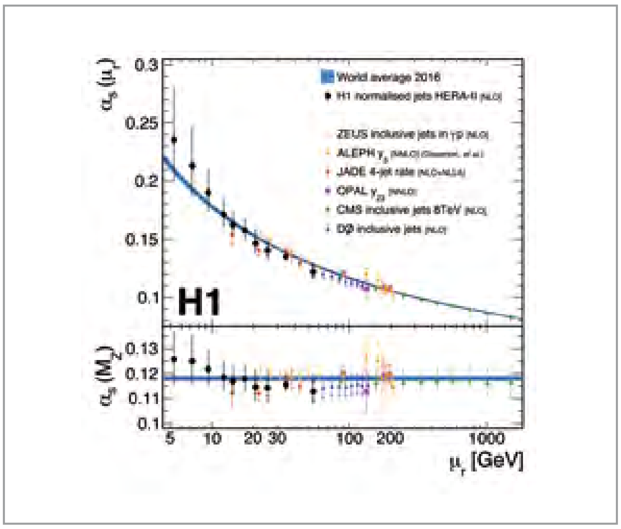

Figure 1

Jet production yields measured by H1 (dots) in comparison to various QCD predictions. The experimental uncertainties are indicated by vertical bars and are visible only at high values of the variable p_T^{jet}. The new NNLO predictions are displayed in green, with the green shaded areas illustrating the theoretical uncertainties, which are large at small p_T^{jet}.

Figure 2

Measurements of the strong coupling constant. The H1 measurements are displayed as black points and compared to results from other experiments. The vertical bars indicate the uncertainties, which are dominated by theoretical uncertainties for most of the H1 points.

Only in 2016 were theoretical physicists able to improve these calculations by including so-called next-to-next-to-leading order (NNLO) predictions [2]. This required the development of new mathematical tools and computer programs. Still, these NNLO calculations necessitate a million hours of computing time and are thus performed by running several thousand computers in parallel.

In Fig. 1, the new H1 jet production data are compared to the new NNLO predictions and to older predictions. The new NNLO calculations improve the description of the data, as compared to the previously available calculations (next-to-leading order, NLO). At the same time, the new predictions exhibit reduced theoretical uncertainties. In most regions, the H1 measurements are more precise than the NNLO predictions, while in other regions it is the other way round. Statistical tests confirm the overall good description of the H1 data by the NNLO predictions on a quantitative level.

The elegant and compact theoretical formulation of QCD is closely related to the fact that it requires only a single *a priori* unknown continuous parameter, the coupling constant α_s. Given this coupling, its energy dependence was predicted in 1973, expressed by a function $\alpha_s(\mu)$ of the energy μ. In QCD, the strength of the interaction decreases with increasing energy, in contrast to, for instance, the electromagnetic interaction. The discovery of this property, also named asymptotic freedom, was finally awarded the Nobel Prize in physics in 2004. This energy dependence was tested using the H1 jet data and the values were compared to other jet-based measurements. As Fig. 2 shows, the predicted energy dependence of α_s, marked by a blue band, is well reproduced by the data.

The H1 jet data may be used to determine the strong coupling constant $\alpha_s(M_Z)$ with high experimental precision. Unfortunately, at present, the determination is still limited in precision because the new NNLO calculations [3] cannot yet be used for this purpose. The challenge for 2017 will be to develop computer programs enabling the use of the NNLO calculations for such studies in order to fully exploit the potential of the precise H1 jet measurements. Beyond the studies of the strong interaction and QCD, this work will then also improve the understanding of the structure of the proton, which is of crucial importance for measurements at the LHC, where protons collide with protons.

Contact:

Daniel Britzger, daniel.britzger@desy
Stefan Schmitt, stefan.schmitt@desy.de

References:

[1] H1 Collaboration, arXiv:1611.03421, accepted by Eur. Phys. J. C.
[2] J. Currie, Th. Gehrmann, J. Niehues, Phys. Rev. Lett. 117 (2016) 042001.
[3] T. Biekötter, M. Klasen and G. Kramer, Phys. Rev. D92 (2015) 7, 074037.

Physics with electrons and positrons.

Physics with lepton beams – and the R&D work for the necessary accelerators and detectors – constitutes the second pillar of DESY's particle physics activities. The focus is on future linear colliders, particularly the International Linear Collider (ILC), and on the upgraded SuperKEKB accelerator with the Belle II experiment at the Japanese national particle physics laboratory KEK. The OLYMPUS experiment at DESY is rounding off the programme (p. 54).

The data collected by the former Belle experiment at the SuperKEKB electron–positron collider are still being scrutinised for physics beyond the Standard Model (p. 42). At the same time, these studies serve to prepare for the analyses to come at the Belle II experiment, commissioning of which started in 2016 (p. 44).

Regarding a future electron–positron linear collider, the two main activities at DESY are target tests to produce viable positron beams (p. 46) as well as calorimeter development (p. 50). These hardware studies are supported by projections for Higgs self-coupling measurements (p. 48), which further foster the science case for such a collider.

Besides furthering "conventional" accelerators such as the ILC, DESY is also pursuing other roads to high energies and new discoveries: Plasma wave acceleration is a promising candidate for achieving highest energies with compact devices, and DESY is crucially involved in understanding the plasma generation mechanism (p. 52).

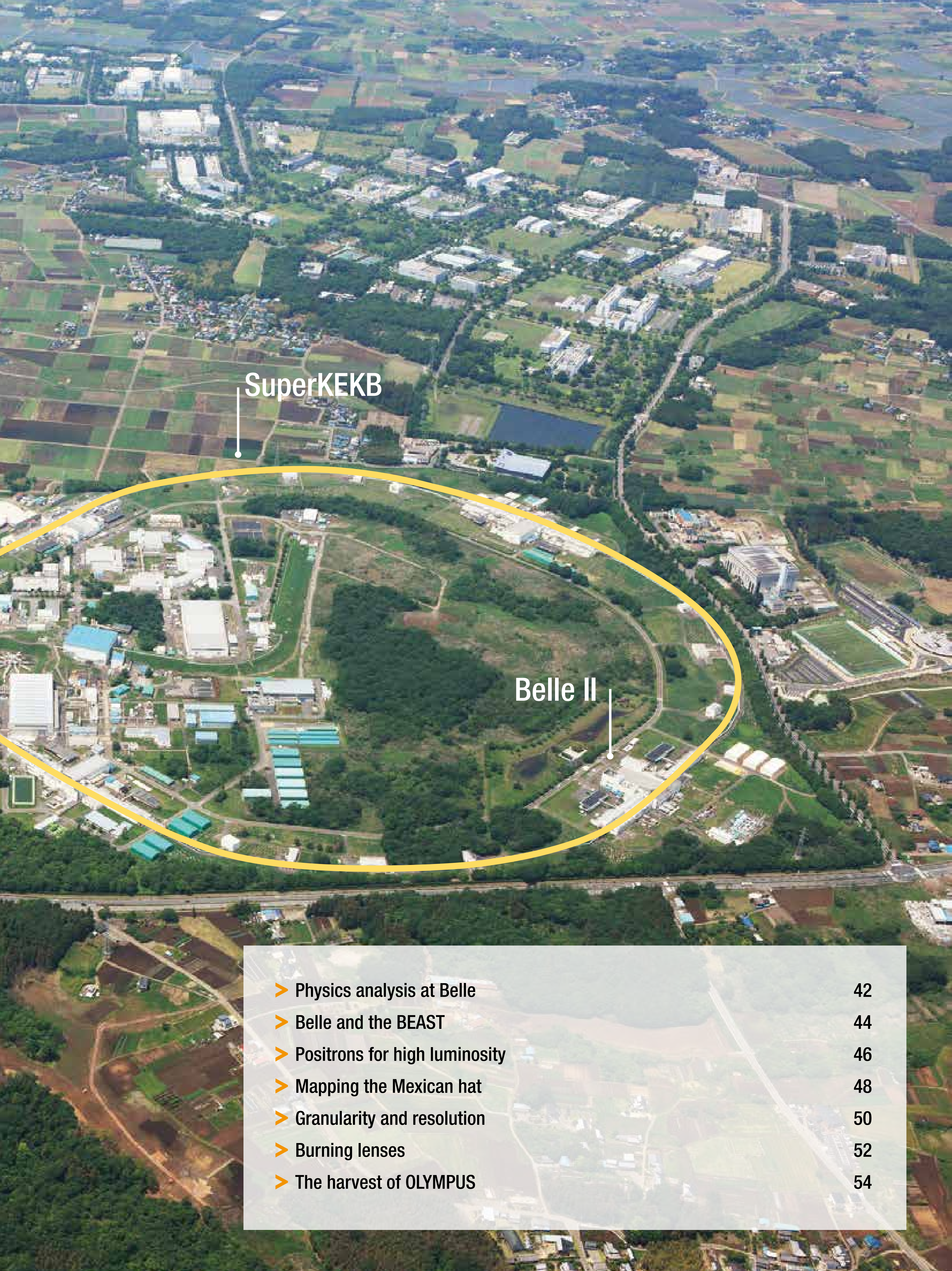
SuperKEKB
Belle II

Physics analysis at Belle.

Cornering new physics from different angles

Recent results in the flavour sector of the Standard Model (SM) exhibit a variety of tensions with the SM predictions. Although none of these measurements alone has yet sufficient significance to claim observation of a deviation from the SM and there is currently no single specific new physics scenario in which all of them could be explained simultaneously, global fits performed by different groups indicate that new physics might be within reach. At DESY, the search focuses on particle candidates that could account for the postulated dark matter in the universe, such as dark photons, and on looking for the effect of heavy new particles appearing in strongly suppressed flavour-changing neutral-current decays of *B* mesons. In light of these results, we might have seen first glimpses of physics beyond the SM in the data collected by the former Belle experiment in Japan.

Analysing rare decays of *B* mesons

While the Belle II experiment, which is currently under construction at the SuperKEKB electron–positron collider in Japan, is expected to lead to a much-awaited step forward in accelerator-driven elementary particle physics, the precious data of its predecessor, the Belle experiment, are still being analysed. Although the Belle data taking ended in 2010, the search for new particles and physics beyond the SM in the Belle data continues.

Several deviations from the SM prediction were recently observed in rare decays of *B* mesons at experiments at the *B*-factories (Belle and Babar) and at the LHC (LHCb). Rare decays are particularly suited for searches for new physics because of their enhanced sensitivity to effects from heavy new particles appearing virtually in quantum loops that mediate the decays. The size of the unique Belle data set, which contains the decays of more than 770 million *B*-meson pairs, is ideal for detailed studies of such rare processes.

In 2013, the LHCb collaboration reported for the first time an anomaly in the angular distribution of the rare $B^0 \to K^*\mu\mu$ decay. The observed deviation from the SM prediction exceeded three standard deviations. With three times more data, the LHCb collaboration updated the result in 2015 and confirmed this discrepancy with comparable significance. Triggered by the 2013 result, the DESY Belle group performed a comprehensive analysis of this and related rare decays that are based on the underlying quark transition $b \to sll$. In contrast to the LHCb measurement, the Belle search was extended to $B \to K^*ll$, where decays of neutral and of charged *B* mesons are studied and either electron or muon pairs can appear in the final state.

Figure 1 (left) shows the angular-dependent variable P'_5 as a function of the invariant mass of the lepton pair (q^2) for the Belle measurement compared with the results previously obtained by LHCb. The largest discrepancy to the SM prediction, marked by blue boxes (DHMV), is found in the q^2 range of 4 to 8 GeV^2/c^4 and is present in both the LHCb and the Belle data. The agreement between the two experimental results is remarkable and reduces the probability that the deviation is just a statistical fluctuation. The local significance of the difference between the Belle data and the SM prediction amounts to 2.5 standard deviations. However, there is an ongoing discussion in the literature whether systematic errors

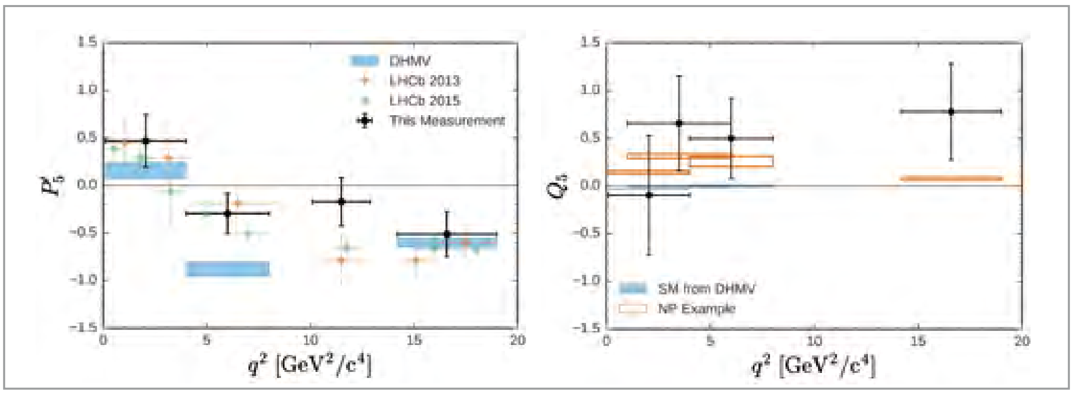

Figure 1

Left: Result of the angular analysis of the process $B \to K^*ll$ using Belle data compared with results of the LHCb experiment and the prediction from the SM. The largest discrepancy to the SM is found in the q^2 range of 4 to 8 GeV^2/c^4. Right: Testing lepton flavour universality by comparing muon with electron mode. The SM predicts values close to zero.

of the theoretical calculations are in fact larger than estimated. Quantities that are free from theoretical uncertainties, such as observables that test the validity of lepton flavour universality, are therefore particularly interesting. SM interactions do not distinguish between different lepton flavours (e, μ or τ). Hence, processes that only differ in the type of leptons should agree except for effects that are expected from their different masses. Any additional deviation is a clear signal of new physics.

One such observable is the ratio R_K between the branching fraction of $B^+ \to K^+\mu^+\mu^-$ and the one of $B^+ \to K^+e^+e^-$, where LHCb also found a 2.6 sigma deviation from the SM expectation. Such a deviation would, for example, be expected if new physics would couple differently to muons than to electrons. Exploiting the clean environment of the rather low-energetic electron–positron collisions at Belle in comparison to the high-energy collisions at LHCb allowed the DESY group to perform the complex angular analysis for the first time separately for electron and muon pairs. Both results show tensions in the angular distribution, but the strongest deviation from the SM is observed in the muon mode in the bin of 4 to 8 GeV^2/c^4 with a local significance of 2.6 sigma.

Figure 1 (right) shows the q^2 dependence of Q_5, which is the difference between P'_5 obtained for muons and for electrons, compared with the SM prediction (DHMV). Also shown is a prediction of a new physics scenario that is based on a global fit to a multitude of measurements in the flavour sector. Several groups in the world are performing such kinds of fits, commonly preferring a new physics contribution specifically for processes involving muons. Within the statistical uncertainty, the Belle data are still compatible with the SM, but the good agreement with the new physics model is intriguing.

The interpretation of these findings remains ambiguous since there is no single specific theoretical model available that simultaneously copes with all the observed discrepancies in the flavour sector. Future experiments will be able to sort out these tensions with more statistics and help to either verify or falsify new physics models. Major progress is expected here in particular with the start of the Belle II experiment, which aims at an increase in integrated luminosity by a factor of 50.

Probing the dark side of particle physics

While dark matter represents a very big fraction in terms of the mass/energy content of the universe (26%) when compared to ordinary matter (5%), the only information we have about it so far comes from the observation of gravitational effects. In fact, the whole concept of dark matter is based on the idea that it does interact gravitationally with ordinary matter while its other interactions are assumed to be extremely weak. Understanding the nature of dark matter is one of the biggest challenges that need to be addressed in the next years.

Supersymmetric models provide a good candidate for dark matter. However, the lack of any experimental evidence for its

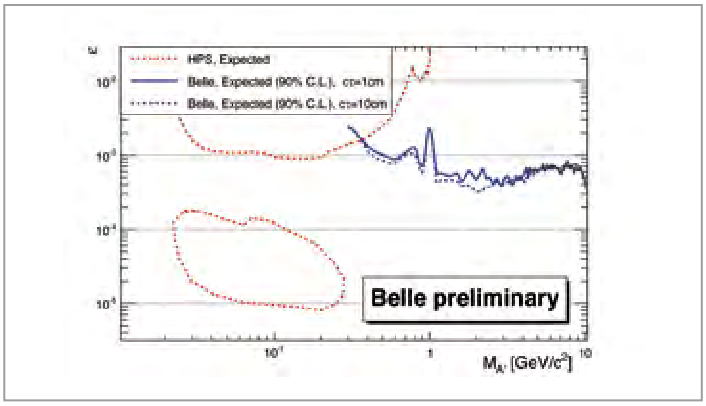

Figure 2

Preliminary projected sensitivity range for the dark-photon (A') search via $e^+e^- \to \gamma A'$ ($\to e^+e^-$, $\mu^+\mu^-$) for different assumptions on its lifetime, in the plane of mixing parameter (ε) versus A' mass. The expected limits for the dedicated Heavy Photon Search (HPS) experiment at Jefferson Lab in the USA are shown for comparison.

realisation in nature up to date suggests that dark matter might be more complicated, comprising a dark sector with a whole zoo of particles (short- or long-lived) that could decay to SM particles and have a wide range of possible masses. The dark photon A' is such a hypothetical constituent, featuring in a number of recently proposed dark-sector models. Through a process known as kinematic mixing, it would act as a mediator between SM and dark-sector particles.

Belle data are being analysed to search for dark-photon production and subsequent decay in radiative processes, in particular in the reaction $e^+e^- \to \gamma A'$ ($\to e^+e$, $\mu^+\mu^-$). At DESY, the search is performed for the specific case in which A' is long-lived, leading to a final state composed of the radiative photon plus two oppositely charged particles (either e^+e^- or $\mu^+\mu^-$) originating from a displaced vertex pointing back to the interaction point. Figure 2 shows the preliminary expected sensitivity range for the search in the plane of mixing parameter (ε) versus A' mass, based on the analysis of a small subsample of the full Belle data corresponding to 30 fb^{-1} and projected to full luminosity.

Preparing for Belle II analyses

With the experience gained with the Belle analyses, the DESY group is in an ideal position to immediately start Belle II analyses once data taking will commence in 2018. In the meantime, the complete Belle data set is used at DESY to fine-tune simulation programs of physical processes involving the fragmentation of quarks, which requires a tremendous computational effort. The goal is to improve the understanding of background processes, from which most future Belle II analyses will benefit.

Contact:

Simon Wehle, simon.wehle@desy.de
Gianluca Inguglia, gianluca.inguglia@desy.de
Carsten Niebuhr, carsten.niebuhr@desy.de

Belle and the BEAST.

SuperKEKB and Belle II commissioning has begun

The first phase of commissioning of the second-generation *B*-factory SuperKEKB, an electron–positron collider at the KEK particle physics laboratory in Japan, was successfully completed in early 2016. In parallel, major detector components, such as the time-of-propagation counter and the central drift chamber, were installed in the Belle II experiment. At DESY, the system integration of a dedicated background monitoring system for Phase 2 of the commissioning has started and will continue until the installation of the system at KEK in 2017. Other important contributions from DESY are the precision measurement of the magnetic field of the Belle II solenoid in the tracking volume and the migration of collaborative tools and services to DESY.

Status of the SuperKEKB and Belle II project

In 2016, several major milestones were achieved with the successful completion of Phase 1 of the SuperKEKB machine commissioning and the installation of the time-of-propagation counter (TOP) and the central drift chamber (CDC) in the upgraded Belle II detector. Figure 1 (left) shows in the front the location of the interaction point (IP), where the 7 GeV electron beam will be brought into collision with the 4 GeV positron beam for the first time in 2018. The ultimate goal is to produce the by far highest peak luminosity (8×10^{35} cm^{-2}s^{-1}) ever reached in a particle collider. In its parking position inside the ring, the Belle II detector is awaiting the installation of the upgraded subdetectors.

The two main goals of Phase 1 were (i) the operation of the main ring and conditioning of the new vacuum system (beam scrubbing) and (ii) the monitoring of the different types of beam background. Figure 1 (right) shows that, during the five months of beam operation, the goals in terms of beam currents and integrated doses were clearly met. Detailed studies of the accompanying background were possible thanks to the installation of several dedicated monitoring devices (dubbed BEAST, for Beam Exorcism for A Stable ExperimenT) around the IP, partially covering the regions that will later be occupied by the final-focus magnets QCSL and QCSR. While the first of these two very complex systems (QCSL) was successfully installed after Phase 1 in August, the second unit (QCSR) will only become available in February 2017.

Entering Phase 2 with BEAST II

With the completion of the final-focus system and after rolling Belle II into beam position in spring 2017, the second phase of the machine commissioning will begin. Besides establishing luminosity production for the first time in the so-called nano-beam scheme, it will be very important to precisely

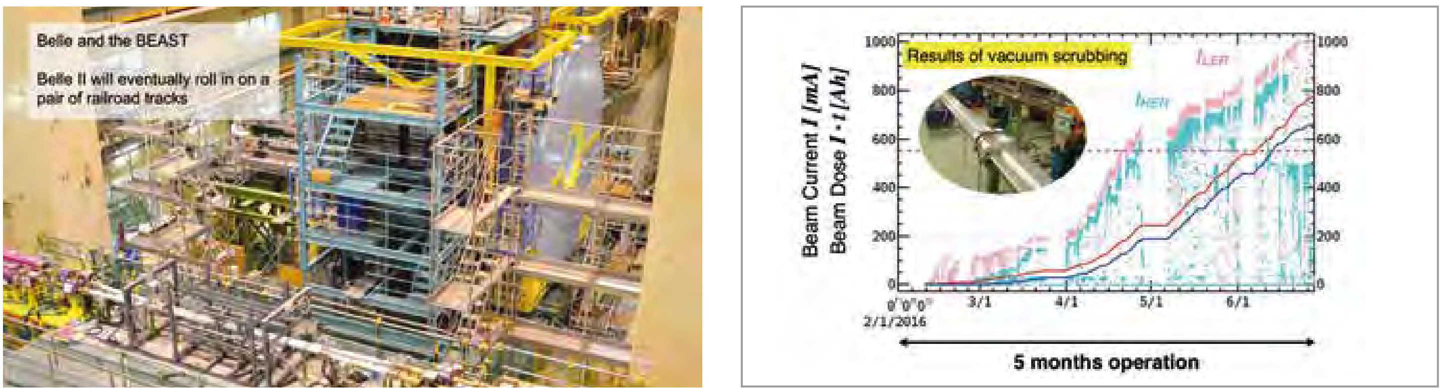

Figure 1

Left: View of the SuperKEKB interaction region and the Belle II detector in its parking position. Dedicated detectors arranged around the interaction point were used for background monitoring during Phase 1 of the machine commissioning in early 2016. Right: Results of beam conditioning of the new SuperKEKB vacuum system. The aims of the machine group in terms of maximum stored beam current and integrated beam dose were reached.

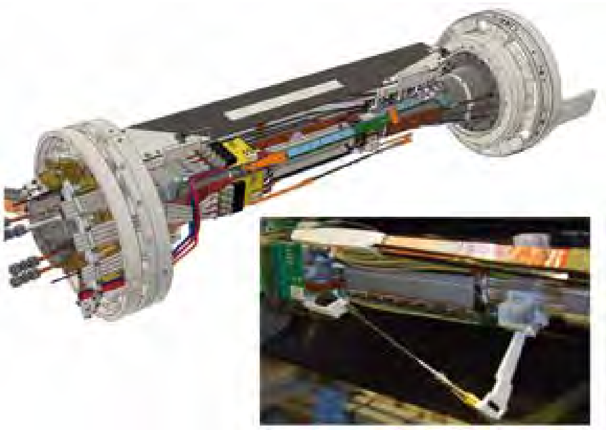

Figure 2

CAD drawing and picture taken during system integration tests at the PERSY setup in the detector laboratory in HERA Hall West. After further tests in the DESY test beam, the final BEAST II system will be used to monitor beam backgrounds during Phase 2 of the SuperKEKB commissioning.

Figure 3

Magnetic-field robot in the TOP detector of Belle II. With this device from CERN, it was possible to measure the entire tracking volume with high precision in the very short time window available.

characterise all background sources with colliding beams. The success of the entire project builds on an increase of the instantaneous luminosity by a factor of 40 during the first few years of operation. Therefore, determining how the various background sources scale with beam intensity and luminosity will be extremely important. Only once this is sufficiently well understood will the very sensitive vertex detector (VXD) be installed in Belle II.

To this end, the collaboration is preparing the so-called BEAST II detector, which will occupy the space of the VXD. It will consist of prototypes of the pixel detector (PXD) and the strip detector (SVD), which were operated together in the DESY test beam in April 2016, as well as a number of complementary detector systems that are sensitive to the different background components. To facilitate the commissioning of these devices, the PErmanently Running System (PERSY) was set up in the DESY detector laboratory in HERA Hall West. Figure 2 shows a CAD drawing of the complete setup and a picture of some of the components of BEAST II during their assembly at PERSY. The BEAST II setup will be extensively tested in the DESY test beam in February 2017 to ensure that a functioning and fully commissioned system is sent to KEK for installation in Belle II in summer 2017.

Prerequisites for precision physics

To reach ultimate precision for physics analyses, an accurate knowledge of the magnetic field distribution inside the tracking volume of Belle II is mandatory. DESY is in charge of providing a precise field map that will serve as input for the reconstruction software. The final magnetic field in the tracking volume results from the superposition of the field of the Belle II solenoid and the stray fields of the QCS magnets, which are about two orders of magnitude stronger than in Belle. Thanks to a very fruitful collaboration with CERN, a precision field map was made in summer 2016. Figure 3 shows the modified CERN field mapper inside the TOP detector before the installation of the CDC.

To determine the influence of the QCS magnets, a second measurement campaign in the final configuration is scheduled for spring 2017. Since the CDC was installed in the meantime, a new dedicated magnetic-field robot is required to allow remote mapping of the very limited space between the CDC and the QCS magnets. The final field map will be determined using the combined information from the two measurement campaigns.

Computing

Collaborative services and tools are essential for any (high-energy physics) experiment that involves a large number of international partners. These tools help to integrate global virtual communities by allowing all members to share and exchange relevant information by way of web-based services. Examples are public and internal web pages, wikis, mailing list services, issue tracking systems, services for meeting organisation and document and authorship management as well as build services and code repositories.

To guarantee stable and reliable services for the future, after considering various other options the Belle II collaboration decided to migrate the current set of services into the existing IT infrastructure at DESY. As a consequence, all Belle II users need a DESY computing account to access the new services.

A particular challenge was the timely completion of the migration process before the KEK computer system shutdown in summer 2016. Thanks to the dedicated efforts of the DESY IT department, this ambitious goal was achieved. The next steps are the final migration of the agenda service (indico) and the development of a membership management service.

Contact:
Carsten Niebuhr, carsten.niebuhr@desy.de

Positrons for high luminosity.

Extreme conditions in a target

Future high-luminosity electron–positron colliders require very powerful particle sources. The production of positrons – ideally polarised positrons – in large numbers is especially challenging, in particular regarding the behaviour of the target needed to produce the positrons, as the target material is subject to extreme thermal loads. At the end of 2016, the DESY linear collider groups performed experiments at the MAMI facility in Mainz, Germany, that were able to simulate, for the first time, the expected behaviour of the target as proposed for the International Linear Collider (ILC), thus contributing important information towards the design of the system.

Testing material fitness for high cyclic load

High luminosity is the common characteristic of all future electron–positron colliders – at high energies as well as low energies. The most developed proposal, the ILC, is designed to operate at energies between 250 GeV and 500 GeV, upgradable to 1 TeV. A critical component in the design is the positron source, in particular the target from which the positrons are generated. At the ILC, the electron beam passes at high energies through a helical undulator, producing a polarised photon beam, which then hits a thin titanium alloy target to generate a polarised positron beam. This scheme has the additional benefit that the provision of polarised positrons enhances the physics potential of the ILC.

Technically, however, this system is very challenging. The photon beam is highly focused, creating an extreme particle density in the positron target. A great challenge is therefore to devise a technical target design that can handle these energy densities in the target and avoid premature aging of the target material. Similar problems arise for the photon dump, which has to absorb the focused photon beam with about 10^{16} photons per second. Such a photon density requires special care to allow a reasonable lifetime and smooth long-term operation of the exit windows to the dump. The ILC collaboration initiated sophisticated design simulations to develop the design for the positron target and the exit windows. In addition, the realistic long-term behaviour of the

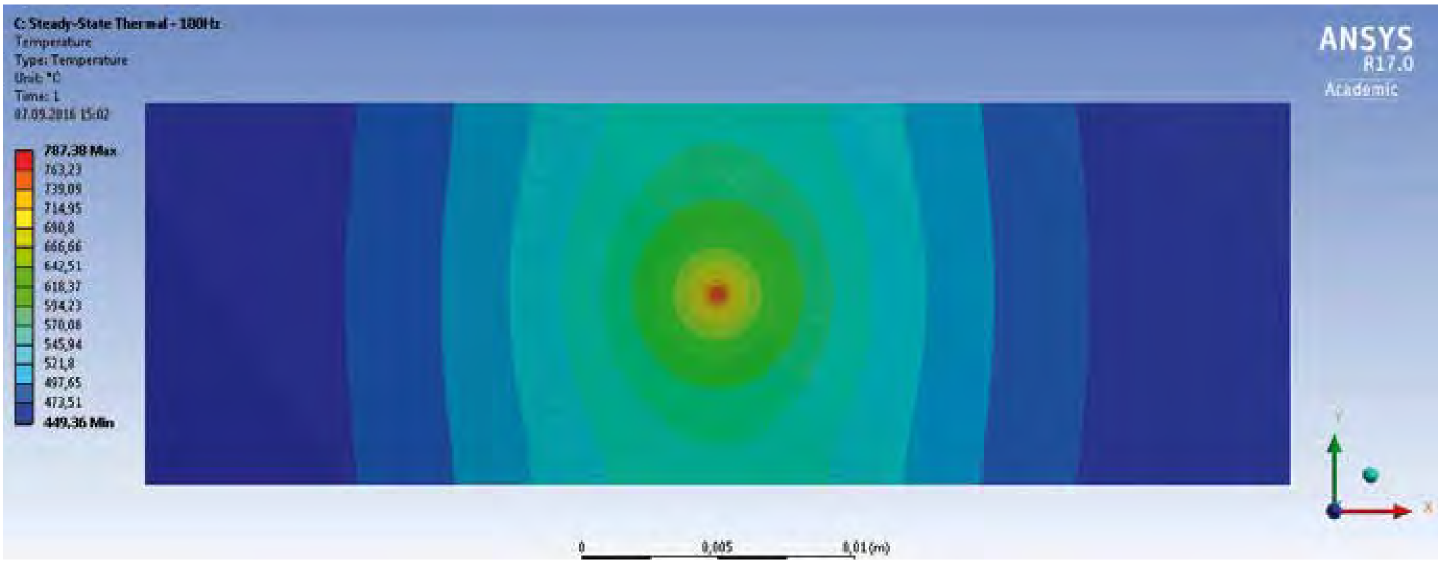

Figure 1

Simulation of the temperature distribution during irradiation; the cyclic load stress is about 250 MPa.

material under high thermomechanical load cycles needs to be tested to demonstrate the feasibility of the design.

The DESY linear collider groups have started such tests at the MAMI Microtron in Mainz, Germany, in collaboration with the universities of Hamburg and Mainz. The MAMI electron beam is used to simulate the load of the ILC photon beam on the positron target and the exit window. By choosing a special time structure of the MAMI beam, it is possible to simulate in one day load cycles in the target material comparable to that expected in the ILC target in one to two years of operation. In this way, the fatigue behaviour of the potential target material can be tested very efficiently.

The first test runs demonstrated an impressive long-term stability of the material. So far, none of the tested targets – thicker samples to represent the cyclic load in the positron target as well as thin samples typical for exit windows – showed serious damage or breakage. The thermomechanical cyclic load was high, and the target samples were heated by the MAMI beam to almost 800°C (Fig. 1). Even when the target was heated to temperatures slightly above the phase transition value of the material, only slight plastic deformations but no serious damage were observed (Fig. 2).

The analysis of the irradiated samples is ongoing in order to measure a potential change of the material parameters after irradiation. For example, the surface emissivity is important as it is foreseen to cool the positron target by thermal radiation. In a next step, the tests will be extended to higher energies in order to test the material degradation under high radiation exposure.

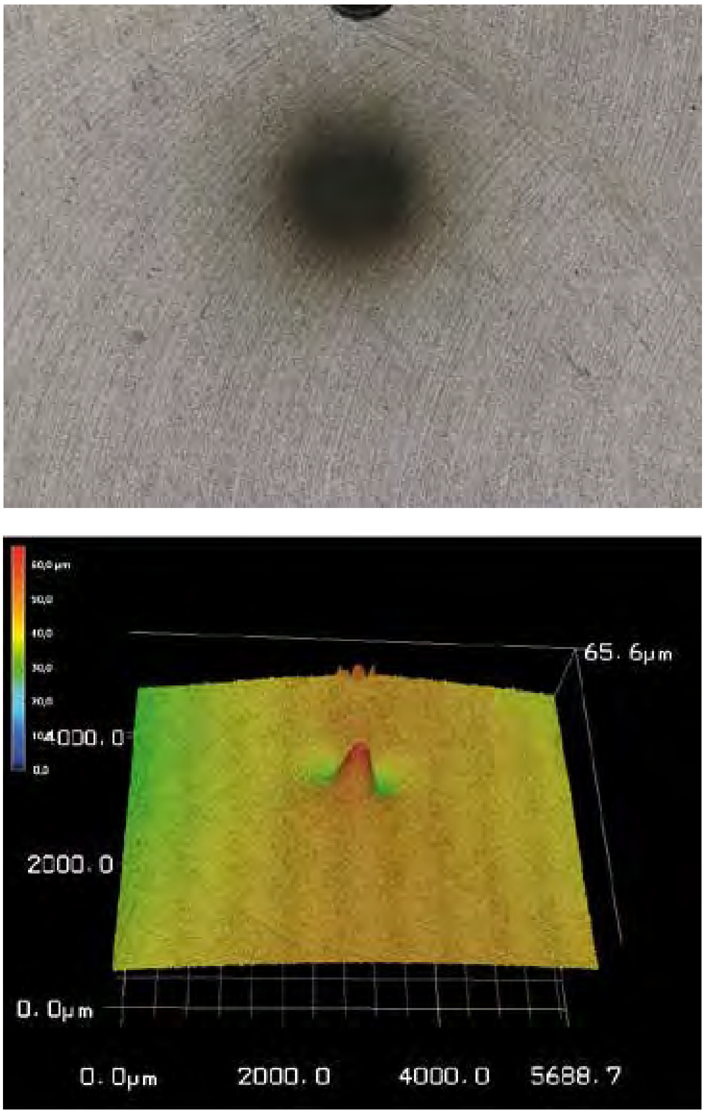

Figure 2

Top: Photograph of the front side of the titanium alloy target after irradiation at MAMI corresponding to about two ILC years. Bottom: The high average temperature causes plastic deformations at the surface of about 25 µm.

Contact:

Sabine Riemann, sabine.riemann@desy.de

Gudrid Moortgat-Pick, gudrid.moortgat-pick@desy.de

Andriy Ushakov, andriy.ushakov@desy.de

References:

[1] ILC Technical Design Report, ed. by T. Behnke et al. (2013).

[2] G. A. Moortgat-Pick et al., Phys. Rept. 460 (2008) 131.

Mapping the Mexican hat.

Establishing the self-interaction of the Higgs boson at the ILC

Since the discovery of a Higgs boson at the LHC in 2012, we already learned a lot about the properties of this new particle. So far, all measurements allow the discovered particle to be consistent with the Higgs boson predicted by the Standard Model (SM) of particle physics. However, its most important property, namely its self-interaction, which is a crucial prerequisite for giving mass to all other particles through electroweak symmetry breaking, has not yet been verified, and it is considered today very unlikely that the LHC experiments will be able to do so. At future colliders, the observation of this self-interaction is very challenging as well, and reliable projections are missing. A new study based on a full detector simulation, carried out mainly at DESY, now showed the feasibility of this measurement at the International Linear Collider (ILC) with a centre-of-mass energy of 500 GeV, including for the first time all relevant backgrounds.

Higgs self-coupling and the early universe

In the SM, all elementary particles gain their masses from the interaction with an omnipresent background field, the Higgs field. This omnipresence requires that the potential associated with the Higgs field has its minimum at a non-zero value of the field, as is for instance realised in the famous "Mexican hat" shape. In the early universe, while expanding and cooling down, the potential underwent a phase transition from the symmetric state (with the minimum of the potential at zero field strength) to its current shape. This process is known as electroweak symmetry breaking. The present shape of the Higgs potential and its evolution in the early universe are determined by the self-coupling λ of the Higgs boson. Thus, the Higgs mechanism will only be fully established once λ has been measured and shown to be non-zero.

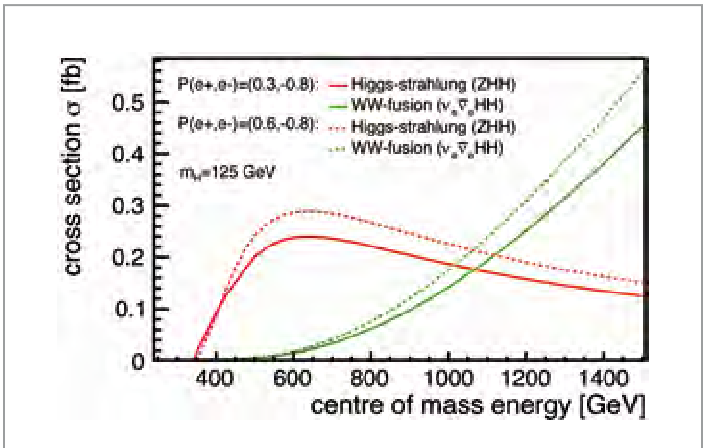

Figure 1

SM cross section for double Higgs production in polarised electron–positron collisions as a function of the centre-of-mass energy [1]. The full lines correspond to the ILC baseline design, which provides a positron polarisation of 30%. The dashed lines correspond to an upgrade to 60% positron polarisation.

Interestingly enough, there is significant motivation for sizable deviations from the SM value of λ in various extensions of the SM. This can still hold true even if all other couplings of the Higgs to SM fermions and gauge bosons are very close to their SM prediction. In particular, a value of λ at least 20% larger than in the SM would be needed for the electroweak phase transition to be of first order, as required for baryogenesis [3].

Double Higgs production

The experimental key to determining the value of λ is the measurement of the cross section for double Higgs production. Depending on the type of collider and its centre-of-mass energy, different production modes dominate. Moreover, processes not containing λ do also contribute to the cross section. Due to the resulting interference, which can even be destructive, the cross section is not proportional to λ^2, but can even shrink with growing λ.

The cross sections for double Higgs production in electron–positron collisions are shown in Fig. 1 as a function of the centre-of-mass energy. For energies around 500 GeV, double Higgsstrahlung $e^+e^- \rightarrow ZHH$ is the only accessible production mechanism, while around 1 TeV, the *WW* fusion mode $e^+e^- \rightarrow \nu_e\nu_e HH$ becomes dominating. The two production processes have very different sensitivities to deviations from the SM, as illustrated by Fig. 2, which shows the *ZHH* cross section at 500 GeV and the $\nu_e\nu_e HH$ cross section at 1 TeV as a function of the actual value of the Higgs self-coupling. While the *ZHH* cross section rises for larger values of λ, the destructive interference mentioned above causes the $\nu_e\nu_e HH$ cross section to go through a broad minimum around $\lambda = 1.5\ \lambda_{SM}$, which makes a precise measurement and an extraction of λ even more difficult in this region.

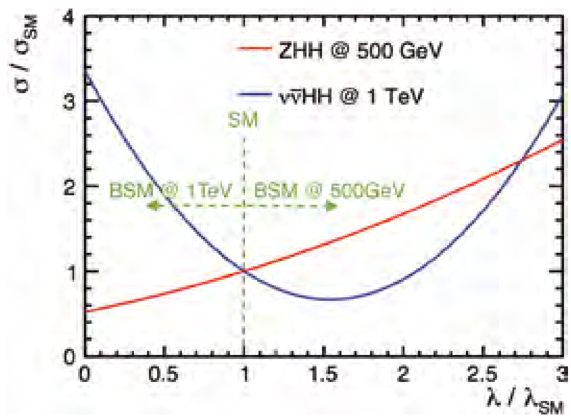

Figure 2

Double Higgs production cross section as a function of the value of the Higgs self-coupling, both in units of their predicted SM values, for Higgsstrahlung at 500 GeV and for *WW* fusion at 1 TeV [1]

New ILC study

Within the International Large Detector (ILD) concept group [4], a new study in full, Geant4-based detector simulation was recently performed [1]. This study introduced several new techniques into the analysis, and – for the first time – also studied the impact of the unavoidable pile-up from low-p_t hadron production in photon–photon collisions. The lion's share of this study, covering the case of both Higgs bosons decaying into *b* jets and considering five different decays modes for the *Z* boson (either to *b* jets as well, or to other quarks, to muons, to electrons, or to neutrinos), was conducted at DESY in the course of a PhD thesis completed in 2016 [1]. The final results were combined with an analysis of $HH \rightarrow bbWW$, covering only the case $Z \rightarrow \nu\nu$.

This detector analysis allows two important conclusions:

1) The low-p_t hadron pile-up does not challenge the feasibility of the Higgs self-coupling measurement at the ILC in any fundamental way, and earlier results, obtained without considering this background, keep their basic validity.
2) The low-p_t hadron pile-up does cause a noticeable degradation, motivating the development of a more sophisticated strategy to remove reconstructed particles from this source, which is currently underway. For these two reasons and for consistency with other studies, projections for the Higgs coupling measurements without the low-p_t hadron background are quoted in the following.

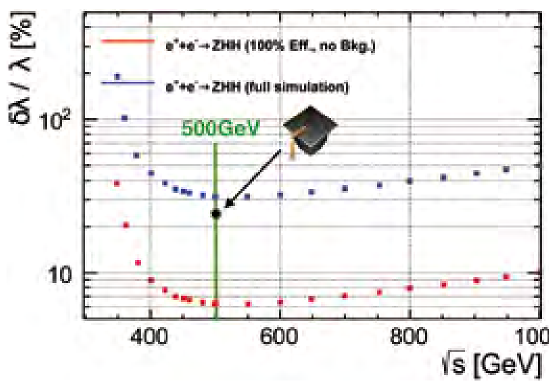

Figure 3

Expected precision on λ when extracted from the measurement of the *ZHH* production cross section at the ILC as a function of the centre-of-mass energy for $\lambda = \lambda_{SM}$. The blue squares indicate the precision of a previous analysis, the red squares illustrate the "theoretical limit" of 100% efficiency and no background.

Results

When considering the full 20-year running programme of the ILC [2] and combining all channels that have been studied in full detector simulation so far, the cross section for double Higgs production at 500 GeV can be expected to be measured with a precision of 17%. This corresponds to an 8 σ discovery of this yet unobserved process. From this measurement, the Higgs self-coupling λ could be extracted with a precision of 27%, as illustrated in Fig. 3.

These numbers are valid if λ attains its SM value. For a larger value of λ, the precision would improve, e.g. for $\lambda = 2\ \lambda_{SM}$, the precision on the cross section would be 12%, while λ could be extracted with a precision of 13%. It should also be noted that the centre-of-mass energy of 500 GeV is an optimal choice for these measurements.

Contact:

Jenny List, jenny.list@desy.de
Ties Behnke, ties.behnke@desy.de

References:

[1] C. Dürig, DESY-THESIS-2016-027.
[2] T. Barklow et al, ILC Operating Scenarios, DESY-15-102.
[3] K.Fujii et al, DESY-15-094.
[4] The International Linear Collider Technical Design Report, DESY-13-062.

Granularity and resolution.

Highest granularity meets best energy resolution for calorimeters

For a long time, DESY has been developing highly granular calorimeters for future linear collider experiments. Such calorimeters are now also being considered for the upgrades of the LHC detectors. Their small cell sizes not only provide detailed spatial information about the energy deposition of particles, but also help to improve the energy information itself, using optimised weighting procedures.

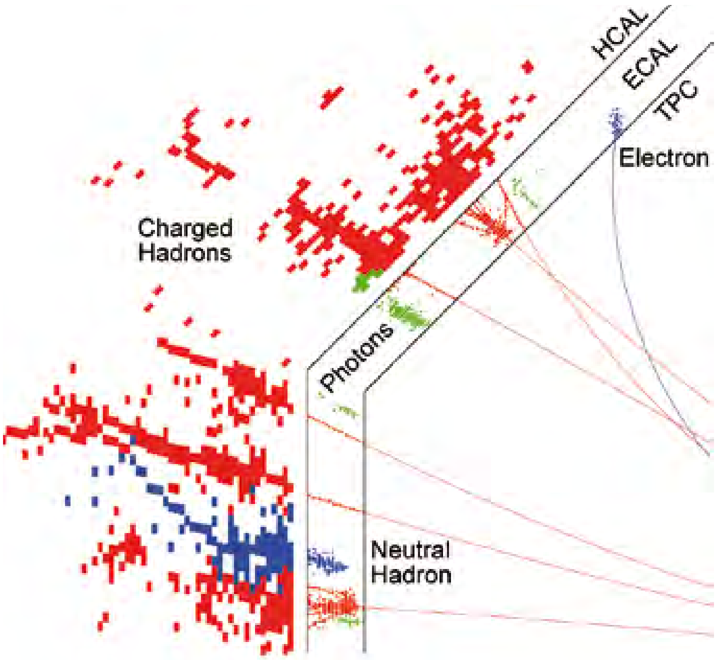

Figure 1

Event display (detail, view along the beam axis) of a simulated multijet event produced in electron–positron annihilation with a centre-of-mass energy of 500 GeV. Shown are charged particle tracks in the time projection chamber (TPC) and energy depositions in the electromagnetic (ECAL) and hadronic calorimeter (HCAL).

Jets are abundant signatures in the final states of high-energy colliding-beam experiments. The bundles of neutral and charged particles carry kinematic information about quarks produced in the primary interaction, for example in the decays of heavy bosons such as *W*, *Z* or Higgs bosons, so their energy needs to be measured precisely. This is most difficult to achieve for neutral hadrons, such as neutrons, while photons and charged particles can be measured comparatively well in electromagnetic calorimeters and tracking devices, respectively.

If the detector is segmented finely enough, the signals produced by the individual particles in the jets can be disentangled, and then for each particle the suitable detector component with the best available performance can be used. In this way, the poor resolution for neutral hadrons affects only about 10% of the measurements. This method, called “particle flow approach”, has driven the development of very finely segmented calorimeters, which only became possible thanks to advances in microelectronics integration and to the advent of novel detector techniques, such as silicon photomultipliers (SiPMs). In more conventional, more coarsely segmented detectors, this method works only in places where particles are separated far enough from each other. In the core of dense jets, in contrast, one can only sum up calorimeter energies, causing the poor performance for neutral hadrons to also affect the charged ones, which constitute 60% of the jet on average.

One of the intrinsic limitations on the precision of hadronic calorimeters are event-to-event fluctuations of the processes in the hadron shower – i.e. the cascade of secondary, tertiary and further particles that is produced when a primary hadron interacts with a block of dense material. These fluctuations are much larger than in electromagnetic showers, due to the much smaller number of particles produced. They affect, for example, the fraction of energy transferred to nuclear excitations, thereby remaining invisible, or the amount of electromagnetic subcascades, which form when neutral pions are produced and decay into energetic photons. Since the response of the calorimeter is typically different for electromagnetic and hadronic cascades of the same energy, a different electromagnetic fraction leads to a different overall response. Since this fraction fluctuates statistically in a wide range, the resolution is degraded.

This limitation was already a major concern in the development of the ZEUS and H1 experiments at HERA, DESY's former electron–proton collider, where "compensation" for this difference was a central theme. ZEUS and H1 tackled the problem in different ways: ZEUS achieved an equalisation of the response for electromagnetic and hadronic showers by carefully tuning the sampling structure of their uranium scintillator calorimeter in such a way that it was "compensating". The ZEUS calorimeter still holds the world record in single-hadron energy resolution for collider experiments. H1 exploited the fact that electromagnetic subcascades are characterised by an enhanced local density of the energy deposition. These zones can be recognised in the reconstruction software and their contribution adjusted to the proper hadron scale by applying suitable weights. This so-called "software compensation" became possible because the H1 liquid-argon calorimeter was the most finely segmented detector at that time.

The weighting techniques pioneered by H1 and other experiments can also be applied to the highly granular particle flow calorimeters, which provide even more detailed information about the local energy deposition density. However, the sophisticated particle flow algorithms are realised in complex software packages, which perform the pattern recognition task of separating the signals from individual particles in dense high-multiplicity environments, and compensation procedures have not been implemented until recently. Figure 1 shows a section of a typical simulated multijet event in the International Large Detector (ILD), produced in an electron–positron collision with 500 GeV centre-of-mass energy. One complication, for example, stems from the fact that the optimal weights to apply to calorimeter signals when summing them up depend not only on the local density of depositions, but also on the total energy of the particle, for which the separation has to be accomplished before. On the other hand, the pattern recognition is not only based on the topology, but uses energy information in addition. Clearly, finding the optimal weights can only be achieved iteratively and the procedure must be robust against assignment ambiguities.

In a close collaboration of DESY scientists with the Pandora group at the University of Cambridge in the UK, H1-style weighting procedures were implemented in the Pandora particle flow software. Figure 2 shows that the effort was well worthwhile; it results in the best jet energy performance realised for the ILC detectors to date, and this over a wide

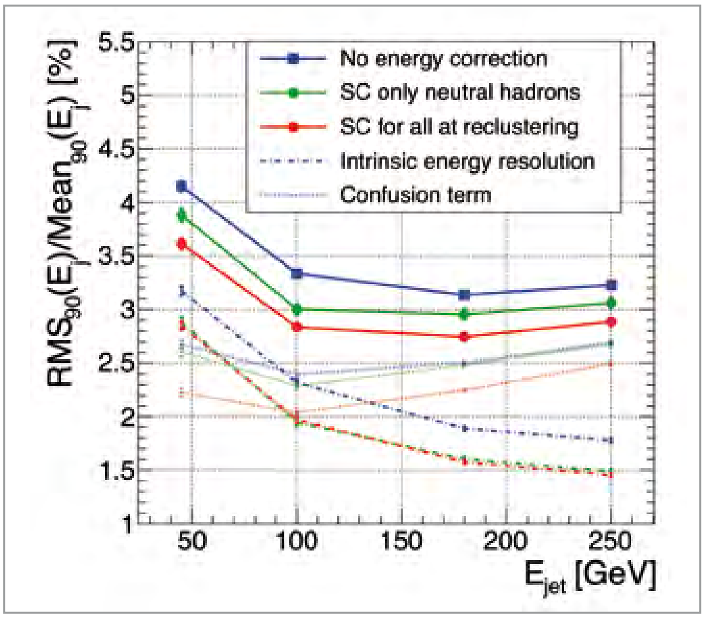

Figure 2

Jet energy resolution as a function of jet energy for different implementations of software compensation (SC) in the particle flow software package Pandora (blue: none; green: only for neutral hadrons identified after the pattern recognition stage; red: additionally also applied in the pattern recognition (reclustering) stage). The dashed lines (perfect pattern recognition) correspond to the intrinsic calorimetric resolution, using Monte Carlo truth information in the pattern recognition, and the dotted lines (quadrature difference) to the contributions from imperfect pattern recognition ("confusion"). The resolution is expressed as RMS90, the root mean square of the smallest interval containing 90% of the events.

range of relevant jet energies from 50 to 250 GeV. Since in the Monte Carlo simulation the true origin of the energy depositions is known, one can disentangle the improvements originating from the better resolution for isolated hadrons from those resulting from assisting the pattern recognition with better energy information. While the former dominate in the lower part of the jet energy range, where particles are mostly well separated, the latter are important at higher energies, where jets become denser and mis-assignments, so-called "confusion", dominates the resolution.

The results show that even for the latest-generation imaging calorimeters, the classical arts of calorimetry as developed for the HERA experiments are essential for obtaining the best possible performance.

Contact:
Felix Sefkow, felix.sefkow@desy.de
Katja Krüger, katja.krueger@desy.de
Huong Lan Tran, huong.lan.tran@desy.de

Burning lenses.

Achieving extreme focusing with active plasma lenses

Electron acceleration in plasma is a promising concept for shrinking the size and cost of high-energy accelerators, owing to the supported extreme accelerating fields – which are about 1000 times stronger than those possible in conventional radio-frequency cavities. One key feature of beams generated and accelerated in plasma is a low beam emittance. This feature is challenging to preserve in the drift section after the beam extraction from the plasma module, however, due to an inherently high beam divergence and a typical energy spread on the percent level. Capturing the beam as closely as possible to the plasma source would allow the beam quality to be conserved. This approach requires novel types of magnetic beam optics, which are currently being developed by the DESY plasma acceleration group. Plasma-based lenses enable focusing strengths an order of magnitude higher than conventional magnetic lens assemblies. In the future, such beam optics will play a crucial part in the development of plasma accelerators for high-energy physics and photon science.

Active plasma lenses

The idea of using plasma as a conductor through which a particle beam can pass, and which can carry a high collinear current of background plasma particles, has been thoroughly tested for heavy-particle beams. Referred to as an active plasma lens (APL), it enables an azimuthal, radially symmetric magnetic field configuration for focusing the charged particle beams. New experiments show that the same concept can be applied to electron beams in plasma structures that are orders of magnitude smaller. The underlying principle is fundamentally different from the passive beam focusing that occurs in transverse plasma wakefields excited by high-current density particle beams or strong lasers.

The APL, as sketched in Fig. 1, consists of a gas channel typically hundreds of micrometres in diameter and a few centimetres in length. When applying a voltage of a few ten kilovolts, electrical breakdown is induced, leading to the formation of a plasma. The plasma supports current transport along the channel, which induces a magnetic field. The magnetic field configuration of such a system can easily be calculated using Ampère's law as being radially symmetric. This allows for symmetric focusing of co-propagating charged particle beams in a single optical element – a considerable advantage of the APL over the most widely used conventional device, the magnetic quadrupole.

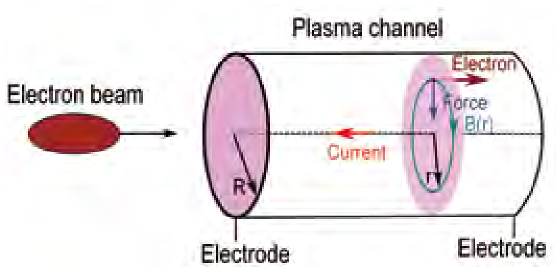

Figure 1

Schematic drawing of the APL setup. The homogeneous current density over the entire channel width creates a focusing magnetic field configuration.

For a plasma channel of 250 µm diameter with a 250 A current, a focusing gradient of g = 3840 T/m has been experimentally demonstrated [1], which surpasses the gradient of commonly used electromagnetic quadrupole lenses by an order of magnitude. Ultimately, such gradients allow for capturing beams with high divergence over short drift sections, as is crucial for high-divergence electron beams from plasma accelerators. An alternative technique that can achieve focusing in both transverse dimensions simultaneously – the solenoid lens – has the disadvantage of a quadratic scaling of the focusing strength with the energy. APLs and quadrupoles have a more favourable linear scaling (Fig. 2).

While the focusing force due to the plasma current can be relatively strong, the acting forces inside a plasma wakefield can be orders of magnitude higher. Therefore, it is important to design the plasma lens in such a way that the traversing electron beam drives no wake.

Probing the quality of plasma lenses

To test the stability of APLs, the DESY plasma acceleration group used the stable and well-characterised electron beams provided by the MAMI microtron at the University of Mainz in Germany. During an experimental campaign in cooperation with the universities of Hamburg and Mainz, the impact of the APL on beam stability and the focusing gradient were measured. The APL was moved transversally to probe the reproducibility of the gradient by measuring the transversal kick the electron beam experiences when

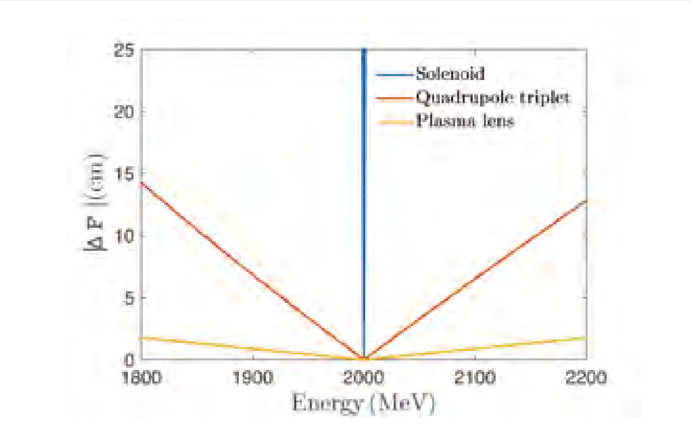

Figure 2

Energy dependence of the focal length of different focusing schemes. The APL (g = 1500 T/m, length = 25 mm) has the smallest absolute deviation because of its small design focal length of only 18 cm. The quadrupole triplet (g = 100 T/m, length = 10 cm) features a smaller relative chromaticity but, due to its larger focal length of 2 m, is still more sensitive to energy spread. The solenoid is by far the most chromatic element due to its quadratic scaling with energy.

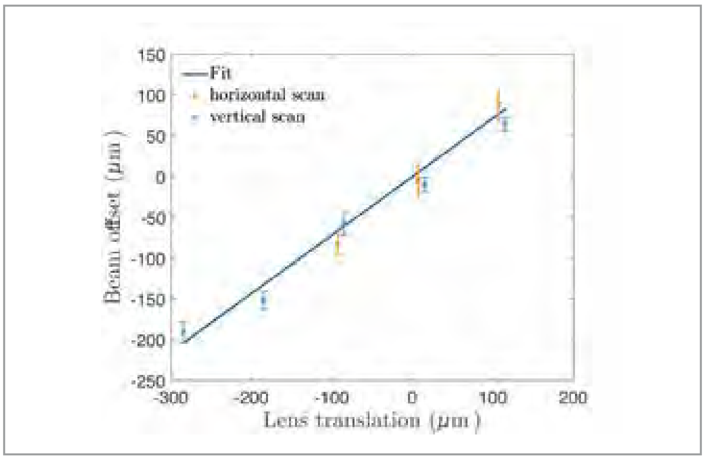

Figure 3

Direct measurement of the magnetic field gradient. The scan was performed by moving the plasma lens transversally – introducing a dipole kick depending on the gradient and the distance moved. The best fit of the measured data yields a gradient of g = 760 T/m corresponding to a current of 950 A. The measured current was 944 A, which shows excellent agreement between the expected magnetic field gradient and the measured value.

passing the lens off-centre. The results of this scan are shown in Fig. 3. This scan also yielded the first-ever direct measurement of the magnetic field gradient of an APL. The measured value of 760 T/m and the predicted value of 755 T/m from independent measurements of the current and the channel diameter were in excellent agreement. The pointing stability with respect to the beam size was measured to be 2% vertically and 3% horizontally. It remained at 11% and 9%, respectively, with the lens in the beamline. The introduced additional fluctuations were likely due to the temporal jitter of the electron beam of 100 ns with respect to the discharge current. The discharge current can be seen in Fig. 4. Its amplitude was stable in the sub-percent range, and the temporal form varied on the nanosecond scale in the initial ramp-up.

The most critical remaining question concerning APLs for electron beam applications is whether their magnetic field gradient is constant over their entire radius. This can only be the case for a homogeneous current density over the entire channel width. Magnetohydrodynamic simulations show that the homogeneity is preserved over half of the radius [1], enabling focusing without emittance growth for beams that are smaller transversally than half the diameter of the channel. A conclusive way of assessing the quality of APLs is to measure the emittance of an electron beam with and without the lens in its path. At the end of 2016, DESY conducted such an experiment at the MAMI microtron in cooperation with the universities of Hamburg and Mainz and Lawrence Berkeley National Laboratory (LBNL) in the USA. The emittance was measured through a quadrupole scan technique using a quadrupole triplet behind the APL. The results are currently being evaluated. They are promising and seem to indicate next to no emittance growth when using different gradients of well above 500 T/m.

These results show that APLs have the potential to play an integral role in advanced accelerator techniques. They allow for compact capturing of electron beams from plasma accelerators while maintaining their high beam quality.

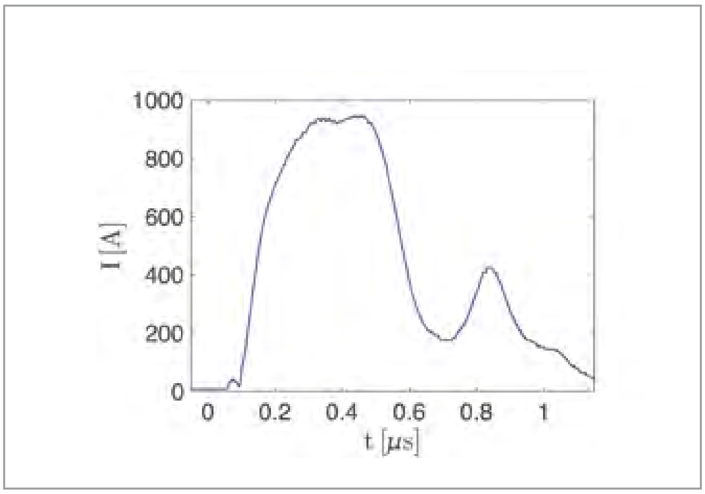

Figure 4

Measured current profile inside the APL. The plateau region around 944 A was used in the experiments. The direct gradient measurement corresponds to a current of 950 A, showing excellent agreement between the predicted gradient and the measured value.

Contact:

Jan-Hendrik Röckemann, jan-hendrik.erbe@desy.de
Lucas Schaper, lucas.schaper@desy.de
Jens Osterhoff, jens.osterhoff@desy.de

Reference:

[1] J. van Tilborg et al., Phys. Rev. Lett. 115 (2015) 184802.

The harvest of OLYMPUS.

Hard two-photon contribution to elastic lepton–proton scattering

The OLYMPUS collaboration has achieved a precise measurement of the positron–proton to electron–proton elastic cross section ratio ($R_{2\gamma}$), a direct measure of the contribution of hard two-photon exchange to the elastic cross section. The OLYMPUS experiment at DESY used the intense beams of electrons and positrons stored in the former DORIS ring at 2.01 GeV, which interacted with an internal windowless hydrogen gas target. The detector consisted of a toroidal magnetic spectrometer instrumented with drift chambers, a system of time-of-flight scintillation counters and a redundant set of luminosity monitors. Radiative effects were taken into account for the extraction of $R_{2\gamma}$. The results, for a wide range of virtual photon polarisation $0.456 < \varepsilon < 0.978$, are smaller than hadronic two-photon exchange calculations predict, but consistent with a phenomenological model.

Measurements of the proton's elastic form factor ratio $\mu_p G_E^p/G_M^p$ using polarisation techniques show a dramatic discrepancy with the ratio obtained using the traditional Rosenbluth technique in unpolarised cross section measurements. One hypothesis for the cause of this discrepancy is a contribution to the cross section from hard two-photon exchange (TPE), which is not included in standard corrections and would affect the two measurement techniques differently. There is no model-independent formalism for calculating hard TPE. Some model-dependent calculations suggest that TPE is responsible for the form factor discrepancy, while others contradict that finding. Hard TPE can be quantified from a measurement of $R_{2\gamma}$, the ratio of the positron–proton to electron–proton elastic cross sections, corrected for the standard set of radiative effects, including soft TPE.

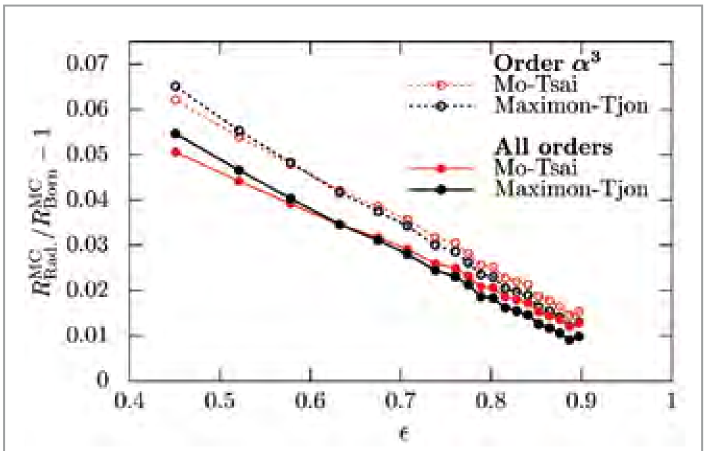

Figure 1

Radiative corrections as a function of virtual photon polarisation ε

The OLYMPUS experiment, as well as two recent experiments at VEPP-3 in Novosibirsk, Russia, and CLAS at Jefferson Lab, USA, measured $R_{2\gamma}$ to specifically determine if hard TPE is sufficient to explain the observed discrepancy in the proton's form factors, or if some additional explanation is needed. Both the magnitude of $R_{2\gamma}$ and its kinematic dependence are relevant. If hard TPE is the cause of the discrepancy, phenomenological models predict $R_{2\gamma}$ should rise with decreasing ε and increasing Q^2. Here, ε is the virtual photon polarisation parameter given by

$$\epsilon = \frac{1}{1 + 2(1+\tau)\tan^2(\theta_l/2)},$$

where θ_l is the lepton scattering angle and $\tau = Q^2 / (4M_p^2)$ with M_p being the proton mass. Q^2 is the negative four-momentum transfer squared.

The OLYMPUS experiment took data during the last operation phase of the DORIS storage ring at DESY. The stored electron (positron) beams passed through an internal unpolarised hydrogen gas target. The detector, which was based on the former MIT-Bates BLAST detector, comprised a toroidal magnetic field with a left/right symmetric arrangement of tracking detectors, time-of-flight scintillation counters and luminosity monitors. These consisted of three independent detector components: Møller/Bhabha calorimeters at 1.29° and two telescopes mounted at 12°, each comprising three gas electron multiplier detectors interleaved with three multiwire proportional chambers. In total, an integrated luminosity of 4.5 fb^{-1} was collected.

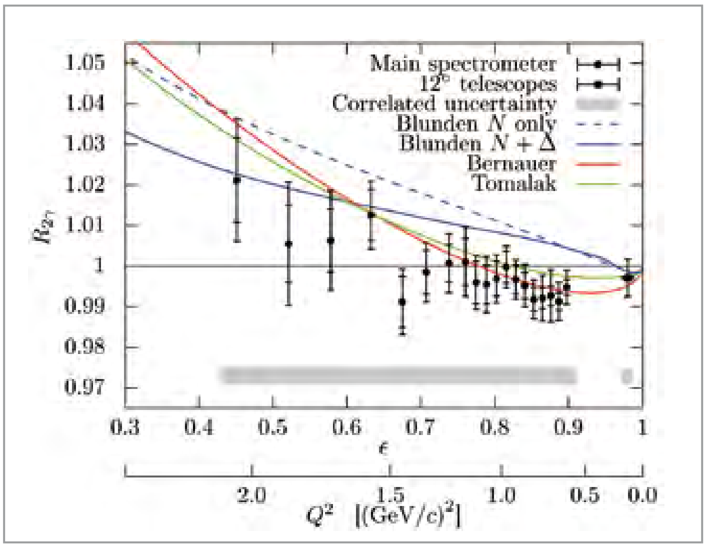

Figure 2

$R_{2\gamma}$ with statistical (inner bars), uncorrelated systematic (added in quadrature, outer bars) and correlated systematic (grey band) uncertainties for all-order radiative corrections, using the Mo-Tsai convention

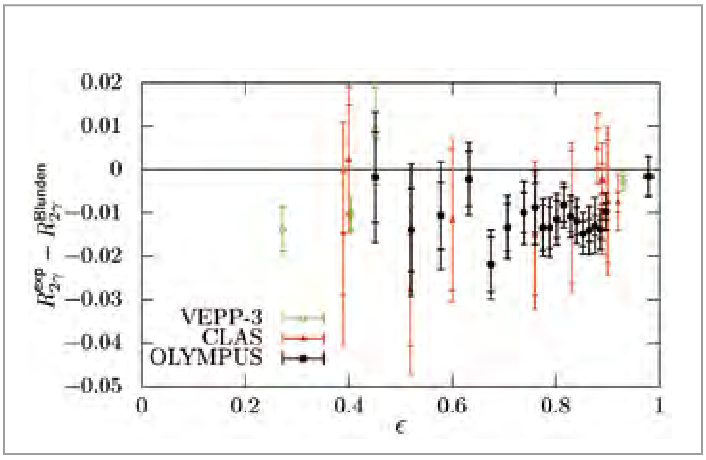

Figure 3

Comparison of the results of recent experiments to the calculation of Blunden

A complete Monte Carlo simulation was developed to account for differences between electrons and positrons with respect to radiative effects, changing beam position and energy, spectrometer acceptance, track reconstruction efficiency, luminosity and elastic event selection. The ratio reported by OLYMPUS is given by

$$R_{2\gamma} = \left[\frac{N_{\mathrm{exp}}(e^+)}{N_{\mathrm{exp}}(e^-)}\right] \Big/ \left[\frac{N_{\mathrm{MC}}(e^+)}{N_{\mathrm{MC}}(e^-)}\right] = \frac{R^{\mathrm{exp}}}{R^{\mathrm{MC}}} ,$$

where N_i are the number of observed and simulated events. The obtained results are based on four independent analyses, using different approaches. In the final analysis, the luminosity determination came from an analysis of multi-interaction events in the Møller/Bhabha calorimeters at 1.29°, permitting a measurement of $R_{2\gamma}$ at $\varepsilon = 0.978$ using the elastic scattering detected in the 12° luminosity monitor system.

Radiative corrections have a large effect on the determination of $R_{2\gamma}$. They are driven by corrections that are odd under lepton charge reversal. Figure 1 shows the size of the corrections, approximately 5–6% at the lowest ε values, and indicates that higher-order effects can alter the correction by as much as 1%.

The OLYMPUS determination of $R_{2\gamma}$ as a function of ε and Q^2 using the Mo-Tsai radiative corrections to all orders is shown in Fig. 2, along with two theoretical calculations and a phenomenological prediction based on a global fit to both unpolarised and polarised measurements of the proton form factors. OLYMPUS finds that the contribution from hard TPE is small at this beam energy, and that $R_{2\gamma}$ is consistent with or below unity over the entire range of ε as well as below the theoretical prediction of Blunden.

A direct comparison of the results from recent experiments is difficult due to the different kinematical regions covered. The OLYMPUS collaboration therefore plotted the difference of all the experimental data to the prediction using Blunden's newest calculations (Fig. 3) to approximately take into account that the data were taken at different ε and Q^2. The data are consistent with each other, but lie mostly below the calculation of Blunden. A similar comparison with the phenomenological prediction of Bernauer shows good agreement.

The OLYMPUS collaboration does not agree with the conclusions of earlier papers. The data shown in Fig. 3 clearly favour a smaller $R_{2\gamma}$. The agreement with the phenomenological prediction of Bernauer suggests that TPE is causing most of the difference in form factor ratio in the measured range. Another theoretical model by Blunden that can explain the difference only at larger Q^2 seems to be ruled out. To clarify the situation, the size of TPE at large Q^2 has to be determined in future measurements.

Contact:

Uwe Schneekloth, uwe.schneekloth@desy.de

References:

http://web.mit.edu/OLYMPUS/
OLYMPUS Collaboration, Phys. Rev. Lett. 118 (2017) 092501.

Astroparticle physics.

Astroparticle physics at DESY spans a broad range of topics, from theoretical studies to a plethora of experimental activities. Of these, the Cherenkov Telescope Array (CTA), the next-generation gamma-ray observatory, is currently the largest endeavour. The DESY CTA group is instrumental in numerous crucial aspects of the experiment, from software to telescope development and physics preparation (p. 58).

DESY has extensive experience in gamma-ray astronomy. The research centre is an important contributor to the H.E.S.S. telescope system in Namibia, the first of the second generation of experiments in this field. While the upgrade with the new camera systems – developed at DESY – was completed, the analysis of the first ten years of H.E.S.S. data led to the discovery of a cosmological accelerator to PeV energies (p. 60). Analysis of data from the Fermi Gamma-Ray Space Telescope is in full swing too. One of the main activities of the DESY Fermi group was the All-Sky Variability Analysis, which led to the publication of a catalogue of over 500 flaring gamma-ray sources (p. 62).

The second major field of experimental activities in astroparticle physics is neutrino physics. DESY is strongly involved in the IceCube neutrino telescope at the South Pole, which continues to deliver high-quality data (p. 64). Here too, the future is in clear focus, with the IceCube-Gen2 project being pursued at full steam. The high-energy cosmic neutrino studies with IceCube are complemented by neutrino searches with gamma-ray telescopes. A new technique hereby is to “fish” for tau neutrinos, a method employed at the MAGIC telescopes on La Palma, Spain (p. 68).

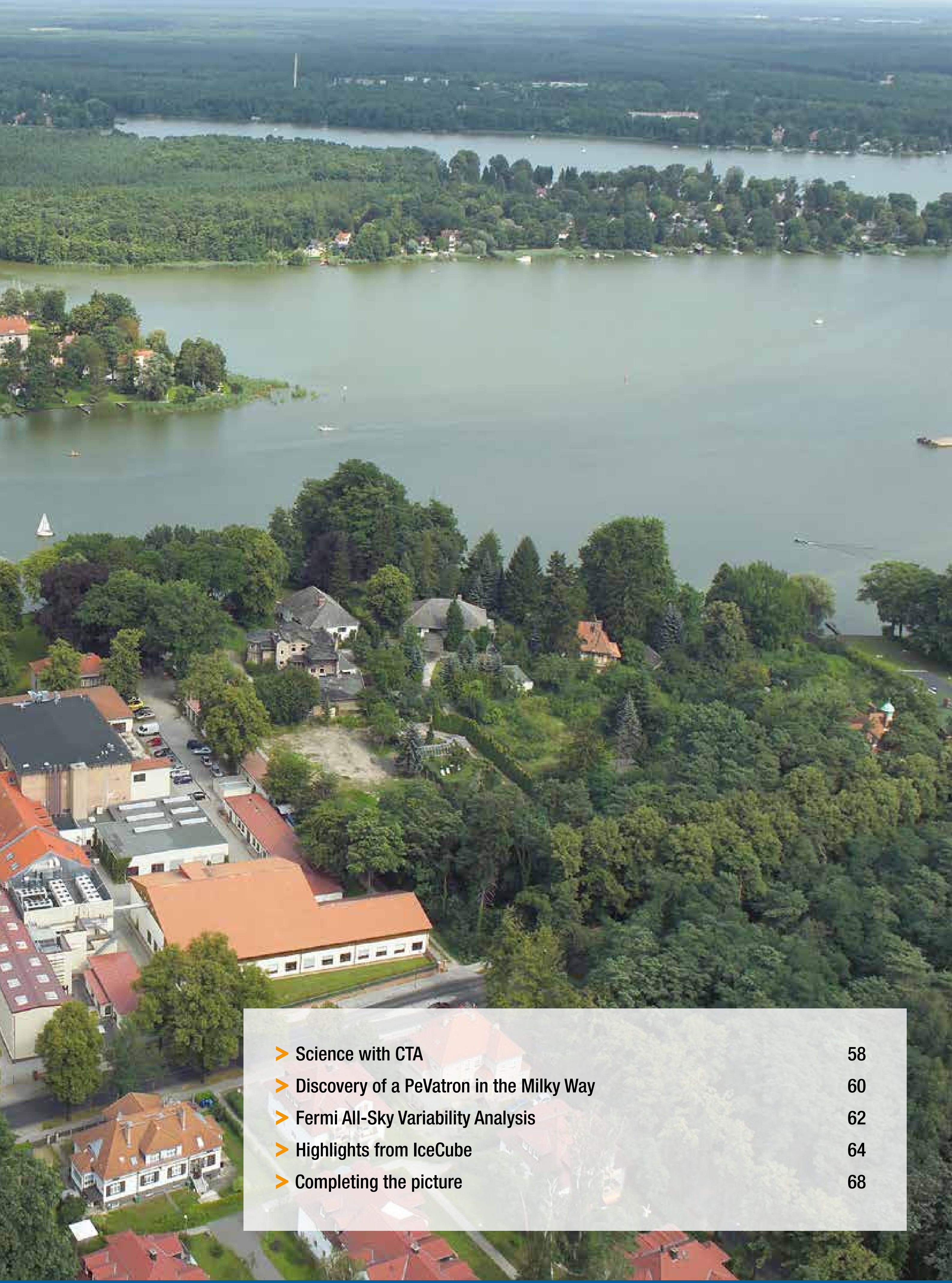

Science with CTA.

… and pre-production readiness of mid-sized telescopes

The next-generation Cherenkov Telescope Array (CTA) gamma-ray observatory will address a broad range of astrophysics and fundamental physics questions. The CTA science programme comprises three main themes: (i) origin and role of relativistic, cosmic particles, (ii) extreme astrophysical environments and (iii) frontiers in physics. In 2016, the main science projects were identified and summarised in the 200-page “Science with CTA” document, which is due to be published in early 2017. On the construction side, the mid-sized telescopes are now ready for industrial pre-production in spring 2017.

Science projects

CTA will be an observatory of Cherenkov telescopes aiming to reach a sensitivity and performance that is in every respect well beyond that of existing instruments: ten times better sensitivity at 1 TeV, full-sky coverage by arrays in both hemispheres higher photon rates for short-timescale phenomena, improved angular resolution and field of view, energies from 20 GeV to over 300 TeV for high redshifts and extreme cosmic accelerators, and enhanced survey and monitoring capabilities.

The science themes and questions are addressed in key science projects (KSPs) (Fig. 1). Furthermore, CTA can tackle a number of science areas not related to gamma rays. DESY personnel is involved in most of the topics, the KSP on star formation is led by a DESY scientist.

Connection of star formation and cosmic rays

Understanding the fundamentals of star-forming processes is one of the great challenges in modern astrophysics. Star

Theme		Question		Dark Matter Programme	Galactic Centre Survey	Galactic Plane Survey	LMC Survey	Extra-galactic Survey	Transients	Cosmic Ray PeVatrons	Star-forming Systems	Active Galactic Nuclei	Galaxy Clusters
1	Understanding the Origin and Role of Relativistic Cosmic Particles	1.1	What are the sites of high-energy particle acceleration in the universe?		✔	✔✔	✔✔	✔✔	✔✔	✔	✔	✔	✔✔
		1.2	What are the mechanisms for cosmic particle acceleration?		✔	✔	✔		✔✔	✔✔	✔	✔✔	✔
		1.3	What role do accelerated particles play in feedback on star formation and galaxy evolution?		✔		✔				✔✔	✔	✔
2	Probing Extreme Environments	2.1	What physical processes are at work close to neutron stars and black holes?		✔	✔	✔			✔✔		✔✔	
		2.2	What are the characteristics of relativistic jets, winds and explosions?		✔	✔	✔	✔	✔✔	✔✔		✔✔	
		2.3	How intense are radiation fields and magnetic fields in cosmic voids, and how do these evolve over cosmic time?					✔	✔			✔✔	
3	Exploring Frontiers in Physics	3.1	What is the nature of Dark Matter? How is it distributed?	✔✔	✔✔		✔						✔
		3.2	Are there quantum gravitational effects on photon propagation?						✔✔	✔		✔✔	
		3.3	Do Axion-like particles exist?					✔	✔			✔✔	

Figure 1

The main CTA science themes and questions are addressed in a number of KSPs (columns on the right). KSPs with relevance to the dark matter programme are labelled in green. The check marks indicate the importance of a KSP for a specific science question.

formation is affected by the ionisation of interstellar matter by relativistic particles (cosmic rays) through chemistry and the interaction of matter with magnetic fields. Cosmic rays also amplify magnetic fields and exert pressure on their environment. Reversely, star formation produces massive stars, which either blow up as supernovae or develop strong winds, which can efficiently accelerate charged particles to highly relativistic speeds and enrich the interstellar medium with heavy elements that feed back on star formation. The acceleration, propagation and interaction of cosmic rays are hence crucial for understanding the evolution of the universe at various scales: from stars to stellar clusters and from molecular clouds to galaxies and galaxy clusters. Gamma rays, produced through cosmic-ray interactions, can be used to image the emission regions. They are the prime messengers to study the properties of relativistic particles in star-forming environments and their roles in the star formation processes.

CTA will observe galactic and extragalactic massive stellar clusters and star-forming regions, in spiral galaxies as well as in ultraluminous infrared galaxies. Prime targets will also be the Large Magellanic Cloud (Fig. 2), the Andromeda galaxy and starburst galaxies. The information obtained will advance our understanding considerably. The benefits of the enhanced performance provided by CTA for studying the connection of star formation and cosmic rays are discussed and quantified in Ref. [1].

Mid-sized telescopes

The mid-sized telescopes (MSTs) of CTA provide the best sensitivity for the central energy range (100 GeV to 50 TeV). With a last round of modifications in 2016, following tests of a second prototype in Arizona, and with improved mirror facets and alignment procedures, the design of the MSTs was finished and optimised for industrial pre-production in spring 2017.

Contact:

Stefan Schlenstedt, stefan.schlenstedt@desy.de
Stefan Ohm, stefan.ohm@desy.de

References:

[1] "Science with CTA", in preparation, The CTA Consortium (2017)

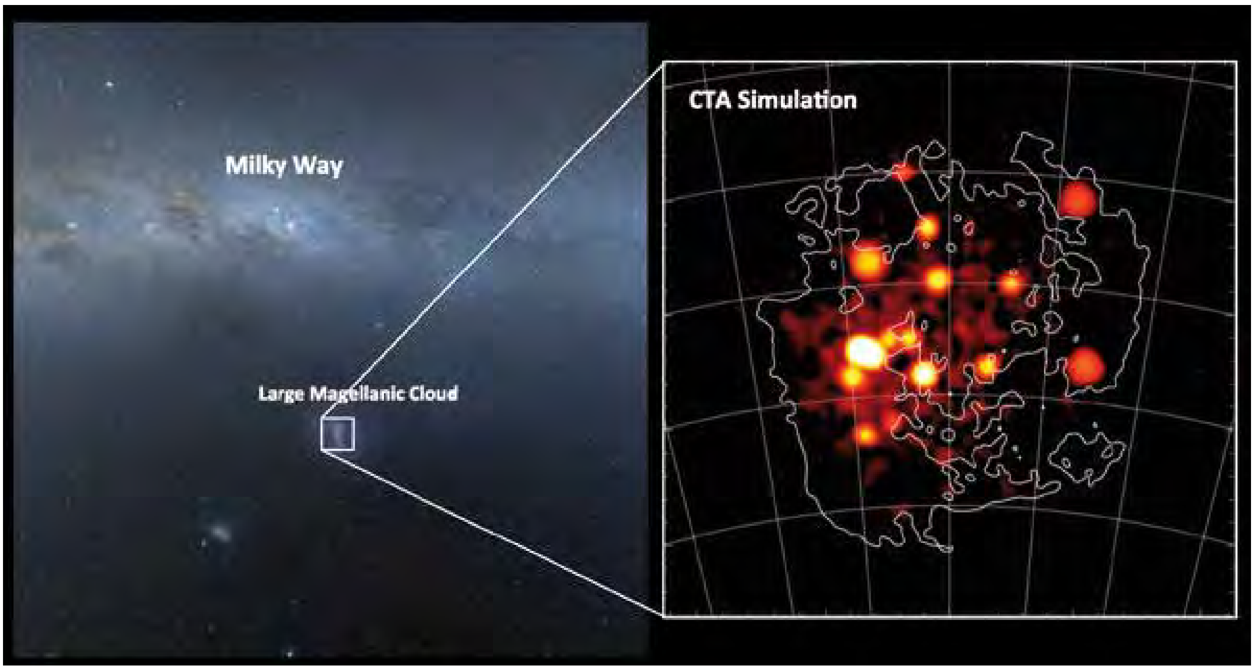

Figure 2

Simulation of high-energy gamma-ray emission as seen with CTA, due to star-forming activity in the Large Magellanic Cloud

Discovery of a PeVatron in the Milky Way.

… and completion of the H.E.S.S. I camera upgrade

In a new analysis of a ten-year observational data set of the High Energy Stereoscopic System (H.E.S.S.), a gamma-ray observatory in Namibia, scientists may have found the origin of the large gamma-ray glow around the centre of our galaxy, the Milky Way. The shape and energy spectrum of this gamma-ray emission indicates that an unprecedentedly violent particle accelerator might sit at its very heart. If so, it is the first time a peta-electronvolt (PeV) particle accelerator is found in the Milky Way, which would be a crucial piece of the puzzle of high-energy cosmic rays. In 2016, DESY personnel successfully built and deployed four new cameras for the 12 m H.E.S.S. I telescopes. This major hardware project of DESY in Zeuthen, which was completed in time and on budget, improves the H.E.S.S. view on the multi-TeV universe.

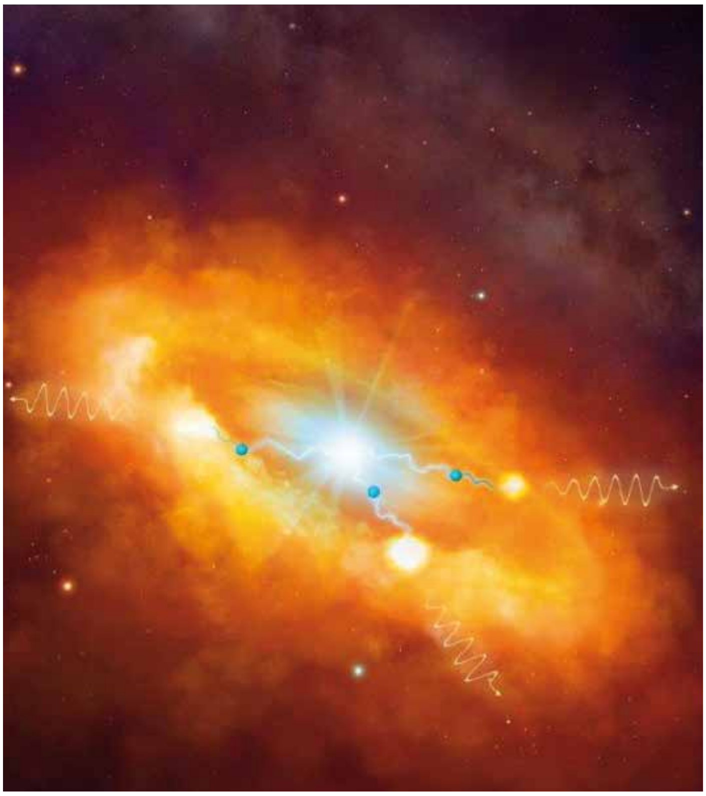

Figure 1

Artist's conception on the inner 500 light years of the Milky Way. Highly energetic particles (blue) are accelerated in the centre and propagate outwards. When interacting with gas and dust, they produce secondary pions, which decay into gamma rays that can travel to Earth and be observed by H.E.S.S.

A cosmic PeVatron

The energy spectrum of cosmic rays reaches, without any major feature, over several orders of magnitude. At energies of a few PeV (1 PeV = 10^{15} eV), it steepens and displays a feature called "the knee" of the cosmic-ray spectrum. This implies that our galaxy hosts PeVatrons – particle accelerators that can actually produce PeV particles. None of the cosmic accelerators currently observed by Cherenkov telescopes have yet seen the characteristic signature of PeV particles, namely, power-law spectra of gamma rays extending without a cut-off or a spectral break to at least tens of TeV (such gamma rays are expected to be produced as secondaries from PeV cosmic-ray interactions).

New observations with H.E.S.S. of the inner 500 light years of the Milky Way have now revealed a diffuse gamma-ray glow with a spectral distribution that reaches up to surprisingly high energies: Without a sign of a cut-off, gamma rays of up to 20–30 TeV were found, which is unexpected for such a large area. When travelling large distances through gas, magnetic fields and background light, particles usually lose their energy very quickly. In addition, the emission shows a concentric intensity profile, which falls with *1/r*, *r* being the distance to the galactic centre. This also indicates that particles are diffusing outwards from the centre of the galaxy.

Both of these newly measured properties suggest that a violent accelerator injects energetic particles on a regular

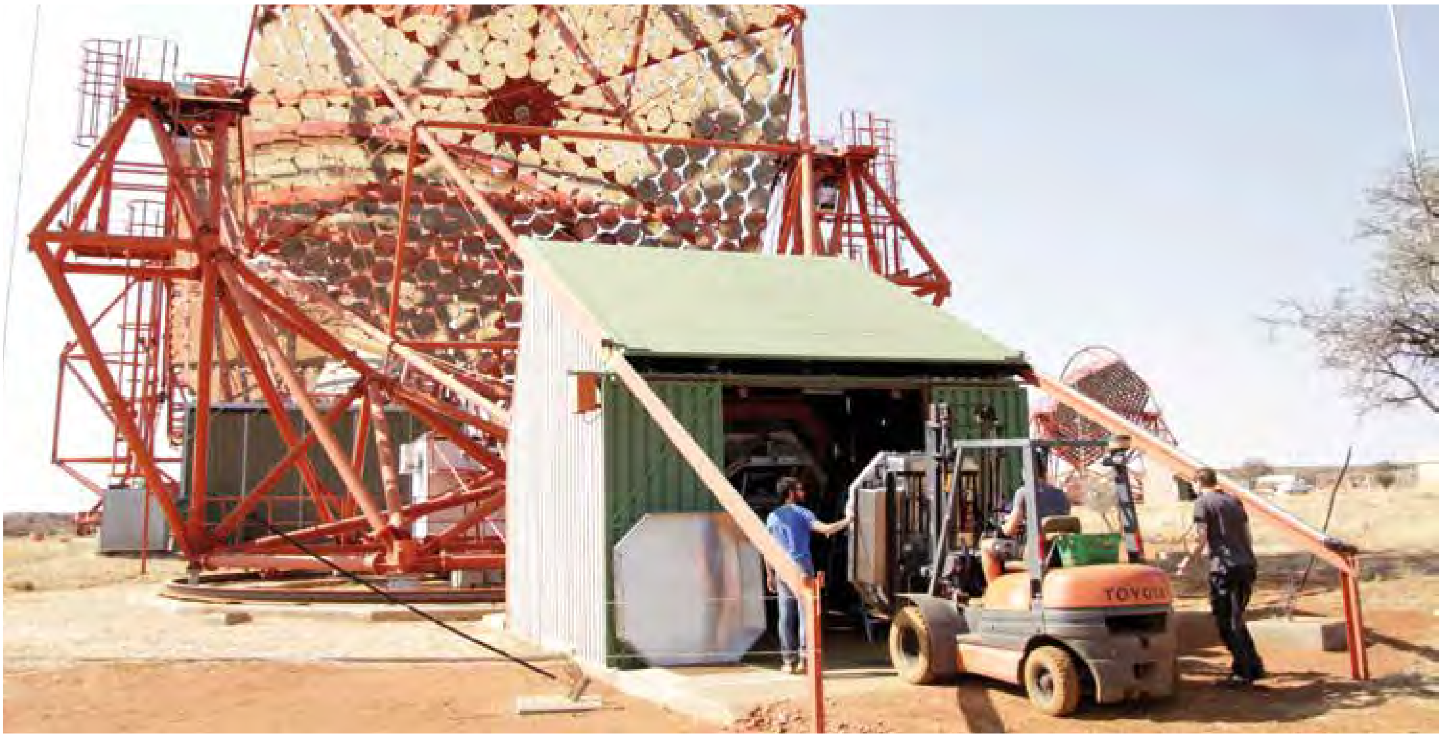

Figure 2

Installation of the back door of camera CT3 at the H.E.S.S. site in the Khomas highland in Namibia. The back door includes a new system for ventilation, filtering and heating of the air that is blown into the camera.

basis (on timescales of 1000 to 10 000 years) into this central molecular zone of our galaxy. Basic calculations show that only if the injected particles have energies that reach a PeV or more, they can plausibly produce the phenomena observed. Thus, H.E.S.S. is measuring gamma rays from the interactions of PeV particles with the gas around the galactic centre (Fig. 1). The study was published in *Nature* [1].

Completion of the H.E.S.S. I camera upgrade

In 2012, DESY joined the H.E.S.S. collaboration with the commitment to upgrade the cameras of the four 12 m H.E.S.S. I telescopes. These sensitive photodetectors consist of photomultiplier tubes as optical sensors as well as electronics, some pneumatic parts, a ventilation system and software. After start-up of the large 28 m H.E.S.S. II telescope in 2012, the data acquisition rate of the H.E.S.S. I cameras was limiting the joint operation. Also, the cameras had been used for more than ten years in the dust of the Namibian savannah, which degraded the sensitive instruments. Consequently, their failure rate increased and the data quality deteriorated.

In spring 2012, DESY started to develop a suitable upgrade, without prior expertise in the construction of such cameras. After only 2.5 years, the first camera was produced and deployed in 2015. It joined routine observations in March 2016, and green light was given for the replacement of the other H.E.S.S. I cameras. Meanwhile, several hundred electronics boards had been produced (with the help of DESY in Hamburg), and all components were assembled and extensively tested at DESY in Zeuthen. In July 2016, the cameras were shipped to the H.E.S.S. site, and in September, ten DESY staff members installed the new hardware, within five weeks, on the H.E.S.S. telescopes (Fig. 2).

As of December 2016, the final commissioning is ongoing, with the hand-over to the H.E.S.S. collaboration planned for January 2017. Besides a much improved availability, the new cameras will provide a lower energy threshold and a better signal digitisation that will enhance the observation of very high energy showers. Signals of such showers can last longer than the 16 ns exposure time that is typically the standard in H.E.S.S. observations. Thus, an improved PeVatron search will be one of the prime goals of the refurbished H.E.S.S. array observing the Southern sky.

Contact:

Stefan Klepser, stefan.klepser@desy.de

References:

[1] H.E.S.S. Collaboration, Abramowski et al., Nature 531 (2016) 476-479.

Fermi All-Sky Variability Analysis.

Locating flaring gamma-ray sources

The Fermi All-Sky Variability Analysis (FAVA) uses data of the Large Area Telescope (LAT) on board the Fermi Gamma-Ray Space Telescope to search for variable and transient phenomena over the entire sky. An automated procedure, developed at DESY, finds weekly flares, locates and identifies (if possible) the sources and determines their spectra. The data from 7.4 years yielded more than 4500 flares from 518 sources. The FAVA results were made freely available through a web portal.

The Fermi LAT [1] is a genuine particle detector orbiting the Earth. Its particle tracker and calorimeter allow measurement of the direction and energy of gamma rays with energies from ≤100 MeV to hundreds of GeV. Since 2008, the LAT has been surveying the sky, providing a full-sky image every three hours. The FAVA initiative exploits this monitoring capability to do a blind search for variable and transient phenomena (flares) over the entire sky. The analysis starts searching for flares by comparing weekly pictures of the sky to the long-term average emission (Fig. 1). This photometric step is fast and reliable but provides only very crude information on the flare. At DESY, we have developed a second stage for FAVA that makes use of likelihood fitting techniques to precisely locate the flares and measure their spectra.

With this improved analysis, FAVA becomes an accurate and effective tool to study and monitor variability across the entire gamma-ray sky. The analysis has been used, for example, in recent searches for gamma-ray counterparts of gravitational waves [2]. Every week, FAVA detects on average 12 high-significance flares and makes them publicly

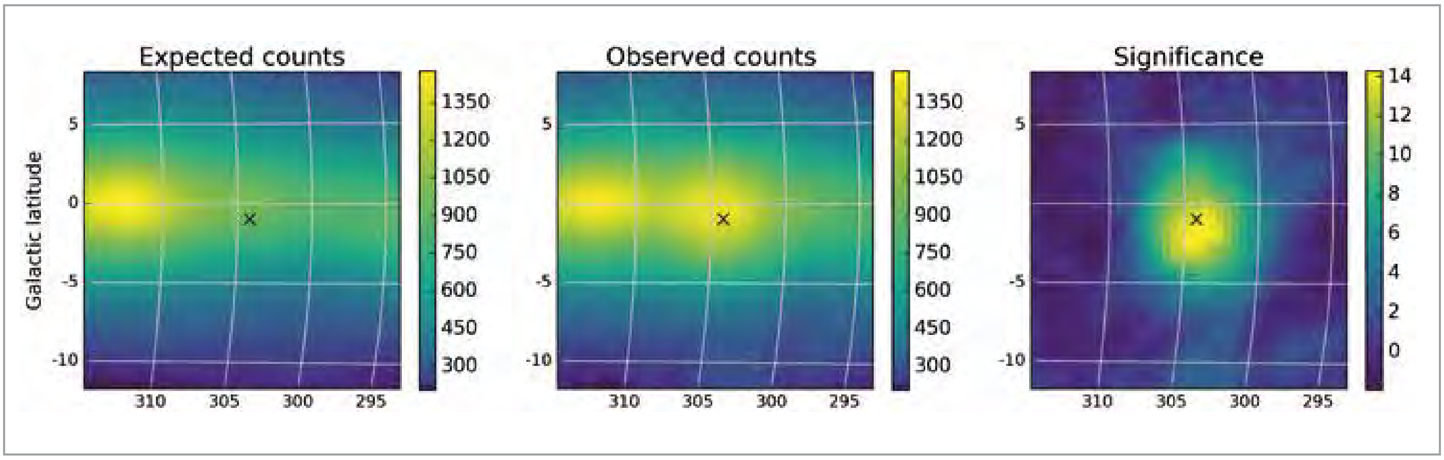

Figure 1

Photometric stage of FAVA. The number of expected counts (left) is derived from a four-year mission average. After accounting for the different exposures, it is compared to the counts observed in a given week (centre). The probability of this excess to be caused by statistical fluctuations is computed and converted into a Gaussian significance (right). The peak in the significance map is used to locate the flare (in this example, a periastron flare of PSR B1259–63/LS 2883, marked as a black x).

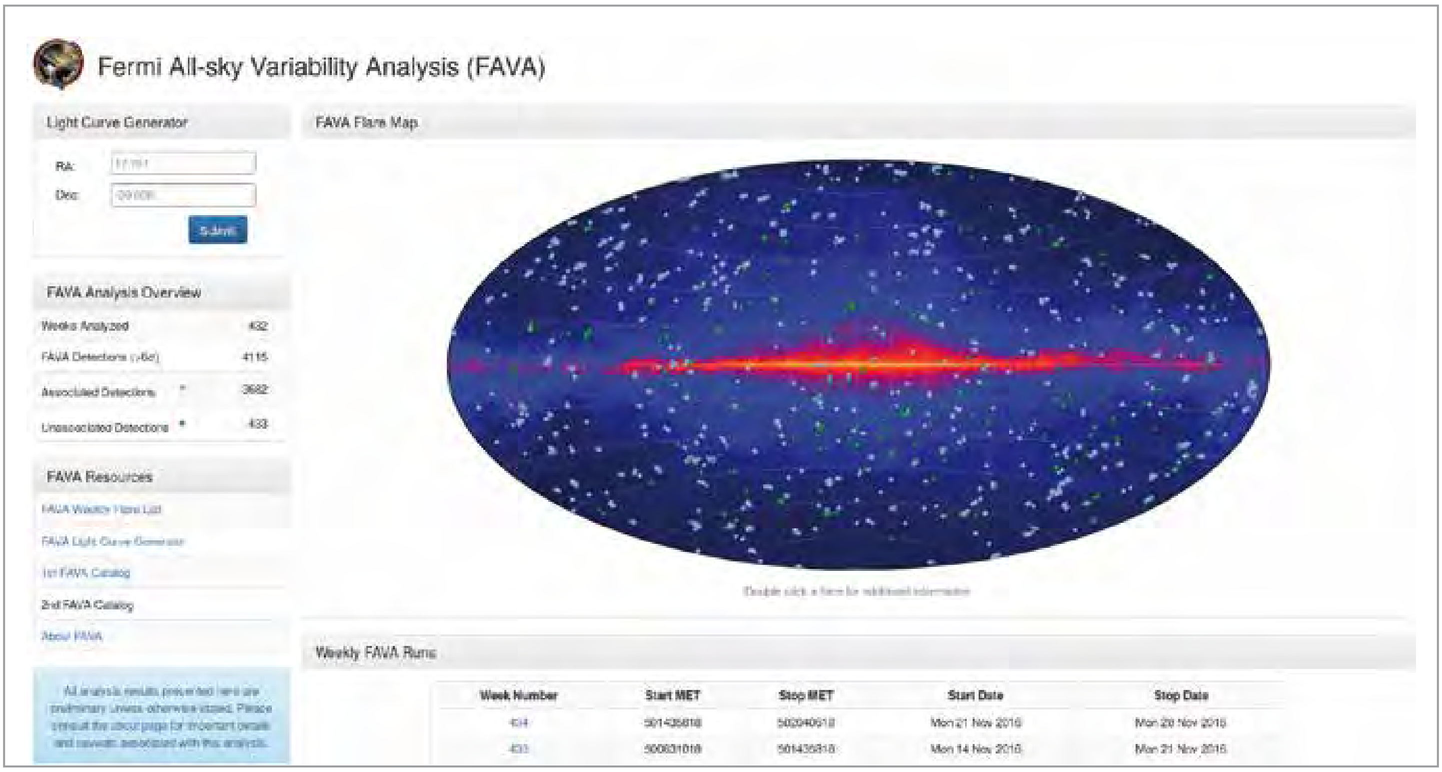

Figure 2:

FAVA web page (http://fermi.gsfc.nasa.gov/ssc/data/access/lat/FAVA/). Flares are shown as grey and green dots. Photometric light curves can be generated for every position on the sky (upper left panel).

available on the web (Fig. 2), providing a useful service to the entire astroparticle and astrophysics community.

At DESY, we have used FAVA to build a catalogue (2FAV, [3]) of flares from 7.4 years of Fermi data. More than 4500 flares were detected at high significance (>6σ). Clustering their positions, 518 flaring sources could be identified. All the diverse classes of variable gamma-ray emitters are represented in the 2FAV catalogue (Fig. 3). The catalogue also contains several tens of previously undetected gamma-ray sources, whose quiescent emission is below the threshold of more traditional analyses but whose flares are bright enough to be detected by FAVA.

Contact:

Matteo Giomi, matteo.giomi@desy.de,
Rolf Bühler, rolf.buehler@desy.de

References:

[1] W. B. Atwood et al. 2009, Astrophys. J. 697 (2009) 1071.
[2] M. Ackermann et al. 2016, Astrophys. J. 823 (2016) no.1, L2.
[3] S. Abdollahi et al. 2016, submitted to the Astrophysical Journal Supplement.

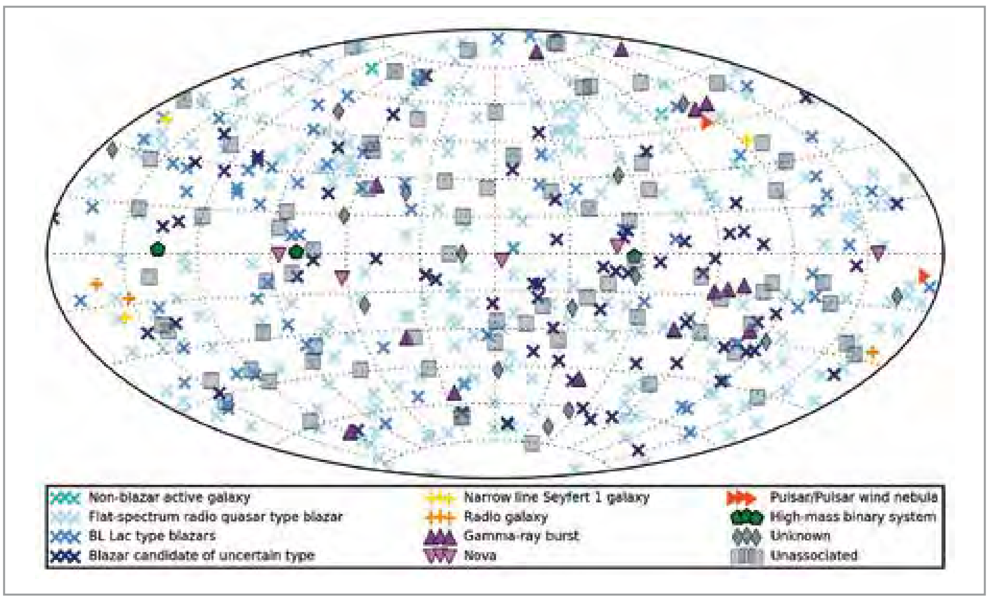

Figure 3

Sky map of the 2FAV sources, differentiated by source class (galactic coordinates, Aitoff projection)

Highlights from IceCube.

… the world's largest particle detector

In the IceCube neutrino observatory, more than 5000 optical sensors turn a cubic kilometre of Antarctic ice below the South Pole into the world's largest particle detector [1]. They record the very rare collisions of high-energy neutrinos produced either in the Earth's atmosphere or in distant astrophysical sources. IceCube was the first instrument that measured the spectrum and flavour composition of high-energy (>100 TeV) cosmic neutrinos [2]. It also demonstrated excellent capabilities in measuring fundamental properties of the neutrinos [3]. DESY is involved in a leading role in IceCube operation and data analysis.

Figure 1
At the heart of an active galaxy, matter falling into a supermassive black hole creates jets of particles travelling near the speed of light. In active galaxies classified as blazars, one of these jets points right towards Earth.
Credit: NASA/Goddard Space Flight Center Conceptual Image Lab

Origin of cosmic neutrinos remains elusive

The jets of relativistic particles that emanate from enormous black holes in the centre of some galaxies have been considered prime candidates for the origin of cosmic rays and neutrinos. In rare cases where such jets point towards Earth, the intensities of radiation and particle beams are amplified by several orders of magnitude, and they outshine most other objects in the sky. Indeed, the extragalactic gamma-ray sky above a few tens of GeV is dominated by these "blazars" (Fig. 1 and [4]). However, a recent IceCube study correlating neutrino arrival directions with large samples of blazars found in gamma rays revealed that these objects cannot be responsible for more than about 25% of the cosmic neutrinos observed by IceCube [5]. Fainter, but more numerous objects must produce the bulk of the observed high-energy neutrinos.

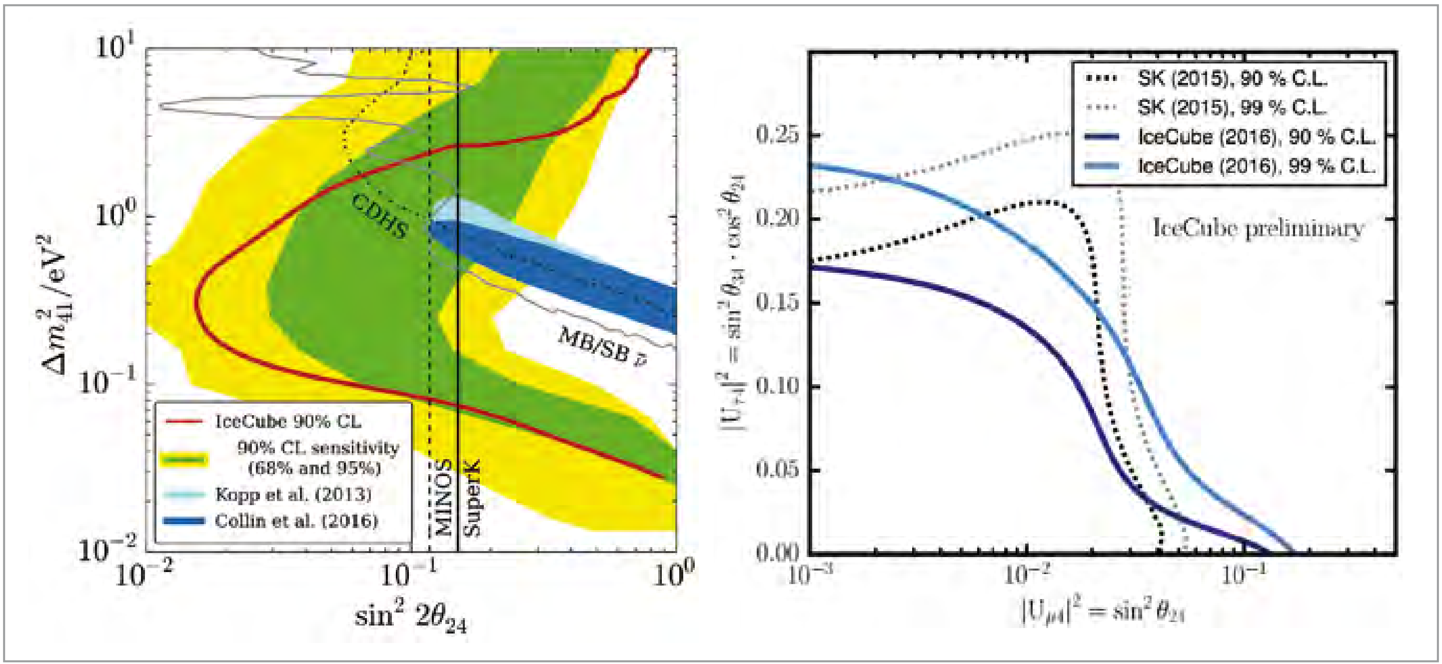

Figure 2

IceCube constraints on sterile neutrino oscillation parameters. Regions to the right of the IceCube lines are excluded.

Left: Comparison to confidence regions from other experiments. A sterile neutrino within the shaded blue region would explain the anomalies observed in some experiments. This area is clearly excluded by the IceCube results. Right: Combined constraints on two different mixing angles in comparison to results from the SuperKamiokande experiment in Japan. See [6,7] for detailed descriptions of these figures.

No evidence for sterile neutrinos

“Sterile” neutrinos are hypothetical particles that do not interact weakly, but “normal” neutrinos could oscillate into sterile neutrinos. They are motivated theoretically as such neutrinos could resolve some outstanding questions in cosmology and particle physics. Sterile neutrinos of masses around 1 eV could explain several anomalies observed in neutrino experiments at particle accelerators and nuclear reactors. In IceCube, the existence of these hypothetical particles would produce distinct distortions in the spatial and spectral arrival patterns of atmospheric neutrinos. IceCube is currently the most sensitive instrument to probe such an eV-scale sterile neutrino. No evidence for its existence was found, excluding the parameter space that would explain the anomalies mentioned above with high confidence (Fig. 2 left). Instead, the currently most stringent upper limits on the mixing angles, the parameters that govern the oscillation between ordinary and sterile neutrinos, can be set [6,7]. Figure 2 shows these constraints derived from two different analyses using high-energy and low-energy atmospheric neutrinos, respectively. The latter was led by DESY researchers.

Next major step in neutrino astronomy

Preparations for the IceCube-Gen2 project, a neutrino telescope promising ten times more cosmic neutrinos and a five times better sensitivity for astrophysical sources than the current IceCube detector, reached a first important milestone. The IceCube collaboration submitted a proposal to the US National Science Foundation to build “Gen2 Phase 1”. This first step would allow the development and construction of an improved hot water drill and the deployment of seven densely spaced and instrumented strings inside IceCube’s DeepCore region. If funded, Gen2 Phase 1 would significantly enhance IceCube’s sensitivity in the few-GeV neutrino energy range. It would also allow the installation of additional IceCube calibration devices and the in-situ testing of new detector technologies for IceCube-Gen2. The baseline sensor technology selected for Gen2 Phase 1 is the multi-photomultiplier digital optical module (mDOM), a sensor using 24 small-diameter (3") photomultiplier tubes in a glass pressure vessel. It is being developed in a collaboration of DESY and the universities of Erlangen and Münster in Germany. DESY is foreseen as one of the two production sites for the modules needed for Gen2 Phase 1.

Contact:

Markus Ackermann, markus.ackermann@desy.de
Timo Karg, timo.karg@desy.de

References:

[1] M.G. Aartsen et al., arXiv e-prints, astro-ph/1612.05093.
[2] M.G. Aartsen et al., Astrophys. J. 809 (2015) 98.
[3] M.G. Aartsen et al., Phys. Rev. D91 (2015) 072004.
[4] M. Ackermann et al., Phys. Rev. Lett. 116 (2016) 151105.
[5] M.G. Aartsen et al., arXiv e-prints, astro-ph/1611.03874.
[6] M.G. Aartsen et al., Phys. Rev. Lett. 117 (2016) 071801.
[7] Andrii Terliuk et al., Proc. of NEUTRINO 2016, London.

Completing the picture.

Neutrino searches with gamma-ray telescopes

Imaging air Cherenkov telescopes, such as MAGIC, H.E.S.S., VERITAS and the forthcoming CTA observatory, are primarily built to investigate cosmic gamma rays at very high energies. However, they are also sensitive tools to study cosmic neutrinos. DESY scientists are leading this effort by developing novel observation and data analysis techniques for the Major Atmospheric Gamma-ray Imaging Cherenkov (MAGIC) telescopes on La Palma, Spain.

Hunting for neutrino counterparts via gamma-ray follow-up

Thanks to the rapid development of observational techniques and physical theories in the past decade, our understanding of cosmic rays and their potential sources has made huge progress. With very high energy gamma-ray and neutrino astronomy, it became possible to probe the most energetic processes in the cosmos. Nevertheless, several key questions remain unanswered: What are the sources of high-energy cosmic rays and neutrinos? Is the neutrino and cosmic-ray emission constant in time, or is it variable? To which extent can the hadronic emission models proposed so far explain the observed data?

It is now clear that it is impossible to answer these questions with a single instrument. We rather need a multimessenger approach where several groups, running different instruments sensitive to different particles and energy ranges, coordinate their observations, exchange data and interpret them together. An example of such an approach is the collaboration – led by DESY scientists – between the MAGIC telescopes (Fig. 1) and the IceCube neutrino detector at the South Pole. The VERITAS and H.E.S.S. collaborations are pursuing similar programmes.

Since 2009, the MAGIC and IceCube groups at DESY have developed a gamma-ray follow-up programme, which

Figure 1

Stunning view of the two MAGIC Cherenkov telescopes at Roque de los Muchachos on the island of La Palma, Spain

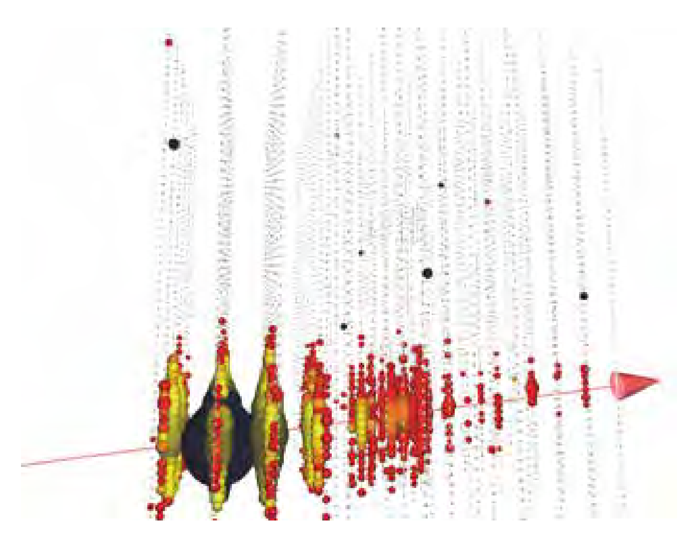

Figure 2:

Visualisation of an event with an energy of more than 100 TeV in IceCube, which initiated a follow-up observation with MAGIC in 2016

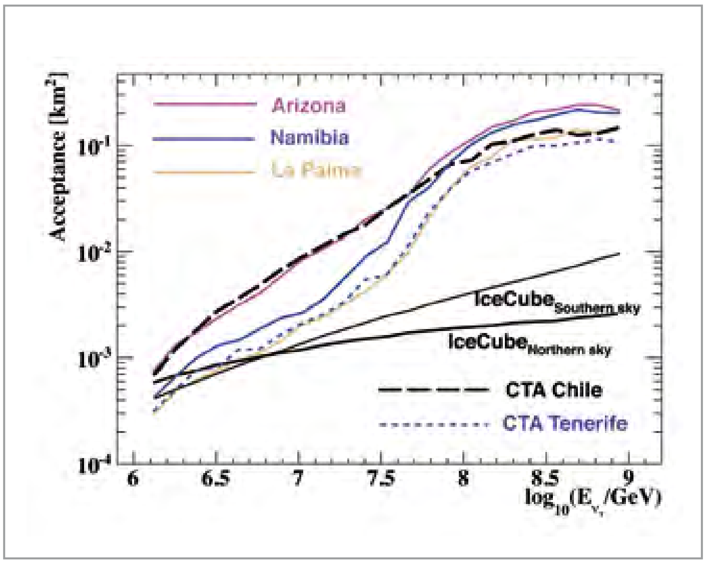

Figure 3

Acceptance (effective area) for point sources of earth-skimming tau neutrinos as estimated for a generic four-telescope observatory and for CTA and IceCube

searches for neutrino flares from known very high energy gamma-ray sources by using advanced machine learning techniques and a smart time-clustering algorithm [1]. MAGIC also participates in the gamma-ray follow-up of single high-energy neutrino events seen in IceCube, a programme that started in 2016. As of December 2016, MAGIC has followed two of five events observed in IceCube (Fig. 2) [2]. No gamma-ray signal has been detected so far, but a coincident detection is likely only a matter of time.

Fishing for tau neutrinos

Tau neutrinos are expected to be produced in astrophysical accelerators only in negligible amounts, but due to neutrino flavour changes (neutrino oscillations), they should appear in the neutrino flux detected at Earth. Indeed, the flavour composition of the neutrinos seen by IceCube is consistent with equal amounts of all three neutrino flavours [3], but up to now, there has been no unambiguous identification of individual tau neutrino events at high energies. The direct detection of tau-neutrino events is important from both the astrophysics and the particle physics standpoint. It will provide new information about the astrophysical neutrino flux and additional confirmation of the astrophysical origin of the IceCube high-energy neutrinos.

Tau neutrinos at PeV energies and above can be detected as they interact in the Earth or in a suitable mountain range, producing a tau lepton, which can escape into the atmosphere and produce a shower event through its decay. Such earth-skimming or slightly upward-going showers are unique signatures of tau neutrinos. These showers can be detected with Cherenkov telescopes pointing at directions just below the horizon.

The acceptance, an effective detection area for neutrinos from point sources, of possible observation schemes are shown in Fig. 3. DESY scientists have shown that at high energies and for comparable exposure times, e.g. in short flares, Cherenkov telescopes can be more sensitive than IceCube [4].

The MAGIC collaboration strives to bring this search method to fruition. In this mode of operation, the MAGIC telescopes, which are located 2200 m above sea level, are pointing towards the sea surface, slightly below the horizon. In this way, MAGIC is “fishing” for air showers induced by tau neutrinos. No such event has been detected so far, but here too, a detection is expected in due time.

Contact:

Elisa Bernardini, elisa.bernardini@desy.de
Konstancja Satalecka, konstancja.satalecka@desy.de
Dariusz Gora, dariusz.gora@desy.de

References:

[1] IceCube Collaboration, JINST 11 (2016) no.11, P11009.
[2] K. Satalecka et al. For the MAGIC Collaboration, AIP Conf. Proc. 1792 (2017) no.1, 070019.
[3] Ice Cube Collaboration, Phys. Rev. Lett. 114 (2015) no.17, 171102.
[4] D. Gora and E. Bernardini, Astropart. Phys. 82 (2016) 77.

Theoretical physics.

The DESY theory group covers a broad range of topics – from particle phenomenology and lattice gauge theory to cosmology and string theory. This scientific breadth is a unique asset of the group and of DESY, as it provides a setting for many fruitful interactions.

In particle phenomenology, results from the Large Hadron Colllider (LHC) at CERN are at the centre of current activities. These include general techniques for precision calculations (p. 76) and their application to Higgs physics (p. 72).

Particle phenomenology activities at DESY are deeply connect to efforts in both lattice gauge theory and cosmology. Lattice gauge theory, pursued by the DESY NIC group, is steadily approaching the goal of producing results for the limits of vanishing lattice spacing, infinite volume and physical quark masses (p. 74). In 2016, theoretical efforts in cosmology led to much progress in our understanding of realistic dark-matter models (p. 81) and of the relation between the cosmological dark matter and baryogenesis puzzles and the strong CP problem of the Standard Model (p. 70).

The fourth core activity of the group, string theory, has recently provided deeper insights into scale-invariant quantum field theories (p. 78) and into the bootstrap method for studying gauge theories (p. 82). The ultimate goal of these studies is to improve our understanding of the theories relevant for particle phenomenology.

The interconnectedness of these activities is underlined by efforts to realise inflation in particle physics and string theory (p. 80) as well as by the Collaborative Research Centre SFB 676 (p. 83), which provides a forum for fostering collaboration between different theoretical and experimental groups.

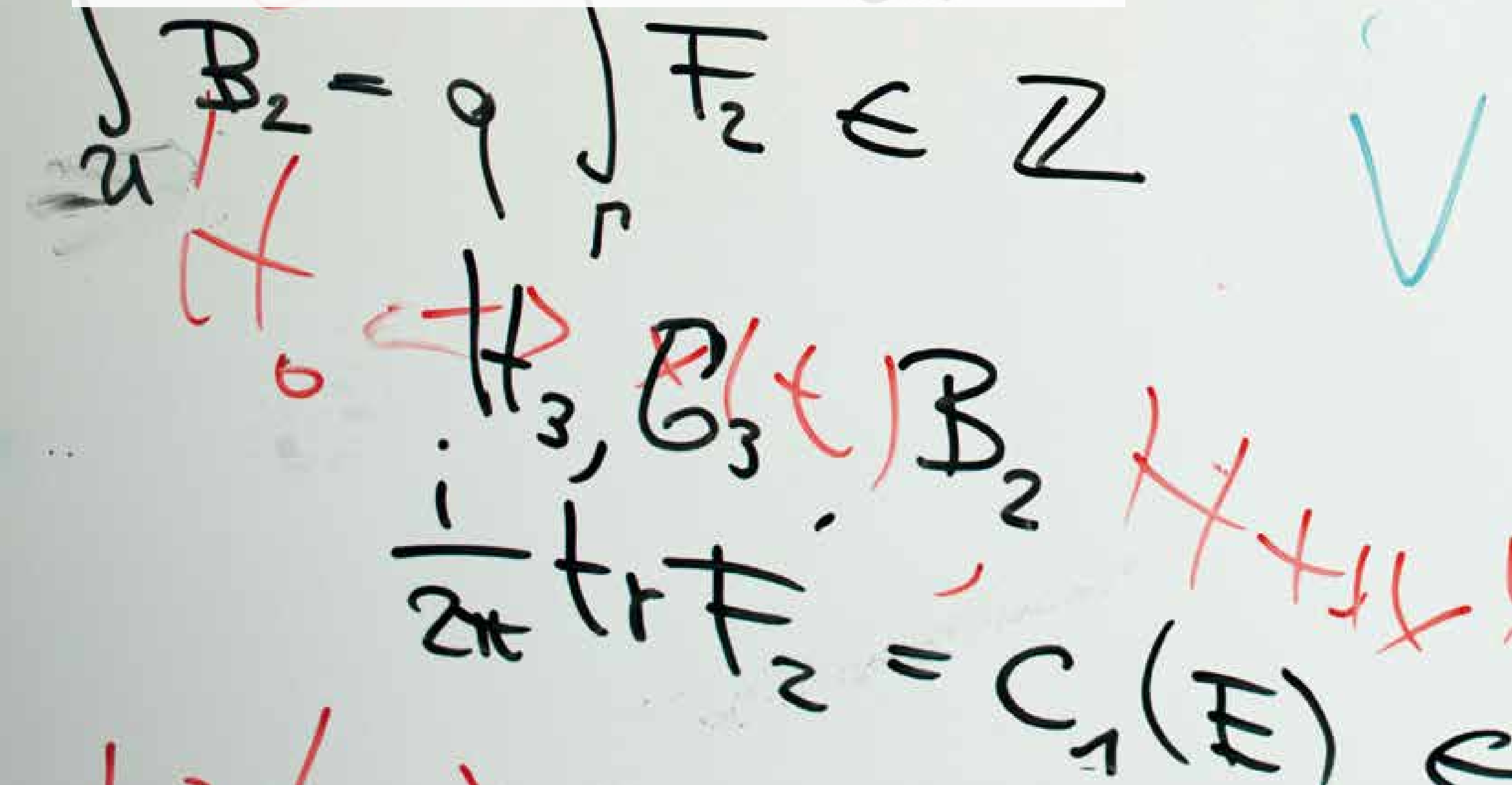

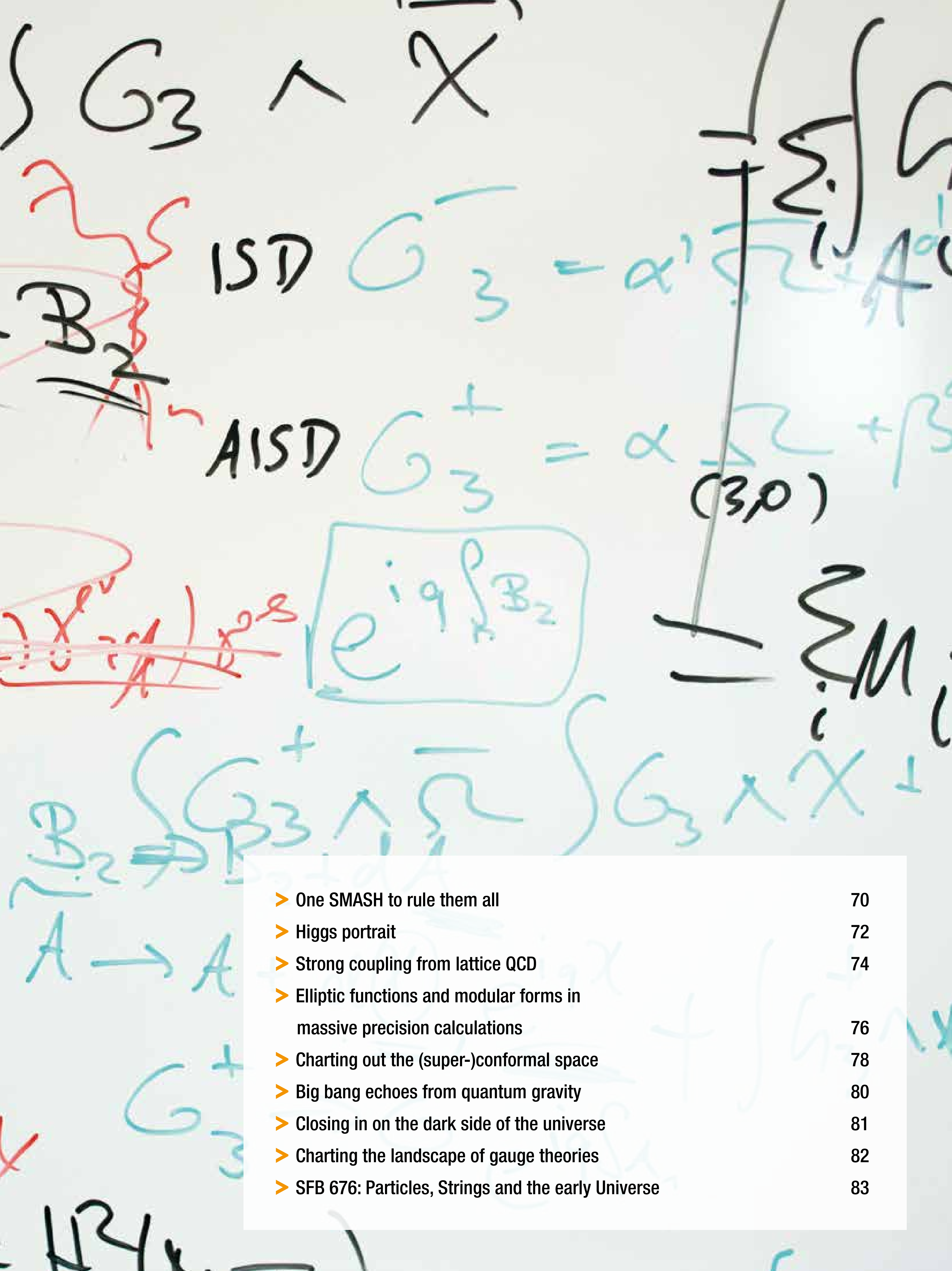
ISD
AISD
(3,0)

One SMASH to rule them all.

A minimal model of particle physics and cosmology

The discovery of the Higgs boson in 2012 marked the completion of the Standard Model of particle physics. However, the latter lacks an explanation of dark matter, cosmic inflation, the matter–antimatter asymmetry in the universe, neutrino oscillations and the feebleness of strong CP violation. A minimal extension of the Standard Model by three extra neutrinos, an extra quark and a scalar particle, which get their masses through the spontaneous breaking of a new global Abelian symmetry at a scale of around 10^{11} GeV, may explain all these puzzles in one go. This model, dubbed SMASH, can be probed decisively by upcoming cosmic microwave background and dark matter experiments.

The Standard Model (SM) describes the interactions of all known elementary particles with remarkable accuracy. So far, collider and other particle physics experiments have seen no significant deviation from its predictions. However, there are big fundamental problems in particle physics and cosmology that require the existence of new physics beyond the SM. Most importantly, there is tantamount evidence, ranging from the shapes of the rotation curves of spiral galaxies to the temperature fluctuations of the cosmic microwave background (CMB), that almost 85% of the matter in the universe is non-baryonic. Moreover, the SM cannot generate the primordial exponential expansion of the universe – known as inflation – that is needed to explain the statistically isotropic, Gaussian and nearly scale-invariant fluctuations of the CMB. The SM also lacks enough CP violation to explain why the universe contains a larger fraction of baryonic matter than of antimatter. Furthermore, in the SM, neutrinos are massless, but tiny masses are required to explain the observed neutrino flavour oscillations. Last but not least, the SM suffers from the strong CP problem: it does not explain the smallness of the θ angle of quantum chromodynamics (QCD), which induces CP-violation in flavour-diagonal interactions, notably a non-zero electric dipole moment of the neutron. In fact, the non-observation of the latter leads to the very strong upper limit $|\theta| < 10^{-10}$, requiring an extreme fine-tuning that cannot even be justified by anthropic reasoning.

Remarkably, as shown with participation of the DESY theory group, these five problems may be intertwined in a simple way, with a solution pointing to a unique new physics scale around 10^{11} GeV [1,2]. This model, dubbed Standard Model Axion Seesaw Higgs portal inflation model, or SMASH for short, consists in extending the SM particle content by three right-handed extra neutrinos, an extra quark and a complex scalar field, which are charged under a new global U(1) symmetry. The latter is assumed to be broken spontaneously at a large scale f_A given by the vacuum expectation value of the scalar field.

Correspondingly, the neutrino mass eigenstates split into a heavy set comprising three states with masses M_i proportional to f_A, composed of mixtures of the new right-handed neutrinos, and a light set of three states with masses inversely proportional to f_A, composed of mixtures of the SM left-handed neutrinos. Thus, the neutrino flavour oscillation puzzle is solved.

The extra quark and the excitation of the modulus of the new scalar field also get large masses proportional to f_A, while the

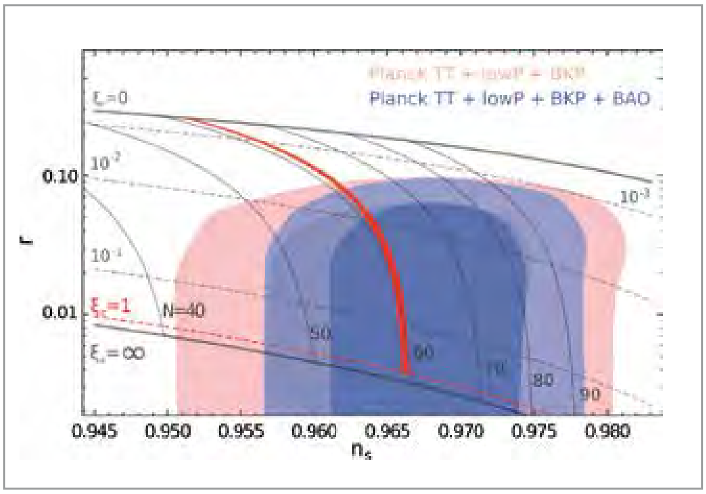

Figure 1

Tensor-to-scalar ratio r versus scalar spectral index n_s predicted by inflation in the SMASH model (red band), compared to the observationally preferred region

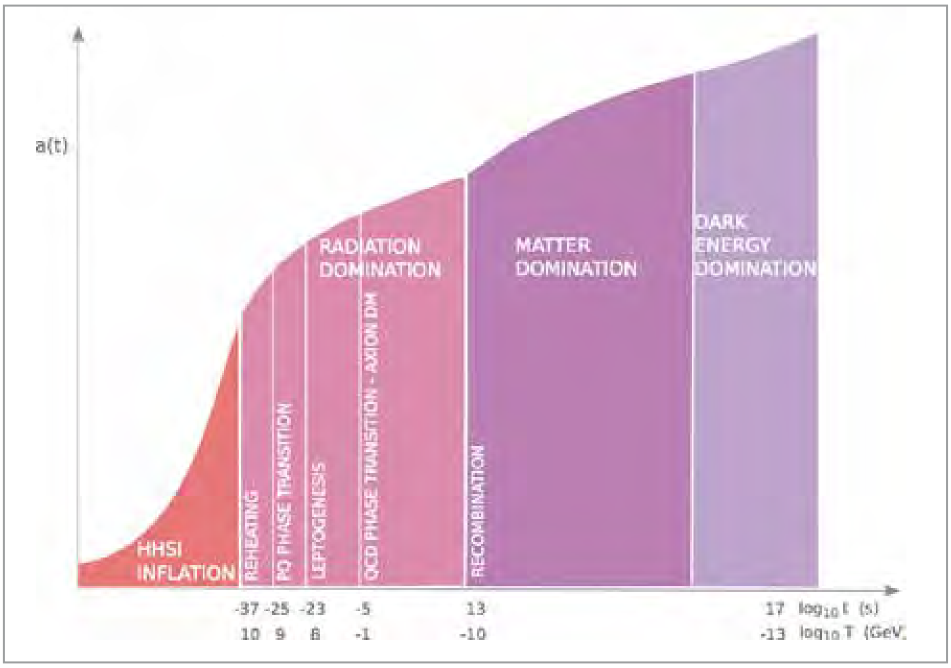

Figure 2

History of the universe. Evolution of the size of the universe as a function of time and temperature as predicted in the SMASH model. The plot emphasises the transition from inflation to epochs whose energy is dominated by radiation, standard matter and finally a cosmological constant.

excitation of the phase of the new scalar field stays very light, its mass being inversely proportional to f_A. Crucially, this phase field acquires a linear coupling to the gluonic topological charge density from a loop correction due to the extra quark. Correspondingly, it cancels the θ angle of QCD and thus solves the strong CP problem. Its excitation can therefore be identified with the axion. Its mass in units of f_A^{-1}, arising from the gluonic topological fluctuations, has recently been determined to a high accuracy, exploiting lattice QCD [3], resulting in m_A = 57.0(7) (10^{11}GeV/f_A) μeV.

Loop effects involving gravitons induce non-minimal gravitational couplings of the Higgs boson and of the new scalar field. These couplings make the scalar potential energy convex and asymptotically flat at very large field values. Correspondingly, a mixture of the modulus of the new scalar field and of the Higgs field can play the role of the inflaton. The predicted values of the CMB observables, such as the amplitude of the spectral index n_s of the scalar perturbations and the tensor-to-scalar ratio r, are perfectly consistent with current observations (Fig. 1) and can be probed decisively by upcoming CMB experiments.

Soon after reheating of the universe and breaking of the new U(1) symmetry, the decays of the right-handed neutrinos produce a lepton asymmetry (Fig. 2), which turns later, when the electroweak symmetry gets broken, into a baryon asymmetry.

Finally, at temperatures around the QCD transition between a quark–gluon and a hadron plasma phase, dark matter is produced in the form of a condensate of extremely non-relativistic axions. To account for all of the cold dark matter in the universe, the U(1) symmetry breaking scale is required to be in the range 3 x 10^{10} GeV < f_A < 1 x 10^{11} GeV, corresponding to an axion mass in the range 50 μeV < m_A < 200 μeV [1–3]. The prediction can be probed decisively in the upcoming decade by axion dark matter direct detection experiments (Fig. 3).

Adding a cosmological constant to account for the present acceleration of the universe, the SMASH model offers a self-contained description of particle physics from the electroweak scale to the Planck scale and of cosmology from inflation until today (Fig. 2).

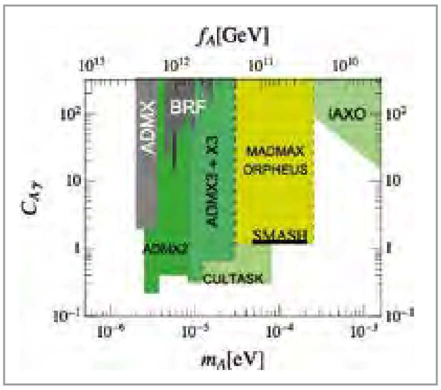

Figure 3

SMASH predictions for the axion–photon coupling: thick solid horizontal line vs. bounds from past (BRF), current (ADMX) and near-future axion dark matter experiments (ADMX2(3), MADMAX, ORPHEUS, X3 and the proposed solar axion experiment IAXO)

Contact:

Andreas Ringwald, andreas.ringwald@desy.de

References:

[1] G. Ballesteros, J. Redondo, A. Ringwald, C. Tamarit, Phys. Rev. Lett. 118 (2017) 071802.
[2] G. Ballesteros, J. Redondo, A. Ringwald, C.Tamarit, arXiv:1610.01639 [hep-ph].
[3] S. Borsanyi et al., Nature 539 (2016) no. 7627, 69.

Higgs portrait.

A tool to venture into landscapes beyond the Standard Model

If the sun has been shining for several billion years, it's because the weak interactions burning its hydrogen into helium are much weaker than the electromagnetic interactions. The cause of the screening of these weak interactions at long distances – in other words, the origin of the mass of the *W* and *Z* gauge bosons – has been puzzling the high-energy physics community for nearly half a century. The discovery of the Higgs boson in 2012 has opened up a new era, and experimental information on the physics behind the breaking of electroweak symmetry can now be collected. This breaking occurs at the high-energy frontier beyond which new physics is expected to supersede the Standard Model. The Higgs boson production and decay rates offer a new way to probe this frontier.

The Higgs boson and the mass problem

The Standard Model (SM) is a triumph of the combination of the two pillars of twentieth-century physics: quantum mechanics and special relativity. Particles are defined as representations of the Poincaré group. Mathematically, these representations are labelled by two quantities: the spin, which is quantised and takes on only discrete values, and the mass, which *a priori* is a continuous parameter. However, the transformation laws for the various elementary particles under the gauge symmetries associated with the fundamental interactions force the masses of these particles to vanish. This is in flagrant contradiction to the experimental measurements.

The Brout–Englert–Higgs (BEH) mechanism provides the solution to this mass conundrum. The discovery of a Higgs boson in July 2012 and the experimental confirmation of the BEH mechanism by the ATLAS and CMS collaborations at the LHC marked a historical step in our understanding of nature: the masses of the elementary particles are not fundamental parameters defined at very high energy but rather emergent quantities appearing at low energy as a result of the particular structure of the vacuum.

Quantum mechanics tells us that, in contrast to the photon, a massive spin-1 particle such as the *W* and *Z* boson has not only two transverse polarisations but also one extra longitudinal mode. At very high energy, the interactions of these longitudinal modes increase incommensurably and challenge the predictivity of the theory. The Higgs boson intervenes to regulate the growth of these interactions. To achieve this role, the Higgs boson's couplings to the massive SM particles – quarks, leptons and gauge bosons – have to be intimately linked to the mass of these particles, and any deviation from this relation would require yet another particle or a new dynamics to complete the task of the Higgs boson – hence the importance of precisely determining all the Higgs couplings.

Measuring the Higgs production and decay rates in the various channels provides an access to these couplings (Fig. 1). Chief among all, the coupling between the Higgs boson and the top quark plays a fundamental role as it controls the stability of the electroweak vacuum over cosmological times and also carries the dominant quantum correction to the Higgs boson mass.

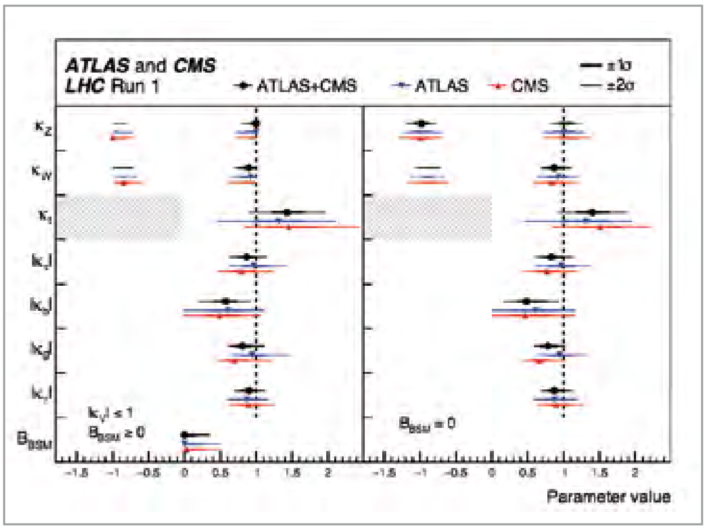

Figure 1

ATLAS and CMS fits to the Higgs coupling modifiers. The measurements are in good agreement with SM predictions, represented by the straight dashed vertical line. But current inclusive measurements remain blind to larger and elusive deviations. See Ref. [1] for details.

Effective field theory approach to Higgs coupling measurements

Beyond the discovery of the Higgs boson, the second most important result inherited from the first operational runs of the LHC is that the beyond-the-SM particle population does not seem to be as light as the naturalness criteria would have suggested. One way it can still manifest itself is through deviations from the SM in the Higgs couplings. In order to capture these effects in a model-independent way, it is handy to consider higher-dimensional interactions among the SM particles supplementing the SM Lagrangian once the heavy degrees of freedom are kept frozen.

Among the 59 generic deformations of the SM at leading order, it was shown that eight of them are particular to Higgs physics since they only impact the Higgs production and decay rates but neither the electroweak nor the jet observables. These deformations tend to have an effect not only on the total rates but also on the kinematical distributions, for instance the Higgs transverse momentum when produced in association with an extra gauge boson. The larger the energy, the larger the impact. But one has to remain careful not to extrapolate the effective interactions into a regime where they cease to be valid, for instance when enough energy is available to excite new degrees of freedom.

In Ref. [2], members of the DESY theory group participated in a study that addressed the following points and proposed a practical recipe to conduct experimental analyses in an effective field theory framework: (i) Under what conditions does the effective theory give a faithful description of the low-energy phenomenology of some explicit models? (ii) When is it justified to truncate the effective theory expansion at the leading order? To what extent can experimental limits on leading-order deformations be affected by the presence of next-to-leading order deformations? Are there physically important examples where next-to-leading order deformations cannot be neglected? (iii) When is it justified to calculate the effective theory predictions at the classical level? In what circumstances may including quantum corrections and/or real-emission corrections modify the predictions in a relevant way?

These questions cannot be addressed in a completely model-independent way, but require a number of (broad) assumptions about the new physics, characterised by its symmetry properties and a collection of selection rules.

Beyond inclusive Higgs measurements

The dominant production mode of the Higgs at the LHC is the so-called gluon fusion channel. This is a purely radiative process mediated by the top quark. The lightness of the Higgs boson plays a malicious role and makes it impossible to disentangle short- and long-distance contributions to the total rate. This limitation is embodied in the Higgs low-energy theorem, which prevents one from resolving the loop contribution itself. New physics could modify the top-quark

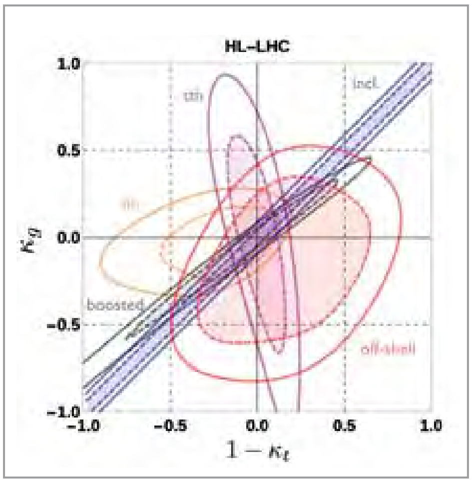

Figure 2
While the dominant inclusive Higgs channels cannot disentangle a modification of the Higgs coupling to the top quark from a contact interaction with the gluons/photons, other channels exploring extreme regions of the kinematical phase space can pin down these couplings individually. See Ref. [3] for details.

Yukawa coupling and also generate a contact interaction with the gluons without leaving any impact on the total rate. Concrete examples are vector-like quarks mixing with the top quark in composite Higgs models or top scalars in supersymmetric extensions of the SM. Still, extra radiation in the form of a boosted jet produced together with the Higgs boson will allow the structure of the top-quark loop to be explored. When the extra radiation carries away a large amount of energy and boosts the Higgs boson, the process effectively probes the high-energy structure of the Higgs–top interactions (Fig. 2).

As for any other quantum particle, the influence of the Higgs boson is not limited to its mass shell. In 2014, the CMS and ATLAS collaborations reported the differential cross section measurement of $pp \to Z^*Z^* \to 4l, 2l2\nu$ at high invariant mass of the ZZ system. This process receives a sizeable contribution from a Higgs produced off-shell by gluon fusion. As such, this process potentially carries information relevant for probing the effective Higgs couplings at large momenta and could thus reveal the energy dependence of the Higgs couplings controlled by higher-dimensional operators with extra derivatives.

It was proposed to use the off-shell Higgs data to constrain the Higgs width. However, this bound actually holds under the assumption that the Higgs couplings remain unaltered over a large range of energy scales and thus applies only to very specific models. Instead, the off-shell measurement offers a unique access to the structure of the Higgs couplings at high energy and thus a check of the fundamental property of the Higgs boson as a unitarising agent of all the scattering amplitudes.

Contact:
Christophe Grojean, christophe.grojean@desy.de

References:

[1] M. Carena, C. Grojean, M. Kado and V. Sharma, Chin. Phys. C40 (2016) 100001.
[2] R. Contino, A. Falkowski, F. Goertz, C. Grojean and F. Riva, JHEP 1607 (2016) 144.
[3] A. Azatov, C. Grojean, A. Paul and E. Salvioni, JHEP 1609 (2016) 123.

Strong coupling from lattice QCD.

DESY NIC group computes high-precision α_s for physics at the LHC

Led by the John von Neumann Institute for Computing (NIC) group at DESY, the ALPHA collaboration has computed one of the most elusive fundamental parameters of nature: the strong coupling, which governs the interactions of quarks and gluons. At high energies, such as the ones reached at the LHC, many processes can be computed in terms of Taylor series of this coupling. A precise input value for these series is thus essential to make full use of the LHC. The ALPHA collaboration simulated the fundamental theory of strong interactions, quantum chromodynamics (QCD), over a large range of energy scales in order to extract the coupling at LHC energies using input from low-energy hadronic observables.

Particle physics and QCD simulations

The Standard Model (SM) of particle physics describes the interactions of the fundamental constituents of matter through electromagnetic, weak and strong forces by means of three different quantum gauge theories. It does so with a surprising precision in terms of very few fundamental constants of nature. Its success is not only a consequence of the mathematical simplicity of its basic equations, but also of the fact that the forces they describe are relatively weak at the typical energy transfers of about 10–100 GeV in particle physics scattering experiments.

The strengths of the interactions are characterised by coupling constants. When the forces are weak, the predictions of the theory can be worked out in terms of an expansion in powers of these coupling constants, a procedure known as perturbation theory. For instance, in quantum electrodynamics (QED), the quantum gauge theory describing the interactions between electrons and photons, the coupling constant is the well-known fine structure constant $\alpha \sim 1/137$. Its smallness guarantees that already a few terms in the power series are sufficient to predict physical quantities with high precision.

In the gauge theory for the strong force, QCD, quarks and gluons assume the roles of the electrons and photons of QED. The QCD coupling is called α_s. One important property of all coupling "constants" in the SM is that they depend on the energy transfer μ in the interaction process. In this sense, they are not really constant but rather a function of μ, which is why the strong coupling is called the running coupling $\alpha_s(\mu)$. At high energy, the strong coupling has been determined to be approximately α_s(100 GeV) ~ 0.11. Although this is much larger than the fine structure constant of QED, perturbation theory still works well. However, if the energy scale μ is decreased the function $\alpha_s(\mu)$ increases. In fact, at μ below 1 GeV, it becomes so large that perturbation theory cannot be relied on any more at all. Particle theorists therefore require another tool that is able to deal with large values of α_s. A *non-perturbative* method is needed to work out the predictions of QCD in this situation.

The simple and elegant theory of QCD is formulated in terms of quarks and gluons. Yet, what is observed in experiments at low energies, say, μ below a few GeV, are protons, neutrons, π mesons and many other particles, all known as hadrons. In fact, a striking property of QCD is "confinement", which means that quarks and gluons themselves cannot be produced in experiments. They are confined inside hadrons.

Computer simulations of QCD formulated on a discrete lattice of space–time points allow for a non-perturbative treatment of the theory in the low-energy regime. As usual when numerical approximations on grids come into play, one must extrapolate the answers to the continuum limit by studying sequences of progressively finer discretisations. In addition, computers demand the restriction of space–time to a finite region, which is an approximation that has to be controlled. In such lattice simulations, it is natural to use a few hadron masses as input to tune the free parameters in lattice QCD and then predict the rest.

Determining the strong coupling

To establish a unified description for all energies, we need to relate the input parameters of perturbative QCD and of lattice QCD to each other. This is a difficult problem, because it requires non-perturbative control as well as the simultaneous

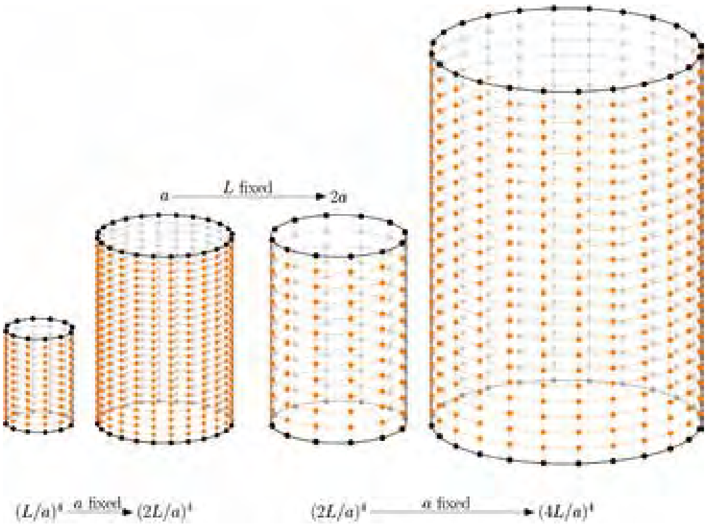

Figure 1

Some of the lattices used to connect larger and larger length scales in the finite-size scaling strategy. More lattices are used with finer resolution a/L to also extrapolate to the continuum limit $a/L \to 0$.

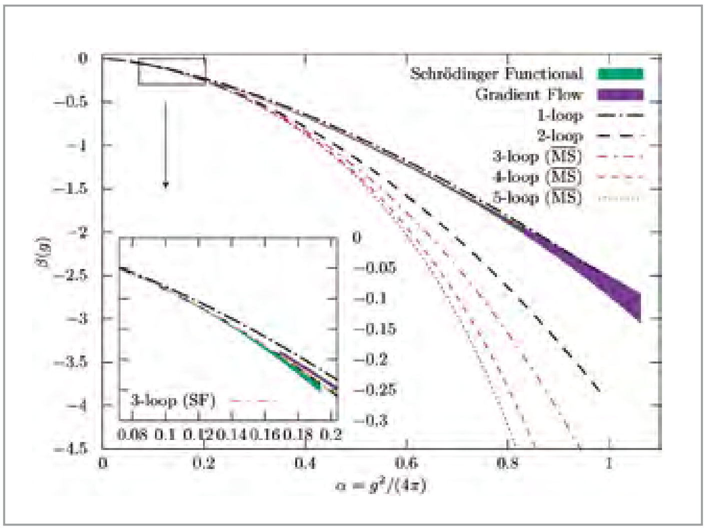

Figure 2

Logarithmic derivative of the QCD coupling, $\beta(g) = \mu \; dg(\mu)/d\mu$. Two different definitions (so-called schemes) are employed in the non-perturbative computations: the "Schrödinger functional" scheme is advantageous in the high-energy/small-α region and the "gradient flow" scheme is very precise at large α. "n-loop" refers to the perturbative series truncated at the order n.

handling of a hadronic scale and a much higher energy scale with both of them discretised finely enough. The ALPHA collaboration is devoted to solving this problem and has developed a recursive finite-size scaling technique to this end.

The decisive idea of this method is to consider a sequence of deliberately finite-sized and mostly even very small boxes ("femto universe") with QCD dynamics inside. The smallest system is chosen such that – due to Heisenberg's uncertainty relation – it can be related by perturbative QCD to high-energy scatterings in an infinite volume. Then successive boxes differ by scale factors of 2 only and are related to each other by taking the continuum limit of simulation results (Fig. 1).

Eventually, one arrives at a box large enough that hadrons fit in. In this way, the multiscale problem is circumvented, and a physical scale ratio is implemented that grows exponentially with the number of steps. This method does not compromise with the multiple scales by handling them on single lattices and is thus amenable to systematic improvement and error control.

Before the method could deliver precise results for QCD, with the relevant up, down and strange quarks included, a number of details had to be developed to perfection (Fig. 2). In addition, the large-volume simulations described in *DESY Particle Physics 2015* needed to be finished. All these milestones were achieved. The ALPHA collaboration was then able to put the pieces together and provide a value for the strong coupling at large energy μ.

Result

The final result of the computations, which were released at the 2016 lattice field theory symposium, is

$$\alpha_s(93\text{ GeV}) = 0.1179(10)(2).$$

This value is in agreement with and more precise than the current world average of a number of different determinations. Most importantly, the ALPHA computation in the three-flavour theory was done at a new level of rigour, using perturbation theory only when α_s is small, but still keeping excellent non-perturbative precision.

The value obtained here can be used with good confidence in the analysis of LHC data, both for the comparison to SM theory and for the search of physics not contained in the SM. In the latter case, the predictions for the background due to known processes usually depend on α_s.

These simulations include only the three lighter of the six quarks. The heavier ones have been added perturbatively. The power series describing these additions are very well behaved. They give rise to the second uncertainty in the value given above. It will be an interesting and worthwhile project to remove any doubt of this use of perturbation theory by including the next-heavier quark in the simulations.

Contact:

Karl Jansen, karl.jansen@desy.de
Stefan Schäfer, stefan.schaefer@desy.de
Hubert Simma, hubert.simma@desy.de
Rainer Sommer, rainer.sommer@desy.de

References:

[1] M. Bruno et al., arXiv:1611.05750.
[2] ALPHA Collaboration, Phys. Rev. D95 (2017) no.1, 014507.
[3] ALPHA Collaboration, Phys. Rev. Lett. 117 (2016) no. 18, 182001.

Elliptic functions and modular forms in massive precision calculations.

New type of integrals in quantum field theory

Precision calculations for observables measured at high-energy colliders can often be performed analytically in case of QED and QCD corrections even at very high order. Both intermediary and final results can be expressed in special function spaces, which successively enlarge with the complication of the calculation, the loop order and the number of parameters involved. Members of the DESY theory group studied a new class of integrals, which appears in various three-loop massive QCD calculations: the non-iterative iterative integrals, following the well-known iterative integrals over general alphabets, which fully describe simpler results.

Iterative integrals

Higher-order precision calculations within QCD and QED in case of not too many scales usually lead to results that can be expressed by iterative integrals. This applies to many results up to two-loop and even higher orders. By iterative integrals, we mean expressions of the form

$$H_{a,b}(x) = \int_0^x dy\, f_a(y)\, H_b(y)\,.$$

The letters $f_a(x)$ form the alphabet for the corresponding iterative integral. In the simplest case, one finds $f_a(x)$ as an element of the set $\{1/x, 1/(1-x), 1/(1+x)\}$. Generalisations are letters of the type $1/(x-b)$, or e.g. the cyclotomic letters $1/(1+x^2)$ and $1/(1-x+x^2)$. There are even more general cases in which square roots of quadratic forms occur. Examples are $1/(1-x)^{1/2}$ and $1/[x\,((1+x)(2+x))^{1/2}]$. All these cases have been studied systematically, see Ref. [1] for recent reviews.

A common property of all these function spaces is that the corresponding iterative integrals form shuffle algebras, which imply mutual relations, as e.g.
$H_a(x)\, H_{b,c,d}(x) = H_{a,b,c,d}(x) + H_{b,a,c,d}(x) + H_{b,c,a,d}(x) + H_{b,c,d,a}(x)$.
Associated to the iterative integrals are the nested sums. One may calculate the Mellin transform of an iterative integral

$$\int_0^1 dx H_A(x)\, x^N = S_B(N)\,,$$

where A and B are certain index sets. An example is

$$\int_0^1 dx \frac{H_0(x)}{1-x}\, x^N = S_2(N) - \zeta_2 = \sum_{k=1}^{N} \frac{1}{k^2} - \zeta_2\,,$$

with $H_0(x) = \ln(x)$. Here,

$$M[f(x)](N) = \int_0^1 dx\, x^N\, f(x)$$

denotes the Mellin transform.

In case the physical problem depends only on up to one scale, there is an algorithm to find all iterative integrals or nested sum representations if the problem can be factorised in first order, see Ref. [2]. The algorithm operates both in x- and in Mellin N-space, i.e. it solves the respective coupled systems of ordinary differential or difference equations. It delivers all the contributing letters of the solution and will thereby even create new alphabets, whenever needed. Furthermore, all known relations between the respective sums and integrals are used to provide a minimal representation.

Not all the integrals emerging, however, will be of the iterative type. Let us consider a typical one-scale problem, as emerging in the three-loop heavy-flavour corrections to deep-inelastic scattering. Here, Feynman integrals contribute that neither factorise in x- nor Mellin N-space at first order, as the algorithm of Ref. [2] shows. The first new terms are usually elliptic integrals. One should note that in general, however, integrals of this type may emerge with simpler arguments in x-space, but factorise to first order in N-space, as the example

$$\int_0^1 \frac{dy}{y} \frac{1}{\sqrt{1-y}\sqrt{1-x/y}} = 2K(1-x)$$

shows, where

$$2M\,[K(1-x)]\,(N) = \left[\frac{4^N}{\binom{2N}{N}} \frac{2}{(2N+1)}\right]^2.$$

In the following, we will consider the non-factorising cases.

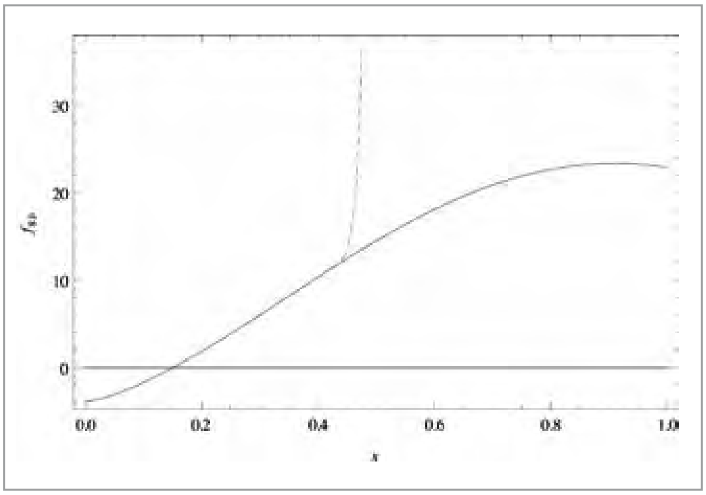

Figure 1

Master integral contributing to the three-loop QCD corrections of the ρ-parameter as a function of x.
Blue line: analytic expansion around $x = 1$;
red line: analytic expansion around $x = 0$. From Ref. [3].

Iterative non-iterative integrals

In case the first-order factorisation cannot be obtained both in x- and N-space, new letters $F_a(x)$ will appear, which have an integral representation

$$F_a(x) = \int_0^1 dy\, g_a\left(y; r(x)\right) ,$$

such that it is impossible to write the function with its x-dependence occurring in the integration boundaries only. $F_a(x)$ now appears as a new type of letter within an otherwise iterative integral

$$H_A(x) = \int_0^x dy_1\, f_a(y_1) \int_0^{y_1} dy_2 \ldots \int_0^{y_{n-1}} dy_n\, F_b(y_n) \ldots .$$

Because the whole expression is still iterative, but $F_a(x)$ is not, we call the respective integrals “iterative non-iterative integrals”. Indeed, this is now the whole possible class remaining. With respect to the representation mentioned above, $H_A(x)$ still exhibits shuffle properties, always keeping the $F_a(x)$ as new entities.

Fast and precise numerical representations can be obtained by expanding analytically around the values $x = 0$ and $x = 1$, or if needed around more points, even in case that a singularity is contained in the interval [0,1], as shown in Fig. 1. The expansions have a wide overlap and finally cover the full solution.

In case $F_a(x)$ can be represented by an elliptic integral $I(q(x))$, with a certain rational function $q(x)$, so-called q-series representations can be derived, i.e.

$$I = \sum_{l=0}^{\infty} a_l\, q^l , \quad q = \exp(i\pi\tau) , \quad \tau = iK(1-r)/K(r) .$$

In the simplest cases, one finds representations in terms of elliptic polylogarithms, see Ref. [3,4]. The theory of modular forms may be used to classify the associated function spaces. The q-series and elliptic polylogarithm representations will play an increasing role, together with the analytic series representations mentioned before, in the treatment of these new structures in higher-loop Feynman integrals. It has to be generally assumed that in higher and higher loops as well as when adding more legs, the respective function spaces grow further. Yet, the possibility to derive analytic results is important to master even larger problems, at least in parts. In this way, faster and more stable numerical representations, which are highly relevant for experimental precision analyses, can also be obtained. Methods originally developed within number theory are now applied in quantum field theory to solve advanced problems. One may assume that even more complicated problems will challenge new developments in number theory and related fields in the future in return.

Contact:
Johannes Blümlein, johannes.bluemlein@desy.de

References:

[1] J. Ablinger and J. Blümlein, arXiv:1304.7071;
J. Ablinger, J. Blümlein and C. Schneider, J. Phys. Conf. Ser. 523 (2014) 012060.
[2] J. Ablinger, A. Behring, J. Blümlein, A. De Freitas, A. von Manteuffel, C. Schneider, Comput. Phys. Commun. 202 (2016) 22-112.
[3] J. Ablinger, A. Behring, J. Blümlein, A. De Freitas, M. van Hoeij, E. Imamoglu, C.G. Raab, and C. Schneider, DESY 16-147.
[4] L. Adams, C. Bogner and S. Weinzierl, J. Math. Phys. 56 (2015) 072303.

Charting out the (super-)conformal space.

A bootstrap approach to quantum field theories

The conformal bootstrap is an old dream in theoretical physics, whereby general consistency requirements and symmetries alone are powerful enough to completely solve specific models. Recent developments have revived this dream and opened up the possibility of exploring new theories for which traditional quantum field theory methods are insufficient.

Reviving the bootstrap programme

Quantum field theories (QFTs) are a natural language for theoretical physics, used to describe physical systems from condensed matter to particle physics. QFTs generically display a non-trivial dependence on a choice of length scale, described by the concept of renormalisation group (RG) flow. Such a flow starts from a fixed point – a conformal field theory (CFT) – followed by a particular, so-called relevant deformation. Not only do CFTs appear in the short-distance description of ultraviolet-complete theories, but the long-distance behaviour of a QFT is also described, in most circumstances, by a (possibly trivial) CFT. In this context, CFTs are ubiquitous for studying and understanding QFTs. A promising, albeit ambitious goal would be to fully characterise all possible CFTs – all fixed points of the RG flow – as a first step towards understanding QFTs in general.

CFTs are strongly constrained by their symmetries, and the idea behind the conformal bootstrap programme is to leverage the symmetries as much as possible. The goals are twofold. Not only do we want to classify the space of allowed theories, but we also want to be able to *solve* each theory, i.e. describe it as completely as possible. This programme was very successful in the past for special classes of two-dimensional theories, but beyond these special classes, and more generally beyond two dimensions, it had fallen short. This changed with a recent revival by Rattazzi, Rychkov, Tonni and Vichi in 2008.

To summarise it very briefly, the bootstrap takes an algebraic viewpoint, defining CFTs as a collection of local operators and all their correlation functions – the CFT data. However, not any random set of CFT data will define a consistent theory, and one must impose the symmetries of the problem and general consistency requirements, such as unitarity and the associativity of the operator product algebra. These are very powerful restrictions that place strong constraints on the CFT data. The recent revival stemmed from a change of emphasis: instead of solving all the restrictions, one simply (numerically) constrains the space of solutions.

A key advantage of the bootstrap approach is that it does not rely on any perturbative description of the theory and it does not require any Lagrangian description. The results are therefore non-perturbative in nature, giving the full answer. All of this makes the bootstrap the ideal tool to study many of the known, interesting, interacting superconformal field theories (SCFTs), which lack a Lagrangian description, thus rendering most of the traditional QFT approaches ineffective. In the past few years, a tremendous amount of work, carried out by various authors, has given us access to information on intrinsically strongly coupled theories, which are hard to access through standard field theory techniques.

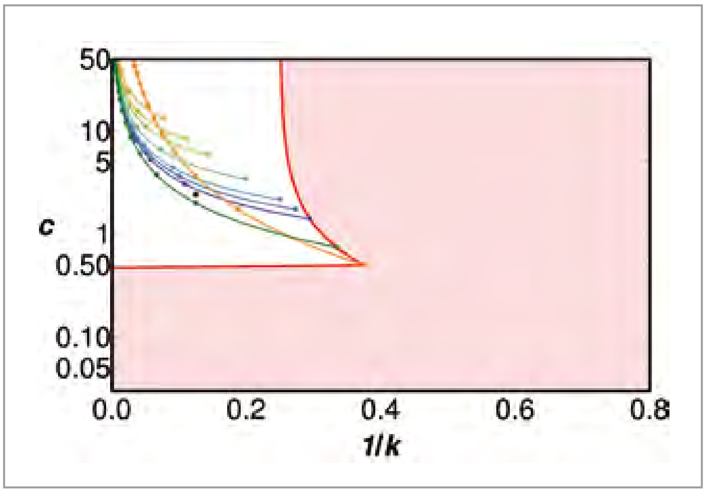

Figure 1

Space of superconformal field theories with an SU(2) flavour symmetry constrained by the conformal bootstrap [1,2]

Charting the superconformal space

Adding supersymmetry allows us to go deeper in the exploration of the space of CFTs. In fact, recent work has shown that SCFTs with enough supersymmetry in four dimensions contain a protected subsector that is exactly solvable [1]. Members of the DESY theory group have been exploring this protected subsector and using it to obtain *analytic* results on SCFTs.

An illustrative example is shown in Fig. 1, where we plot a slice of the space of $N = 2$ SCFTs, with a global SU(2) “flavour” symmetry. This slice is parameterised by two numbers one can universally associate to CFTs, the c and k anomaly coefficients, or central charges. All known interacting theories appear to occupy a mysteriously small portion of this parameter space. This is illustrated in Fig. 1 by the coloured dots, which mark the position of a representative set of known theories, with lines connecting families of theories. In [1,2], we discovered the existence of unitarity bounds disallowing a big portion, shaded in red in Fig. 1, of the mysteriously empty region and drastically constraining the space of allowed SCFTs. Aside from these encouraging results, to move the exploration of the space of SCFTs beyond this protected subsector, we must also employ *numerical* bootstrap techniques.

Solving superconformal theories?

Quintessential examples of theories one would hope to solve using bootstrap techniques are the maximally supersymmetric six-dimensional CFTs. Standard power-counting arguments tell us that there can be no interacting theories in six dimensions. Nevertheless, non-trivial examples, lacking a conventional Lagrangian description, have been constructed using string-theoretic methods. Moreover, these theories play a central role in theoretical physics, giving rise to a rich plethora of lower-dimensional theories via compactifications.

The numerical bootstrap approach to these theories seems promising [3], yielding the first results for observables not protected by supersymmetry, and further research is being carried out in the DESY theory group. Another prime example is given by interacting four-dimensional $N = 3$ SCFTs, which until the work of García-Etxebarria and Regalado in 2016, were generally believed not to exist. In [4], we took the first steps towards the bootstrap study of $N = 3$ SCFTs, using a combination of numerical techniques and the afore-mentioned solvable subsector.

Contact:

Madalena Lemos, madalena.lemos@desy.de

References:

[1] C. Beem et al, Commun. Math. Phys. 336 (2015) no. 3, 1359.
[2] M. Lemos and P. Liendo, JHEP 1604 (2016) 004.
[3] C. Beem, M. Lemos, L. Rastelli and B. C. van Rees, Phys. Rev. D 93 (2016) no. 2, 025016.
[4] M. Lemos, P. Liendo, C. Meneghelli and V. Mitev, arxiv: 1612.01536.

Big bang echoes from quantum gravity.

From microwaves in the sky to inflation in string theory

Observational cosmology suggests that a very early phase of cosmic inflation was at the origin of the hot big bang. Future observations of the cosmic microwave background (CMB) may produce evidence for the primordial gravitational waves generated during inflation. If they do, the required energy scale of inflation is so high that this may enable us to listen to big bang echoes from quantum gravity. This is the aspiration of the European Research Council (ERC) Consolidator Grant “STRINGFLATION” funded at DESY.

The term “inflation” denotes a form of quasi-exponential expansion of the very early universe driven by the potential energy density of a slowly rolling scalar field. Inflation generated the primordial density fluctuations responsible for all of the visible structures of the universe today, such as those that can be seen in the high-precision CMB data from the Planck satellite. Moreover, inflation should also have produced a spectrum of primordial gravitational waves. Their intensity relative to the intensity of density fluctuations depends on the energy scale of inflation.

If such primordial gravitational waves do indeed exist, they would have imprinted a particular pattern in the polarisation of the electromagnetic radiation of the CMB, the so-called *B*-mode or curl pattern. Ongoing observations of polarisation, such as those made by the Planck satellite or ground-based telescopes like BICEP2 or the Keck Array in Antarctica, already significantly constrain this pattern and may detect it in the near future. Detecting such a signal would imply that the energy scale of inflation is sufficiently high that string theory can modify the inflationary predictions – and may thus be testable.

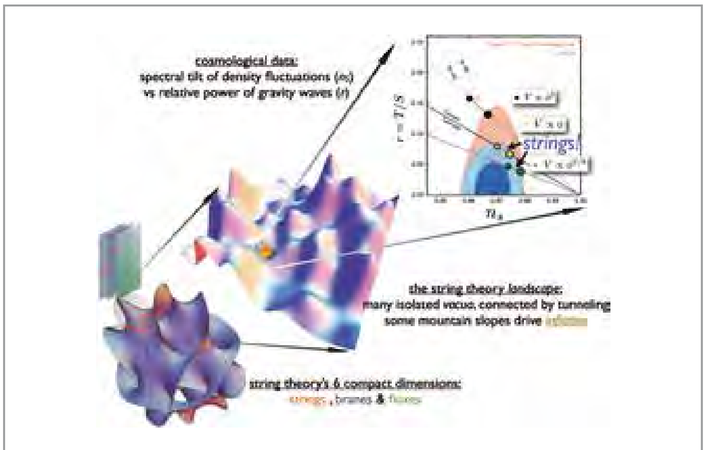

Figure 1

String theory produces a landscape of vacua, some containing inflationary slopes. High enough slopes generate gravitational waves detectable by future CMB polarisation probes. Compared to naive field theory, their stringy origin “deforms” the shape of the slopes and their inflationary predictions.

In the past years, members of the DESY theory group constructed high-scale models of inflation in string theory. The study showed, moreover, that there seems to be a generic tendency in the string landscape to “flatten” away the strength of gravitational waves from the naive field theory expectation. The group found that this “flattening” leads to many string inflation models with gradually suppressed gravitational wave power [1]. Finally, in 2015, the group applied very general consequences of black-hole physics for quantum gravity to descriptions of high-scale inflation in string theory, which produced a general constraint compatible with the “flattening” behaviour [2].

Based on these results, the recently awarded ERC grant, funding of which started in fall 2015, will enable the group during the next five years to analyse the systematics and general dynamics of high-scale inflation in string theory. This may in the end provide a link for observationally testing the theory.

ERC Consolidator Grant

“STRINGFLATION: Inflation in string theory – connecting quantum gravity with observations”

erc

Contact:

Alexander Westphal, alexander.westphal@desy.de
http://www.desy.de/~westphal/

References:

[1] arXiv:1405.3652, arXiv:1509.00024.
[2] arXiv:1512.03768, arXiv:1409.5350.

Closing in on the dark side of the universe.

Improving the understanding of dark matter

There is more to our universe than meets the eye – much more! It has become evident in recent years that the majority of matter in our universe is very different from the stuff we are made of: it is invisible to our eyes and all our instruments (at least so far). The quest for a theoretical understanding of this mysterious dark matter is at the heart of the European Research Council (ERC) Starting Grant "NewAve".

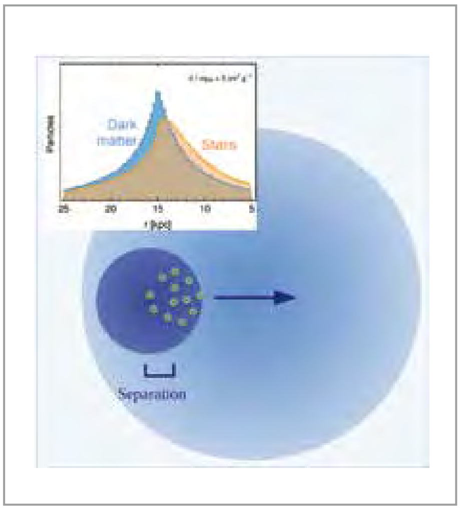

Figure 1
Illustration of a galaxy falling towards the centre of a galaxy cluster and the resulting separation between the dark-matter halo and stars. The inlay shows the result of a numerical simulation of the distribution of dark matter and stars for the system A3827, from which the required self-interaction cross section can be inferred.

The existence of dark matter in our universe is by now firmly established through various astrophysical observations. However, despite tremendous theoretical and experimental efforts over the past few decades, dark matter remains elusive and one of the great unknowns until today.

It is very likely that dark matter consists of new unknown fundamental particles. Its theoretical description therefore naturally falls into the realm of theoretical particle physics.

To solve the dark-matter puzzle, dedicated experimental searches are crucial: direct detection experiments aim to measure dark-matter particles that scatter off ordinary atoms in shielded underground detectors; indirect detection experiments aim to observe the dark-matter annihilation products with satellites and ground-based telescopes; accelerator experiments such as the LHC attempt to directly produce dark matter by colliding ordinary particles at very high energies. All these channels probe the interaction of dark matter with ordinary matter, and experimental efforts have mainly concentrated on the three techniques described above.

In addition, there could also be interactions within the dark sector, leading to scattering among dark-matter particles. Studying possible astrophysical imprints of such dark-matter self-interactions is one of the many aspects of this ERC grant. One possibility to infer whether dark matter really is collisional is to study a galaxy moving through a large dark-matter background density, e.g. a galaxy falling towards the centre of a galaxy cluster. The dark-matter halo of the in-falling galaxy will be slowed down due to the dark-matter self-interactions, while the collisionless stars will not be affected. This can lead to a separation between the dark-matter halo and the stars, which is potentially observable, as illustrated in Fig. 1. Interestingly, there have been recent hints for such a separation. The required self-interaction cross section has been estimated within the context of this ERC project, with a visualisation of the results in the inlay of Fig. 1.

Beyond the study of self-interactions, the overall goal of this ERC project is to exploit the complementarity of all the different search strategies mentioned above and to improve our theoretical understanding of dark matter, helping to advance our knowledge about one of the biggest puzzles of our time.

ERC Starting Grant

"NewAve: New avenues towards solving the dark matter puzzle"

erc

Contact:
Kai Schmidt-Hoberg, kai.schmidt-hoberg@desy.de

Charting the landscape of gauge theories.

… with integrability and conformal bootstrap techniques

Gauge theories provide the theoretical framework for our understanding of the fundamental building blocks of nature – a microscopic description of the matter particles and the forces that govern them. These theories are very well understood at the level of individual particles that interact weakly through the exchange of force carriers. However, treatment of gauge theories becomes very hard when aiming to study stronger interactions and/or collective phenomena. Such studies are the topic of a DESY group funded through the Emmy Noether Programme of Deutsche Forschungsgemeinschaft (DFG).

Arguably, one of the cornerstones of our modern understanding of theoretical physics is Noether's theorem, which states that each symmetry leads to a conservation law. Such conservation laws can be used to simplify the system, as they imply that there are some degrees of freedom – related to the conserved quantities – for which the problem does not need to be solved. In this respect, an ideal theory would have as many degrees of freedom as symmetries and thus be immediately solvable, or "integrable". The hydrogen atom is a famous example, which Wolfgang Pauli managed to solve in a very simple manner after realising that there were more symmetries governing the problem than originally thought.

A proven, fruitful theoretical approach is to consider generalisations of the space–time symmetries. Conformal symmetry extends rotations and translations by rescaling of the coordinates. Theories with this conformal symmetry exist in nature, governing the study of critical phenomena. Moreover, many gauge theories have this symmetry at very high energy. When going to lower energies, the symmetry is broken, but in a controlled way. Supersymmetry is a symmetry that relates particles with different statistics, bosons and fermions. It has been a powerful tool allowing theorists to uncover underlying structures of gauge theories that would not have been discovered otherwise and to compute some observables exactly.

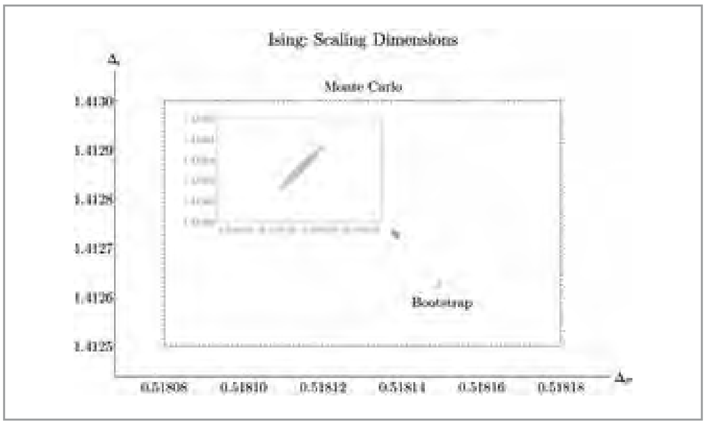

Figure 1

Determination of the leading scaling dimensions in the 3D Ising model. The dashed box is the range of Monte Carlo predictions. The blue region is given by the conformal bootstrap method [2].

Almost all the modern developments in the field are based on revisiting symmetries, discovering new ones and finding novel ways to use them and make them manifest. One way to phrase the problem of trying to understand gauge theories is "charting the landscape of gauge theories", which means that the allowed space of theories can be determined using only general principles: symmetries and quantum mechanics. This approach has led to a revival of the conformal bootstrap programme [1], the pursuit of which has yielded very impressive results and opened up a new era of understanding quantum field theory in general. One famous result is the solution of the 3D Ising model to a numerical accuracy much better than that achieved by any Monte Carlo simulation (Fig. 1). Similar methods can also be applied to quantum chromodynamics (QCD), which, interestingly, becomes conformal for a certain matter content and specific values of the coupling constant.

The Emmy Noether group at DESY is working on the endeavours described above.

Emmy Noether Programme (DFG)

"Exact results in gauge theories"

DFG

Contact:

Elli Pomoni, elli.pomoni@desy.de

References:

[1] David Simmons-Duffin, arXiv:1602.07982.

[2] F. Kos, D. Poland, D. Simmons-Duffin and A. Vichi, JHEP 1606 (2016) 036.

SFB 676: Particles, Strings and the early Universe.

Unravelling the structure of matter and space-time

The Collaborative Research Centre SFB 676 of the University of Hamburg (UHH) and DESY, which is funded by Deutsche Forschungsgemeinschaft (DFG), focuses on the interface of particle physics, string theory and cosmology. The research topics range from physics at the LHC experiments, elucidating the nature of the elementary building blocks of matter, through astrophysical and cosmological observations, uncovering the nature of dark matter and the history of the early universe, to theoretical and mathematical activities, including supersymmetric particle theories and the unification of particle physics and cosmology within string theory.

Figure 1

Presentation during the SFB 676 Block Meeting.

In the past years, particle physics, string theory and cosmology have seen significant progress and some far-reaching discoveries, most notably the discovery of the Higgs boson at the LHC and the discovery of gravitational waves. In the SFB 676, about 150 researchers make use of these new developments to obtain interdisciplinary insights into the fundamental laws of nature. Launched in 2006, the SFB is currently in its third and final funding period, which runs from mid-2014 to mid-2018. Its 17 research projects are distributed over three research areas: A) string theory, B) particle physics and C) cosmology.

In area A, advances in mathematical methods have improved the understanding of scale-invariant quantum systems, $N = 2$ supergravity theories and logarithmic conformal field theories. In area B, the SFB researchers profit from the remarkable LHC performance, collecting more than 40 fb^{-1} in 2016 at a centre-of-mass energy of 13 TeV. The collected data set will allow detailed studies of the Higgs boson and searches for physics beyond the Standard Model with unprecedented sensitivities. In area C, researchers identified a stupendous cosmic particle accelerator formed by the combination of a galaxy cluster merger and an eruption from a supermassive black hole; a prediction of the axion dark-matter mass using lattice QCD simulations was obtained; and a new collaboration between the astroparticle physics and QCD groups presented improved predictions for atmospheric prompt neutrino fluxes relevant for the IceCube neutrino observatory. A complete list of publications can be found on the SFB web page.

SFB members were also very active in projects accompanying the core research. With support of the SFB, UHH hosted the Spring Meeting of the Matter and Cosmos Section of Deutsche Physikalische Gesellschaft (DPG) with 1400 attending physicists in early 2016. The SFB 676 also co-organised the "Women's Career Day" in February. On 17 November, the public outreach event "Science on Tap" ("Wissen vom Fass") was organised in Hamburg for the second time with strong support of the SFB. The scientists' presentations were very well received in about 50 bars throughout the city, and the event obtained wide media attention.

In 2016, the SFB underwent important organisational changes: the project initiator and long-term spokesperson, Jan Louis, was appointed vice-president of UHH, and Johannes Haller took over the role of spokesperson. Furthermore, the managing director Wiebke Kircheisen left the SFB at the end of 2016, and the management was taken over by Michael Grefe.

Contact:

Johannes Haller, johannes.haller@physik.uni-hamburg.de
Michael Grefe, michael.grefe@uni-hamburg.de

References:

http://wwwiexp.desy.de/sfb676/

Experimental facilities and services.

The experimental and theoretical research activities at DESY would not be possible without the contributions and support from numerous groups and people.

One example is the development of new silicon photomultipliers by the DESY electronics development group, which provides an important ingredient for the next generation of pixel detectors (p. 88). Another example is electromagnetic compatibility tests of electronic devices (p. 90), which since 2016 can be performed in house at DESY.

Computing too is a crucial ingredient. The DESY IT group is constantly striving to improve its services for all users and needs – from the Grid and the National Analysis Facility (NAF) to high-performance computing platforms (p. 92). Big data in particular has gained in importance, leading to a European initiative spearheaded by DESY (p. 93).

Another important service offered by DESY is its test beam facility at the DESY II synchrotron. Scientists from all over the world are using the facility to subject newly developed detector components, e.g. for the International Linear Collider (ILC) or the LHC upgrades, to tests with electron or positron beams (p. 96).

The DESY library group, meanwhile, is promoting the open-access movement and working towards increasing the user-friendliness of the publishing process at DESY (p. 94).

Last but not least, in 2016, the ALPS II experiment at DESY was able to secure additional resources and reached some important milestones in anticipation of the start of the experiment, foreseen for 2019 (p. 86).

Light brightens up ALPS II prototype.

Laser light successfully stored in 20 m long optical resonator

The Any Light Particle Search collaboration is preparing the ALPS II experiment at DESY, which will use the "light-shining-through-a-wall" technique to probe for hypothetical very weakly interacting ultralight particles (WISPs), in particular axion-like particles (ALPs). This requires the operation of long optical resonators to boost the effective power of lasers by a factor of a few thousand. In 2016, the ALPS collaboration reached a corresponding milestone.

The existence of very weakly interacting ultralight particles (or weakly interacting sub-eV particles, WISPs for short) is theoretically motivated by extensions of the Standard Model (SM) based on string theory and by the possibility to explain CP conservation in strong interactions through the Peccei–Quinn mechanism. Phenomenologically, puzzling astrophysics observations such as the transparency of the universe to highest-energy photons and phenomena in the developments of stars may hint at the existence of ALPs and axions.

As ALPS II is designed to generate and detect WISPs in the laboratory, it can probe their existence without depending on cosmology (i.e. assuming WISPs make up dark matter) and astrophysics (i.e. assuming WISPs are emitted by the sun). In the first section of ALPS II, laser light is shone through a strong magnetic field. Here, ALPs might be generated by interactions of optical photons with the magnetic field. The second section of ALPS II is separated from the first one by a light-tight wall, which only ALPs and other WISPs could pass through. These particles would stream through a strong magnetic field behind the wall, allowing for a reconversion into photons. This effect would give the impression of "light shining through a wall" (LSW). At ALPS II, the magnetic field before and behind the wall will be provided by 20 dipole magnets from DESY's former HERA proton accelerator.

However, with the simplified LSW approach, ALPS II would not be able to reach the sensitivity required to probe for the ALPs motivated by the astrophysics phenomena mentioned above. Therefore, two optical resonators will be implemented in the experiment:

- A resonator before the wall will "recycle" the laser light through back-and-forth reflections, with the aim to increase the effective power of the laser light by a factor of 5000.
- A resonator behind the wall will increase the reconversion of WISPs into photons by a factor of 40 000.

The overall status of ALPS II is summarised in Ref. [1].

A particular challenge when setting up long-baseline, low-loss optical resonators is to maintain the resonance condition in spite of the ambient seismic noise. At ALPS II, the length of the resonator has to match a multiple of the laser light wavelength of 1064 nm with an accuracy of a few 10^{-12} m. The ALPS collaboration already demonstrated corresponding

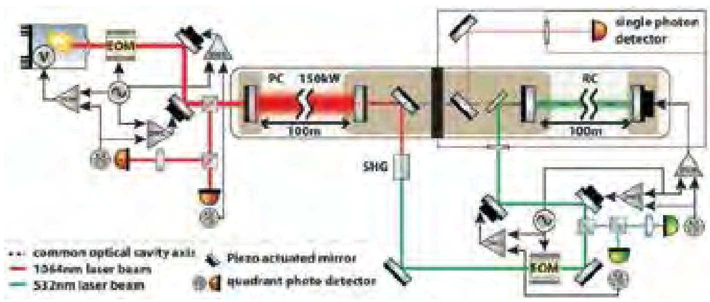

Figure 1

Schematic layout of the ALPS II optics system. Note the two resonators before (PC) and behind (RC) the light-tight wall, controlled with infrared and green light, respectively. Details are given in Ref. [2].

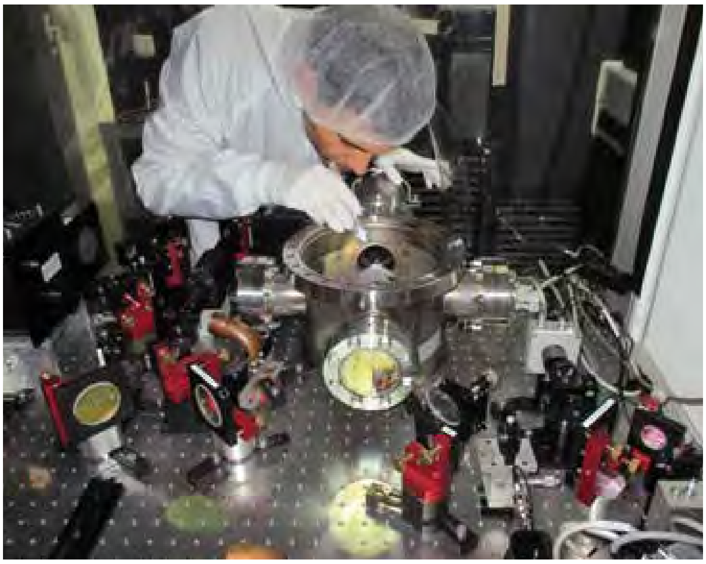

Figure 2

Inspecting the in-coupling mirror of the resonator before the wall

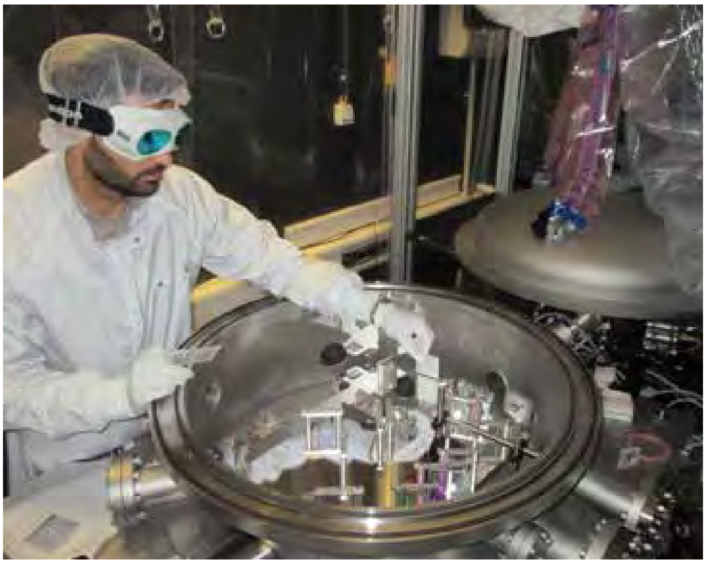

Figure 3

Central breadboard installed in the big ALPS II vacuum tank

techniques based on experience at gravitational-wave interferometers (see for example *DESY Particle Physics 2014 & 2015*). A schematic layout of the optics setup is shown in Fig. 1.

Previous problems with the limited performance of the resonator before the wall could finally be traced back to mirrors not fulfilling the order specifications. Using newly delivered mirrors, a 20 m long resonator was set up in the ALPS laboratory and characterised in great detail [2]. It could be shown that with the techniques developed for and used at ALPS II, the resonator could be operated with low losses over long time periods while coupling in more than 95% of the laser light power shining towards the resonator. Frequency noise, pointing noise, laser power noise and the performance of the corresponding feedback stabilisation systems were analysed. With all control electronics activated, the relative resonator transmission power noise was just 4×10^{-4}. The results indicate that the operation of 100 m long resonators in the HERA tunnel should be possible without problems.

However, some unexplained internal resonator losses of 230 ± 50 ppm were observed, most likely caused by dust or point defects on the mirrors scattering some light. Investigations are ongoing (Fig. 2).

In a next step, the so-called central breadboard, the interface between the resonators before and behind the wall (Fig. 3 and 1) was installed in the big vacuum chamber. Among other components, it houses the end mirrors of both resonators and a dedicated potassium titanyl phosphate (KTP) crystal (labelled “SHG” for “second-harmonic generation” in Fig. 1) to generate 532 nm (green) light from the light leaking through the end mirror of the resonator before the wall. This green light is used to control the resonator behind the wall. With the central breadboard in place, the circulating power in the resonator before the wall was increased carefully. At the end of 2016, power values up to 75 kW (50% of the ultimate ALPS II goal) were achieved, but thermal effects hindered a stable operation at this level. In addition, the generation of green light was demonstrated.

In 2017, the optical setup is expected to reach the specifications lined out in the 2012 technical design report. In addition, preparation of installation work in the HERA tunnel and HERA dipole magnet straightening will start, with the aim for ALPS II to start taking data in 2019.

Contact:
Axel Lindner, axel.lindner@desy.de

References:

[1] A. D. Spector, arXiv:1611.05863.
[2]: A. D. Spector, J. H. Põld, R. Bähre, A. Lindner and B. Willke, Opt. Express 24 (2016) 29237-29245.

Tracking and imaging.

Taking advantage of digital silicon photomultipliers

The vertical integration of pixel detectors and readout electronics is likely to gain in significance in particle physics and photon science experiments. To meet this challenge, DESY is developing a detector system using digital silicon photomultipliers (SiPMs) in a hybrid approach, which allows for readout of each pixel without limitation in fill factor. By utilising an active quenching and recharging circuitry, no additional quench resistor is necessary, and the dead time can be minimised. The resulting signal can be used in its digital form, and only an inverter is necessary for event discrimination. In contrast to conventional analogue SiPMs, pixel-to-pixel gain non-uniformity with respect to temperature can be ignored. The pixel electronics offers options to turn off noisy pixels, reduce after-pulsing through an adjustable hold-off time and count hits. A detector system with an array of digital SiPMs enables energy and timing measurements.

Pixel detector systems pose high demands on spatial and timing resolution. Supposing a pixel pitch of 50 µm and a frame rate of 3 MHz, a system of 40 000 pixels per cm² would produce a sustained data throughput of around 8 GB/s/cm² at a power request of ~4.3 W/cm² for delivering the whole imaging information. A smart adaptation or a higher integration density is a suitable solution to concentrate the data. For example, field programmable gate arrays (FPGAs) allow a higher throughput per link. A 3D integration is a layered architecture of several electronic components. This allows us to minimise the edge region by shifting circuit blocks into the next layer and to integrate more functionalities such as data storage and reduction. This approach is supported by the bunch schemes of the International Linear Collider (ILC) and the European XFEL X-ray laser, where data taking occurs in bunch trains followed by memory readout during long train-to-train gap.

DESY is developing a novel detector system consisting of several digital SiPM hybrid modules. One module comprises four layers (Fig. 1). The first layer is a dSIMPI sensor array from Max Planck Semiconductor Laboratory Munich (HLL) with 128 x 64 pixels. The second layer contains two application-specific integrated circuits (ASICs), integrating a quenching circuit in a one-to-one coupling configuration. Each pixel electronic occupies the same area as the sensor pixel, limiting the space of the electronics to 50 x 50 µm². Each ASIC reads out a 64-by-64 pixel array and contains additional peripheral circuits. Both ASICs are bump-bonded to the sensor. DESY and the company PacTech are working closely together to facilitate the solder ball placement technique for 30 µm diameter solder spheres on the 50 µm pitch array. The sensor and with it the ASICs are wire-bonded to two thin-film carriers that make up the third and fourth layer of the module. The purpose of these layers is the signal transmission, power supply decoupling and filtering.

Such hybrid modules are three-side tillable so that large-scale pixel detectors can be built. To process the full imaging information, a fast data acquisition (DAQ) system is needed. The MicroTCA.4 standard is already being extensively used for DAQ purposes at DESY. For example, the Helmholtz advanced mezzanine card allows DAQ applications at data rates around 50 Gbit/s. A corresponding rear transition module with an application-specific design completes the DAQ system.

The ASIC consists of 16 units, each processing a 16-by-16 pixel array. Figure 2 shows a simplified block diagram of a single unit. Upon event detection, the first firing pixel draws a current from a wired OR-connection of all pixels, stopping a time-to-digital converter (TDC) input line (fast trigger) within

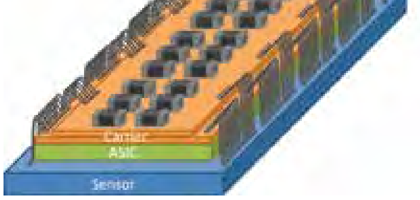

Figure 1

The digital SiPM hybrid module is a four-layer stack made up of a sensor, two ASICs and two ultrathin carriers assembled with passive devices.

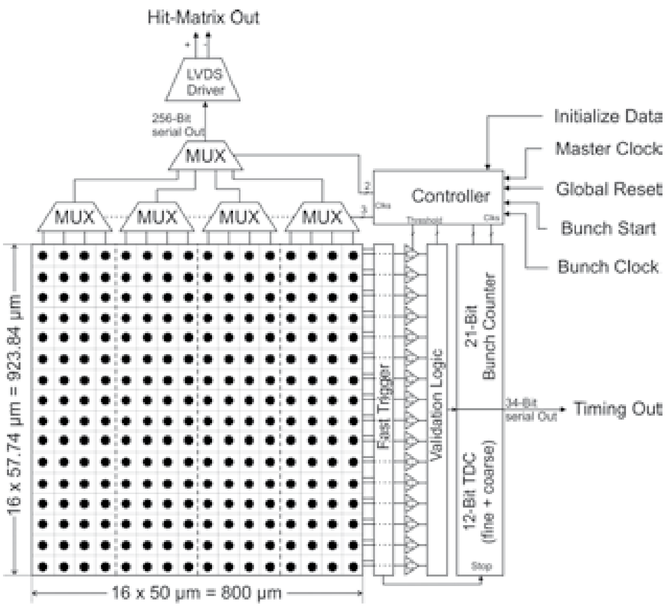

Figure 2

Block diagram of a single ASIC unit processing a 16-by-16 pixel array

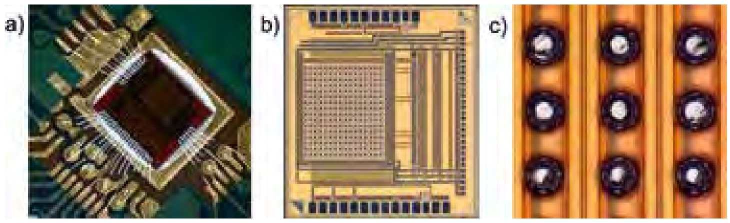

Figure 3

Photograph of the first (a) and second (b) prototype chip; detail of the bump matrix with 30 µm solder spheres (c)

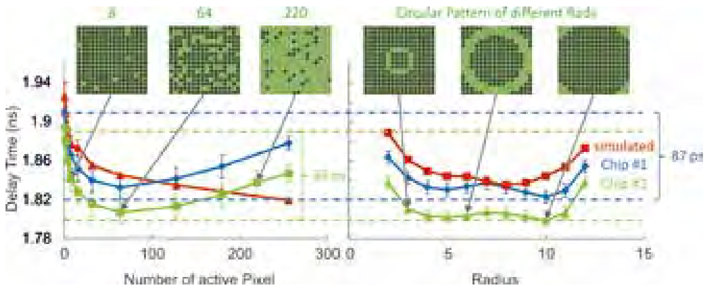

Figure 4

Measured and simulated fast-trigger propagation delays for random (left) and circular pattern (right) at room temperature

2 ns. Additional validation logic in combination with 16 comparators, each wired OR-connected to all pixels in one row and with four adjustable thresholds, generates a combinatorial trigger signal. In this way, undesirable events can be discarded. The hit matrix is read out by an interleaved row-wise 16-to-1 multiplexer. A controller block receives the external 3 MHz bunch clock (e.g. from the ILC), a 408 MHz master clock, a start signal and a reset, and generates all internal clock signals. Furthermore, the controller's status register can be initially loaded with data to set the validation thresholds and mask noisy pixels. The TDC is divided into a 5 bit fine and 7 bit coarse TDC. The fine TDC, which consists of a delay-locked loop (DLL) with 32 differential delay elements, a phase–frequency detector, a charge pump and a thermometer-to-binary encoder, provides a 77 ps timing resolution. The coarse TDC's ripple counter is incremented after every DLL cycle, resulting in a timing resolution of 2.45 ns (408 MHz clock period). The time stamp information comprises the 12 bits from the TDC and 21 bits from a bunch counter. The total sustained data throughput per ASIC amounts to ~14 Gbit/s (16 x 816 Mbit/s hit data, 1 x 816 Mbit/s timing data) at 3 MHz frame rate.

To verify the concept and related simulations, two prototypes in 130 nm IBM 8M1P CMOS technology with a 16-by-16 pixel unit were designed and fabricated (Fig. 3). The first one (Fig. 3a) comprises the complete pixel electronics, a fast trigger and a single-row combinatorial trigger configuration. A control register is implemented to enable every individual pixel and adjust the in-pixel hit counting depth as well as the threshold of the comparator. This prototype was designed to gain experience as to which timing range the fast trigger and the combinatorial trigger are working in, in order to define the required TDC resolution and the width of a veto time window within which an undesired event can be discarded.

The trigger signal delays of two chips were measured as a function of the active pixels and compared with simulation results (Fig. 4). The individual enabling of every pixel in combination with a test input allows the determination of active pixels and operation without a sensor matrix. It is possible to load the pixel matrix with regular or random patterns. All pixel test inputs see the same test pulse simultaneously. The propagation delay induced by the ASIC electronics from test input to fast-trigger output was measured at room temperature and found to cover a range around 86 ps for both chips, showing that the TDC bin width of 77 ps mentioned above is sufficiently low.

The second prototype (Fig. 3b) comprises all circuit blocks of the ASIC unit shown in Fig. 2. As of December 2016, the chips have arrived and test preparation is in progress. It will soon be possible to test both prototypes together with a 16-by-16 dSIMPI array from HLL. Sixteen chips have been successfully processed with 30 µm solder spheres (Fig. 3c) and are ready for flip-chip bonding.

Contact:
Inge Diehl, inge.diehl@desy.de
Karsten Hansen, karsten.hansen@desy.de

Electromagnetic compatibility of electronic devices.

Achieving system integrity through EMC-conform design and testing

At DESY's FLASH free-electron laser, the upcoming European XFEL X-ray laser and the planned International Linear Collider (ILC), electrical power consumption is modulated at the bunch train repetition rate of several Hz. Therefore, to ensure the electromagnetic compatibility (EMC) of electronic devices, the electronics design has to consider the full frequency range from low frequencies (DC or few Hz) up to the high frequencies (GHz) of digital rising edges. Checking for possible disturbances and sensitivities from the initial device conception up to the final design promises reliable operation in the harsh beamline environment. To carry out such tests in house, DESY invested in suitable measuring and testing technology. As a result, the success of a design can now be proven at DESY by standardised methods and comparison to agreed limits such as CE certification.

In electronics, the "ground" reference potential has different functions: (i) reference for each signal, (ii) current return and (iii) shielding against electromagnetic interference. Therefore, it is important to minimise the currents applied to the ground system. The basis for EMC is already defined during the initial device conception.

Designing the AGIPD

In the case of the Adaptive Gain Integrating Pixel Detector (AGIPD) for example, a high-speed 1 Mpx camera for the European XFEL (Fig. 1), all fast signals between boards are kept differential without current in the ground. The I^2C bus, which features slow rise times and small currents, was chosen for slow control. The connector for analogue inputs was selected to define the reference point. The power supply connected to the other end of the board needs to be floating for low frequencies, and high frequencies are filtered by ferrite capacitor combinations. With an adequate circuit design, it was achieved that the grounding planes are used as current returns for a length of 10 cm in an area of low sensitivity only. In the amplifier region, no current is induced into the ground system.

Thanks to the selection of only low-profile surface-mount device (SMD) components, the field emission is limited, because its strength decreases strongly with the distance of the radiating component to the reference plane. During layout of the printed circuit board (PCB), it was checked carefully that each functional current has a close-by dedicated return path to avoid vagabonding currents. This was supported by routing every trace above the reference planes. Where needed, the circuit diagram was adjusted in close collaboration of circuit and PCB designer.

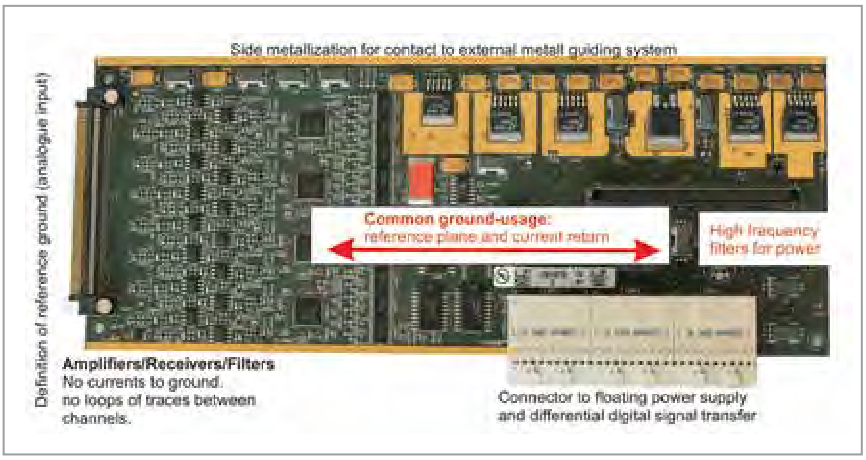

Figure 1

AGIPD detector for the European XFEL: 64-channel analogue board with 64 differential filters (DC to 33 MHz), 64 analogue-to-digital converters (ADCs) and 80 differential digital output lines at 500 Mbit/s, operated synchronised to the 10 Hz bunch train structure

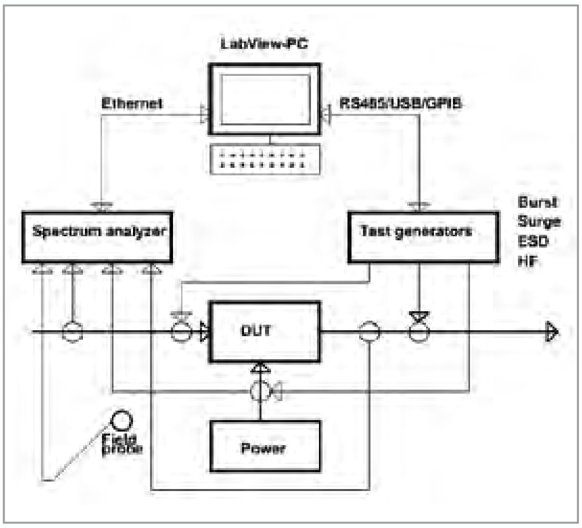

Figure 2

Typical configuration to probe a device under test (DUT)

Figure 3

Emission test, controlled by LabView software

Even in well-designed systems, parasitic coupling to surrounding metal pieces will occur. Because that kind of effects might show up as late as during system integration or even during operation in the harsh beamline environment, the sides of the PCBs are designed to allow three options for grounding different parts of the circuit board. By closing or opening a few solder connections, the system can be adapted to low- or high-frequency disturbances from the beamline environment.

In 2016, a full AGIPD detector was assembled, consuming around 500 A of direct current (DC) at low voltages. No optimisation was needed to reach the required performance at the system integration level in the laboratory.

EMC testing at DESY

By means of suitable measurements, the behaviour of electronics can be assessed before practical operation and weak points can be eliminated. Previously, these measurements had to be carried out in external test laboratories, which led to repeated delays and high costs. To remedy this situation, the DESY Service Centre Electronics invested in the training of employees and the procurement of suitable measuring and testing technology.

Through test generators, standardised interference signals are impressed by means of suitable coupling modules on all input and output lines as well as on the power supply lines, and the behaviour of the circuit is checked. Since there is a variety of interfering mechanisms, various signals differing in amplitude, time duration, waveform and energy have to be generated. To standardise and automate these tests, a LabView software was developed, which controls the various generators through a uniform interface and then creates test logs. This reduces the load on the operator and ensures a standardised and complete test of the response of the test object to line-connected disturbances. The response of the device to radiated electromagnetic waves can be tested at external facilities with short access times.

It is equally important to determine the emitted interference of the test object, to find the cause of these disturbances if the limits are exceeded and to check the effectiveness of the measures taken after revision. The LabView software developed for this purpose controls a spectrum analyser, which is connected to the device under test (DUT) by means of suitable coupling modules or probes. This makes it possible to locate and document sources of inadmissibly high emissions (Fig. 3).

With the possibilities now available at DESY, a development-accompanying EMC pre-compliance test is now possible at DESY and by DESY employees. To obtain a CE certification, which may be necessary later, an examination must still be carried out in an accredited EMC laboratory, after measurements at DESY have shown that it is very probable that the DUT will pass the EMC tests required by law.

Contact:
Peter Göttlicher, peter.goettlicher@desy.de
Otto-Christian Zeides, otto-christian.zeides@desy.de

HEP computing and storage infrastructure consolidation.

Providing computing and storage services to the scientific community

The resource requests for computing and storage in high-energy physics (HEP) are increasing. In 2016, DESY therefore consolidated and modernised its batch systems and fast storage space to provide the most efficient environment for data analysis.

Modernising the fast project space for the NAF

Since its creation in 2007, a key ingredient of the National Analysis Facility (NAF) at DESY [1] has been a fast and flexible storage system for projects, which complements the dCache Grid storage system used for high-volume storage and data exchange. This fast storage system is constantly being modernised to adapt it to changing user needs. Previous products used were Lustre and then the IBM SONAS appliance. In 2016, the choice fell on a setup based on the IBM Spectrum Scale system, which was already in use at DESY for PETRA III data taking. The system relies on IBM data and metadata server using the IBM Spectrum Scale RAID technology to ensure best data integrity and availability. The DESY IT group performed the migration from SONAS to the new system, baptised DUST, with minimal impact to users.

DUST offers a total net capacity of 1.3 PB. The storage space is exported via four cluster export service nodes, running Ganesha NFS, with a total aggregated bandwidth of 80 Gbit/s. To increase speed and reduce latency, these four nodes are equipped with fast solid-state drives acting as read-only buffer, so that the load on the back-end storage system is reduced. At the end of 2016, nearly 2/3 of the space was in use. An increase in capacity and bandwidth of DUST is planned for 2017. The system has the potential to scale up to multiple tens of PB in capacity and more than 400 Gbit/s aggregated data delivery speed. The initial setup was planned such that a flexible growth in capacity, metadata performance and bandwidth can easily be performed as needs evolve.

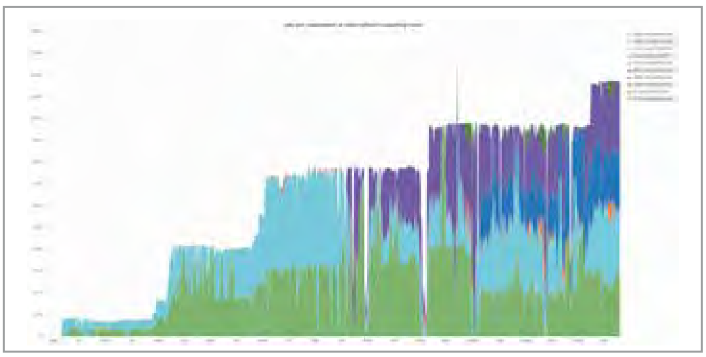

Figure 1

Total number of jobs running on the NAF. The different colours denote the various experiments.

Homogeneous computing cluster for Grid and NAF

As one of the major providers of computing and storage resources for HEP communities, DESY operates computing infrastructures for local and global users [2]. Historically, these infrastructures were logically separated in batch systems serving either HEP experiments directly, as a global Grid site, or local individual users, as the NAF.

Both infrastructures are now being merged into one batch system based on the HTCondor batch system. Within the consolidated infrastructure, HEP experiments such as (i) ATLAS, CMS and LHCb operating at the LHC within the WLCG [3], (ii) Belle II and the ILC experiments as major non-LHC experiments and (iii) several small virtual organisations (VOs) provide a continuous workload through the global Grid infrastructure. In addition, individual users will be able to use the combined infrastructure for a dynamic, fast-response work-flow, which contributes higher entropy to the batch pool thereby optimising the resource utilisation. To meet the needs of both use cases, DESY is pioneering the simplification of computing nodes by externalising dependencies, which allows for both greater flexibility and enhanced ease of operation. Together with the merger of batch systems, this will allow a more efficient use and management of the computing resources.

Contact:

Yves Kemp, yves.kemp@desy.de

Thomas Hartmann, thomas.hartmann@desy.de

References:

[1] http://naf.desy.de.

[2] http://grid.desy.de.

[3] http://wlcg.web.cern.ch.

dCache and Europe's digital future.

Contributing to the European Open Science Cloud vision

With the publication of the Horizon 2020 work programmes in 2014, the European Commission launched the challenging endeavour to create a Europe-wide computing platform, ensuring the operation of the European Strategy Forum on Research Infrastructures (ESFRI) and other world-class research infrastructures. From the very beginning, dCache.org, an international big-data open-source software collaboration headquartered at DESY, contributed to various initiatives targeting the realisation of the European Open Science Cloud (EOSC).

dCache – big data for science

Since 2010, DESY has been operating the headquarters and project support infrastructures for dCache.org, an international collaboration of Fermilab, the Nordic Data Grid Facility, the University of Applied Sciences in Berlin and DESY. dCache.org provides an open-source software technology to manage massive amounts of data on a variety of storage technologies, facilitating data storage, data access, security and data life cycle management. Within the domain of the Worldwide LHC Computing Grid (WLCG), the dCache technology is used to hold more than 150 PB of data on disk and tape storage devices, distributed over 70 laboratories around the world.

dCache and the European INDIGO-DataCloud

Given the distribution of the dCache technology within Europe and the big-data features it already provided, dCache.org was a natural choice for becoming partner of the European INDIGO-DataCloud consortium, which aims to develop an open-source data and computing platform for science in Europe. The INDIGO project started in April 2015 and will last until September 2017; this includes funding for dCache of about half a million euros. This financial support allows dCache.org to extend the dCache technology towards improved data life cycle and authentication functionalities.

Most important, however, are new mechanisms within dCache that allow users to customise the quality of storage spaces for their various scientific applications. Storage quality may range from a single copy on cheap media for temporary storage to multiple copies on high-performance solid-state disks, spinning disks or long-lasting tape technologies for long-term archiving. As DESY is operating several dCache instances, its users immediately profit from those improved features. In particular, the DESY user storage sync-and-share cloud installation, realised with OwnCloud built on top of dCache, will provide those features as soon as it is sufficiently tested.

European Open Science Cloud (EOSC)

With the end of the INDIGO-DataCloud project, financial support for software development from the European Commission will be significantly reduced. It is assumed that a sufficient number of the developed cloud software components are now ready for production. Therefore, the next step towards realising the EOSC will be a pilot project aiming mainly to prepare a governance model for such a complex European entity. At the technical level, the pilot project will evaluate possible interoperability issues and provide a catalogue of thematic and cloud-based services. The pilot project was launched in January 2017 and will run for 24 months.

DESY is involved in work packages validating data and infrastructure interoperability, and leading a "science demonstrator" on photons and neutrons in cooperation with European XFEL, EMBL, ESRF and ESS. The objective of such a science demonstrator is to prove that particular scientific workflows can be ported to private and public cloud systems. In consequence, those research infrastructures would benefit from a common European cloud and would be able to share resources. In a second step, sharing scientific results is envisioned, in the hope that the overall scientific profit will be more than just the sum of the individual findings. Building the EOSC is certainly one of the most exciting activities en route to a powerful and efficient European science community.

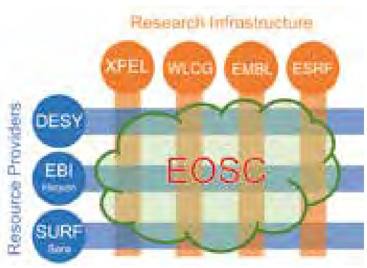

Figure 1
Design of the European Open Science Cloud

Contact:
Patrick Fuhrmann, patrick.fuhrmann@desy.de

From database to platform.

Transition of the DESY publication database PubDB

The DESY publication database (PubDB) is becoming the central pivot point for publishing at DESY. It provides a variety of features: Up-to-date publication lists for web pages created by means of the ZMS content management system can be generated dynamically, increasing the visibility of scientific results and leading to faster submissions by authors – a win–win situation for both the researchers and DESY. PubDB provides the full-text version of all material published by DESY; a DOI is minted as a stable identifier for all open-access articles. Data are automatically exchanged with other providers such as INSPIRE and OpenAIRE.

Since 2001, DESY has been acting as a publisher and has held the right to assign International Standard Book Numbers (ISBNs). While the relevance of traditional printed versions is in decline, fast, easy and persistent online access to content becomes more and more important. Unfortunately, DESY's report series, preprints, theses, proceedings and books are hosted on different platforms, some of which have a high risk of becoming obsolete. To preserve this valuable content and provide persistent uniform access, the documents are being moved into the versatile publication database PubDB. In 2016, the DESY library group successfully migrated more than 550 reports form the Accelerator division, some of which are now available online for the first time.

Listing publications – for reference

A list of publications is an integral part of most scientific online presence. In the past, DESY groups, institutes and beamline scientists were using static, manually maintained web pages for all relevant publications. Collecting and normalising these lists is time-consuming and not fail-save. Furthermore, the lists were sometimes out-dated, since the person who updates the list is usually not the person who has written the publications. Now, it is possible to create such lists dynamically from PubDB.

To provide the data, the DESY library group developed an output format that uses the standardised notation of the German national library (ZDB), the world's largest database for periodicals. Furthermore, all served data (authors, title, periodicals, etc.) are hyperlinked back to PubDB and contain enhanced metadata information. Hyperlinking and metadata become more and more important because search engines such as Google use these data for their ranking. The increased visibility of their publications is an important point for the DESY researchers and groups.

Another advantage of using PubDB instead of static lists is the standardised, easy and fast input by Digital Object Identifier (DOI) in the submit masks of the database. The importing feature makes use of a lot of authority records, e.g. for authors, DESY groups and publisher data such as periodicals, which greatly enhances the overall quality. By including the full text of a publication, authors can ensure that their research output is available to a greater audience free of charge. Typically, submitting a journal entry in PubDB takes about a minute or less. After the group editor has approved an entry, the new record is automatically included in the group's publication list.

Historically, PubDB was restricted to content by DESY authors or results obtained at DESY. To overcome this restriction, the possibility to included "hosted content" was introduced, which allows users to create a complete list of their personal publications. "Using the PubDB publication list, we ensure a timely and consistent listing of all publications across various pages and

Figure 1

Publication list of the Controlled Molecule Imaging (CMI) group at CFEL.

https://www.controlled-molecule-imaging.org/publication/scientific/#2015

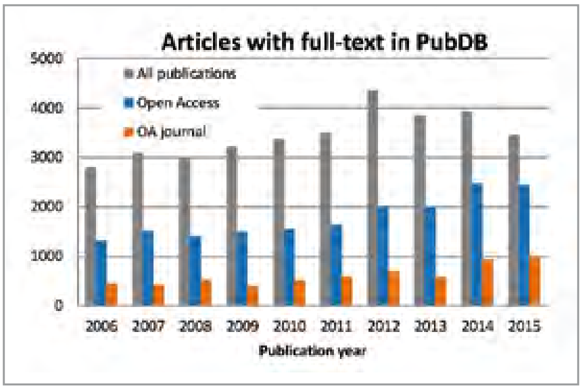

Figure 2

Number of publications with full text in PubDB. Grey: number of all publications (with and without full text); blue: open-access portion; orange: open-access publications in journals.

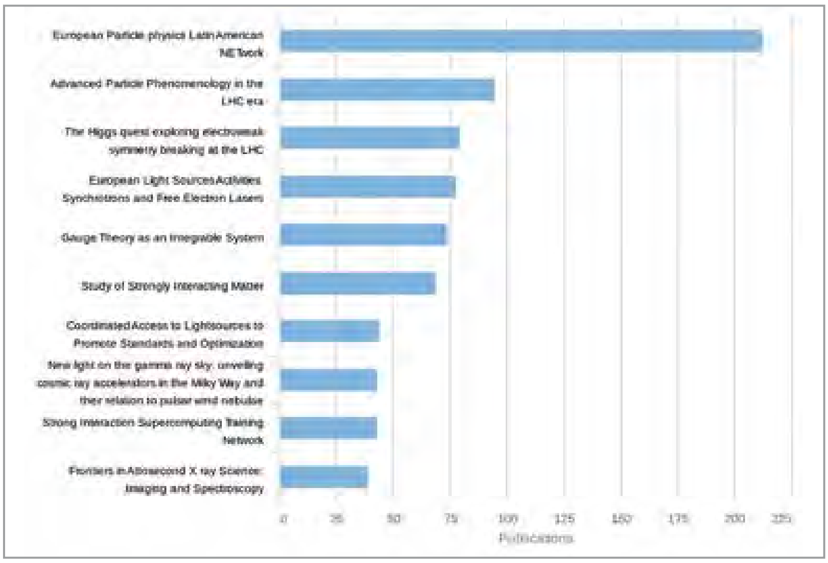

Figure 3

Number of DESY publications listed in OpenAIRE by grant (if known). Unfortunately, the grant information is not standardised and sometimes missing. From OpenAIRE via HighCharts.

sublists on our websites. This provides professional and reliable dissemination of our work," says Prof. Jochen Küpper from CFEL, whose web publication list is generated from PubDB (Fig. 1).

To use the PubDB publication lists in the centrally provided web pages, which are created by means of the ZMS content management system, users can run the centrally supported INVENIO plugin. The library group provides support in case help to configure the plugin is needed.

Hosting full texts – for reading

PubDB is not just a system to list and index publications, it has always been a valuable source of the corresponding full-text versions (Fig. 2). To make full use of this feature, DOIs are now minted automatically for every document with an open-access license. By default, a generic DOI is assigned, dedicated DOIs are possible on request. Such a DOI not only serves as a unique and stable identifier, it also allows for easy and well-defined reference beyond the existence of a report number. The latter is especially important for contributions to proceedings in order to make them easily citable.

The DOI is registered at datacite.org with metadata available from PubDB, including e.g. high-quality author information taken from authority records of known individuals. Where available, the data include Open Researcher and Contributor IDs (ORCIDs) provided by datacite.org. This is an essential feature for cross-platform author identification.

To provide publications through PubDB, the library group started with the DESY thesis series, trying to render full texts in the pdf/a format, which includes embedded fonts and facilitates archival. This is not always possible in post-processing due to missing information. Initial submission in the pdf/a format is therefore desirable.

Next, the online publications of DESY proceedings were moved from a static web page or single-pdf only to PubDB, which allows the association of documents. Using this feature, the record of the proceedings books now also lists the individual contributions (usually as hosted content), providing a convenient way to present both the complete publication and individual contributions and to mint DOIs. More report series will follow and be moved to PubDB.

Exchanging metadata – for finding

Metadata are also submitted to OpenAIRE.eu, a portal promoting the implementation of open access in Europe, supported by the European Research Council (ERC). The goal is to make as much EU-funded research output as possible freely available to everyone everywhere. OpenAIRE agglomerates information from big players such as PubMed Central and institutional repositories such as PubDB. It provides various tools to search for publications, such as a listing by grant (Fig. 3).

The high-energy physics information system INSPIRE, which automatically searches and links PubDB entries, profits from fast data exchange including not just metadata but also full-text versions. This enables the extraction and (partial) identification of references from the pdf as well as full-text search in INSPIRE.

Contact:
Kirsten Sachs, kirsten.sachs@desy.de
Robert Thiele, robert.thiele@desy.de

The beam is on.

The DESY II test beam facility in 2016

DESY operates the DESY II test beam facility for detector R&D projects from a wide range of communities. After the winter shutdown starting in November 2015, the facility was back in user operation in March 2016 and proved to be even more popular than in 2015. User groups ranging from the upcoming LHC upgrades to small groups pursuing generic R&D made extensive use of the facility, appreciating the unique infrastructure at DESY, such as the EUDET-style pixel beam telescopes or the large-bore magnets, as well as the very reliable beam availability. User operation will resume in February 2017.

The DESY II test beam facility is located on the DESY Hamburg site (Fig. 1) and makes use of the DESY II synchrotron, which predominantly serves as an injector for the synchrotron radiation source PETRA III. DESY II delivers electron and positron beams with energies of 1–6 GeV to three test beamlines via a secondary target. All beamlines can be individually controlled by the users. The ease of use and the excellent infrastructure available make the DESY II test beam a very popular facility with a global user community. The test beam team constantly adds improvements to the beamlines and strives to keep it a world-class facility for detector R&D. With the AIDA-2020 project, the EU supports test beams around Europe, including access to the DESY II test beam facility under the transnational access programme, which helps users from outside Germany to come to DESY and perform their tests at the facility.

Activities of the test beam team in 2016 mainly concentrated on consolidating the infrastructure of the facility. The aging gas warning system was replaced with a state-of-the-art setup, the beam diagnostics were further improved, and high-speed fibre links between the beam areas and the huts were installed, a move requested by many user groups.

Figure 1

DESY II test beam facility in Hall 2 (Bldg. 27) on the DESY Hamburg site

Highlights from 2016

In 2016, the DESY II test beam facility operated for 41 weeks in total including several maintenance weeks. Of the 105 user weeks available, 66% were used, with all beamlines occupied 30% of the time. The average beam time used by the groups was 68%, which is a very high value for such a facility. Overall, 292 users from 21 countries came to the facility, among them 67% from Germany, 15% from other EU countries and 18% from outside the EU. In 2016, 37% of the users came to DESY for the first time to use the facility.

Among the user communities, the LHC groups dominated with 49% of requests. As usual, however, groups from many different fields, ranging from Belle II and ILC detector R&D to experiments at FAIR, made use of the facility. The beam telescopes were again in high demand, with 70% of the groups requesting one. Thanks to the installation of the DURANTA telescope in 2015, two telescopes were available, so that all the user requests could be satisfied.

Selected highlights from 2016 showcase the capability and versatility of the facility. The Belle II team set a new record for group size, with 65 users – including the Belle II spokesperson – taking part in a four-week test beam campaign. A slice of the entire silicon tracking system together with the full trigger and readout system was installed in the PCMAG 1 T solenoid and successfully tested (Fig. 2). The whole data acquisition chain demonstrated long-term stability with a rate only limited by the particle rate. The novel two-phase CO_2 cooling system was also tested successfully. The beam period concluded with the measurement of the pixel detector (PXD) efficiency using tracks reconstructed by means of the silicon strip tracker (SVD).

Figure 2

DESY Director Helmut Dosch taking a tour of the Belle II setup at Beamline 24

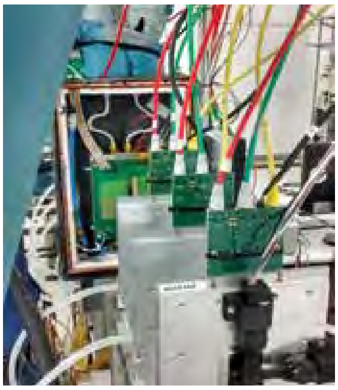

Figure 3

ATLAS ITk test setup installed in the DURANTA telescope. The test sensor is located in the black cooling box.

Figure 4

Two of the participants of the “Particle Physics for Teachers” course assembling the LEHRERCAL calorimeter to measure electromagnetic showers.

For the ATLAS Phase 2 inner tracker (ITk) upgrade, the end of 2016 marked a milestone with the delivery of the technical design report (TDR). The year therefore involved an intense time of test beams to evaluate the performance of the ITk strip detector modules before and after neutron irradiation, focusing on efficiency and collected signal charge (Fig. 3). The detailed data analysis confirmed that these sensors are not only suitable for the Phase 2 upgrade but exceed expectations, which was a key result to be included in the TDR.

Teachers to the test beam!

The DESY II test beam facility is also an important and vital infrastructure to train the next generation of detector experts for particle physics and other disciplines. Therefore, it is very encouraging that again about half of the users were students. Also, every year, DESY summer students are given the opportunity to take part in several test beam measurements. But why stop at students? In 2016, the facility was part of the first advanced training course “Particle Physics for Teachers” organised by Karen Ong, head of the DESY school lab. Besides attending lectures on particle physics, detectors and accelerators, the teachers had the opportunity to perform experiments themselves using the DESY research infrastructure. As one of the key facilities, the DESY II test beam provided multi-GeV electrons for those studies. The participants were asked to measure the development of electromagnetic showers in a calorimeter built by the test beam team specially for educational purposes (Fig. 4). After an intense week, the participants left full of enthusiasm for particle physics and DESY, something they will no doubt pass on to the next generation of students.

Outlook for 2017

The 2017 run will start in February. So far, 24 groups have made requests for 44 weeks of beam time. The majority of user requests (75%) come from the LHC community and, for the first time, from all four LHC experiments. Four out of five groups have requested the use of one of the telescopes, underlining their popularity. In 2017, new infrastructure, supported by AIDA-2020, will be made available to the users: A common slow-control system will enable the users to log environmental data such as temperature or humidity. A first prototype of a new large-area beam telescope based on silicon strip sensors will also be operated with beam for the first time.

Beyond 2017 – a fourth beamline at DESY

The three available beamlines are very well used, but there are user requests that currently cannot be met. At the top of the list are higher-intensity electron beams as well as muon and pion beams. With the shutdown of the DORIS synchrotron in 2013, the old transfer line to DORIS became available. This transfer line would allow a primary extraction of the beam out of DESY II without interfering with PETRA III operation. This beam could then be shaped to the user needs regarding intensity and spot size, and it could be used to produce pion and muon beams with several GeV. Currently, studies are ongoing to establish the feasibility of the project, and a workshop in summer 2017 will give users the opportunity to further specify their requirements for such a beamline.

Summary

2016 has been another successful year for the DESY II test beam facility, and we are looking forward to the upcoming highlights of 2017. This success would not have been possible without the support from many individuals and groups from the DESY particle physics and accelerator divisions, and we would like to take this opportunity to thank everybody involved for their efforts.

Contact:
testbeam-coor@desy.de
Ralf Diener, ralf.diener@desy.de
Norbert Meyners, norbert.meyners@desy.de
Marcel Stanitzki, marcel.stanitzki@desy.de

References:
http://testbeam.desy.de


NUCLEAR
SCIENCE
VOL. 12
1962
OF
NUCLEAR
SCIENCE
VOL. 13
1963
K
K
K
K
Ann
15

References

Committees.

DESY Foundation Council

Representatives of the Federal Republic of Germany

G. Winkler
(Federal Foreign Office)

MinR'in **O. Keppler**
(Federal Ministry of Education and Research)

Dr.-Ing. **B. Vierkorn-Rudolph** (Chair)
(Federal Ministry of Education and Research)

Representatives of the Free and Hanseatic City of Hamburg

LRD Dr. **R. Greve**
(Ministry of Education and Research)

C. Zierau
(Ministry of Education and Research)

Representatives of the Federal State of Brandenburg

Dr. **C. Menzel**
(Ministry of Finance)

C. Feller
(Ministry of Science, Research and Culture)

Representatives from science and industry

Prof. Dr. **U. Beisiegel**
(President, Georg-August-Universität Göttingen)

Dr. **M. Kraas**
(Olympus Surgical Technologies)

Dr. **G. Mecke**
(AIRBUS)

Dr. **C. Quitmann**
(Lund University)

Guests

Chair of the DESY Scientific Council
Prof. Dr. **P. Drell** (SLAC, USA)

Chair of the DESY Scientific Committee
Dr. **M. Kasemann**

President of the Hermann von Helmholtz Association
Prof. Dr. **O. Wiestler**

DESY Equal Opportunity Officer
S. Faverot-Spengler

Chair of DESY Works Council
K. Lando

DESY Board of Directors

Dr. **R. Brinkmann**
(Accelerator Division)

Prof. Dr. **H. Dosch**
(Chairman of the DESY Board of Directors)

Prof. Dr. **J. Mnich**
(Particle Physics and Astroparticle Physics Division)

C. Scherf (until 31 October 2015)
C. Harringa (acting since 1 November 2015)
(Administrative Division)

Prof. Dr. **E. Weckert**
(Photon Science Division)

Prof. Dr. **C. Stegmann**
(Representative of the Directorate in Zeuthen)

DESY Scientific Council

Dr. **R. Abela**
PSI (CH)

Prof. Dr. **O. Botner**
Uppsala University (SE)

Prof. Dr. **J. Daillant**
Soleil Synchrotron (FR)

Prof. Dr. **P. Drell** (Chair)
SLAC (USA)

Prof. Dr. **K. Hämäläinen**
University of Helsinki (FIN)

Prof. Dr. **K. Jakobs**
University of Freiburg (DE)

Prof. Dr. **Y.-K. Kim**
University of Chicago (USA)

Prof. Dr. **S. Larsen**
MAX IV Laboratory (SE)

Dr. **L. Merminga**
TRIUMF (CA)

Prof. Dr. **S. Ritz**
University of California (USA)

Prof. Dr. **L. Rivkin**
PSI (CH)

Dr. **E. Shaposhnikova**
CERN (CH)

Prof. Dr. **J. Womersley**
STFC (UK)

Prof. Dr. **L. Young**
ANL (USA)

and the chairs of

DESY MAC: Prof. Dr. **A. Jankowiak**
HZB (DE)

DESY PRC: Dr. **R. Yoshida**
ANL (USA)

DESY PSC: Dr. **Ch. David**
PSI (CH)

DESY Scientific Committee: Dr. **M. Kasemann**
DESY

European XFEL: Prof. Dr. **M. Altarelli**
European XFEL (DE)

DESY Scientific Committee

M. Aldaya Martin (DESY)
R. Aßmann (DESY)
F. Beckmann (HZG)
T. Behnke (DESY)
M. Bieler (DESY)
I. Bloch (DESY)
K. Borras (DESY)
W. Buchmüller (DESY)
A. Burkhardt (DESY)
K. Büßer (DESY)
F. Calegari (DESY)
H. Chapman (DESY)
M. Diehl (DESY)
R. Doehrmann (DESY)
J. Dreyling-Eschweiler (DESY)
W. Drube (DESY)
S. Fiedler (EMBL)
T. Finnern (DESY)
B. Foster (DESY)
A. Frey (KET)
E. Gallo (DESY)
H. Graafsma (DESY)
I.-M. Gregor (DESY)
Ch. Grojean (DESY)
G. Grübel (DESY)
V. Gülzow (DESY)
B. Heinemann (DESY)
M. Hempel (DESY)
K. Honkavaara (DESY)
K. Jansen (DESY)
R. Kammering (DESY)
M. Kasemann (DESY, Chair)
C. Kluth (DESY)
M. Kowalski (DESY)
G. Kube (DESY)
F. X. Kärtner (DESY)
M. Martins (U Hamburg)
N. Meyners (DESY)
K. Mönig (DESY)
S. Molodtsov (European XFEL)
B. Murphy (KfS)
A. Mußgiller (DESY)
T. Naumann (DESY)
C. Niebuhr (DESY)
D. Nölle (DESY)
K. Peters (DESY)
E. Plönjes-Palm (DESY)
M. Pohl (DESY)
D. Reuther (DESY)
R. Röhlsberger (DESY)
R. Santra (DESY)
M. Schmitz (DESY)
V. Schomerus (DESY)
S. Schreiber (DESY)
Ch. Schroer (DESY)
H. Schulte-Schrepping (DESY)
A. Schulz (DESY)
Ch. Schwanenberger (DESY)
U. Schwanke (HU Berlin)
A. Schwarz (DESY)
T. Schörner-Sadenius (DESY)
G. Servant (DESY)
S. Spannagel (DESY)
A. Stierle (DESY)
K. Tackmann (DESY)
S. Techert (DESY)
M. Tischer (DESY)
R. Treusch (DESY)
Y. Umhey (DESY)
J. Viefhaus (DESY)
M. Vogt (DESY)
N. Walker (DESY)
G. Weiglein (DESY)
H. Weise (DESY)
H.-Ch. Wille (DESY)
K. Wittenburg (DESY)
W. Wurth (DESY)
H. Yan (DESY)

Machine Advisory Committee (MAC)

Dr. **M. Borland** (ANL, USA)
Dr. **A. Faus-Golfe** (IFIC Valencia, SP)
Dr. **M. Ferrario** (INFN, IT)
Dr. **Z. Huang** (SLAC, USA)
Prof. Dr. **A. Jankowiak** (HZB, DE, Chair)
Dr. **P. Raimondi** (ESRF, FR)
Prof. Dr. **A. Wolski** (U Liverpool, UK)

Physics Research Committee (PRC)

Prof. Dr. **M. Beneke** (RWTH Aachen, DE)
Prof. Dr. **P. Burrows** (U Oxford, UK)
Prof. Dr. **A. Boehnlein** (JLab, USA)
Prof. Dr. **L. Covi (**U Göttingen, DE)
Prof. Dr. **L. Feld** (RWTH Aachen, DE)
Prof. Dr. **J. Fuster Verdú** (IFIC Valencia, SP)
Prof. Dr. **L. Köpke** (U Mainz, DE)
Prof. Dr. **R. Ong** (UCLA, USA)
Prof. Dr. **L. Rosenberg** (U Washington, USA)
Prof. Dr. **R. Wallny** (ETH Zürich, CH)
Dr. **R. Yoshida** (ANL, USA, Chair)

Ex-officio members:
Prof. Dr. **H. Dosch** (DESY)
Prof. Dr. **J. Mnich** (DESY)
Prof. Dr. **E. Weckert** (DESY)
Dr. **R. Brinkmann** (DESY)
Prof. Dr. **C. Stegmann** (DESY)

German Committee for Particle Physics (KET)

Prof. Dr. **S. Bethke** (MPP München)
Prof. Dr. **K. Borras** (DESY)
Prof. Dr. **V. Büscher** (U Mainz)
Prof. Dr. **K. Desch** (U Bonn)
Dr. **M. Elsing** (CERN)
Prof. Dr. **A. Frey** (U Göttingen)
Prof. Dr. **T. Hebbeker** (RWTH Aachen)
Prof. Dr. **W. Hollik** (MPP München)
Prof. Dr. **M. Kobel** (TU Dresden)
Prof. Dr. **J. Mnich** (DESY)
Prof. Dr. **P. Schlepe**r (U Hamburg)
Prof. Dr. **M. Schumacher** (U Freiburg)
Prof. Dr. **G. Weiglein** (DESY)
Prof. Dr. **C. Zeitnitz** (U Wuppertal, Chair)
Prof. Dr. **D. Zeppenfeld** (KIT)

German Committee for Astroparticle Physics (KAT)

Prof. Dr. **J. Bluemer** (KIT)
Prof. Dr. **K. Danzmann** (U Hannover)
Dr. **A. Haungs** (KIT)
Prof. Dr. **M. Lindner** (MPP München)
Prof. Dr. **L. Oberauer** (TU München)
Prof. Dr. **M. Pohl** (DESY)
Prof. Dr. **E. Resconi** (TU München)
Prof. Dr. **C. Stegmann** (DESY)
Prof. Dr. **S. Wagner** (U Heidelberg)
Prof. Dr. **C. Weinheimer** (U Münster)
Prof. Dr. **K. Zuber** (TU Dresden)

Memberships.

Accelerator Test Facility (ATF), Program Advisory Committee
Ralph Aßmann

ACOT - Advisory Committee of TRIUMF (Canada)
Kerstin Borras

AIDA-2020
Felix Sefkow (Coordinator)

Akademie der Wissenschaften Hamburg
Wilfried Buchmüller

ArXiv Member Advisory Board
Martin Köhler

ATLAS Collaboration Board
Klaus Mönig

ATLAS Tracker Upgrade Management Board
Ingrid Gregor

AWAKE Experiment CERN Collaboration Board
Ralph Aßmann

BELLE II Institutional Board
Carsten Niebuhr

BELLE II Scrutiny Group
Bernd Löhr

BMBF "Physik der kleinsten Teilchen", Gutachterausschuss
Joachim Mnich

CALICE Steering Board
Felix Sefkow (Chair)

CERN Science Policy Committee
Reinhard Brinkmann, Beate Heinemann

CMS Collaboration Board
Kerstin Borras, Matthias Kasemann

CMS Tracker Institution Board
Günter Eckerlin

Computing Resources Review Board (CERN)
Volker Gülzow

Deutsches Forschungsnetz DFN, Betriebsausschuss
Volker Gülzow

Deutsches Forschungsnetz DFN, Verwaltungsrat
Joachim Mnich

DPG National Prize Committee
Georg Weiglein

DPG Wissenschaftlicher Beirat des Physikzentrums
Georg Weiglein

ERC Panel
Georg Weiglein

EuCARD2 European Coordination for Accelerator R&D
Ralph Aßmann, Nicoleta-Ionela Baboi, Jens Osterhoff

EuPRAXIA
Ralph Aßmann, Reinhard Brinkmann,
Jens Osterhoff (Chair of WP9)

European Committee for Future Accelerators (ECFA)
Kerstin Borras (Plenary Member),
Joachim Mnich (Ex-officio member)

European Network for Novel Accelerators (EuroNNAc), Steering Group
Jens Osterhoff

European Particle Physics Communication Network
Thomas Zoufal

European Physical Society Accelerator Group (EPS AG)
Ralph Aßmann

Excellence Cluster Universe, Scientific Advisory Committee
Wilfried Buchmüller

Future Circular Collider (FCC), Collaboration Board
Ralph Aßmann

Galileo Galilei Institute (INFN), Scientific Committee
Christophe Grojean

GATIS Marie Curie Project, Supervisory Board
Volker Schomerus (Chair)

Gauß-Allianz
Volker Gülzow

German Executive LHC Outreach Group (GELOG)
Matthias Kasemann, Thomas Naumann, Christian Mrotzek,
Barbara Warmbein, Thomas Zoufal

GridKa Technical Advisory Board
Martin Gasthuber, Brigit Lewendel

Hamilton Mathematics Institute, Trinity College Dublin, Advisory Board
Volker Schomerus

Helmholtz AK Bibliotheks- und Informationsmanagement
Martin Köhler

Helmholtz Arbeitskreis Open Science
Florian Schwennsen

Helmholtz Data Federation Executive Board
Volker Gülzow, Brigit Lewendel

Helmholtz IT-Koordinierungsausschuss (KoDa)
Volker Gülzow

Helmholtz Lenkungsausschuss Materie
Reinhard Brinkmann, Helmut Dosch, Volker Gülzow,
Joachim Mnich, Christian Stegmann, Edgar Weckert

Helmholtz Programme Matter and Technologies
Ties Behnke (Programme spokesperson)

Helmholtz Think Tank
Kerstin Borras, Hans Weise

Helsinki Physics Institute, Scientific Advisory Board
Wilfried Buchmüller

Humboldt Awards, Selection Committee
Wilfried Buchmüller

ICFA Beam Dynamics Panel
Rainer Wanzenberg

IEEE CANPS Technical Committee
Günter Eckerlin, Kay Rehlich

IEEE Radiation Instrumentation Steering Committee
Ingrid Gregor

IEEE Real-Time Systems, Scientific Committee
Günter Eckerlin

ILC European Action Plan Working Group
Nicholas Walker

ILC Physics and Experiment Board and Executive Board
Ties Behnke, Karsten Büßer

ILD Institute Assembly
Felix Sefkow

INDIGO Collaboration and Project Management Board
Patrick Fuhrmann

INSPIRE Directorate
Kirsten Sachs

INSPIRE High-Energy Physics Literature Database, International Advisory Board
Jürgen Reuter

Institut d'Etudes Scientifiques de Cargese (IESC), Scientific Committee
Géraldine Servant

Interactions Collaboration Board
Christian Mrotzek

International Committee for Future Accelerators (ICFA)
Joachim Mnich (Chair)

John Adams Institute, Advisory Board
Reinhard Brinkmann

John von Neumann Institute for Computing (NIC)
Joachim Mnich

Joint Institute for Nuclear Research (JINR), Programme Advisory Committee for Particle Physics
Joachim Mnich

Joint Institute of Nuclear Research (JINR), Scientific Council
Joachim Mnich

KIT Center for Elementary Particle and Astroparticle Physics (KCETA), Advisory Board
Joachim Mnich

Komitee für Astroteilchenphysik (KAT)
Martin Pohl, Christian Stegmann

Komitee für Beschleunigerphysik (KfB)
Jens Osterhoff, Hans Weise

Komitee für Elementarteilchenphysik (KET)
Kerstin Borras, Joachim Mnich, Georg Weiglein

LCC Physics and Detector Executive Board
Ties Behnke, Karsten Büßer

LHC Physics Center Management Board (LPC MB)
Kerstin Borras

LHC Resources Review Board
Manfred Fleischer

LHC Resources Scrutiny Group
Frank Gaede, Carsten Niebuhr

Linear Collider Board (LCB)
Joachim Mnich

Linear Collider Collaboration, Executive Committee
Brian Foster

Max-Planck-Institut für Gravitationsphysik, Potsdam, Advisory Committee
Wilfried Buchmüller

MPI Munich, Scientific Advisory Board
Joachim Mnich (Chair)

Munich Institute for Astro- and Particle Physics (MIAPP), Scientific Committee
Géraldine Servant

NIKHEF Scientific Advisory Committee (SAC)
Joachim Mnich

Oxford e-Science Research Centre Management Committee, University of Oxford
Brian Foster (Chair)

Particle Data Group
Brian Foster, Klaus Mönig, Andreas Ringwald, Georg Weiglein

Paul Scherrer Institut, Particle Physics Review
Joachim Mnich

PIER Executive Board (Research field Particle & Astroparticle Physics)
Georg Weiglein

SCOAP3 Repository Steering Working Group
Florian Schwennsen

SFB 676 Vorstand
Elisabetta Gallo, Christian Schwanenberger

SPS and PS Experiments Committee (SPSC), CERN
Markus Diehl

STFC, Accelerator Strategy Board (ASB)
Reinhard Brinkmann

SuperKEKB Machine Advisory Committee
Ralph Aßmann

TTC Executive Committee
Hans Weise

TTC Technical Board
Wolf-Dietrich Möller, Detlef Reschke

US LHC Accelerator Research Program Advisory Committee
Kay Wittenburg

Publications.

ALPS

Published

S. Alekhin et al.
A facility to search for hidden particles at the CERN SPS: the SHiP physics case.
Reports on progress in physics, 79(12):124201, and PUBDB-2016-04863.
doi: 10.1088/0034-4885/79/12/124201.

N. Bastidon, D. Horns and A. Lindner.
Quantum Efficiency Characterization and Optimization of a Tungsten Transition-Edge Sensor for ALPS II.
Journal of low temperature physics, 184(1):88, and PUBDB-2017-00297.
doi: 10.1007/s10909-015-1408-5.

S. Borsanyi et al.
Calculation of the axion mass based on high-temperature lattice quantum chromodynamics.
Nature / Physical science, 539(7627):69, and PUBDB-2016-04674, DESY-16-105.
doi: 10.1038/nature20115.

B. Döbrich et al.
ALPtraum: ALP production in proton beam dump experiments.
Journal of high energy physics, 2016(2):18, and PUBDB-2016-01167, DESY-15-237; arXiv:1512.03069.
doi: 10.1007/JHEP02(2016)018.

T. Fischer et al.
Probing axions with the neutrino signal from the next Galactic supernova.
Physical review / D, 94(8):085012, and PUBDB-2016-04423, DESY-16-094.
doi: 10.1103/PhysRevD.94.085012.

M. Giannotti et al.
Cool WISPs for stellar cooling excesses.
Journal of cosmology and astroparticle physics, 2016(05):057, and PUBDB-2016-02031, DESY-15-245; arXiv:1512.08108.
doi: 10.1088/1475-7516/2016/05/057.

Particle Data Collaboration.
Review of Particle Physics.
Chinese physics / C, 40(10):100001, and PUBDB-2016-04859.
doi: 10.1088/1674-1137/40/10/100001.

A. Ringwald and K. i. Saikawa.
Axion dark matter in the post-inflationary Peccei-Quinn symmetry breaking scenario.
Physical review / D, D93(8):085031, and PUBDB-2016-01891, DESY-15-250; arXiv:1512.06436.
doi: 10.1103/PhysRevD.93.085031.

A. Spector et al.
Characterization of Optical Systems for the ALPS II Experiment.
Optics express, 24(25):29237, and PUBDB-2016-06059, DESY 16-187.
doi: 10.1364/OE.24.029237.

ATLAS

Published

ATLAS Collaboration.
Identification of boosted, hadronically decaying W bosons and comparisons with ATLAS data taken at $\sqrt{s} = 8$ TeV.
The European physical journal / C, 76(3):154, and PUBDB-2016-01747, CERN-PH-EP-2015-204; arXiv:1510.05821.
doi: 10.1140/epjc/s10052-016-3978-z.

ATLAS Collaboration.
Measurements of top-quark pair differential cross-sections in the lepton+jets channel in pp collisions at $\sqrt{s} = 8$ TeV using the ATLAS detector.
The European physical journal / C, 76(10):538, and PUBDB-2016-04088, CERN-PH-EP-2015-239; arXiv:1511.04716.
doi: 10.1140/epjc/s10052-016-4366-4.

ATLAS Collaboration.
Search for new phenomena in different-flavour high-mass dilepton final states in pp collisions at $\sqrt{s} = 13$ Tev with the ATLAS detector.
The European physical journal / C, 76(10):541, and PUBDB-2016-04089, CERN-EP-2016-168; arXiv:1607.08079.
doi: 10.1140/epjc/s10052-016-4385-1.

A. Affolder et al.
Charge collection studies in irradiated HV-CMOS particle detectors.
Journal of Instrumentation, 11(04):P04007, and PUBDB-2017-00277.
doi: 10.1088/1748-0221/11/04/P04007.

M. Alhroob et al.
Implementations of Custom Sonar Instruments for Binary Gas Mixture and Flow Analysis in the ATLAS Experiment at the CERN LHC.
IEEE transactions on nuclear science, 63(3):1659, and PUBDB-2017-00284.
doi: 10.1109/TNS.2016.2561290.

ATLAS Collaboration.
A measurement of material in the ATLAS tracker using secondary hadronic interactions in 7 TeV pp collisions.
Journal of Instrumentation, 11(11):P11020, and PUBDB-2016-06122, arXiv:1609.04305.
doi: 10.1088/1748-0221/11/11/P11020.

ATLAS Collaboration.
A new method to distinguish hadronically decaying boosted Z bosons from W bosons using the ATLAS detector.
The European physical journal / C, 76(5):238, and PUBDB-2016-02050, CERN-PH-EP-2015-194; arXiv:1509.04939.
doi: 10.1140/epjc/s10052-016-4065-1.

ATLAS Collaboration.
A Search for an Excited Muon Decaying to a Muon and Two Jets in pp Collisions at $\sqrt{s} = 8$ TeV with the ATLAS Detector.
New journal of physics, 18(7):073021, and PUBDB-2016-03101, CERN-PH-EP-2015-298; arXiv:1601.05627.
doi: 10.1088/1367-2630/18/7/073021.

ATLAS Collaboration.
A search for prompt lepton-jets in pp collisions at $\sqrt{s}$ = 8 TeV with the ATLAS detector.
Journal of high energy physics, 2016(2):62, and PUBDB-2016-01133, CERN-PH-EP-2015-242; arXiv:1511.05542.
doi: 10.1007/JHEP02(2016)062.

ATLAS Collaboration.
A search for top squarks with R-parity-violating decays to all-hadronic final states with the ATLAS detector in $\sqrt{s}$ = 8 TeV proton-proton collisions.
Journal of high energy physics, 1606(6):67, and PUBDB-2016-02768, CERN-PH-EP-2015-296; arXiv:1601.07453.
doi: 10.1007/JHEP06(2016)067.

ATLAS Collaboration.
Beam-induced and cosmic-ray backgrounds observed in the ATLAS detector during the LHC 2012 proton-proton running period.
Journal of Instrumentation, 11(05):P05013, and PUBDB-2016-02068, CERN-EP-2016-029; arXiv:1603.09202.
doi: 10.1088/1748-0221/11/05/P05013.

ATLAS Collaboration.
Centrality, rapidity and transverse momentum dependence of isolated prompt photon production in lead-lead collisions at $\sqrt{s_{NN}} = 2.76$ TeV measured with the ATLAS detector.
Physical review / C, 93(3):034914, and PUBDB-2016-01748, CERN-PH-EP-2015-142; arXiv:1506.08552.
doi: 10.1103/PhysRevC.93.034914.

ATLAS Collaboration.
Charged-particle distributions at low transverse momentum in $\sqrt{s} = 13$ TeV pp interactions measured with the ATLAS detector at the LHC.
The European physical journal / C, 76(9):502, and PUBDB-2016-03964, CERN-EP-2016-099; arXiv:1606.01133.
doi: 10.1140/epjc/s10052-016-4335-y.

ATLAS Collaboration.
Charged-particle distributions in pp interactions at $\sqrt{s} = 8$ TeV measured with the ATLAS detector.
The European physical journal / C, 76(7):403, and PUBDB-2016-02788, CERN-EP-2016-020; arXiv:1603.02439.
doi: 10.1140/epjc/s10052-016-4203-9.

ATLAS Collaboration.
Charged-particle distributions in $\sqrt{s}$ = 13 TeV pp interactions measured with the ATLAS detector at the LHC.
Physics letters / B, 758:67, and PUBDB-2017-00342, CERN-EP-2016-014; arXiv:1602.01633.
doi: 10.1016/j.physletb.2016.04.050.

ATLAS Collaboration.
Combination of searches for WW, WZ, and ZZ resonances in pp collisions at $\sqrt{s} = 8$ TeV with the ATLAS detector.
Physics letters / B, 755:285, and PUBDB-2016-01749, CERN-PH-EP-2015-269; arXiv:1512.05099.
doi: 10.1016/j.physletb.2016.02.015.

ATLAS Collaboration.
Constraints on non-Standard Model Higgs boson interactions in an effective Lagrangian using differential cross sections measured in the $H \rightarrow \gamma\gamma$ decay channel at $\sqrt{s} = 8$ TeV with the ATLAS detector.
Physics letters / B, 753:69, and PUBDB-2017-00348, CERN-PH-EP-2015-182; arXiv:1508.02507.
doi: 10.1016/j.physletb.2015.11.071.

ATLAS Collaboration.
Dark matter interpretations of ATLAS searches for the electroweak production of supersymmetric particles in $\sqrt{s} = 8$ TeV proton-proton collisions.
Journal of high energy physics, 2016(9):175, and PUBDB-2016-03988, arXiv:1608.00872; CERN-PH-EP-2016-165.
doi: 10.1007/JHEP09(2016)175.

ATLAS Collaboration.
Dijet production in $\sqrt{s}$ =7 TeV pp collisions with large rapidity gaps at the ATLAS experiment.
Physics letters / B, 754:214, and PUBDB-2016-01017, CERN-PH-EP-2015-227; arXiv:1511.00502.
doi: 10.1016/j.physletb.2016.01.028.

ATLAS Collaboration.
Erratum to: ATLAS Run 1 searches for direct pair production of third-generation squarks at the Large Hadron Collider.
The European physical journal / C, 76(3):153, and PUBDB-2017-00349, CERN-PH-EP-2015-138.
doi: 10.1140/epjc/s10052-016-3935-x.

ATLAS Collaboration.
Erratum to: Study of the spin and parity of the Higgs boson in diboson decays with the ATLAS detector.
The European physical journal / C, 76(3):152, and PUBDB-2017-00344, CERN-PH-EP-2015-114.
doi: 10.1140/epjc/s10052-016-3934-y.

ATLAS Collaboration.
Evidence for single top-quark production in the s-channel in proton–proton collisions at $\sqrt{s} = 8$ TeV with the ATLAS detector using the Matrix Element Method.
Physics letters / B, 756:228, and PUBDB-2016-01384, CERN-PH-EP-2015-286; arXiv:1511.05980.
doi: 10.1016/j.physletb.2016.03.017.

ATLAS Collaboration.
Identification of high transverse momentum top quarks in pp collisions at $\sqrt{s} = 8$ TeV with the ATLAS detector.
Journal of high energy physics, 1606(6):93, and PUBDB-2017-00345, CERN-EP-2016-010; arXiv:1603.03127.
doi: 10.1007/JHEP06(2016)093.

ATLAS Collaboration.
Luminosity determination in pp collisions at $\sqrt{s}$ = 8 TeV using the ATLAS detector at the LHC.
The European physical journal / C, 76(12):653, and PUBDB-2016-06040, CERN-EP-2016-117; arXiv:1608.03953.
doi: 10.1140/epjc/s10052-016-4466-1.

ATLAS Collaboration.
Measurement of $D^{*\pm}$, $D^{\pm}$ and $D_s^{\pm}$ meson production cross sections in pp collisions at $\sqrt{s} = 7$ TeV with the ATLAS detector.
Nuclear physics / B, 907:717, and PUBDB-2016-02082, CERN-PH-EP-2015-288; arXiv:1512.02913.
doi: 10.1016/j.nuclphysb.2016.04.032.

ATLAS Collaboration.
Measurement of event-shape observables in $Z \to \ell^+\ell^-$ events in pp collisions at $\sqrt{s} = 7$ TeV with the ATLAS detector at the LHC.
The European physical journal / C, 76(7):375, and PUBDB-2016-02776, CERN-EP-2016-015; arXiv:1602.08980.
doi: 10.1140/epjc/s10052-016-4176-8.

ATLAS Collaboration.
Measurement of exclusive $\gamma\gamma \to W^+W^-$ production and search for exclusive Higgs boson production in pp collisions at $\sqrt{s} = 8$ TeV using the ATLAS detector.
Physical review / D, 94(3):032011, and PUBDB-2016-03717.
doi: 10.1103/PhysRevD.94.032011.

ATLAS Collaboration.
Measurement of jet activity in top quark events using the $e\mu$ final state with two b-tagged jets in pp collisions at $\sqrt{s} = 8$ TeV with the ATLAS detector.
Journal of high energy physics, 1609(9):074, and PUBDB-2016-03961, CERN-EP-2016-122; arXiv:1606.09490.
doi: 10.1007/JHEP09(2016)074.

ATLAS Collaboration.
Measurement of jet charge in dijet events from $\sqrt{s}$ = 8 TeV pp collisions with the ATLAS detector.
Physical review / D, 93(5):052003, and PUBDB-2016-01323, CERN-PH-EP-2015-207; arXiv:1509.05190.
doi: 10.1103/PhysRevD.93.052003.

ATLAS Collaboration.
Measurement of the angular coefficients in Z-boson events using electron and muon pairs from data taken at $\sqrt{s} = 8$ TeV with the ATLAS detector.
Journal of high energy physics, 1608(8):159, and PUBDB-2016-03715, CERN-EP-2016-087; arXiv:1606.00689.
doi: 10.1007/JHEP08(2016)159.

ATLAS Collaboration.
Measurement of the $b\bar{b}$ dijet cross section in pp collisions at $\sqrt{s} = 7$ TeV with the ATLAS detector.
The European physical journal / C, 76(12):670, and PUBDB-2016-06153, CERN-EP-2016-091; arXiv:1607.08430.
doi: 10.1140/epjc/s10052-016-4521-y.

ATLAS Collaboration.
Measurement of the centrality dependence of the charged-particle pseudorapidity distribution in proton–lead collisions at $\sqrt{s_{\rm NN}} = 5.02$ TeV with the ATLAS detector.
The European physical journal / C, 76(4):199, and PUBDB-2016-01797, CERN-PH-EP-2015-160; arXiv:1508.00848.
doi: 10.1140/epjc/s10052-016-4002-3.

ATLAS Collaboration.
Measurement of the charge asymmetry in highly boosted top-quark pair production in $\sqrt{s}$ = 8 TeV pp collision data collected by the ATLAS experiment.
Physics letters / B, 756:52, and PUBDB-2016-01326, CERN-PH-EP-2015-303; arXiv:1512.06092.
doi: 10.1016/j.physletb.2016.02.055.

ATLAS Collaboration.
Measurement of the charge asymmetry in top-quark pair production in the lepton-plus-jets final state in pp collision data at $\sqrt{s} = 8$ TeV with the ATLAS detector.
The European physical journal / C, 76(2):87, and PUBDB-2016-01147, CERN-PH-EP-2015-217; arXiv:1509.02358.
doi: 10.1140/epjc/s10052-016-3910-6.

ATLAS Collaboration.
Measurement of the charged-particle multiplicity inside jets from $\sqrt{s} = 8$ TeV pp collisions with the ATLAS detector.
The European physical journal / C, 76(6):322, and PUBDB-2016-02774, CERN-PH-EP-2016-001; CERN-EP-2016-001; arXiv:1602.00988.
doi: 10.1140/epjc/s10052-016-4126-5.

ATLAS Collaboration.
Measurement of the correlations between the polar angles of leptons from top quark decays in the helicity basis at $\sqrt{s} = 7$ TeV using the ATLAS detector.
Physical review / D, 93(1):012002, and PUBDB-2016-00357, CERN-PH-EP-2015-241; arXiv:1510.07478.
doi: 10.1103/PhysRevD.93.012002.

ATLAS Collaboration.
Measurement of the CP-violating phase ϕ_s and the B_s^0 meson decay width difference with $B_s^0 \to J/\psi\phi$ decays in ATLAS.
Journal of high energy physics, 1608(8):147, and PUBDB-2016-03673, CERN-PH-EP-2015-166; arXiv:1601.03297.
doi: 10.1007/JHEP08(2016)147.

ATLAS Collaboration.
Measurement of the dependence of transverse energy production at large pseudorapidity on the hard-scattering kinematics of proton-proton collisions at $\sqrt{s} = 2.76$ TeV with ATLAS.
Physics letters / B, 756:10, and PUBDB-2016-01325, CERN-PH-EP-2015-293; arXiv:1512.00197.
doi: 10.1016/j.physletb.2016.02.056.

ATLAS Collaboration.
Measurement of the differential cross-section of highly boosted top quarks as a function of their transverse momentum in $\sqrt{s}$ = 8 TeV proton-proton collisions using the ATLAS detector.
Physical review / D, 93(3):032009, and PUBDB-2016-01322, CERN-PH-EP-2015-237; arXiv:1510.03818.
doi: 10.1103/PhysRevD.93.032009.

ATLAS Collaboration.
Measurement of the differential cross-sections of prompt and non-prompt production of J/ψ and $\psi(2S)$ in pp collisions at $\sqrt{s} = 7$ and 8 TeV with the ATLAS detector.
The European physical journal / C, 76(5):283, and PUBDB-2016-02077, CERN-PH-EP-2015-292; arXiv:1512.03657.
doi: 10.1140/epjc/s10052-016-4050-8.

ATLAS Collaboration.
Measurement of the double-differential high-mass Drell-Yan cross section in pp collisions at $\sqrt{s}$ = 8 TeV with the ATLAS detector.
Journal of high energy physics, 2016(8):9, and PUBDB-2016-02840, CERN-EP-2016-079; arXiv:1606.01736.
doi: 10.1007/JHEP08(2016)009.

ATLAS Collaboration.
Measurement of the inclusive isolated prompt photon cross section in pp collisions at $\sqrt{s} = 8$ TeV with the ATLAS detector.
Journal of high energy physics, 2016(8):5, and PUBDB-2016-02838, CERN-EP-2016-035; arXiv:1605.03495.
doi: 10.1007/JHEP08(2016)005.

ATLAS Collaboration.
Measurement of the Inelastic Proton-Proton Cross Section at $\sqrt{s}$ = 13 TeV with the ATLAS Detector at the LHC.
Physical review letters, 117(18):182002, and PUBDB-2016-05248, CERN-EP-2016-140; arXiv:1606.02625.
doi: 10.1103/PhysRevLett.117.182002.

ATLAS Collaboration.
Measurement of the photon identification efficiencies with the ATLAS detector using LHC Run-1 data.
The European physical journal / C, 76(12):666, and PUBDB-2016-06152, CERN-EP-2016-110; arXiv:1606.01813.
doi: 10.1140/epjc/s10052-016-4507-9.

ATLAS Collaboration.
Measurement of the production cross-section of a single top quark in association with a W boson at 8 TeV with the ATLAS experiment.
Journal of high energy physics, 1601(1):64, and PUBDB-2016-00549, CERN-PH-2015-230; CERN-PH-EP-2015-230; arXiv:1510.03752.
doi: 10.1007/JHEP01(2016)064.

ATLAS Collaboration.
Measurement of the relative width difference of the B^0-$\bar{B}^0$ system with the ATLAS detector.
Journal of high energy physics, 1606(6):081, and PUBDB-2017-00250, CERN-EP-2016-085; arXiv:1605.07485.
doi: 10.1007/JHEP06(2016)081.

ATLAS Collaboration.
Measurement of the top quark mass in the $t\bar{t} \rightarrow$ dilepton channel from $\sqrt{s} = 8$ TeV ATLAS data.
Physics letters / B, 761:350, and PUBDB-2016-03925, CERN-EP-2016-114; arXiv:1606.02179.
doi: 10.1016/j.physletb.2016.08.042.

ATLAS Collaboration.
Measurement of the transverse momentum and ϕ^*_η distributions of Drell–Yan lepton pairs in proton–proton collisions at $\sqrt{s} = 8$ TeV with the ATLAS detector.
The European physical journal / C, 76(5):291, and PUBDB-2016-02079, CERN-PH-EP-2015-275; arXiv:1512.02192.
doi: 10.1140/epjc/s10052-016-4070-4.

ATLAS Collaboration.
Measurement of the $t\bar{t}$ production cross-section using $e\mu$ events with b-tagged jets in pp collisions at $\sqrt{s} = 13$ TeV with the ATLAS detector.
Physics letters / B, B761:136, and PUBDB-2016-03713, CERN-EP-2016-088; arXiv:1606.02699.
doi: 10.1016/j.physletb.2016.08.019.

ATLAS Collaboration.
Measurement of the ZZ Production Cross Section in pp Collisions at $\sqrt{s}$ = 13 TeV with the ATLAS Detector.
Physical review letters, 116(10):101801, and PUBDB-2016-01385, CERN-PH-EP-2015-318; arXiv:1512.05314.
doi: 10.1103/PhysRevLett.116.101801.

ATLAS Collaboration.
Measurement of top quark pair differential cross-sections in the dilepton channel in pp collisions at $\sqrt{s}$ = 7 and 8 TeV with ATLAS.
Physical review / D, 94(9):092003, and PUBDB-2016-05345, CERN-EP-2016-144; arXiv:1607.07281.
doi: 10.1103/PhysRevD.94.092003.

ATLAS Collaboration.
Measurement of total and differential W^+W^- production cross sections in proton-proton collisions at $\sqrt{s} = 8$ TeV with the ATLAS detector and limits on anomalous triple-gauge-boson couplings.
Journal of high energy physics, 1609(9):029, and PUBDB-2016-03926, CERN-PH-EP-2015-323; arXiv:1603.01702.
doi: 10.1007/JHEP09(2016)029.

ATLAS Collaboration.
Measurement of $W^\pm$ and Z-boson production cross sections in pp collisions at $\sqrt{s} = 13$ TeV with the ATLAS detector.
Physics letters / B, 759:601, and PUBDB-2016-02779, CERN-EP-2016-069; arXiv:1603.09222.
doi: 10.1016/j.physletb.2016.06.023.

ATLAS Collaboration.
Measurement of W boson angular distributions in events with high transverse momentum jets at $\sqrt{s} = 8$ TeV using the ATLAS detector.
Physics letters / B, 765:132, and PUBDB-2016-06414, CERN-EP-2016-182; arXiv:1609.07045.
doi: 10.1016/j.physletb.2016.12.005.

ATLAS Collaboration.
Measurements of fiducial cross-sections for $t\bar{t}$ production with one or two additional b-jets in pp collisions at $\sqrt{s}$ =8 TeV using the ATLAS detector.
The European physical journal / C, 76(1):11, and PUBDB-2016-00248, CERN-PH-EP-2015-200; arXiv:1508.06868.
doi: 10.1140/epjc/s10052-015-3852-4.

ATLAS Collaboration.
Measurements of the charge asymmetry in top-quark pair production in the dilepton final state at $\sqrt{s} = 8$ TeV with the ATLAS detector.
Physical review / D covering particles, fields, gravitation, and cosmology, 94(3):032006, and PUBDB-2017-00254, CERN-

EP-2016-051; arXiv:1604.05538.
doi: 10.1103/PhysRevD.94.032006.

ATLAS Collaboration.
Measurements of the Higgs boson production and decay rates and coupling strengths using pp collision data at $\sqrt{s}$ = 7 and 8 TeV in the ATLAS experiment.
The European physical journal / C, 76(1):6, and PUBDB-2017-00350, CERN-PH-EP-2015-125; arXiv:1507.04548.
doi: 10.1140/epjc/s10052-015-3769-y.

ATLAS Collaboration.
Measurements of $W^{\pm}Z$ production cross sections in pp collisions at $\sqrt{s} = 8$ TeV with the ATLAS detector and limits on anomalous gauge boson self-couplings.
Physical review / D, 93(9):092004, and PUBDB-2016-02066, CERN-EP-2016-017; arXiv:1603.02151.
doi: 10.1103/PhysRevD.93.092004.

ATLAS Collaboration.
Measurements of $Z\gamma$ and $Z\gamma\gamma$ production in pp collisions at $\sqrt{s}$ = 8 TeV with the ATLAS detector.
Physical review / D, 93(11):112002, and PUBDB-2016-02170, CERN-EP-2016-049; arXiv:1604.05232.
doi: 10.1103/PhysRevD.93.112002.

ATLAS Collaboration.
Muon reconstruction performance of the ATLAS detector in proton–proton collision data at $\sqrt{s}$ =13 TeV.
The European physical journal / C, 76(5):292, and PUBDB-2016-02076, CERN-EP-2016-033; arXiv:1603.05598.
doi: 10.1140/epjc/s10052-016-4120-y.

ATLAS Collaboration.
Observation of long-range elliptic azimuthal anisotropies in $\sqrt{s}$ =13 and 2.76 TeV pp collisions with the ATLAS detector.
Physical review letters, 116(17):172301, and PUBDB-2016-01857, CERN-PH-EP-2015-251; arXiv:1509.04776.
doi: 10.1103/PhysRevLett.116.172301.

ATLAS Collaboration.
Performance of b-Jet Identification in the ATLAS Experiment.
Journal of Instrumentation, 11(04):P04008, and PUBDB-2016-01757, CERN-PH-EP-2015-216; arXiv:1512.01094.
doi: 10.1088/1748-0221/11/04/P04008.

ATLAS Collaboration.
Performance of pile-up mitigation techniques for jets in pp collisions at $\sqrt{s}$ = 8 TeV using the ATLAS detector.
The European physical journal / C, 76(11):581, and PUBDB-2016-05249, CERN-PH-EP-2015-206; arXiv:1510.03823.
doi: 10.1140/epjc/s10052-016-4395-z.

ATLAS Collaboration.
Probing lepton flavour violation via neutrinoless $\tau \longrightarrow 3\mu$ decays with the ATLAS detector.
The European physical journal / C, 76(5):232, and PUBDB-2016-01856, CERN-PH-EP-2015-315; arXiv:1601.03567.
doi: 10.1140/epjc/s10052-016-4041-9.

ATLAS Collaboration.
Reconstruction of hadronic decay products of tau leptons with the ATLAS experiment.
The European physical journal / C, 76(5):295, and PUBDB-2016-02080, CERN-PH-EP-2015-294; arXiv:1512.05955.
doi: 10.1140/epjc/s10052-016-4110-0.

ATLAS Collaboration.
Search for a high-mass Higgs boson decaying to a W boson pair in pp collisions at $\sqrt{s} = 8$ TeV with the ATLAS detector.
Journal of high energy physics, 2016(1):32, and PUBDB-2016-00342, CERN-PH-EP-2015-185; arXiv:1509.00389.
doi: 10.1007/JHEP01(2016)032.

ATLAS Collaboration.
Search for an additional, heavy Higgs boson in the $H \rightarrow ZZ$ decay channel at $\sqrt{s} = 8$ TeV in pp collision data with the ATLAS detector.
The European physical journal / C, 76(1):45, and PUBDB-2016-01016, CERN-PH-EP-2015-154; arXiv:1507.05930.
doi: 10.1140/epjc/s10052-015-3820-z.

ATLAS Collaboration.
Search for anomalous couplings in the Wtb vertex from the measurement of double differential angular decay rates of single top quarks produced in the t-channel with the ATLAS detector.
Journal of high energy physics, 1604(4):23, and PUBDB-2016-01758, CERN-PH-EP-2015-236; arXiv:1510.03764.
doi: 10.1007/JHEP04(2016)023.

ATLAS Collaboration.
Search for bottom squark pair production in proton–proton collisions at $\sqrt{s} = 13$ TeV with the ATLAS detector.
The European physical journal / C, 76(10):547, and PUBDB-2016-05246, CERN-EP-2016-138; CERN-PH-2016-138; arXiv:1606.08772.
doi: 10.1140/epjc/s10052-016-4382-4.

ATLAS Collaboration.
Search for charged Higgs bosons in the $H^{\pm} \rightarrow tb$ decay channel in pp collisions at $\sqrt{s} = 8$ TeV using the ATLAS detector.
Journal of high energy physics, 1603(3):127, and PUBDB-2016-01744, CERN-PH-EP-2015-290; arXiv:1512.03704.
doi: 10.1007/JHEP03(2016)127.

ATLAS Collaboration.
Search for charged Higgs bosons produced in association with a top quark and decaying via $H^{\pm} \rightarrow \tau\nu$ using pp collision data recorded at $\sqrt{s} = 13$ TeV by the ATLAS detector.
Physics letters / B, 759:555, and PUBDB-2016-02777, CERN-EP-2016-056; arXiv:1603.09203.
doi: 10.1016/j.physletb.2016.06.017.

ATLAS Collaboration.
Search for dark matter in association with a Higgs boson decaying to b-quarks in pp collisions at $\sqrt{s} = 13$ TeV with the ATLAS detector.
Physics letters / B, 765:11, and PUBDB-2016-06175, CERN-EP-2016-181; arXiv:1609.04572.
doi: 10.1016/j.physletb.2016.11.035.

ATLAS Collaboration.
Search for dark matter produced in association with a hadronically decaying vector boson in pp collisions at $\sqrt{s} = 13$ TeV with the ATLAS detector.
Physics letters / B, 763:251, and PUBDB-2016-05251, CERN-EP-2016-180; arXiv:1608.02372.
doi: 10.1016/j.physletb.2016.10.042.

ATLAS Collaboration.
Search for dark matter produced in association with a Higgs boson decaying to two bottom quarks in pp collisions at $\sqrt{s} = 8$ TeV with the ATLAS detector.
Physical review / D, 93(7):072007, and PUBDB-2016-01801, CERN-PH-EP-2015-247; arXiv:1510.06218.
doi: 10.1103/PhysRevD.93.072007.

ATLAS Collaboration.
Search for direct top squark pair production in final states with two tau leptons in pp collisions at $\sqrt{s} = 8$ TeV with the ATLAS detector.
The European physical journal / C, 76(2):81, and PUBDB-2016-01146, CERN-PH-EP-2015-188; arXiv:1509.04976.
doi: 10.1140/epjc/s10052-016-3897-z.

ATLAS Collaboration.
Search for flavour-changing neutral current top-quark decays to qZ in pp collision data collected with the ATLAS detector at $\sqrt{s} = 8$ TeV.
The European physical journal / C, 76(1):12, and PUBDB-2016-00347, arXiv:1508.05796; CERN-PH-EP-2015-183.
doi: 10.1140/epjc/s10052-015-3851-5.

ATLAS Collaboration.
Search for gluinos in events with an isolated lepton, jets and missing transverse momentum at $\sqrt{s} = 13$ TeV with the ATLAS detector.
The European physical journal / C, 76(10):565, and PUBDB-2016-05247, CERN-EP-2016-037; arXiv:1605.04285.
doi: 10.1140/epjc/s10052-016-4397-x.

ATLAS Collaboration.
Search for heavy long-lived charged R-hadrons with the ATLAS detector in 3.2 fb^{-1} of proton–proton collision data at $\sqrt{s} = 13$ TeV.
Physics letters / B, 760:647, and PUBDB-2016-02790, CERN-EP-2016-131; arXiv:1606.05129.
doi: 10.1016/j.physletb.2016.07.042.

ATLAS Collaboration.
Search for heavy resonances decaying to a Z boson and a photon in pp collisions at $\sqrt{s} = 13$ TeV with the ATLAS detector.
Physics letters / B, 764:11, and PUBDB-2016-05441, CERN-EP-2016-163; arXiv:1607.06363.
doi: 10.1016/j.physletb.2016.11.005.

ATLAS Collaboration.
Search for Higgs and Z Boson Decays to $\phi\gamma$ with the ATLAS Detector.
Physical review letters, 117(11):111802, and PUBDB-2016-03959, CERN-EP-2016-130; arXiv:1607.03400.
doi: 10.1103/PhysRevLett.117.111802.

ATLAS Collaboration.
Search for invisible decays of a Higgs boson using vector-boson fusion in pp collisions at $\sqrt{s} = 8$ TeV with the ATLAS detector.
Journal of high energy physics, 1601(1):172, and PUBDB-2016-01018, CERN-PH-EP-2015-186; arXiv:1508.07869.
doi: 10.1007/JHEP01(2016)172.

ATLAS Collaboration.
Search for magnetic monopoles and stable particles with high electric charges in 8 TeV pp collisions with the ATLAS detector.
Physical review / D, D93(5):052009, and PUBDB-2016-01745, CERN-PH-EP-2015-174; arXiv:1509.08059.
doi: 10.1103/PhysRevD.93.052009.

ATLAS Collaboration.
Search for metastable heavy charged particles with large ionization energy loss in pp collisions at $\sqrt{s} = 13$ TeV using the ATLAS experiment.
Physical review / D, 93(11):112015, and PUBDB-2016-02775, CERN-EP-2016-063; arXiv:1604.04520.
doi: 10.1103/PhysRevD.93.112015.

ATLAS Collaboration.
Search for Minimal Supersymmetric Standard Model Higgs bosons H/A and for a Z' boson in the $\tau\tau$ final state produced in pp collisions at $\sqrt{s} = 13$ TeV with the ATLAS Detector.
The European physical journal / C, 76(11):585, and PUBDB-2016-05250, CERN-EP-2016-164; arXiv:1608.00890.
doi: 10.1140/epjc/s10052-016-4400-6.

ATLAS Collaboration.
Search for new phenomena in dijet mass and angular distributions from pp collisions at $\sqrt{s} = 13$ TeV with the ATLAS detector.
Physics letters / B, 754:302, and PUBDB-2016-01015, CERN-PH-EP-2015-311; arXiv:1512.01530.
doi: 10.1016/j.physletb.2016.01.032.

ATLAS Collaboration.
Search for new phenomena in events with a photon and missing transverse momentum in pp collisions at $\sqrt{s} = 13$ TeV with the ATLAS detector.
Journal of high energy physics, 1606(6):59, and PUBDB-2016-02766, CERN-EP-2016-060; arXiv:1604.01306.
doi: 10.1007/JHEP06(2016)059.

ATLAS Collaboration.
Search for new phenomena in events with at least three photons collected in pp collisions at $\sqrt{s} = 8$ TeV with the ATLAS detector.
The European physical journal / C, 76(4):210, and PUBDB-2016-01802, CERN-PH-EP-2015-187; arXiv:1509.05051.
doi: 10.1140/epjc/s10052-016-4034-8.

ATLAS Collaboration.
Search for new phenomena in final states with an energetic jet and large missing transverse momentum in pp collisions at $\sqrt{s} = 13$ TeV using the ATLAS detector.
Physical review / D, 94(3):032005, and PUBDB-2016-03499, CERN-EP-2016-075; arXiv:1604.07773.
doi: 10.1103/PhysRevD.94.032005.

ATLAS Collaboration.
Search for new phenomena in final states with large jet multiplicities and missing transverse momentum with ATLAS using $\sqrt{s} = 13$ TeV proton-proton collisions.
Physics letters / B, 757:334, and PUBDB-2016-02081, CERN-PH-EP-2016-026; CERN-EP-2016-026; arXiv:1602.06194.
doi: 10.1016/j.physletb.2016.04.005.

ATLAS Collaboration.
Search for new phenomena with photon+jet events in proton-proton collisions at $\sqrt{s} = 13$ TeV with the ATLAS detector.
Journal of high energy physics, 2016(3):41, and PUBDB-2016-01386, CERN-PH-EP-2015-320; arXiv:1512.05910.
doi: 10.1007/JHEP03(2016)041.

ATLAS Collaboration.
Search for new resonances decaying to a W or Z boson and a Higgs boson in the $\ell^+\ell^- b\bar{b}$, $\ell\nu b\bar{b}$, and $\nu\bar{\nu}b\bar{b}$ channels with pp collisions at $\sqrt{s} = 13$ TeV with the ATLAS detector.
Physics letters / B, 765:32, and PUBDB-2016-06173, CERN-EP-2016-148; arXiv:1607.05621.
doi: 10.1016/j.physletb.2016.11.045.

ATLAS Collaboration.
Search for new resonances in events with one lepton and missing transverse momentum in pp collisions at $\sqrt{s} = 13$ TeV with the ATLAS detector.
Physics letters / B, 762:334, and PUBDB-2016-05346, CERN-EP-2016-143; arXiv:1606.03977.
doi: 10.1016/j.physletb.2016.09.040.

ATLAS Collaboration.
Search for Pair Production of Gluinos Decaying Via Stop and Sbottom in Events with b-Jets and Large Missing Transverse Momentum in pp Collisions at $\sqrt{s} = 13$ TeV with the ATLAS Detector.
Physical review / D, 94(3):032003, and PUBDB-2016-03100, CERN-EP-2016-061; arXiv:1605.09318.
doi: 10.1103/PhysRevD.94.032003.

ATLAS Collaboration.
Search for pair production of Higgs bosons in the $b\bar{b}b\bar{b}$ final state using proton-proton collisions at $\sqrt{s} = 13$ TeV with the ATLAS detector.
Physical review / D, 94(5):052002, and PUBDB-2016-03924, CERN-EP-2016-142; arXiv:1606.04782.
doi: 10.1103/PhysRevD.94.052002.

ATLAS Collaboration.
Search for resonances in diphoton events at $\sqrt{s}$ = 13 TeV with the ATLAS detector.
Journal of high energy physics, 1609(9):001, and PUBDB-2016-03918, CERN-EP-2016-120; arXiv:1606.03833.
doi: 10.1007/JHEP09(2016)001.

ATLAS Collaboration.
Search for resonances in the mass distribution of jet pairs with one or two jets identified as b-jets in proton–proton collisions at $\sqrt{s} = 13$ TeV with the ATLAS detector.
Physics letters / B, 759:229, and PUBDB-2017-00253, CERN-EP-2016-066; CERN-EP-2016-66; arXiv:1603.08791.
doi: 10.1016/j.physletb.2016.05.064.

ATLAS Collaboration.
Search for scalar leptoquarks in pp collisions at $\sqrt{s}$ = 13 TeV with the ATLAS experiment.
New journal of physics, 18(9):093016, and PUBDB-2017-00251, CERN-EP-2016-074; arXiv:1605.06035.
doi: 10.1088/1367-2630/18/9/093016.

ATLAS Collaboration.
Search for single production of a vector-like quark via a heavy gluon in the $4b$ final state with the ATLAS detector in pp collisions at $\sqrt{s} = 8$ TeV.
Physics letters / B, 758:249, and PUBDB-2017-00343, CERN-PH-EP-2015-321; arXiv:1602.06034.
doi: 10.1016/j.physletb.2016.04.061.

ATLAS Collaboration.
Search for single production of vector-like quarks decaying into Wb in pp collisions at $\sqrt{s} = 8$ TeV with the ATLAS detector.
The European physical journal / C, 76(8):442, and PUBDB-2016-03303, CERN-PH-EP-2015-319; arXiv:1602.05606.
doi: 10.1140/epjc/s10052-016-4281-8.

ATLAS Collaboration.
Search for single top-quark production via flavour-changing neutral currents at 8 TeV with the ATLAS detector.
The European physical journal / C, 76(2):55, and PUBDB-2016-01019, CERN-PH-EP-2015-172; arXiv:1509.00294.
doi: 10.1140/epjc/s10052-016-3876-4.

ATLAS Collaboration.
Search for squarks and gluinos in events with hadronically decaying tau leptons, jets and missing transverse momentum in proton-proton collisions at $\sqrt{s} = 13$ TeV recorded with the ATLAS detector.
The European physical journal / C, 76(12):683, and PUBDB-2016-06211, CERN-EP-2016-145; arXiv:1607.05979.
doi: 10.1140/epjc/s10052-016-4481-2.

ATLAS Collaboration.
Search for squarks and gluinos in final states with jets and missing transverse momentum at $\sqrt{s}$ =13 TeV with the ATLAS detector.
The European physical journal / C, 76(7):392, and PUBDB-2016-02783, CERN-EP-2016-080; arXiv:1605.03814.
doi: 10.1140/epjc/s10052-016-4184-8.

ATLAS Collaboration.
Search for strong gravity in multijet final states produced in pp collisions at $\sqrt{s}$ = 13 TeV using the ATLAS detector at the LHC.
Journal of high energy physics, 1603(3):26, and PUBDB-2016-01387, CERN-PH-EP-2015-312; arXiv:1512.02586.
doi: 10.1007/JHEP03(2016)026.

ATLAS Collaboration.
Search for TeV-scale gravity signatures in high-mass final states with leptons and jets with the ATLAS detector at $\sqrt{s} = 13$ TeV.
Physics letters / B, 760:520, and PUBDB-2016-02789, CERN-EP-2016-109; arXiv:1606.02265.
doi: 10.1016/j.physletb.2016.07.030.

ATLAS Collaboration.
Search for the electroweak production of supersymmetric particles in $\sqrt{s}$=8 TeV pp collisions with the ATLAS detector.
Physical review / D, 93(5):052002, and PUBDB-2016-01324, CERN-PH-EP-2015-218; arXiv:1509.07152.
doi: 10.1103/PhysRevD.93.052002.

ATLAS Collaboration.
Search for the Higgs boson produced in association with a W boson and decaying to four b-quarks via two spin-zero particles in pp collisions at 13 TeV with the ATLAS detector.
The European physical journal / C, 76(11):605, and PUBDB-2016-05440, CERN-EP-2016-135; arXiv:1606.08391.
doi: 10.1140/epjc/s10052-016-4418-9.

ATLAS Collaboration.
Search for the production of single vector-like and excited quarks in the Wt final state in pp collisions at $\sqrt{s}$ = 8 TeV with the ATLAS detector.
Journal of high energy physics, 1602(2):110, and PUBDB-2016-01321, CERN-PH-EP-2015-235; arXiv:1510.02664.
doi: 10.1007/JHEP02(2016)110.

ATLAS Collaboration.
Search for the Standard Model Higgs boson decaying into $b\bar{b}$ produced in association with top quarks decaying hadronically in pp collisions at $\sqrt{s}$ = 8 TeV with the ATLAS detector.
Journal of high energy physics, 2016(5):160, and PUBDB-2016-02078, CERN-EP-2016-058; arXiv:1604.03812.
doi: 10.1007/JHEP05(2016)160.

ATLAS Collaboration.
Search for the Standard Model Higgs boson produced by vector-boson fusion and decaying to bottom quarks in $\sqrt{s} = 8$ TeV pp collisions with the ATLAS detector.
Journal of high energy physics, 1611(11):112, and PUBDB-2017-00252, CERN-EP-2016-076; arXiv:1606.02181.
doi: 10.1007/JHEP11(2016)112.

ATLAS Collaboration.
Search for the standard model Higgs boson produced in association with a vector boson and decaying into a tau pair in pp collisions at $\sqrt{s} = 8$ TeV with the ATLAS detector.
Physical review / D, 93(9):092005, and PUBDB-2016-02067, CERN-PH-2015-226; CERN-PH-EP-2015-226; arXiv:1511.08352.
doi: 10.1103/PhysRevD.93.092005.

ATLAS Collaboration.
Search for top squarks in final states with one isolated lepton, jets, and missing transverse momentum in $\sqrt{s} = 13$ TeV pp collisions with the ATLAS detector.
Physical review / D, D94(5):052009, and PUBDB-2016-03966, CERN-EP-2016-113; arXiv:1606.03903.
doi: 10.1103/PhysRevD.94.052009.

ATLAS Collaboration.
Searches for heavy diboson resonances in pp collisions at $\sqrt{s} = 13$ TeV with the ATLAS detector.
Journal of high energy physics, 2016(9):173, and PUBDB-2016-03983, CERN-EP-2016-106; arXiv:1606.04833.
doi: 10.1007/JHEP09(2016)173.

ATLAS Collaboration.
Searches for scalar leptoquarks in pp collisions at $\sqrt{s}$ = 8 TeV with the ATLAS detector.
The European physical journal / C, 76(1):5, and PUBDB-2016-00353, CERN-PH-EP-2015-179; arXiv:1508.04735.
doi: 10.1140/epjc/s10052-015-3823-9.

ATLAS Collaboration.
Study of hard double-parton scattering in four-jet events in pp collisions at $\sqrt{s} = 7$ TeV with the ATLAS experiment.
Journal of high energy physics, 1611(11):110, and PUBDB-2016-06039, CERN-EP-2016-183; arXiv:1608.01857.
doi: 10.1007/JHEP11(2016)110.

ATLAS Collaboration.
Study of the $B_c^+ \to J/\psi D_s^+$ and $B_c^+ \to J/\psi D_s^{*+}$ decays with the ATLAS detector.
The European physical journal / C, 76(1):4, and PUBDB-2016-00351, CERN-PH-EP-2015-163; arXiv:1507.07099.
doi: 10.1140/epjc/s10052-015-3743-8.

ATLAS Collaboration.
Study of the rare decays of B_s^0 and B^0 into muon pairs from data collected during the LHC Run 1 with the ATLAS detector.
The European physical journal / C, 76(9):513, and PUBDB-2016-03968, CERN-EP-2016-064; arXiv:1604.04263.
doi: 10.1140/epjc/s10052-016-4338-8.

ATLAS Collaboration.
Test of CP Invariance in vector-boson fusion production of the Higgs boson using the $Optimal\ Observable$ method in the ditau decay channel with the ATLAS detector.
The European physical journal / C, 76(12):658, and PUBDB-2016-06041, CERN-EP-2016-002; arXiv:1602.04516.
doi: 10.1140/epjc/s10052-016-4499-5.

ATLAS Collaboration.
The performance of the jet trigger for the ATLAS detector during 2011 data taking.
The European physical journal / C, 76(10):526, and PUBDB-2016-03977, CERN-EP-2016-031; arXiv:1606.07759.
doi: 10.1140/epjc/s10052-016-4325-0.

ATLAS Collaboration.
Transverse momentum, rapidity, and centrality dependence of inclusive charged-particle production in $\sqrt{s_{NN}}$ = 5.02 TeV p + Pb collisions measured by the ATLAS experiment.
Physics letters / B, 763:313, and PUBDB-2016-05342, CERN-EP-2016-077; arXiv:1605.06436.
doi: 10.1016/j.physletb.2016.10.053.

ATLAS Collaboration and CMS Collaboration.
Measurements of the Higgs boson production and decay rates and constraints on its couplings from a combined ATLAS and CMS analysis of the LHC pp collision data at $\sqrt{s}$ = 7 and 8 TeV.
Journal of high energy physics, 1608(8):045, and PUBDB-2016-04739, CERN-EP-2016-100; ATLAS-HIGG-2015-07; CMS-HIG-15-002; arXiv:1606.02266.
doi: 10.1007/JHEP08(2016)045.

ATLAS TDAQ Collaboration.
The ATLAS Data Acquisition and High Level Trigger system.
Journal of Instrumentation, 11(06):P06008, and PUBDB-2017-00351.
doi: 10.1088/1748-0221/11/06/P06008.

V. Benítez et al.
Sensors for the End-cap prototype of the Inner Tracker in the ATLAS Detector Upgrade.
Nuclear instruments & methods in physics research / A, 833:226, and PUBDB-2017-00353.
doi: 10.1016/j.nima.2016.07.023.

J. Butterworth et al.
PDF4LHC recommendations for LHC Run II.
Journal of physics / G, 43(2):023001, and PUBDB-2017-00302, OUTP-15-17P; SMU-HEP-15-12; TIF-UNIMI-2015-14; LCTS-2015-27; CERN-PH-TH-2015-249; arXiv:1510.03865.
doi: 10.1088/0954-3899/43/2/023001.

V. Cavaliere et al.
Design of a hardware track finder (Fast Tracker) for the ATLAS trigger.
Journal of Instrumentation, 11(02):C02056, and PUBDB-2017-00292.
doi: 10.1088/1748-0221/11/02/C02056.

M. Dyndal and L. Schoeffel.
Four-lepton production from photon-induced reactions in *pp* collisions at the LHC.
Acta physica Polonica / B, 47(6):1645, and PUBDB-2017-00319, arXiv:1511.02065.
doi: 10.5506/APhysPolB.47.1645.

V. Fadeyev et al.
Investigation of HV/HR-CMOS technology for the ATLAS Phase-II Strip Tracker Upgrade.
Nuclear instruments & methods in physics research / A, 831:189, and PUBDB-2017-00322.
doi: 10.1016/j.nima.2016.05.092.

K. Hara et al.
Charge collection and field profile studies of heavily irradiated strip sensors for the ATLAS inner tracker upgrade.
Nuclear instruments & methods in physics research / A, 831:181, and PUBDB-2017-00333.
doi: 10.1016/j.nima.2016.04.035.

L. B. A. Hommels et al.
Detailed studies of full-size ATLAS12 sensors.
Nuclear instruments & methods in physics research / A, 831:167, and PUBDB-2017-00338.
doi: 10.1016/j.nima.2016.03.042.

B. T. Huffman et al.
Radiation hardness of two CMOS prototypes for the ATLAS HL-LHC upgrade project.
02. Topical Workshop on Electronics for Particle Physics 2015, Lisbon (Portugal), 28 Sep 2015 - 2 Oct 2015.
Inst. of Physics, London.
doi: 10.1088/1748-0221/11/02/C02005.

H. Jansen et al.
Performance of the EUDET-type beam telescopes.
EPJ Techniques and Instrumentation, 3(1):7, and PUBDB-2016-05430, DESY-16-055; arXiv:1603.09669.
doi: 10.1140/epjti/s40485-016-0033-2.

N. Lehmann et al.
Real time tracker based upon local hit correlation circuit for silicon strip sensors.
Nuclear instruments & methods in physics research / A, 806:21, and PUBDB-2017-00369.
doi: 10.1016/j.nima.2015.09.109.

Z. Liang et al.
Study of built-in amplifier performance on HV-CMOS sensor for the ATLAS phase-II strip tracker upgrade.
10th International “Hiroshima” Symposium on the Development and Application of Semiconductor Tracking Detectors, Xian (China), 25 Sep 2015 - 29 Sep 2015.
Elsevier, Amsterdam.
doi: 10.1016/j.nima.2016.05.007.

M. Mikestikova et al.
Study of surface properties of ATLAS12 strip sensors and their radiation resistance.
10th International “Hiroshima” Symposium on the Development and Application of Semiconductor Tracking Detectors, Xian (China), 25 Sep 2015 - 29 Sep 2015.
Elsevier, Amsterdam.
doi: 10.1016/j.nima.2016.03.056.

R. Mori et al.
Evaluation of the performance of irradiated silicon strip sensors for the forward detector of the ATLAS Inner Tracker Upgrade.
10th International “Hiroshima” Symposium on the Development and Application of Semiconductor Tracking Detectors, Xian (China), 25 Sep 2015 - 29 Sep 2015.
Elsevier, Amsterdam.
doi: 10.1016/j.nima.2016.04.044.

L. Poley et al.
Alternative glues for the production of ATLAS silicon strip modules for the Phase-II upgrade of the ATLAS Inner Detector.
Journal of Instrumentation, 11(05):P05017, and PUBDB-2016-02543, DESY-16-027; arXiv:1508.05912.
doi: 10.1088/1748-0221/11/05/P05017.

L. Poley et al.
Characterisation of strip silicon detectors for the ATLAS Phase-II Upgrade with a micro-focused X-ray beam.
Journal of Instrumentation, 11(07):P07023, and PUBDB-2016-03426, DESY-16-047; arXiv:1603.04846.
doi: 10.1088/1748-0221/11/07/P07023.

M. Ullán et al.
Embedded pitch adapters: A high-yield interconnection solution for strip sensors.
Nuclear instruments & methods in physics research / A, 831:221, and PUBDB-2017-00426.
doi: 10.1016/j.nima.2016.04.019.

Ph.D. Thesis

A.-R. Draeger.
Prediction of the $t\bar{t}$ and $W+$ Jets Background in a Search for New Physics with Jets and Missing Transverse Energy at CMS.
Universität Hamburg, Hamburg, 2016.

N. Kondrashova.
Measurements of Z boson plus jet production cross section using $\sqrt{s}=8$ TeV data and studies of jet quark-gluon decomposition.
Universität Hamburg, Hamburg, 2016.

G. Sedov.
Measurement of Z boson production using $Z \rightarrow ee$ decays with one of the electrons detected in the forward calorimeters of the ATLAS detector using 4.6 fb^{-1} of data collected at $\sqrt{s}=7$ TeV.
Universität Hamburg, Hamburg, 2016.

Astroparticle physics

Published

M. G. Aartsen et al.
Neutrino oscillation studies with IceCube-DeepCore.
Nuclear physics / B, 908:161, and PUBDB-2017-00278.
doi: 10.1016/j.nuclphysb.2016.03.028.

M. G. Aartsen et al.
Searches for relativistic magnetic monopoles in IceCube.
The European physical journal / C, 76(3):133, and PUBDB-2017-00193.
doi: 10.1140/epjc/s10052-016-3953-8.

A. U. Abeysekara et al.
A Search for Brief Optical Flashes Associated with the SETI Target KIC 8462852.
The astrophysical journal / 2, 818(2):L33, and PUBDB-2017-00203.
doi: 10.3847/2041-8205/818/2/L33.

A. U. Abeysekara et al.
VERITAS and multiwavelength observations of the BL Lacertae object 1ES 1741+196.
Monthly notices of the Royal Astronomical Society, 459(3):2550, and PUBDB-2016-04082.
doi: 10.1093/mnras/stw664.

F. Acero et al.
Development of the Model of Galactic Interstellar Emission for Standard Point-Source Analysis of FERMI Large Area Telescope Data.
The astrophysical journal / Supplement series, 223(2):26, and PUBDB-2016-06164.
doi: 10.3847/0067-0049/223/2/26.

F. Acero et al.
The First FERMI LAT Supernova Remnant Catalog.
The astrophysical journal / Supplement series, 224(1):8, and PUBDB-2016-06157.
doi: 10.3847/0067-0049/224/1/8.

M. Ackermann et al.
2FHL: The Second Catalog of Hard FERMI-LAT Sources.
The astrophysical journal / Supplement series, 222(1):5, and PUBDB-2016-06168.
doi: 10.3847/0067-0049/222/1/5.

M. Ackermann et al.
FERMI Large Area Telescope Detection of Extended Gamma-Ray Emission from the Radio Galaxy Fornax A.
The astrophysical journal, 826(1):1, and PUBDB-2016-05877.
doi: 10.3847/0004-637X/826/1/1.

M. Ackermann et al.
FERMI LAT Stacking Analysis of SWIFT Localized GRBs.
The astrophysical journal, 822(2):68, and PUBDB-2016-06160.
doi: 10.3847/0004-637X/822/2/68.

M. Ackermann et al.
FERMI-LAT Observations of the LIGO Event GW150914.
The astrophysical journal / 2, 823(1):L2, and PUBDB-2016-06159.
doi: 10.3847/2041-8205/823/1/L2.

M. Ackermann et al.
Minute-Timescale 100 MeV γ-Ray Variability During the Giant Outburst of Quasar 3C 279 Observed by FERMI-LAT in 2015 June.
The astrophysical journal / 2, 824(2):L20, and PUBDB-2016-06149.
doi: 10.3847/2041-8205/824/2/L20.

M. Ackermann et al.
Resolving the Extragalactic γ-Ray Background above 50 GeV with the Fermi Large Area Telescope.
Physical review letters, 116(15):151105, and PUBDB-2016-06171.
doi: 10.1103/PhysRevLett.116.151105.

M. L. Ahnen et al.
Detection of very high energy gamma-ray emission from the gravitationally lensed blazar QSO B0218+357 with the MAGIC telescopes.
Astronomy and astrophysics, 595:A98, and PUBDB-2016-06251, arXiv:1609.01095.
doi: 10.1051/0004-6361/201629461.

M. L. Ahnen et al.
Long-term multi-wavelength variability and correlation study of Markarian 421 from 2007 to 2009.
Astronomy and astrophysics, 593:A91, and PUBDB-2016-05883, arXiv:1605.09017.
doi: 10.1051/0004-6361/201628447.

M. L. Ahnen et al.
MAGIC observations of the February 2014 flare of 1ES 1011+496 and ensuing constraint of the EBL density.
Astronomy and astrophysics, 590:A24, and PUBDB-2016-04000.
doi: 10.1051/0004-6361/201527256.

M. L. Ahnen et al.
Search for VHE gamma-ray emission from Geminga pulsar and nebula with the MAGIC telescopes.
Astronomy and astrophysics, 591:A138, and PUBDB-2016-04021.
doi: 10.1051/0004-6361/201527722.

M. L. Ahnen et al.
Super-orbital variability of LS I +61°303 at TeV energies.
Astronomy and astrophysics, 591:A76, and PUBDB-2016-04084.
doi: 10.1051/0004-6361/201527964.

M. Ajello et al.
Deep Morphological and Spectra Study of the SNR RCW 86 with FERMI-LAT.
The astrophysical journal, 819(2):98, and PUBDB-2016-06165.
doi: 10.3847/0004-637X/819/2/98.

M. Ajello et al.
FERMI-LAT Observations of High-Energy γ-Ray Emission Toward the Galactic Center.
The astrophysical journal, 819(1):44, and PUBDB-2016-06162.
doi: 10.3847/0004-637X/819/1/44.

M. Ajello et al.
NuSTAR, Swift, and GROND observations of the flaring MeV blazar PMN J0641−0320.
The astrophysical journal, 826(1):76, and PUBDB-2016-04024.
doi: 10.3847/0004-637X/826/1/76.

J. Aleksić et al.
Insights into the emission of the blazar 1ES 1011+496 through unprecedented broadband observations during 2011 and 2012.
Astronomy and astrophysics, 591:A10, and PUBDB-2016-06242, arXiv:1603.06776.
doi: 10.1051/0004-6361/201527176.

J. Aleksić et al.
The major upgrade of the MAGIC telescopes, Part I: The hardware improvements and the commissioning of the system.
Astroparticle physics, 72:61, and PUBDB-2016-06236, arXiv:1409.6073.
doi: 10.1016/j.astropartphys.2015.04.004.

J. Aleksić et al.
The major upgrade of the MAGIC telescopes, Part II: A performance study using observations of the Crab Nebula.
Astroparticle physics, 72:76, and PUBDB-2016-06237, arXiv:1409.5594.
doi: 10.1016/j.astropartphys.2015.02.005.

E. Aliu et al.
A search for very high energy gamma rays from the missing link binary pulsar J1023+0038 with VERITAS.
The astrophysical journal, 831(2):193, and PUBDB-2017-00012, arXiv:1609.01692.
doi: 10.3847/0004-637X/831/2/193.

S. Ansoldi et al.
Teraelectronvolt pulsed emission from the Crab Pulsar detected by MAGIC.
Astronomy and astrophysics, 585:A133, and PUBDB-2016-01251.
doi: 10.1051/0004-6361/201526853.

ANTARES Collaboration and IceCube Collaboration.
The First Combined Search for Neutrino Point-Sources in the Southern Hemispherewith the ANTARES and IceCube Neutrino Telescopes.
The astrophysical journal, 823(1):65, and PUBDB-2016-06271.
doi: 10.3847/0004-637X/823/1/65.

ANTARES Collaboration and IceCube Collaboration and LIGO Scientific Collaboration and Virgo Collaboration.
High-energy neutrino follow-up search of gravitational wave event GW150914 with ANTARES and IceCube.
Physical review / D covering particles, fields, gravitation, and cosmology, 93(12):122010, and PUBDB-2016-06434, arXiv:1602.05411.
doi: 10.1103/PhysRevD.93.122010.

W. D. Apel et al.
A comparison of the cosmic-ray energy scales of Tunka-133 and KASCADE-Grande via their radio extensions Tunka-Rex and LOPES.
Physics letters / B, 763:179, and PUBDB-2016-05881.
doi: 10.1016/j.physletb.2016.10.031.

S. Archambault et al.
Discovery of very high energy gamma rays from 1ES 1440+122.
Monthly notices of the Royal Astronomical Society, 461(1):202, and PUBDB-2016-05878, arXiv:1608.02769.
doi: 10.1093/mnras/stw1319.

S. Archambault et al.
Exceptionally Bright TEV Flares from the Binary LS I +61° 303.
The astrophysical journal / 2, 817(1):L7, and PUBDB-2016-01142.
doi: 10.3847/2041-8205/817/1/L7.

A. Archer et al.
TeV gamma-ray observations of the Galactic Center ridge by VERITAS.
The astrophysical journal, 821(2):129, and PUBDB-2016-02015.
doi: 10.3847/0004-637X/821/2/129.

A. Archer et al.
Very High Energy Observations of the Binaries V 404 CYG and 4U 0115+634 During Giant X-Ray Outbursts.
The astrophysical journal, 831(1):113, and PUBDB-2016-05880, arXiv:1608.06464.
doi: 10.3847/0004-637X/831/1/113.

A. Baushev.
Can the dark matter annihilation signal be significantly boosted by substructures?
Journal of cosmology and astroparticle physics, 2016(01):018, and PUBDB-2016-01143, arXiv:1506.08609.
doi: 10.1088/1475-7516/2016/01/018.

V. Bonnivard et al.
CLUMPY: Jeans analysis, γ-ray and ν fluxes from dark matter (sub-)structures.
Computer physics communications, 200:336, and PUBDB-2016-00735, arXiv:1506.07628.
doi: 10.1016/j.cpc.2015.11.012.

R. Brose, I. Telezhinsky and M. Pohl.
Transport of magnetic turbulence in supernova remnants.
Astronomy and astrophysics, 593:A20, and PUBDB-2017-00194.
doi: 10.1051/0004-6361/201527345.

R. Bühler and M. Giomi.
The imprint of pulsar parameters on the morphology of Pulsar Wind Nebulae.
Monthly notices of the Royal Astronomical Society, 462(3):2762, and PUBDB-2016-06145.
doi: 10.1093/mnras/stw1773.

X. Chen et al.
Particle diffusion and localized acceleration in inhomogeneous AGN jets – II. Stochastic variation.
Monthly notices of the Royal Astronomical Society, 458(3):3260, and PUBDB-2017-00196.
doi: 10.1093/mnras/stw528.

CMS Collaboration.
New Fast Beam Conditions Monitoring (BCM1F) system for CMS.
Journal of Instrumentation, 11(01):C01088, and PUBDB-2017-00318.
doi: 10.1088/1748-0221/11/01/C01088.

A. Corstanje et al.
Timing calibration and spectral cleaning of LOFAR time series data.
Astronomy and astrophysics, 590:A41, and PUBDB-2017-00295, arXiv:1603.08354.
doi: 10.1051/0004-6361/201527809.

Fermi LAT Collaboration.
Measurement of the high-energy gamma-ray emission from the Moon with the Fermi Large Area Telescope.
Physical review / D, 93(8):082001, and PUBDB-2016-01799, arXiv:1604.03349.
doi: 10.1103/PhysRevD.93.082001.

Fermi-LAT Collaboration.
Contemporaneous Broadband Observations of Three High-Redshift BL Lac Objects.
The astrophysical journal, 820(1):72, and PUBDB-2016-01712, arXiv:1602.04510.
doi: 10.3847/0004-637X/820/1/72.

Fermi-LAT Collaboration.
Deep view of the Large Magellanic Cloud with six years of Fermi-LAT observations.
Astronomy and astrophysics, 586:A71, and PUBDB-2016-01709, arXiv:1509.06903.
doi: 10.1051/0004-6361/201526920.

Fermi-LAT Collaboration.
Search for gamma-ray emission from the Coma Cluster with six years of Fermi-LAT data.
The astrophysical journal, 819(2):149, and PUBDB-2016-01711, arXiv:1507.08995.
doi: 10.3847/0004-637X/819/2/149.

Fermi-LAT Collaboration.
Search for Spectral Irregularities due to Photon–Axionlike-Particle Oscillations with the Fermi Large Area Telescope.
Physical review letters, 116(16):161101, and PUBDB-2016-06170.
doi: 10.1103/PhysRevLett.116.161101.

J. X. Ge, J. H. He and H. Yan.
Effects of turbulent dust grain motion to interstellar chemistry.
Monthly notices of the Royal Astronomical Society, 455(4):3570, and PUBDB-2016-06329.
doi: 10.1093/mnras/stv2560.

M. Giomi, L. Gerard and G. Maier.
Optimal strategies for observation of active galactic nuclei variability with Imaging Atmospheric Cherenkov Telescopes.
Astroparticle physics, 80:8, and PUBDB-2016-01798.
doi: 10.1016/j.astropartphys.2016.03.006.

D. Gora and E. Bernardini.
Detection of tau neutrinos by imaging air Cherenkov telescopes.
Astroparticle physics, 82:77, and PUBDB-2016-04086.
doi: 10.1016/j.astropartphys.2016.06.002.

H. E. S. S. Collaboration.
Acceleration of petaelectronvolt protons in the Galactic Centre.
Nature / Physical science, 531(7595):476, and PUBDB-2017-00281, arXiv:1603.07730.
doi: 10.1038/nature17147.

H. E. S. S. Collaboration.
Characterizing the γ-ray long-term variability of PKS 2155-304 with H.E.S.S. and Fermi-LAT.
Astronomy and astrophysics, 598(11):A39, and PUBDB-2017-00447, arXiv:1610.03311.
doi: 10.1051/0004-6361/201629419.

H. E. S. S. Collaboration.
First limits on the very-high energy gamma-ray afterglow emission of fast radio bursts. H.E.S.S. observations of FRB 150418.
Astronomy and astrophysics, 597(5):A115, and PUBDB-2017-00445.
doi: 10.1051/0004-6361/201629117.

H. E. S. S. Collaboration.
Search for dark matter annihilations towards the inner Galactic halo from 10 years of observations with H.E.S.S.
Physical review letters, 117(11):111301, and PUBDB-2017-00279, arXiv:1607.08142.
doi: 10.1103/PhysRevLett.117.111301.

J. Heinze et al.
Cosmogenic Neutrinos Challenge the Cosmic-Ray Proton DIP Model.
The astrophysical journal, 825(2):122, and PUBDB-2016-06103, arXiv:1512.05988.
doi: 10.3847/0004-637X/825/2/122.

M. Hempel et al.
Measurements of the performance of a beam condition monitor prototype in a 5 GeV electron beam.
Nuclear instruments & methods in physics research / A, 826:65, and PUBDB-2016-02014.
doi: 10.1016/j.nima.2016.04.038.

HESS Collaboration.
H.E.S.S. Limits on Linelike Dark Matter Signatures in the 100 GeV to 2 TeV Energy Range Close to the Galactic Center.
Physical review letters, 117(15):151302, and PUBDB-2016-05876, arXiv:1609.08091.
doi: 10.1103/PhysRevLett.117.151302.

IceCube Collaboration.
All-flavour search for neutrinos from dark matter annihilations in the Milky Way with IceCube/DeepCore.
The European physical journal / C, 76(10):531, and PUBDB-2016-04080.
doi: 10.1140/epjc/s10052-016-4375-3.

IceCube Collaboration.
An All-Sky Search for Three Flavors of Neutrinos from Gamma-Ray Bursts with theIceCube Neutrino Observatory.
The astrophysical journal, 824(2):115, and PUBDB-2016-06273, arXiv:1601.06484.
doi: 10.3847/0004-637X/824/2/115.

IceCube Collaboration.
Anisotropy in Cosmic-Ray Arrival Directions in the Southern Hemisphere Based on Six Years of Data from the IceCube Detector.
The astrophysical journal, 826(2):220, and PUBDB-2016-06262, arXiv:1603.01227.
doi: 10.3847/0004-637X/826/2/220.

IceCube Collaboration.
Characterization of the Atmospheric Muon Flux in IceCube.
Astroparticle physics, 78:1, and PUBDB-2016-00599, arXiv:1506.07981.
doi: 10.1016/j.astropartphys.2016.01.006.

IceCube Collaboration.
Constraints on Ultrahigh-Energy Cosmic-Ray Sources from a Search for Neutrinos above 10 PeV with IceCube.
Physical review letters, 117(24):241101, and PUBDB-2016-06458, arXiv:1607.05886.
doi: 10.1103/PhysRevLett.117.241101.

IceCube Collaboration.
Improved limits on dark matter annihilation in the Sun with the 79-string IceCube detector and implications for supersymmetry.
Journal of cosmology and astroparticle physics, 2016(04):022, and PUBDB-2016-06268, arXiv:1601.00653.
doi: 10.1088/1475-7516/2016/04/022.

IceCube Collaboration.
Lowering IceCube's Energy Threshold for Point Source Searches in the Southern Sky.
The astrophysical journal / 2, 824(2):L28, and PUBDB-2016-06430, arXiv:1605.00163.
doi: 10.3847/2041-8205/824/2/L28.

IceCube Collaboration.
Observation and Characterization of a Cosmic Muon Neutrino Flux from the Northern Hemisphere Using Six Years of IceCube DATA.
The astrophysical journal, 833(1):3, and PUBDB-2016-06460, arXiv:1607.08006.
doi: 10.3847/0004-637X/833/1/3.

IceCube Collaboration.
Search for astrophysical tau neutrinos in three years of IceCube data.
Physical review / D, 93:022001, and PUBDB-2016-00513.
doi: DOI: 10.1103/PhysRevD.93.022001.

IceCube Collaboration.
Search for Sources of High-Energy Neutrons with Four Years of Data from the IceTop Detector.
The astrophysical journal, 830(2):129, and PUBDB-2016-06455, arXiv:1607.05614.
doi: 10.3847/0004-637X/830/2/129.

IceCube Collaboration.
Searches for Sterile Neutrinos with the IceCube Detector.
Physical review letters, 117(7):071801, and PUBDB-2016-06462, arXiv:1605.01990.
doi: 10.1103/PhysRevLett.117.071801.

IceCube Collaboration.
The Search for Transient Astrophysical Neutrino Emission with IceCube-Deepcore.
The astrophysical journal, 816(2):75, and PUBDB-2016-00522.
doi: 10.3847/0004-637X/816/2/75.

IceCube Collaboration and MAGIC Collaboration and VERITAS Collaboration.
Very high-energy gamma-ray follow-up program using neutrino triggers from IceCube.
Journal of Instrumentation, 11(11):P11009, and PUBDB-2016-06538.
doi: 10.1088/1748-0221/11/11/P11009.

T. Karg et al.
Report from the Multi-Messenger Working Group at UHECR-2014 Conference.
International Symposium for Ultra-High Energy Cosmic Rays, Springdale (USA), 12 Oct 2014 - 15 Oct 2014.
The Physical Society of Japan, Tokyo.
doi: 10.7566/JPSCP.9.010021.

H. Katagiri et al.
FERMI/LAT Study of Gamma-Ray Emission in the Direction of the Monoceros Loop Supernova Remnant.
The astrophysical journal, 831(1):106, and PUBDB-2017-00296.
doi: 10.3847/0004-637X/831/1/106.

S. A. Khalek et al.
The ALFA Roman Pot detectors of ATLAS.
Journal of Instrumentation, 11(11):P11013, and PUBDB-2017-00013, arXiv:1609.00249.
doi: 10.1088/1748-0221/11/11/P11013.

J. Knödlseder et al.
GammaLib and ctools.
Astronomy and astrophysics, 593:A1, and PUBDB-2016-05874, arXiv:1606.0039.
doi: 10.1051/0004-6361/201628822.

O. Lishilin et al.
First Results of the Plasma Wakefield Acceleration Experiment at PITZ.
2nd European Advanced Accelerator Concepts Workshop, La Biodola, Isola d'Elba (Italy), 13 Sep 2015 - 19 Sep 2015.
North-Holland Publ. Co., Amsterdam.
doi: 10.1016/j.nima.2016.01.005.

MAGIC Collaboration.
Deep observation of the NGC1275 region with MAGIC: search of diffuse γ-ray emission from cosmic rays in the Perseus cluster.
Astronomy and astrophysics, 589:A33, and PUBDB-2016-04075.
doi: 10.1051/0004-6361/201527846.

MAGIC Collaboration.
Limits to dark matter annihilation cross-section from a combined analysis of MAGIC and Fermi-LAT observations of dwarf satellite galaxies.
Journal of cosmology and astroparticle physics, 2016(02):039, and PUBDB-2016-06238, arXiv:1601.06590.
doi: 10.1088/1475-7516/2016/02/039.

MAGIC Collaboration.
Multi-Wavelength Observations of the Blazar 1ES 1011+496 in Spring 2008.
Monthly notices of the Royal Astronomical Society, 459:2286, and PUBDB-2016-06248, arXiv:1603.07308.
doi: 10.1093/mnras/stw710.

MAGIG Collaboration and Fermi-LAT Collaboration.
Investigating the peculiar emission from the new VHE gamma-ray source H1722+119.
Monthly notices of the Royal Astronomical Society, 459(3):3271, and PUBDB-2016-04043.
doi: 10.1093/mnras/stw689.

J. Martín, D. F. Torres and G. Pedaletti.
Molecular environment, reverberation, and radiation from the pulsar wind nebula in CTA 1.
Monthly notices of the Royal Astronomical Society, 459(4):3868, and PUBDB-2016-06539, arXiv:1603.09328.
doi: 10.1093/mnras/stw684.

K.-I. Nishikawa et al.
Microscopic Processes in Global Relativistic Jets Containing Helical Magnetic Fields.
Galaxies, 4(4):38, and PUBDB-2017-00110.
doi: 10.3390/galaxies4040038.

K.-I. Nishikawa et al.
Evolution of Global Relativistic Jets: Collimations and Expansion with kKHI and the Weibel Instability.
The astrophysical journal, 820(2):94, and PUBDB-2017-00201.
doi: 10.3847/0004-637X/820/2/94.

NuSTAR Collaboration and VERITAS Collaboration and MAGIC Collaboration.
Multiwavelenght Study of Quiescent States of Mrk 421 with Unprecedented Hard X-Ray Coverage Provided by NuSTAR in 2013.
The astrophysical journal, 819(2):156, and PUBDB-2016-04035.
doi: 10.3847/0004-637X/819/2/156.

S. Ohm.
Starburst galaxies as seen by gamma-ray telescopes.
Comptes rendus physique, 17(6):585, and PUBDB-2016-04077.
doi: 10.1016/j.crhy.2016.04.003.

Pierre Auger Collaboration.
Azimuthal asymmetry in the risetime of the surface detector signals of the Pierre Auger Observatory.
Physical review / D covering particles, fields, gravitation, and cosmology, 93(7):072006, and PUBDB-2017-00248, FERMILAB-PUB-16-094-AD-AE-CD-TD; arXiv:1604.00978.
doi: 10.1103/PhysRevD.93.072006.

Pierre Auger Collaboration.
Search for ultrarelativistic magnetic monopoles with the Pierre Auger observatory.
Physical review / D covering particles, fields, gravitation, and cosmology, 94(8):082002, and PUBDB-2017-00249, FERMILAB-PUB-16-373-AD-AE-CD-TD; arXiv:1609.04451.
doi: 10.1103/PhysRevD.94.082002.

R. W. Rasmussen and W. Winter.
Perspectives for tests of neutrino mass generation at the GeV scale: Experimental reach versus theoretical predictions.
Physical review / D covering particles, fields, gravitation, and cosmology, 94(7):073004, and PUBDB-2017-00300, DESY-16-136; arXiv:1607.07880.
doi: 10.1103/PhysRevD.94.073004.

R. Santos-Lima et al.
Limits on the ion temperature anisotropy in the turbulent intracluster medium.
Monthly notices of the Royal Astronomical Society, 460(3):2492, and PUBDB-2016-06330, DESY-16-037; arXiv:1601.03837.
doi: 10.1093/mnras/stw1079.

F. G. Schröder et al.
The Tunka radio extension (Tunka-Rex): Radio measurements of cosmic rays in Siberia.
Nuclear instruments & methods in physics research / A, 824:652, and PUBDB-2017-00306, arXiv:1509.01495.
doi: 10.1016/j.nima.2015.08.075.

Scientific, LIGO and Virgo Collaboration and ASKAP Collaboration and BOOTES Collaboration and DES Collaboration and DEC Collaboration and Fermi-GBM Collaboration and Fermi-LAT Collaboration and GRAWITA Collaboration and INTEGRAL Collaboration and iPTF Collaboration and Network, InterPlanetary and J-GEM Collaboration and Survey, La Silla-QUEST and Telescope, Liverpool and LOFAR Collaboration and MASTER Collaboration and MAXI Collaboration and MWA Collaboration and Pan-STARRS Collaboration

and PESSTO Collaboration and Sky, Pi of the and SkyMapper Collaboration and Swift Collaboration and TAROT Collaboration and Zadko Collaboration and Observatory, Algerian National and C2PU Collaboration and TOROS Collaboration and VISTA Collaboration.
Supplement: Localization and broadband follow-up of the gravitational-wave transient GW150914.
The astrophysical journal / Supplement series, 225(1):8, and PUBDB-2017-00405, LIGO-P1600137-V1; FERMILAB-PUB-16-149-AE-E; LIGO-P1600137-V2; arXiv:1604.07864.
doi: 10.3847/0067-0049/225/1/8.

N. L. Strotjohann et al.
Highly variable AGN from the XMM-Newton Slew Survey.
Astronomy and astrophysics, 592:A74, and PUBDB-2017-00307, arXiv:1605.02749.
doi: 10.1051/0004-6361/201628241.

J. A. Toalá et al.
X-Ray Observations of Bow Shocks Around Runaway O Stars. The Case of ζ OPH and BD+43°3654.
The astrophysical journal, 821(2):79, and PUBDB-2017-00200.
doi: 10.3847/0004-637X/821/2/79.

G. Tovmassian et al.
Astroclimatic Characterization of Vallecitos: A candidate site for the Cherenkov Telescope Array at San Pedro Mártir.
Publications of the Astronomical Society of the Pacific, 128(961):035004, and PUBDB-2017-00311, arXiv:1601.02383.
doi: 10.1088/1538-3873/128/961/035004.

Tunka-Rex Collaboration.
Radio measurements of the energy and the depth of the shower maximum of cosmic-ray air showers by Tunka-Rex.
Journal of cosmology and astroparticle physics, 1601(01):052, and PUBDB-2017-00289, arXiv:1509.05652.
doi: 10.1088/1475-7516/2016/01/052.

VERITAS Collaboration.
Upper limits from five years of blazar observations with the VERITAS Cherenkov Telescopes.
The astronomical journal, 151(6):142, and PUBDB-2017-00198.
doi: 10.3847/0004-6256/151/6/142.

VERITAS Collaboration.
Very high energy outburst of Markarian 501 in May 2009.
Astronomy and astrophysics, 594:A76, and PUBDB-2016-05875, arXiv:1608.01569.
doi: 10.1051/0004-6361/201628744.

V. Wieland et al.
Nonrelativistic Perpendicular Shocks Modeling Young Supernova Remnants : Nonstationary Dynamics and Particle Acceleration at Forward and Reverse Shocks.
The astrophysical journal, 820(1):62, and PUBDB-2017-00202.
doi: 10.3847/0004-637X/820/1/62.

W. Winter.
Atmospheric Neutrino Oscillations for Earth Tomography.
Nuclear physics / B, 908:250, and PUBDB-2016-01613, DESY-15-227.
doi: 10.1016/j.nuclphysb.2016.03.033.

S. Xu, H. Yan and A. Lazarian.
Damping of Magnetohydrodynamic Turbulence in Partially Ionized Plasma: Implications for Cosmic Ray Propagation.
The astrophysical journal, 826(2):166, and PUBDB-2016-06328.
doi: 10.3847/0004-637X/826/2/166.

A. A. Zdziarski et al.
The high-energy gamma-ray detection of G73.9+0.9, a supernova remnant interacting with a molecular cloud.
Monthly notices of the Royal Astronomical Society, 455(2):1451, and PUBDB-2016-01252.
doi: 10.1093/mnras/stv2167.

Ph.D. Thesis

C. Skole.
Search for extremely short transientgamma-ray sources with the VERITAS observatory.
Humboldt-Universität zu Berlin, 2016.

Belle II

Published

Belle Collaboration.
Energy Scan of the $e^+e^- \to h_b(nP)\pi^+\pi^-$ $(n = 1, 2)$ Cross Sections and Evidence for $\Upsilon(11020)$ Decays into Charged Bottomonium-like States.
Physical review letters, 117(14):142001, and PUBDB-2016-03956, BELLE-CONF-1503; arXiv:1508.06562.
doi: 10.1103/PhysRevLett.117.142001.

Belle Collaboration.
First model-independent Dalitz analysis of $B^0 \to DK^{*0}$, $D \to K_S^0\pi^+\pi^-$ decay.
Progress of theoretical and experimental physics, 2016(4):043C01, and PUBDB-2016-02187, arXiv:1509.01098.
doi: 10.1093/ptep/ptw030.

Belle Collaboration.
First Observation of Doubly Cabibbo-Suppressed Decay of a Charmed Baryon: $\Lambda_c^+ \to pK^+\pi^-$.
Physical review letters, 117(1):011801, and PUBDB-2016-02797, BELLE-PREPRINT-2015-22; KEK-PREPRINT-2015-62; BELLE-2015-22; KEK-2015-62; arXiv:1512.07366.
doi: 10.1103/PhysRevLett.117.011801.

Belle Collaboration.
First observation of $\gamma\gamma \to p\bar{p}K^+K^-$ and search for exotic baryons in pK systems.
Physical review / D, 93(11):112017, and PUBDB-2016-02721, BELLE-PREPRINT-2016-02; KEK-PREPRINT-2016-1; arXiv:1604.02525.
doi: 10.1103/PhysRevD.93.112017.

Belle Collaboration.
First Observation of the Decay $B^0 \to \psi(2S)\pi^0$.
Physical review / D, 93(3):031101, and PUBDB-2016-01257, BELLE-PREPRINT-15-20; KEK-PREPRINT-15-54; arXiv:1512.06895.
doi: 10.1103/PhysRevD.93.031101.

Belle Collaboration.
Inclusive and exclusive measurements of B decays to χ_{c1} and χ_{c2} at Belle.
Physical review / D, 93(5):052016, and PUBDB-2016-01687, arXiv:1512.02672.
doi: 10.1103/PhysRevD.93.052016.

Belle Collaboration.
Measurement of D^0–$\bar{D}^0$ mixing and search for CP violation in $D^0 \to K^+K^-, \pi^+\pi^-$ decays with the full Belle data set.
Physics letters / B, 753:412, and PUBDB-2016-00414, arXiv:1509.08266.
doi: 10.1016/j.physletb.2015.12.025.

Belle Collaboration.
Measurement of the branching ratio of $\bar{B}^0 \to D^{*+}\tau^-\bar{\nu}_\tau$ relative to $\bar{B}^0 \to D^{*+}\ell^-\bar{\nu}_\ell$ decays with a semileptonic tagging method.
Physical review / D, 94(7):072007, and PUBDB-2016-05686, KEK-PREPRINT-2016-8; BELLE-PREPRINT-2016-8; arXiv:1607.07923.
doi: 10.1103/PhysRevD.94.072007.

Belle Collaboration.
Measurement of the CKM angle φ_1 in $B^0 \to \bar{D}^{(*)0}h^0$, $\bar{D}^0 \to K_S^0\pi^+\pi^-$ decays with time-dependent binned Dalitz plot analysis.
Physical review / D, 94(5):052004, and PUBDB-2016-05641, arXiv:1607.05813.
doi: 10.1103/PhysRevD.94.052004.

Belle Collaboration.
Measurement of the decay $B \to D\ell\nu_\ell$ in fully reconstructed events and determination of the Cabibbo-Kobayashi-Maskawa matrix element $|V_{cb}|$.
Physical review / D, 93(3):032006, and PUBDB-2016-01256, BELLE-PREPRINT-2015-16; KEK-PREPRINT-2015-43; arXiv:1510.03657.
doi: 10.1103/PhysRevD.93.032006.

Belle Collaboration.
Measurement of the lepton forward-backward asymmetry in $B \to X_s\ell^+\ell^-$ decays with a sum of exclusive modes.
Physical review / D covering particles, fields, gravitation, and cosmology, 93(35):032008, and PUBDB-2017-00384, BELLE-PREPRINT-2014-1; KEK-PREPRINT-2013-60; arXiv:1402.7134.
doi: 10.1103/PhysRevD.93.032008.

Belle Collaboration.
Measurements of the Υ(10860) and Υ(11020) resonances via $\sigma(e^+e^- \to \Upsilon(nS)\pi^+\pi^-)$.
Physical review / D, D93(1):011101, and PUBDB-2016-00984, arXiv:1501.01137; Belle preprint 2014-19, KEK Preprint 2014-33.
doi: 10.1103/PhysRevD.93.011101.

Belle Collaboration.
Observation of the decay $B_s^0 \to K^0\overline{K}^0$.
Physical review letters, 116(16):161801, and PUBDB-2016-01756, BELLE-PREPRINT-2015-19; KEK-PREPRINT-2015-53; UNIVERSITY-OF–CINCINNATI-PREPRINT-UCHEP-15-07; arXiv:1512.02145.
doi: 10.1103/PhysRevLett.116.161801.

Belle Collaboration.
Observation of $Z_b(10610)$ and $Z_b(10650)$ Decaying to B Mesons.
Physical review letters, 116(21):212001, and PUBDB-2016-03955, arXiv:1512.07419.
doi: 10.1103/PhysRevLett.116.212001.

Belle Collaboration.
Search for a dark vector gauge boson decaying to $\pi^+\pi^-$ using $\eta \to \pi^+\pi^-\gamma$ decays.
Physical review / D covering particles, fields, gravitation, and cosmology, 94(9):092006, and PUBDB-2016-06269, arXiv:1609.05599; Belle Preprint 2016-10, KEK Preprint 2016-19.
doi: 10.1103/PhysRevD.94.092006.

Belle Collaboration.
Search for a massive invisible particle X^0 in $B^+ \to e^+X^0$ and $B^+ \to \mu^+X^0$ decays.
Physical review / D, 94(1):012003, and PUBDB-2016-02723, BELLE-PREPRINT-2016-03; KEK-PREPRINT-2016-2; arXiv:1605.04430.
doi: 10.1103/PhysRevD.94.012003.

Belle Collaboration.
Search for $B^0 \to \pi^-\tau^+\nu_\tau$ with hadronic tagging at Belle.
Physical review / D, 93(3):032007, and PUBDB-2016-01254, KEK-PREPRINT-2015-23; arXiv:1509.06521.
doi: 10.1103/PhysRevD.93.032007.

Belle Collaboration.
Search for the decay $B^0 \to \phi\gamma$.
Physical review / D, 93(11):111101(R), and PUBDB-2016-03506, UCHEP-16-01; arXiv:1603.06546.
doi: 10.1103/PhysRevD.93.111101.

Belle Collaboration.
Search for the rare decay $D^0 \to \gamma\gamma$ at Belle.
Physical review / D, 93(5):051102, and PUBDB-2016-01388, arXiv:1512.02992.
doi: 10.1103/PhysRevD.93.051102.

Belle Collaboration.
Search for XYZ states in $\Upsilon(1S)$ inclusive decays.
Physical review / D, 93(11):112013, and PUBDB-2016-02722, BELLE-PREPRINT-2016-04; KEK-PREPRINT-2016-3; BELLE-2016-04; KEK-2016-3; arXiv:1605.00990.
doi: 10.1103/PhysRevD.93.112013.

Belle Collaboration.
Studies of charmed strange baryons in the ΛD final state at Belle.
Physical review / D, 94(3):032002, and PUBDB-2016-03307, arXiv:1605.09103.
doi: 10.1103/PhysRevD.94.032002.

Belle Collaboration.
Study of π^0 pair production in single-tag two-photon collisions.
Physical review / D, 93(3):032003, and PUBDB-2016-01253, BELLE-PREPRINT-2015-15; KEK-PREPRINT-2015-24; arXiv:1508.06757.
doi: 10.1103/PhysRevD.93.032003.

Belle Collaboration.
Study of $\mathbf{B^0} \to {}^{+-}$ decays and implications for the CKM angle $_2$.
Physical review / D, 93(3):032010, and PUBDB-2016-01255, arXiv:1510.01245.
doi: 10.1103/PhysRevD.93.032010.

Belle Collaboration.
Study of Excited Ξ_c States Decaying into Ξ_c^0 and Ξ_c^+ Baryons.
Physical review / D, 94(5):052011, and PUBDB-2016-05642, BELLE-PREPRINT-2016-07; KEK-PREPRINT-2016-7; arXiv:1607.07123.
doi: 10.1103/PhysRevD.94.052011.

Ph.D. Thesis

S. Wehle.
Angular Analysis of $B \to K^*\ell\ell$ and Search for $B^+ \to K^+\tau\tau$ at the Bellle Experiment.
Universität Hamburg, Hamburg, 2016.

CMS

Published

A. Accardi et al.
A Critical Appraisal and Evaluation of Modern PDFs.
The European physical journal / C, 76(8):471, and PUBDB-2016-03357, DESY-16-041; DO-TH-16-05; JLAB-THY-16-2231; LTH-1081; arXiv:1603.08906.
doi: 10.1140/epjc/s10052-016-4285-4.

S. Alekhin et al.
Isospin asymmetry of quark distributions and implications for single top-quark production at the LHC.
Physical review / D covering particles, fields, gravitation, and cosmology, 94(11):114038, and PUBDB-2017-00570, DESY-15-161; arXiv:1508.07923.
doi: 10.1103/PhysRevD.94.114038.

ATLAS Collaboration and CMS Collaboration.
Measurements of the Higgs boson production and decay rates and constraints on its couplings from a combined ATLAS and CMS analysis of the LHC pp collision data at $\sqrt{s} = 7$ and 8 TeV.
Journal of high energy physics, 1608(8):045, and PUBDB-2016-04739, CERN-EP-2016-100; ATLAS-HIGG-2015-07; CMS-HIG-15-002; arXiv:1606.02266.
doi: 10.1007/JHEP08(2016)045.

S. P. Baranov.
Possible solution of the quarkonium polarization problem.
Physical review / D, 93(5):054037, and PUBDB-2016-04666, DESY-15-222.
doi: 10.1103/PhysRevD.93.054037.

M. Berggren et al.
Non-simplified SUSY: $\tilde{\tau}$ -coannihilation at LHC and ILC.
The European physical journal / C, 76(4):183, and PUBDB-2016-01686, DESY-15-145; arXiv:1508.04383.
doi: 10.1140/epjc/s10052-016-3914-2.

B. Blok and P. Gunnellini.
Dynamical approach to MPI in W+dijet and Z+dijet production within the PYTHIA event generator.
The European physical journal / C, 76(4):202, and PUBDB-2016-01796, PUBDB-2015-04334; arXiv:1510.07436; DESY-15-226.
doi: 10.1140/epjc/s10052-016-4035-7.

R. M. Chatterjee, M. Guchait and R. Placakyte.
QCD analysis of the CMS inclusive differential Z production data at $\sqrt{s} = 8$ TeV.
Physical review / D covering particles, fields, gravitation, and cosmology, D94(3):034035, and PUBDB-2017-00303, arXiv:1603.09619.
doi: 10.1103/PhysRevD.94.034035.

CMS Collaboration.
A search for pair production of new light bosons decaying into muons.
Physics letters / B, 752:146, and PUBDB-2015-04648, CMS-HIG-13-010; CERN-PH-EP-2015-116; arXiv:1506.00424.
doi: 10.1016/j.physletb.2015.10.067.

CMS Collaboration.
Azimuthal decorrelation of jets widely separated in rapidity in pp collisions at $\sqrt{s} = 7$ TeV.
Journal of high energy physics, 1608(8):139, and PUBDB-2016-04287, CMS-FSQ-12-002; CERN-PH-EP-2015-309; arXiv:1601.06713.
doi: 10.1007/JHEP08(2016)139.

CMS Collaboration.
Combined search for anomalous pseudoscalar HVV couplings in VH(H $\to b\bar{b}$) production and H $\to$ VV decay.
Physics letters / B, 759:672, and PUBDB-2016-04284, CMS-HIG-14-035; CERN-PH-EP-2015-331; arXiv:1602.04305.
doi: 10.1016/j.physletb.2016.06.004.

CMS Collaboration.
Correlations between jets and charged particles in PbPb and pp collisions at $\sqrt{s_{NN}} = 2.76$ TeV.
Journal of high energy physics, 1602(2):156, and PUBDB-2016-04277, CMS-HIN-14-016; CERN-PH-EP-2015-329; arXiv:1601.00079.
doi: 10.1007/JHEP02(2016)156.

CMS Collaboration.
Decomposing transverse momentum balance contributions for quenched jets in PbPb collisions at $\sqrt{s_{NN}} = 2.76$ TeV.
Journal of high energy physics, 1611(11):55, and PUBDB-2016-06676, CMS-HIN-15-011; CERN-EP-2016-199; arXiv:1609.02466.
doi: 10.1007/JHEP11(2016)055.

G. Jain et al.
Design optimization of pixel sensors using device simulations for the phase-II CMS tracker upgrade.
Frontier Detector for Frontier Physics, La Biodola (Italy), 24 May 2015 - 30 May 2015.
North-Holland Publ. Co., Amsterdam.
doi: 10.1016/j.nima.2015.08.053.

CMS Collaboration.
Erratum to: Comparison of the Z/γ^* + jets to γ + jets cross sections in pp collisions at $\sqrt{s} = 8$.
Journal of high energy physics, 2016(4):10, and PUBDB-2017-00437, CMS-SMP-14-005; CERN-PH-EP-2015-089; arXiv:1505.06520.
doi: 10.1007/JHEP04(2016)010.

CMS Collaboration.
Event generator tunes obtained from underlying event and multiparton scattering measurements.
The European physical journal / C, 76(3):155, and PUBDB-2016-01846, CMS-GEN-14-001; CERN-PH-EP-2015-291; arXiv:1512.00815.
doi: 10.1140/epjc/s10052-016-3988-x.

CMS Collaboration.
Evidence for exclusive $\gamma\gamma \rightarrow W^+W^-$ production and constraints on anomalous quartic gauge couplings in pp collisions at $\sqrt{s} = 7$ and 8 TeV.
Journal of high energy physics, 1608(8):119, and PUBDB-2016-04731, CMS-FSQ-13-008; CERN-EP-2016-073; arXiv:1604.04464.
doi: 10.1007/JHEP08(2016)119.

CMS Collaboration.
Forward–backward asymmetry of Drell–Yan lepton pairs in pp collisions at $\sqrt{s} = 8$ TeV.
The European physical journal / C, 76(6):325, and PUBDB-2016-04288, CMS-SMP-14-004; CERN-PH-EP-2015-295; arXiv:1601.04768.
doi: 10.1140/epjc/s10052-016-4156-z.

CMS Collaboration.
Inclusive and differential measurements of the $t\bar{t}$ charge asymmetry in pp collisions at $\sqrt{s}$=8 TeV.
Physics letters / B, 757:154, and PUBDB-2016-01832, CMS-TOP-12-033; CERN-PH-EP-2015-141; arXiv:1507.03119.
doi: 10.1016/j.physletb.2016.03.060.

CMS Collaboration.
Measurement of differential and integrated fiducial cross sections for Higgs boson production in the four-lepton decay channel in pp collisions at $\sqrt{s} = 7$ and 8 TeV.
Journal of high energy physics, 1604(4):005, and PUBDB-2016-04278, CMS-HIG-14-028; CERN-PH-EP-2015-285; arXiv:1512.08377.
doi: 10.1007/JHEP04(2016)005.

CMS Collaboration.
Measurement of differential cross sections for Higgs boson production in the diphoton decay channel in pp collisions at $\sqrt{s} = 8$ TeV.
The European physical journal / C, 76(1):13, and PUBDB-2016-01100, CMS-HIG-14-016; CERN-PH-EP-2015-195; arXiv:1508.07819.
doi: 10.1140/epjc/s10052-015-3853-3.

CMS Collaboration.
Measurement of dijet azimuthal decorrelation in pp collisions at $\sqrt{s} = 8$ TeV.
The European physical journal / C, 76(10):536, and PUBDB-2016-04310, CMS-SMP-14-015; CERN-PH-EP-2016-013; CERN-EP-2016-013; CERN-SMP-14-015; arXiv:1602.04384.
doi: 10.1140/epjc/s10052-016-4346-8.

CMS Collaboration.
Measurement of electroweak production of a W boson and two forward jets in proton-proton collisions at $\sqrt{s} = 8$ TeV.
Journal of high energy physics, 1611(11):147, and PUBDB-2016-06643, CMS-SMP-13-012; CERN-EP-2016-093; arXiv:1607.06975.
doi: 10.1007/JHEP11(2016)147.

CMS Collaboration.
Measurement of inclusive jet production and nuclear modifications in pPb collisions at $\sqrt{s_{NN}} = 5.02$ TeV.
The European physical journal / C, 76(7):372, and PUBDB-2016-04276, CMS-HIN-14-001; CERN-PH-EP-2015-334; arXiv:1601.02001.
doi: 10.1140/epjc/s10052-016-4205-7.

CMS Collaboration.
Measurement of long-range near-side two-particle angular correlations in pp collisions at $\sqrt{s} = 13$ TeV.
Physical review letters, 116(17):172302, and PUBDB-2016-04272, CMS-FSQ-15-002; CERN-PH-EP-2015-271; arXiv:1510.03068.
doi: 10.1103/PhysRevLett.116.172302.

CMS Collaboration.
Measurement of spin correlations in $t\bar{t}$ production using the matrix element method in the muon+jets final state in pp collisions at $\sqrt{s} = 8$ TeV.
Physics letters / B, 758:321, and PUBDB-2016-04274, CMS-TOP-13-015; CERN-PH-EP-2015-289; arXiv:1511.06170.
doi: 10.1016/j.physletb.2016.05.005.

CMS Collaboration.
Measurement of $\mathrm{t\bar{t}}$ production with additional jet activity, including b quark jets, in the dilepton decay channel using pp collisions at $\sqrt{s} = 8$ TeV.
The European physical journal / C, 76(7):379, and PUBDB-2016-02796, CMS-TOP-12-041; CERN-PH-EP-2015-240; arXiv:1510.03072.
doi: 10.1140/epjc/s10052-016-4105-x.

CMS Collaboration.
Measurement of the charge asymmetry in top quark pair production in pp collisions at $\sqrt{s} = 8$ TeV using a template method.
Physical review / D covering particles, fields, gravitation, and cosmology, D93(3):034014, and PUBDB-2017-00429, CMS-TOP-13-013; CERN-PH-EP-2015-189; arXiv:1508.03862.
doi: 10.1103/PhysRevD.93.034014.

CMS Collaboration.
Measurement of the differential cross section and charge asymmetry for inclusive $\mathrm{pp} \rightarrow \mathrm{W}^{\pm} + X$ production at $\sqrt{s} = 8$ TeV.
The European physical journal / C, 76(8):469, and PUBDB-2016-04303, CMS-SMP-14-022; CERN-EP-2016-043; arXiv:1603.01803.
doi: 10.1140/epjc/s10052-016-4293-4.

CMS Collaboration.
Measurement of the differential cross sections for top quark pair production as a function of kinematic event variables in pp collisions at $\sqrt{s} = 7$ and 8 TeV.
Physical review / D, 94(5):052006, and PUBDB-2016-03780, CMS-TOP-12-042; CERN-EP-2016-139; arXiv:1607.00837.
doi: 10.1103/PhysRevD.94.052006.

CMS Collaboration.
Measurement of the double-differential inclusive jet cross section in proton–proton collisions at $\sqrt{s} = 13$ TeV.
The European physical journal / C, 76(8):451, and PUBDB-2016-04313, CMS-SMP-15-007; CERN-EP-2016-104; arXiv:1605.04436.
doi: 10.1140/epjc/s10052-016-4286-3.

CMS Collaboration.
Measurement of the inclusive jet cross section in pp collisions at $\sqrt{s} = 2.76$ TeV.
The European physical journal / C, 76(5):265, and PUBDB-2016-04281, CMS-SMP-14-017; CERN-PH-EP-2015-299; arXiv:1512.06212.
doi: 10.1140/epjc/s10052-016-4083-z.

CMS Collaboration.
Measurement of the inelastic cross section in proton–lead collisions at $\sqrt{s_{NN}} = 5.02$ TeV.
Physics letters / B, 759:641, and PUBDB-2016-04273, CMS-FSQ-13-006; CERN-PH-EP-2015-210; arXiv:1509.03893.
doi: 10.1016/j.physletb.2016.06.027.

CMS Collaboration.
Measurement of the integrated and differential $t\bar{t}$ production cross sections for high-p_T top quarks in pp collisions at $\sqrt{s} = 8$ TeV.
Physical review / D, 94(7):072002, and PUBDB-2016-04729, CMS-TOP-14-012; CERN-EP-2016-078; arXiv:1605.00116.
doi: 10.1103/PhysRevD.94.072002.

CMS Collaboration.
Measurement of the ratio $B(B_s^0 \rightarrow J/\psi f_0(980))$ / $B(B_s^0 \rightarrow J/\psi \phi(1020))$ in pp collisions at $\sqrt{s} = 7$ TeV.
Physics letters / B, 756:84, and PUBDB-2016-01830, CMS-BPH-14-002; CERN-PH-EP-2015-003; arXiv:1501.06089.
doi: 10.1016/j.physletb.2016.02.047.

CMS Collaboration.
Measurement of the top quark mass using charged particles in pp collisions at $\sqrt{s} = 8$ TeV.
Physical review / D, 93(9):092006, and PUBDB-2016-04290, CMS-TOP-12-030; CERN-EP-2016-062; arXiv:1603.06536.
doi: 10.1103/PhysRevD.93.092006.

CMS Collaboration.
Measurement of the top quark mass using proton-proton data at $\sqrt{(s)} = 7$ and 8 TeV.
Physical review / D, 93(7):072004, and PUBDB-2016-01840, CMS-TOP-14-022; CERN-PH-EP-2015-234; arXiv:1509.04044.
doi: 10.1103/PhysRevD.93.072004.

CMS Collaboration.
Measurement of the top quark pair production cross section in proton-proton collisions at $\sqrt{s} = 13$ TeV.
Physical review letters, 116(5):052002, and PUBDB-2016-01012, CMS-TOP-15-003; CERN-PH-EP-2015-280; arXiv:1510.05302.
doi: 10.1103/PhysRevLett.116.052002.

CMS Collaboration.
Measurement of the $\mathrm{t\bar{t}}$ production cross section in the all-jets final state in pp collisions at $\sqrt{s} = 8$ TeV.
The European physical journal / C, 76(3):128, and PUBDB-2016-04270, CMS-TOP-14-018; CERN-PH-EP-2015-243; arXiv:1509.06076.
doi: 10.1140/epjc/s10052-016-3956-5.

CMS Collaboration.
Measurement of the $t\bar{t}$ production cross section in the $e\mu$ channel in proton-proton collisions at $\sqrt{s} = 7$ and 8 TeV.
Journal of high energy physics, 1608(8):029, and PUBDB-2016-04297, CMS-TOP-13-004; CERN-EP-2016-044; arXiv:1603.02303.
doi: 10.1007/JHEP08(2016)029.

CMS Collaboration.
Measurement of the W boson helicity fractions in the decays of top quark pairs to lepton + jets final states produced in pp collisions at $\sqrt{s} = 8$ TeV.
Physics letters / B, 762:512, and PUBDB-2016-04741, CMS-TOP-13-008; CERN-EP-2016-118; arXiv:1605.09047.
doi: 10.1016/j.physletb.2016.10.007.

CMS Collaboration.
Measurement of the $\mathrm{W^+W^-}$ cross section in pp collisions at $\sqrt{s} = 8$ TeV and limits on anomalous gauge couplings.
The European physical journal / C, 76(7):401, and PUBDB-2016-04076, CMS-SMP-14-016; CERN-PH-EP-2015-122;

arXiv:1507.03268.
doi: 10.1140/epjc/s10052-016-4219-1.

CMS Collaboration.
Measurement of the $Z\gamma \rightarrow \nu\bar{\nu}\gamma$ production cross section in pp collisions at $\sqrt{s} = 8$ TeV and limits on anomalous $ZZ\gamma$ and $Z\gamma\gamma$ trilinear gauge boson couplings.
Physics letters / B, 760:448, and PUBDB-2016-04307, CMS-SMP-14-019; CERN-EP-2016-007; arXiv:1602.07152.
doi: 10.1016/j.physletb.2016.06.080.

CMS Collaboration.
Measurement of the ZZ production cross section and $Z \rightarrow \ell^+\ell^-\ell'^+\ell'^-$ branching fraction in pp collisions at $\sqrt{s} =$ 13 TeV.
Physics letters / B, 763:280, and PUBDB-2016-06641, CMS-SMP-16-001; CERN-EP-2016-174; arXiv:1607.08834.
doi: 10.1016/j.physletb.2016.10.054.

CMS Collaboration.
Measurement of top quark polarisation in t-channel single top quark production.
Journal of high energy physics, 1604(4):73, and PUBDB-2016-01842, CMS-TOP-13-001; CERN-PH-EP-2015-282; arXiv:1511.02138.
doi: 10.1007/JHEP04(2016)073.

CMS Collaboration.
Measurement of transverse momentum relative to dijet systems in PbPb and pp collisions at $\sqrt{s_{NN}} = 2.76$ TeV.
Journal of high energy physics, 2016(1):6, and PUBDB-2016-00222, CMS-HIN-14-010; CERN-PH-EP-2015-260; arXiv:1509.09029.
doi: 10.1007/JHEP01(2016)006.

CMS Collaboration.
Measurements of $t\bar{t}$ charge asymmetry using dilepton final states in pp collisions at $\sqrt{s} = 8$ TeV.
Physics letters / B, 760:365, and PUBDB-2016-04291, CMS-TOP-15-009; CERN-EP-2016-059; arXiv:1603.06221.
doi: 10.1016/j.physletb.2016.07.006.

CMS Collaboration.
Measurements of $t\bar{t}$ spin correlations and top quark polarization using dilepton final states in pp collisions at $\sqrt{s} = 8$ TeV.
Physical review / D, 93(5):052007, and PUBDB-2016-01848, CMS-TOP-14-023; CERN-PH-EP-2015-333; arXiv:1601.01107.
doi: 10.1103/PhysRevD.93.052007.

CMS Collaboration.
New Fast Beam Conditions Monitoring (BCM1F) system for CMS.
Journal of Instrumentation, 11(01):C01088, and PUBDB-2017-00318.
doi: 10.1088/1748-0221/11/01/C01088.

CMS Collaboration.
Υ(nS) polarizations versus particle multiplicity in pp collisions at $\sqrt{s} = 7$ TeV.
Physics letters / B, 761:31, and PUBDB-2016-04294, CMS-HIN-15-003; CERN-PH-EP-2015-310; arXiv:1603.02913.
doi: 10.1016/j.physletb.2016.07.065.

CMS Collaboration.
Observation of top quark pairs produced in association with a vector boson in pp collisions at $\sqrt{s} = 8$ TeV.
Journal of high energy physics, 1601(1):96, and PUBDB-2016-01105, CMS-TOP-14-021; CERN-PH-EP-2015-248; arXiv:1510.01131.
doi: 10.1007/JHEP01(2016)096.

CMS Collaboration.
Phenomenological MSSM interpretation of CMS searches in pp collisions at $\sqrt{s} = 7$ and 8 TeV.
Journal of high energy physics, 1610(10):129, and PUBDB-2016-04736, CMS-SUS-15-010; CERN-EP-2016-094; arXiv:1606.03577.
doi: 10.1007/JHEP10(2016)129.

CMS Collaboration.
Reconstruction and identification of τ lepton decays to hadrons and ν_τ at CMS.
Journal of Instrumentation, 11(01):P01019, and PUBDB-2016-01103, CMS-TAU-14-001; CERN-PH-EP-2015-261; arXiv:1510.07488.
doi: 10.1088/1748-0221/11/01/P01019.

CMS Collaboration.
Search for a Higgs boson decaying into $\gamma^*\gamma \rightarrow \ell\ell\gamma$ with low dilepton mass in pp collisions at $\sqrt{s} = 8$ TeV.
Physics letters / B, 753:341, and PUBDB-2016-01099, CMS-HIG-14-003; CERN-PH-EP-2015-137; arXiv:1507.03031.
doi: 10.1016/j.physletb.2015.12.039.

CMS Collaboration.
Search for a low-mass pseudoscalar Higgs boson produced in association with a $b\bar{b}$ pair in pp collisions at $\sqrt{s} = 8$ TeV.
Physics letters / B, 758:296, and PUBDB-2016-04275, CMS-HIG-14-033; CERN-PH-EP-2015-284; arXiv:1511.03610.
doi: 10.1016/j.physletb.2016.05.003.

CMS Collaboration.
Search for a massive resonance decaying into a Higgs boson and a W or Z boson in hadronic final states in proton-proton collisions at $\sqrt{s} = 8$ TeV.
Journal of high energy physics, 2016(2):145, and PUBDB-2016-01831, CMS-EXO-14-009; CERN-PH-EP-2015-096; arXiv:1506.01443.
doi: 10.1007/JHEP02(2016)145.

CMS Collaboration.
Search for a very light NMSSM Higgs boson produced in decays of the 125 GeV scalar boson and decaying into τ leptons in pp collisions at $\sqrt{s} = 8$ TeV.
Journal of high energy physics, 1601(1):79, and PUBDB-2016-01102, CMS-HIG-14-019; CERN-PH-EP-2015-264; arXiv:1510.06534.
doi: 10.1007/JHEP01(2016)079.

CMS Collaboration.
Search for anomalous single top quark production in association with a photon in pp collisions at $\sqrt{s} = 8$ TeV.
Journal of high energy physics, 1604(4):35, and PUBDB-2016-01843, CMS-TOP-14-003; CERN-PH-EP-2015-287;

arXiv:1511.03951.
doi: 10.1007/JHEP04(2016)035.

CMS Collaboration.
Search for dark matter and unparticles produced in association with a Z boson in proton-proton collisions at $\sqrt{s} = 8$ TeV.
Physical review / D, 93(5):052011, and PUBDB-2016-01844, CMS-EXO-12-054; CERN-PH-EP-2015-297; arXiv:1511.09375.
doi: 10.1103/PhysRevD.93.052011.

CMS Collaboration.
Search for direct pair production of scalar top quarks in the single- and dilepton channels in proton-proton collisions at $\sqrt{s} = 8$ TeV.
Journal of high energy physics, 1607(7):027, and PUBDB-2016-04285, CMS-SUS-14-015; CERN-PH-EP-2016-004; CERN-EP-2016-004; arXiv:1602.03169.
doi: 10.1007/JHEP07(2016)027.

CMS Collaboration.
Search for direct pair production of supersymmetric top quarks decaying to all-hadronic final states in pp collisions at $\sqrt{s} = 8$ TeV.
The European physical journal / C, 76(8):460, and PUBDB-2016-04304, CMS-SUS-13-023; CERN-EP-2016-040; arXiv:1603.00765.
doi: 10.1140/epjc/s10052-016-4292-5.

CMS Collaboration.
Search for excited leptons in proton-proton collisions at $\sqrt{s} = 8$ TeV.
Journal of high energy physics, 1603(3):125, and PUBDB-2016-01836, CMS-EXO-14-015; CERN-PH-EP-2015-281; arXiv:1511.01407.
doi: 10.1007/JHEP03(2016)125.

CMS Collaboration.
Search for heavy Majorana neutrinos in $e^\pm e^\pm$+ jets and $e^\pm \mu^\pm$+ jets events in proton-proton collisions at $\sqrt{s} = 8$ TeV.
Journal of high energy physics, 1604(4):169, and PUBDB-2016-04301, CMS-EXO-14-014; CERN-EP-2016-032; arXiv:1603.02248.
doi: 10.1007/JHEP04(2016)169.

CMS Collaboration.
Search for heavy resonances decaying to two Higgs bosons in final states containing four b quarks.
The European physical journal / C, 76(7):371, and PUBDB-2016-04305, CMS-EXO-12-053; CERN-EP-2016-041; arXiv:1602.08762.
doi: 10.1140/epjc/s10052-016-4206-6.

CMS Collaboration.
Search for Higgs boson off-shell production in proton-proton collisions at 7 and 8 TeV and derivation of constraints on its total decay width.
Journal of high energy physics, 1609(9):051, and PUBDB-2016-04727, CMS-HIG-14-032; CERN-EP-2016-054; arXiv:1605.02329.
doi: 10.1007/JHEP09(2016)051.

CMS Collaboration.
Search for lepton flavour violating decays of heavy resonances and quantum black holes to an $e\mu$ pair in proton-proton collisions at $\sqrt{s} = 8$ TeV.
The European physical journal / C, 76(6):317, and PUBDB-2016-04730, CMS-EXO-13-002; CERN-EP-2016-068; arXiv:1604.05239.
doi: 10.1140/epjc/s10052-016-4149-y.

CMS Collaboration.
Search for lepton flavour violating decays of the Higgs boson to $e\tau$ and $e\mu$ in proton-proton collisions at $\sqrt{s}$=8 TeV.
Physics letters / B, 763:472, and PUBDB-2016-04744, CMS-HIG-14-040; CERN-EP-2016-112; arXiv:1607.03561.
doi: 10.1016/j.physletb.2016.09.062.

CMS Collaboration.
Search for long-lived charged particles in proton-proton collisions at $\sqrt{s} = 13$ TeV.
Physical review / D covering particles, fields, gravitation, and cosmology, D94(11):112004, and PUBDB-2016-06675, CMS-EXO-15-010; CERN-EP-2016-204; arXiv:1609.08382.
doi: 10.1103/PhysRevD.94.112004.

CMS Collaboration.
Search for massive WH resonances decaying into the $\ell\nu b\bar{b}$ final state at $\sqrt{s} = 8$ TeV.
The European physical journal / C, 76(5):237, and PUBDB-2016-04286, CMS-EXO-14-010; CERN-PH-2015-332; CERN-PH-EP-2015-332; arXiv:1601.06431.
doi: 10.1140/epjc/s10052-016-4067-z.

CMS Collaboration.
Search for narrow resonances decaying to dijets in proton-proton collisions at $\sqrt{s} = 13$ TeV.
Physical review letters, 116(7):071801, and PUBDB-2016-01847, CMS-EXO-15-001; CERN-PH-EP-2015-317; arXiv:1512.01224.
doi: 10.1103/PhysRevLett.116.071801.

CMS Collaboration.
Search for narrow resonances in dijet final states at $\sqrt{s} = 8$ TeV with the novel CMS technique of data scouting.
Physical review letters, 117(3):031802, and PUBDB-2016-04728, CMS-EXO-14-005; CERN-EP-2016-090; arXiv:1604.08907.
doi: 10.1103/PhysRevLett.117.031802.

CMS Collaboration.
Search for neutral MSSM Higgs bosons decaying to $\mu^+\mu^-$ in pp collisions at $\sqrt{s} = 7$ and 8 TeV.
Physics letters / B, 752:221, and PUBDB-2016-00221, CMS-HIG-13-024; CERN-PH-EP-2015-148; arXiv:1508.01437.
doi: 10.1016/j.physletb.2015.11.042.

CMS Collaboration.
Search for neutral resonances decaying into a Z boson and a pair of b jets or τ leptons.
Physics letters / B, 759:369, and PUBDB-2016-04293, CMS-HIG-15-001; CERN-EP-2016-039; arXiv:1603.02991.
doi: 10.1016/j.physletb.2016.05.087.

CMS Collaboration.
Search for new phenomena in monophoton final states in proton-proton collisions at $\sqrt{s} = 8$ TeV.
Physics letters / B, 755:102, and PUBDB-2016-01096, CMS-EXO-12-047; CERN-PH-EP-2014-253; arXiv:1410.8812.
doi: 10.1016/j.physletb.2016.01.057.

CMS Collaboration.
Search for new physics in final states with two opposite-sign, same-flavor leptons, jets, and missing transverse momentum in pp collisions at $\sqrt{s} = 13$ TeV.
Journal of high energy physics, 1612(12):13, and PUBDB-2016-06638, CMS-SUS-15-011; CERN-EP-2016-132; arXiv:1607.00915.
doi: 10.1007/JHEP12(2016)013.

CMS Collaboration.
Search for new physics in same-sign dilepton events in proton–proton collisions at $\sqrt{s} = 13$ TeV.
The European physical journal / C, 76(8):439, and PUBDB-2016-04314, CMS-SUS-15-008; CERN-EP-2016-119; arXiv:1605.03171.
doi: 10.1140/epjc/s10052-016-4261-z.

CMS Collaboration.
Search for new physics with the M_{T2} variable in all-jets final states produced in pp collisions at $\sqrt{s} = 13$ TeV.
Journal of high energy physics, 1610(10):006, and PUBDB-2016-04292, CMS-SUS-15-003; CERN-EP-2016-067; arXiv:1603.04053.
doi: 10.1007/JHEP10(2016)006.

CMS Collaboration.
Search for pair production of first and second generation leptoquarks in proton-proton collisions at $\sqrt{s} = 8$ TeV.
Physical review / D covering particles, fields, gravitation, and cosmology, 93(3):032004, and PUBDB-2017-00436, CMS-EXO-12-041; CERN-PH-EP-2015-197; arXiv:1509.03744.
doi: 10.1103/PhysRevD.93.032004.

CMS Collaboration.
Search for pair-produced vectorlike B quarks in proton-proton collisions at $\sqrt{s}$ = 8 TeV.
Physical review / D, 93(11):112009, and PUBDB-2016-04073, CMS-B2G-13-006; CERN-PH-EP-2015-170; arXiv:1507.07129.
doi: 10.1103/PhysRevD.93.112009.

CMS Collaboration.
Search for Resonant Production of High-Mass Photon Pairs in Proton-Proton Collisions at $\sqrt{s}$ = 8 and 13 TeV.
Physical review letters, 117(5):051802, and PUBDB-2016-04735, CMS-EXO-16-018; CERN-EP-2016-154; arXiv:1606.04093.
doi: 10.1103/PhysRevLett.117.051802.

CMS Collaboration.
Search for Resonant $t\bar{t}$ Production in Proton-Proton Collisions at $\sqrt{s}$ = 8 TeV.
Physical review / D, 93(1):012001, and PUBDB-2016-00220, CMS-B2G-13-008; CERN-PH-EP-2015-126; arXiv:1506.03062; FERMILAB-PUB-15-276-CMS.
doi: 10.1103/PhysRevD.93.012001.

CMS Collaboration.
Search for R-parity violating decays of a top squark in proton-proton collisions at $\sqrt{s}$ = 8 TeV.
Physics letters / B, 760:178, and PUBDB-2016-04311, CMS-EXO-14-013; CERN-PH-EP-2016-005; CERN-EP-2016-005; arXiv:1602.04334.
doi: 10.1016/j.physletb.2016.06.039.

CMS Collaboration.
Search for s channel single top quark production in pp collisions at $\sqrt{s} = 7$ and 8 TeV.
Journal of high energy physics, 1609(9):027, and PUBDB-2016-04296, CMS-TOP-13-009; CERN-EP-2016-045; arXiv:1603.02555.
doi: 10.1007/JHEP09(2016)027.

CMS Collaboration.
Search for single production of scalar leptoquarks in proton-proton collisions at $\sqrt{s} = 8$ TeV.
Physical review / D, 93(3):032005, and PUBDB-2016-01841, CMS-EXO-12-043; CERN-PH-EP-2015-149; arXiv:1509.03750.
doi: 10.1103/PhysRevD.93.032005.

CMS Collaboration.
Search for supersymmetry in electroweak production with photons and large missing transverse energy in pp collisions at $\sqrt{s} = 8$ TeV.
Physics letters / B, 759:479, and PUBDB-2016-04306, CMS-SUS-14-016; CERN-EP-2016-012; arXiv:1602.08772.
doi: 10.1016/j.physletb.2016.05.088.

CMS Collaboration.
Search for supersymmetry in events with a photon, a lepton, and missing transverse momentum in pp collisions at $\sqrt{s}$ =8 TeV.
Physics letters / B, 757:6, and PUBDB-2016-01834, CMS-SUS-14-013; CERN-PH-EP-2015-169; arXiv:1508.01218.
doi: 10.1016/j.physletb.2016.03.039.

CMS Collaboration.
Search for supersymmetry in events with soft leptons, low jet multiplicity, and missing transverse energy in proton–proton collisions at $\sqrt{s} = 8$ TeV.
Physics letters / B, 759:9, and PUBDB-2016-04279, CMS-SUS-14-021; CERN-PH-EP-2015-307; arXiv:1512.08002.
doi: 10.1016/j.physletb.2016.05.033.

CMS Collaboration.
Search for supersymmetry in pp collisions at $\sqrt{s} = 8$ TeV in final states with boosted W bosons and b jets using razor variables.
Physical review / D covering particles, fields, gravitation, and cosmology, 93(9):092009, and PUBDB-2017-00430, CMS-SUS-14-007; CERN-PH-EP-2016-008; CERN-EP-2016-008; arXiv:1602.02917.
doi: 10.1103/PhysRevD.93.092009.

CMS Collaboration.
Search for supersymmetry in pp collisions at $\sqrt{s} = 13$ TeV in the single-lepton final state using the sum of masses of large-radius jets.
Journal of high energy physics, 1608(8):122, and PUBDB-2016-04312, CMS-SUS-15-007; CERN-EP-2016-111; arXiv:1605.04608.
doi: 10.1007/JHEP08(2016)122.

CMS Collaboration.
Search for supersymmetry in the multijet and missing transverse momentum final state in pp collisions at 13 TeV.
Physics letters / B, 758:152, and PUBDB-2016-04308, CMS-SUS-15-002; CERN-EP-2016-036; arXiv:1602.06581.
doi: 10.1016/j.physletb.2016.05.002.

CMS Collaboration.
Search for the associated production of a Higgs boson with a single top quark in proton-proton collisions at $\sqrt{s} = 8$ TeV.
Journal of high energy physics, 1606(6):177, and PUBDB-2016-04271, CMS-HIG-14-027; CERN-PH-EP-2015-255; arXiv:1509.08159.
doi: 10.1007/JHEP06(2016)177.

CMS Collaboration.
Search for the production of an excited bottom quark decaying to tW in proton-proton collisions at $\sqrt{s} = 8$ TeV.
Journal of high energy physics, 1601(1):166, and PUBDB-2016-01104, CMS-B2G-14-005; CERN-PH-EP-2015-246; arXiv:1509.08141.
doi: 10.1007/JHEP01(2016)166.

CMS Collaboration.
Search for two Higgs bosons in final states containing two photons and two bottom quarks in proton-proton collisions at 8 TeV.
Physical review / D, 94(5):052012, and PUBDB-2016-04734, CMS-HIG-13-032; CERN-EP-2016-050; arXiv:1603.06896.
doi: 10.1103/PhysRevD.94.052012.

CMS Collaboration.
Search for vector-like charge 2/3 T quarks in proton-proton collisions at $\sqrt{s}$ = 8 TeV.
Physical review / D, 93(1):012003, and PUBDB-2016-01108, CMS-B2G-13-005; CERN-PH-EP-2015-228; arXiv:1509.04177.
doi: 10.1103/PhysRevD.93.012003.

CMS Collaboration.
Search for W' decaying to tau lepton and neutrino in proton-proton collisions at $\sqrt{(s)} = 8$ TeV.
Physics letters / B, 755:196, and PUBDB-2016-01835, CMS-EXO-12-011; CERN-PH-EP-2015-190; arXiv:1508.04308.
doi: 10.1016/j.physletb.2016.02.002.

CMS Collaboration.
Search for $W' \to tb$ in proton-proton collisions at $\sqrt{s} = 8$ TeV.
Journal of high energy physics, 1602(2):122, and PUBDB-2016-01839, CMS-B2G-12-009; CERN-PH-EP-2015-231; arXiv:1509.06051.
doi: 10.1007/JHEP02(2016)122.

CMS Collaboration.
Searches for a heavy scalar boson H decaying to a pair of 125 GeV Higgs bosons hh or for a heavy pseudoscalar boson A decaying to Zh, in the final states with h $\to \tau\tau$.
Physics letters / B, 755:217, and PUBDB-2016-01106, CMS-HIG-14-034; CERN-PH-EP-2015-211; arXiv:1510.01181.
doi: 10.1016/j.physletb.2016.01.056.

CMS Collaboration.
Studies of inclusive four-jet production with two b-tagged jets in proton-proton collisions at 7 TeV.
Physical review / D covering particles, fields, gravitation, and cosmology, 94(11):112005, and PUBDB-2016-06653, CMS-FSQ-13-010; CERN-EP-2016-191; arXiv:1609.03489.
doi: 10.1103/PhysRevD.94.112005.

CMS Collaboration.
Study of B Meson Production in p+Pb Collisions at $\sqrt{s_{NN}}$=5.02 TeV Using Exclusive Hadronic Decays.
Physical review letters, 116(3):032301, and PUBDB-2016-01101, CMS-HIN-14-004; CERN-PH-EP-2015-209; arXiv:1508.06678.
doi: 10.1103/PhysRevLett.116.032301.

CMS Collaboration.
Study of Z boson production in pPb collisions at $\sqrt{sNN} = 5.02$ TeV.
Physics letters / B, 759:36, and PUBDB-2016-04280, CMS-HIN-15-002; CERN-PH-EP-2015-302; arXiv:1512.06461.
doi: 10.1016/j.physletb.2016.05.044.

CMS Collaboration.
Transverse momentum spectra of inclusive b jets in pPb collisions at $\sqrt{s_{NN}} = 5.02$ TeV.
Physics letters / B, 754:59, and PUBDB-2016-01107, CMS-HIN-14-007; CERN-PH-EP-2015-205; arXiv:1510.03373.
doi: 10.1016/j.physletb.2016.01.010.

CMS-HCAL.
Dose rate effects in the radiation damage of the plastic scintillators of the CMS Hadron Endcap Calorimeter.
Journal of Instrumentation, 11(10):T10004, and PUBDB-2017-00363, arXiv:1608.07267.
doi: 10.1088/1748-0221/11/10/T10004.

J. D'Hondt et al.
Signatures of top flavour-changing dark matter.
Journal of high energy physics, 2016(3):60, and PUBDB-2016-01412, DESY-15-231; arXiv:1511.07463.
doi: 10.1007/JHEP03(2016)060.

Group, LHC Forward Physics Working.
LHC Forward Physics.
Journal of physics / G, 43(11):110201, and PUBDB-2016-06125, CERN-PH-LPCC-2015-001; SLAC-PUB-16364; DESY-15-167; FERMILAB-PUB-16-572-PPD; arXiv:1611.05079.
doi: 10.1088/0954-3899/43/11/110201.

F. Hautmann, H. Jung and H. Van Haevermaet.
Treating jet correlations in high pile-up at hadron colliders.
Physics letters / B, B754:260, and PUBDB-2016-01616, DESY-15-147; RAL-P-2015-007; arXiv:1508.07811.
doi: 10.1016/j.physletb.2015.12.079.

H. Jansen.
A Pascalian lateral drift sensor.
Nuclear instruments & methods in physics research / A, 831:242, and PUBDB-2016-05587.
doi: 10.1016/j.nima.2016.01.092.

H. Jansen.
Resolution studies with the DATURA beam telescope.
12. International Workshop on Semiconductor Pixel Detectors for Particles and Imaging, Rome (Italy), 5 Sep 2016 - 9 Sep 2016.
Inst. of Physics, London.
doi: 10.1088/1748-0221/11/12/C12031.

H. Jansen et al.
Performance of the EUDET-type beam telescopes.
EPJ Techniques and Instrumentation, 3(1):7, and PUBDB-2016-05430, DESY-16-055; arXiv:1603.09669.
doi: 10.1140/epjti/s40485-016-0033-2.

V. Khachatryan et al.
Measurement of the CP-violating weak phase ϕ_s and the decay width difference $\Delta\Gamma_s$ using the $B_s^0 \rightarrow J/\psi(1020)$ decay channel in pp collisions at $\sqrt{s}$=8 TeV.
Physics letters / B, 757:97, and PUBDB-2016-01833, CMS-BPH-13-012; CERN-PH-EP-2015-192; arXiv:1507.07527.
doi: 10.1016/j.physletb.2016.03.046.

J. Kieseler, K. Lipka and S.-O. Moch.
Calibration of the Top-Quark Monte Carlo Mass.
Physical review letters, 116(16):162001, and PUBDB-2016-01899, DESY-15-190; arXiv:1511.00841.
doi: 10.1103/PhysRevLett.116.162001.

H. Kowalski, L. N. Lipatov and D. A. Ross.
The Behaviour of the Green Function for the BFKL Pomeron with Running Coupling.
The European physical journal / C, 76(1):23, and PUBDB-2016-01397, DESY-15-152; arXiv:1508.05744.
doi: 10.1140/epjc/s10052-015-3865-z.

M. Lisovyi, A. Verbytskyi and O. Zenaiev.
Combined analysis of charm-quark fragmentation-fraction measurements.
The European physical journal / C, 76(7):397, and PUBDB-2017-00372, MPP-2015-257; arXiv:1509.01061.
doi: 10.1140/epjc/s10052-016-4246-y.

M. Ö. Sahin, D. Krücker and I.-A. Melzer-Pellmann.
Performance and optimization of support vector machines in high-energy physics classification problems.
Nuclear instruments & methods in physics research / A, 838:137, and PUBDB-2016-04006, DESY-16-004; arXiv:1601.02809.
doi: 10.1016/j.nima.2016.09.017.

S. Spannagel.
Status of the CMS Phase I pixel detector upgrade.
10th International "Hiroshima" Symposium on the Development and Application of Semiconductor Tracking Detectors, Xi'an (China), 25 Sep 2015 - 29 Sep 2015.
North-Holland Publ. Co., Amsterdam.
doi: 10.1016/j.nima.2016.03.028.

Tracker group CMS Collaboration.
Trapping in proton irradiated p^+-n-n^+ silicon sensors at fluences anticipated at the HL-LHC outer tracker.
Journal of Instrumentation, 11(04):P04023, and PUBDB-2017-00276, arXiv:1505.01824.
doi: 10.1088/1748-0221/11/04/P04023.

Ph.D. Thesis

M. Bergholz.
Vergleich relevanter Parameter von Multipixelsensoren für Spurdetektoren nach Bestrahlung mit hohen Proton- und Neutronflüssen.
BTU Cottbus, Hamburg, 2016.

G. Dolinska.
Measurement of the Cross Sections of $t\bar{t}$ Production in the Boosted Regime with the CMS Detector at $\sqrt{s} = 8$ TeV.
Universität Hamburg, Hamburg, 2016.

A.-R. Draeger.
Prediction of the $t\bar{t}$ and W + Jets Background in a Search for New Physics with Jets and Missing Transverse Energy at CMS.
Universität Hamburg, Hamburg, 2016.

J. Garay Garcia.
Search for Higgs-Boson Production in Association with Top-Quark Pairs in H→ $b\bar{b}$ Decays at $\sqrt{s}$ = 8 and 13 TeV with the CMS Experiment.
Universität Hamburg, Hamburg, 2016.

A. Gizhko.
Measurement of beauty quark mass at HERA and impact on Higgs production in association with beauty quarks at LHC.
Universität Hamburg, Hamburg, 2016.

M. Hoffmann.
Search for the decay of a heavy Higgs boson decaying to two light Higgs bosons using a kinematic fit.
Universität Hamburg, Hamburg, 2016.

I. Korol.
Measurement of Double Differential $t\bar{t}$ Production Cross Sections with the CMS Detector.
Universität Hamburg, Hamburg, 2016.

T. Lapsien.
Studies of top tagging identification methods and development of a new heavy object tagger.
Universität Hamburg, Hamburg, 2016.

T. Lenz.
A search for new heavy particles in events with highly ionising, short tracks at the CMS experiment.
Universität Hamburg, Hamburg, 2016.

A. Lobanov.
Search for gluino production in final states with an isolated lepton and b-tagged jets using 13 TeV collisions at CMS.
Universität Hamburg, Hamburg, 2016.

S. Spannagel.
Test Beam Measurements for the Upgrade of the CMS Pixel Detector and Measurement of the Top Quark Mass from Differential Cross Sections.
Universität Hamburg, Hamburg, 2016.

H1

Published

I. Abt et al.
Combined electroweak and QCD fit to HERA data.
Physical review / D, 94(5):052007, and PUBDB-2016-03907, DESY-16-063; arXiv:1604.05083.
doi: 10.1103/PhysRevD.94.052007.

S. Alekhin et al.
Isospin asymmetry of quark distributions and implications for single top-quark production at the LHC.
Physical review / D covering particles, fields, gravitation, and cosmology, 94(11):114038, and PUBDB-2017-00570, DESY-15-161; arXiv:1508.07923.
doi: 10.1103/PhysRevD.94.114038.

V. Bertone et al.
A determination of $m_c(m_c)$ from HERA data using a matched heavy-flavor scheme.
Journal of high energy physics, 2016(8):050, and PUBDB-2016-03580, OUTP-16-10P; DESY-16-078; arXiv:1605.01946.
doi: 10.1007/JHEP08(2016)050.

D. Britzger.
Precision QCD measurements in DIS at HERA.
Modern physics letters / A, 31(28):1630025, and PUBDB-2017-00585.
doi: 10.1142/S0217732316300251.

H1 Collaboration.
Search for QCD instanton-induced processes at HERA in the high-Q^2 Domain.
The European physical journal / C, 76:381, and PUBDB-2016-03741, DESY 16-050; arXiv:1603.05567.
doi: 10.1140/epjc/s10052-016-4194-6.

M. Wing.
Final combined deep inelastic scattering cross sections at HERA.
3. Excited QCD 2016, Lisbon (Portugal), 6 Mar 2016 - 12 Mar 2016.
Inst. of Physics, Jagellonian Univ., Cracow.
doi: 10.5506/APhysPolBSupp.9.485.

D. South and M. Turcato.
Review of searches for rare processes and physics beyond the Standard Model at HERA.
The European physical journal / C, 76:336, and PUBDB-2017-00583.
doi: 10.1140/epjc/s10052-016-4152-3.

Ph.D. Thesis

M. v. d. Driesch.
On parton showers and multi parton interaction.
Universität Hamburg, Hamburg, 2016.

R. Zlebcik.
Diffractive Dijet Production with a Leading Proton in ep Collisions at HERA.
Charles University, Prague, Hamburg, 2016.

HERMES

Published

N. d'Hose, S. Niccolai and A. Rostomyan.
Experimental overview of Deeply Virtual Compton Scattering.
The European physical journal / A, 52(6):151, and PUBDB-2017-00310.
doi: 10.1140/epja/i2016-16151-9.

HERMES Collaboration.
Erratum to: Spin density matrix elements in exclusive ω electroproduction on ^{1}H and ^{2}H targets at 27.5 GeV beam energy.
The European physical journal / C, 76(3):162, and PUBDB-2016-06719, DESY-14-116; arXiv:1407.2119.
doi: 10.1140/epjc/s10052-016-3996-x.

V. Korotkov and HERMES Collaboration.
Recent results on TMDs from the HERMES experiment.
XVI Dubna Workshop on High Energy Spin Physics, Dubna (Russia), 8 Sep 2015 - 12 Sep 2015.
IOP Publ., Bristol.
doi: 10.1088/1742-6596/678/1/012051.

S. I. Manaenkov.
Study of spin-density matrix in exclusive electroproduction of ω meson at HERMES.
XVI Dubna Workshop on High Energy Spin Physics, Dubna (Russia), 8 Sep 2015 - 12 Sep 2015.
IOP Publ., Bristol.
doi: 10.1088/1742-6596/678/1/012043.

H. Marukyan and HERMES Collaboration.
Overview of recent HERMES results.
XVI Dubna Workshop on High Energy Spin Physics, Dubna (Russia), 8 Sep 2015 - 12 Sep 2015.
IOP Publ., Bristol.
doi: 10.1088/1742-6596/678/1/012038.

IPP

Master Thesis

M. Szczepanski.
Analysis, design and development of a Campus Feature Module for a CAFM System in DESY.
Silesian University of Technology, 2016.

Linear Collider

Published

H. Abramowicz, A. Caldwell and B. Foster.
Particle Physics after the Higgs.
Annalen der Physik, 528(1-2):16, and PUBDB-2016-06155.
doi: 10.1002/andp.201670017.

I. Abt et al.
Study of HERA ep data at low Q^2 and low x_{Bj} and the need for higher-twist corrections to standard perturbative QCD fits.
Physical review / D, 94(3):034032, and PUBDB-2016-04400, DESY-16-064; arXiv:1604.02299.
doi: 10.1103/PhysRevD.94.034032.

C. M. Berggren.
Discovering Supersymmetry and Dark Matter at the International Linear Collider.
37th International Conference on High Energy Physics, Valencia (Spain), 2 Jul 2014 - 9 Jul 2014.
Elsevier, Amsterdam [u.a.]
doi: 10.1016/j.nuclphysbps.2015.09.086.

M. Berggren et al.
Non-simplified SUSY: $\tilde{\tau}$ -coannihilation at LHC and ILC.
The European physical journal / C, 76(4):183, and PUBDB-2016-01686, DESY-15-145; arXiv:1508.04383.
doi: 10.1140/epjc/s10052-016-3914-2.

M. Bertucci et al.
Defect detection inside superconducting 1.3 GHz cavities by means of x-ray fluorescence spectroscopy.
Review of scientific instruments, 87(1):013103, and PUBDB-2017-00299.
doi: 10.1063/1.4939611.

A. Caldwell et al.
Path to AWAKE: Evolution of the concept.
Nuclear instruments & methods in physics research / A, 829:3, and PUBDB-2016-06463.
doi: 10.1016/j.nima.2015.12.050.

CALICE Collaboration.
DHCAL with minimal absorber: measurements with positrons.
Journal of Instrumentation, 11(05):P05008, and PUBDB-2016-06381, arXiv:1603.01652.
doi: 10.1088/1748-0221/11/05/P05008.

CALICE Collaboration.
First results of the CALICE SDHCAL technological prototype.
Journal of Instrumentation, 11(04):P04001, and PUBDB-2016-06354.
doi: 10.1088/1748-0221/11/04/P04001.

CALICE Collaboration.
Hadron shower decomposition in the highly granular CALICE analogue hadron calorimeter.
Journal of Instrumentation, 11(06):P06013, and PUBDB-2016-06357, arXiv:1602.08578.
doi: 10.1088/1748-0221/11/06/P06013.

CALICE Collaboration.
Resistive Plate Chamber digitization in a hadronic shower environment.
Journal of Instrumentation, 11(06):P06014, and PUBDB-2016-06415, arXiv:1604.04550.
doi: 10.1088/1748-0221/11/06/P06014.

U. Dorda et al.
SINBAD—The accelerator $R\&D$ facility under construction at DESY.
Nuclear instruments & methods in physics research / A, 829:233, and PUBDB-2016-01462.
doi: 10.1016/j.nima.2016.01.067.

O. Kononenko et al.
2D hydrodynamic simulations of a variable length gas target for density down-ramp injection of electrons into a laser wakefield accelerator.
2nd European Advanced Accelerator Concepts Workshop, La Biodola, Isola d'Elba (Italy), 13 Sep 2015 - 19 Sep 2015.
North-Holland Publ. Co., Amsterdam.
doi: 10.1016/j.nima.2016.03.104.

O. Lishilin et al.
First Results of the Plasma Wakefield Acceleration Experiment at PITZ.
2nd European Advanced Accelerator Concepts Workshop, La Biodola, Isola d'Elba (Italy), 13 Sep 2015 - 19 Sep 2015.
North-Holland Publ. Co., Amsterdam.
doi: 10.1016/j.nima.2016.01.005.

J. List.
Precision Measurements of Supersymmetry at the International Linear Collider.
37th International Conference on High Energy Physics, Valencia (Spain), 2 Jul 2014 - 9 Jul 2014.
Elsevier, Amsterdam [u.a.]
doi: 10.1016/j.nuclphysbps.2015.09.412.

T. J. Mehrling et al.
Efficient numerical modelling of the emittance evolution of beams with finite energy spread in plasma wakefield accelerators.
Nuclear instruments & methods in physics research / A, 829:367, and PUBDB-2016-01526.
doi: 10.1016/j.nima.2016.01.091.

F. Sefkow et al.
Experimental Tests of Particle Flow Calorimetry.
Reviews of modern physics, 88(1):015003, and PUBDB-2016-05532, DESY-14-032; KYUSHU-RCAPP-2015-01; LAL-15-235; arXiv:1507.05893.
doi: 10.1103/RevModPhys.88.015003.

W. Singer et al.
Production of Superconducting 1.3-GHz Cavities for the European X-Ray Free Electron Laser.
Physical review accelerators and beams, 19(9):092001, and PUBDB-2017-00386.
doi: 10.1103/PhysRevAccelBeams.19.092001.

C. Svetina et al.
Photon transport of the superradiant TeraFERMI THz beamline at the FERMI free-electron laser.
Journal of synchrotron radiation, 23(1):106, and PUBDB-2015-05155.
doi: 10.1107/S1600577515021414.

B. Vormwald, J. List and A. Vauth.
A calibration system for Compton polarimetry at e^+e^- linear colliders.
Journal of Instrumentation, 11(01):P01014, and PUBDB-2016-06215.
doi: 10.1088/1748-0221/11/01/P01014.

Master Thesis

S. Bohlen.
Detection of Inverse Compton Scattering in Plasma Wakefield Experiments.
Universität Hamburg, Hamburg, 2016.

D. Borissenko.
Designing and Commissioning of a Setup for Timing-Jitter Measurements Using Electro-Optic Temporal Decoding.
Universität Hamburg, Hamburg, 2016.

J.-N. Gruse.
Calibration of laser diagnostics for laser plasma-wakefield acceleration.
Universität Hamburg, Hamburg, 2016.

T. Koevener.
THz spectrometer calibration at FELIX.
Universität Hamburg, Hamburg, 2016.

Ph.D. Thesis

C. F. Duerig.
Measuring the Higgs Self-coupling at the International Linear Collider.
Universität Hamburg, Hamburg, 2016.

O. Hartbrich.
Scintillator Calorimeters for a Future Linear Collider Experiment.
Bergische Universität Wuppertal, Hamburg, 2016.

F. J. Mueller.
Development of a Triple GEM Readout Module for a Time Projection Chamber & Measurement Accuracies of Hadronic Higgs Branching Fractions in $\nu\nu$H at a 350 GeV ILC.
Universität Hamburg, Hamburg, 2016.

C. Neubueser.
Comparison of Two Highly Granular Hadronic Calorimeter Concepts.
Universität Hamburg, Hamburg, 2016.

H. Sert.
Light Higgsinos at the ILC: Precision Measurements and Detector Requirements.
Universität Hamburg, Hamburg, 2016.

Y. Tamashevich.
Diagnostics and treatment of 1.3 GHz Nb cavities.
Universität Hamburg, Hamburg, 2016.

S. Wunderlich.
Development and Commissioning of a Double-Prism Spectrometer for the Diagnosis of Femtosecond Electron Bunches.
Universität Hamburg, Hamburg, 2016.

OLYMPUS

Published

J. Bernauer et al.
Measurement and tricubic interpolation of the magnetic field for the OLYMPUS experiment.
Nuclear instruments & methods in physics research / A, 823:9, and PUBDB-2016-02977.
doi: 10.1016/j.nima.2016.03.115.

Theory

Published

A. Abdel-Rehim et al.
Direct Evaluation of the Quark Content of Nucleons from Lattice QCD at the Physical Point.
Physical review letters, 116(25):252001, and PUBDB-2016-04018.
doi: 10.1103/PhysRevLett.116.252001.

A. Abdel-Rehim et al.
Erratum: Nucleon and pion structure with lattice QCD simulations at physical value of the pion mass [Phys. Rev. D 92 , 114513 (2015)].
Physical review / D, 93(3):039904, and PUBDB-2016-01141.
doi: 10.1103/PhysRevD.93.039904.

J. Ablinger et al.
Calculating three loop ladder and V-topologies for massive operator matrix elements by computer algebra.
Computer physics communications, 202:33, and PUBDB-2016-05661, arXiv:1509.08324.
doi: 10.1016/j.cpc.2016.01.002.

A. Accardi et al.
A Critical Appraisal and Evaluation of Modern PDFs.
The European physical journal / C, 76(8):471, and PUBDB-2016-03357, DESY-16-041; DO-TH-16-05; JLAB-THY-16-2231; LTH-1081; arXiv:1603.08906.
doi: 10.1140/epjc/s10052-016-4285-4.

A. Accardi et al.
Electron Ion Collider: The Next QCD Frontier.
The European physical journal / A, 52:268, and PUBDB-2017-00275, BNL-98815-2012-JA; JLAB-PHY-12-1652; arXiv:1212.1701.
doi: 10.1140/epja/i2016-16268-9.

S. Alekhin, J. Blümlein and S.-O. Moch.
α_s from global fits of parton distribution functions.
Modern physics letters / A, 31(25):1630023, and PUBDB-2016-03502, DESY-16-051; DO-TH-16-07; MITP-16-026.
doi: 10.1142/S0217732316300238.

S. Alekhin et al.
A facility to search for hidden particles at the CERN SPS: the SHiP physics case.
Reports on progress in physics, 79(12):124201, and PUBDB-2016-04863.
doi: 10.1088/0034-4885/79/12/124201.

S. Alekhin et al.
Isospin asymmetry of quark distributions and implications for single top-quark production at the LHC.
Physical review / D covering particles, fields, gravitation, and cosmology, 94(11):114038, and PUBDB-2017-00570, DESY-15-161; arXiv:1508.07923.
doi: 10.1103/PhysRevD.94.114038.

C. Alexandrou et al.
Neutron electric dipole moment using $N_f = 2+1+1$ twisted mass fermions.
Physical review / D covering particles, fields, gravitation, and cosmology, 93(7):074503, and PUBDB-2017-00352, arXiv:1510.05823; DESY-15-188.
doi: 10.1103/PhysRevD.93.074503.

A. Ali.
Rare B-meson decays at the crossroads.
International journal of modern physics / A, 31(23):1630036, and PUBDB-2016-04683, DESY-16-134.
doi: 10.1142/S0217751X16300362.

A. Ali et al.
$B_c^{\pm}$ decays into tetraquarks.
Physical review / D, 94(3):034036, and PUBDB-2016-04410, DESY-16-045.
doi: 10.1103/PhysRevD.94.034036.

A. Ali et al.
Heavy quark symmetry and weak decays of the b baryons in pentaquarks with a $c\bar{c}$ component.
Physical review / D, 94(5):054001, and PUBDB-2016-04672, DESY-16-102.
doi: 10.1103/PhysRevD.94.054001.

A. Ali et al.
Transverse energy-energy correlations at next-to-leading order in α_s at the LHC.
37th International Conference on High Energy Physics, Valencia (Spain), 2 Jul 2014 - 9 Jul 2014.
Elsevier, Amsterdam [u.a.]
doi: 10.1016/j.nuclphysbps.2015.10.056.

S. Alioli et al.
Underlying-event sensitive observables in Drell–Yan production using GENEVA.
The European physical journal / C, 76(11):614, and PUBDB-2016-05268, DESY-16-088.
doi: 10.1140/epjc/s10052-016-4458-1.

A. Almasy, N. A. Lo Presti and A. Vogt.
Generalized threshold resummation in inclusive DIS and semi-inclusive electron-positron annihilation.
Journal of high energy physics, 2016(1):28, and PUBDB-2016-00448, DESY-15-228; ZU-TH-42-15; LTH-1066; arXiv:1511.08612.
doi: 10.1007/JHEP01(2016)028.

ALPHA Collaboration.
Determination of the QCD Λ Parameter and the Accuracy of Perturbation Theory at High Energies.
Physical review letters, 117(18):182001, and PUBDB-2016-05770, DESY-16-053; IFT-UAM-CSIC-16-029; CERN-TH-2016-060; TCD-MATH-16-04; WUB-16-00; arXiv:1604.06193.
doi: 10.1103/PhysRevLett.117.182001.

A. Ammon et al.
On the efficient numerical solution of lattice systems with low-order couplings.
Computer physics communications, 198:71, and PUBDB-2015-06138.
doi: 10.1016/j.cpc.2015.09.004.

A. Ammon et al.
Overcoming the sign problem in one-dimensional QCD by new integration rules with polynomial exactness.
Physical review / D covering particles, fields, gravitation, and cosmology, 94(11):114508, and PUBDB-2016-06344.
doi: 10.1103/PhysRevD.94.114508.

T. Asaka et al.
Reinterpretation of the Starobinsky model.
Progress of theoretical and experimental physics, 2016(12):123E01, and PUBDB-2016-06503, DESY-15-114.
doi: 10.1093/ptep/ptw161.

P. Athron et al.
GM2Calc: precise MSSM prediction for (g-2) of the muon.
The European physical journal / C, 76(2):62, and PUBDB-2016-01164, DESY-15-193.
doi: 10.1140/epjc/s10052-015-3870-2.

A. Azatov et al.
Resolving gluon fusion loops at current and future hadron colliders.
Journal of high energy physics, 09:123, and PUBDB-2016-04954, arXiv:1608.00977.
doi: 10.1007/JHEP09(2016)123.

E. Bagnaschi and A. Vicini.
The Higgs transverse momentum distribution in gluon fusion as a multiscale problem.
Journal of high energy physics, 2016(1):56, and PUBDB-2016-01156, DESY-15-067; arXiv:1505.00735.
doi: 10.1007/JHEP01(2016)056.

E. Bagnaschi et al.
Resummation ambiguities in the Higgs transverse-momentum spectrum in the Standard Model and beyond.
Journal of high energy physics, 2016(1):90, and PUBDB-2016-01159, DESY-15-155; arXiv:1510.08850.
doi: 10.1007/JHEP01(2016)090.

E. Bagnaschi et al.
Vacuum stability and supersymmetry at high scales with two Higgs doublets.
Journal of high energy physics, 2016(3):158, and PUBDB-2016-01921, DESY-15-238.
doi: 10.1007/JHEP03(2016)158.

F. T. Bahr et al.
Continuum limit of the leading-order HQET form factor in Bs→Kℓν decays.
Physics letters / B, 757:473, and PUBDB-2016-01948, DESY-16-009.
doi: 10.1016/j.physletb.2016.03.088.

I. Balitsky, V. Kazakov and E. Sobko.
Structure constant of twist-2 light-ray operators in the Regge limit.
Physical review / D, 93(6):061701, and PUBDB-2016-01657, DESY-15-086.
doi: 10.1103/PhysRevD.93.061701.

A. Banerjee and K. Panigrahi.
On circular strings in $(AdS_3 \times S^3)_\varkappa$.
Journal of high energy physics, 1609(9):061, and PUBDB-2017-00290, arXiv:1607.04208.
doi: 10.1007/JHEP09(2016)061.

D. Banerjee et al.
An Improved Single-Plaquette Gauge Action.
Journal of high energy physics, 1603(03):116, and PUBDB-2017-00282, arXiv:1512.04984.
doi: 10.1007/JHEP03(2016)116.

D. Banerjee et al.
Finite-Volume Energy Spectrum, Fractionalized Strings, and Low-Energy Effective Field Theory for the Quantum Dimer Model on the Square Lattice.
Physical review / B covering condensed matter and materials physics, 94(11):115120, and PUBDB-2017-00283, arXiv:1511.00881.
doi: 10.1103/PhysRevB.94.115120.

M. C. Bañuls et al.
Chiral condensate in the Schwinger model with matrix product operators.
Physical review / D, 93(9):094512, and PUBDB-2016-02660.
doi: 10.1103/PhysRevD.93.094512.

T. Bargheer, G. Papathanasiou and V. Schomerus.
The two-loop symbol of all multi-Regge regions.
Journal of high energy physics, 2016(5):12, and PUBDB-2016-02009, DESY-15-257; arXiv:1512.07620.
doi: 10.1007/JHEP05(2016)012.

T. Becher et al.
Factorization and resummation for jet processes.
Journal of high energy physics, 2016(11):019, and PUBDB-2016-05267, DESY-16-052.
doi: 10.1007/JHEP11(2016)019.

I. Ben-Dayan and R. Takahashi.
Constraints on small-scale cosmological fluctuations from SNe lensing dispersion.
Monthly notices of the Royal Astronomical Society, 455(1):552, and PUBDB-2015-05428, DESY-15-053.
doi: 10.1093/mnras/stv2356.

I. Ben-Dayan et al.
Vacuum energy sequestering and conformal symmetry.
Journal of cosmology and astroparticle physics, 2016(05):002, and PUBDB-2016-01914, DESY-15-119.
doi: 10.1088/1475-7516/2016/05/002.

G. Bergner et al.
The light bound states of supersymmetric SU(2) Yang-Mills theory.
Journal of high energy physics, 2016(3):80, and PUBDB-2016-01918, DESY-15-221.
doi: 10.1007/JHEP03(2016)080.

N. Bernal, C. S. Fong and N. Fonseca.
Sharing but not caring: dark matter and the baryon asymmetry of the universe.
Journal of cosmology and astroparticle physics, 2016(09):30, and PUBDB-2016-04416, arXiv:1605.07188.
doi: 10.1088/1475-7516/2016/09/005.

J. Blümlein.
A kinematic condition on intrinsic charm.
Physics letters / B, 753:619, and PUBDB-2016-05662, arXiv:1511.00229.
doi: 10.1016/j.physletb.2015.12.068.

J. Blümlein, G. Falcioni and A. De Freitas.
The complete $O\left(\alpha_s^2\right)$ non-singlet heavy flavor corrections to the structure functions $g_{1,2}^{ep}\left(x,Q^2\right)$, $F_{1,2,L}^{ep}\left(x,Q^2\right)$, $F_{1,2,3}^{\nu(\bar{\nu})}\left(x,Q^2\right)$ and the associated sum rules.
Nuclear physics / B, 910:568, and PUBDB-2016-05586, DESY-15-171; DO-TH-15-14.
doi: 10.1016/j.nuclphysb.2016.06.018.

J. Blümlein, K. H. Phan and T. Riemann.
General ϵ-representation for scalar one-loop Feynman integrals.
18th International Conference in Quantum Chromodynamics, Montpellier (France), 29 Jun 2015 - 3 Jul 2015.
Elsevier, Amsterdam [u.a.]
doi: 10.1016/j.nuclphysbps.2016.02.045.

D. Bombardelli et al.
An integrability primer for the gauge-gravity correspondence: an introduction.
Journal of physics / A, 49(32):320301, and PUBDB-2016-03326, DESY-16-083.
doi: 10.1088/1751-8113/49/32/320301.

R. Bonciani et al.
Two-loop master integrals for the mixed EW-QCD virtual corrections to Drell-Yan scattering.
Journal of high energy physics, 2016(9):91, and PUBDB-2016-04411, DESY-16-066; arXiv:1604.08581.
doi: 10.1007/JHEP09(2016)091.

M. Bonvini, A. S. Papanastasiou and F. J. Tackmann.
Matched predictions for the $b\bar{b}$ H cross section at the 13 TeV LHC.
Journal of high energy physics, 2016(10):53, and PUBDB-2016-04415, DESY-16-076.
doi: 10.1007/JHEP10(2016)053.

S. Borsanyi et al.
Axion cosmology, lattice QCD and the dilute instanton gas.
Physics letters / B, 752:175, and PUBDB-2015-05434, DESY-15-151.
doi: 10.1016/j.physletb.2015.11.020.

S. Borsanyi et al.
Calculation of the axion mass based on high-temperature lattice quantum chromodynamics.
Nature / Physical science, 539(7627):69, and PUBDB-2016-04674, DESY-16-105.
doi: 10.1038/nature20115.

B. Broy.
Corrections to n_s and n_t from high scale physics.
Physical review / D, 94(10):103508, and PUBDB-2016-05273, DESY-16-181.
doi: 10.1103/PhysRevD.94.103508.

B. Broy, D. Coone and D. Roest.
Plateau inflation from random non-minimal coupling.
Journal of cosmology and astroparticle physics, 2016(6):036, and PUBDB-2016-02432, DESY-16-069.
doi: 10.1088/1475-7516/2016/06/036.

B. Broy et al.
Starobinsky-type inflation from α'-corrections.
Journal of cosmology and astroparticle physics, 2016(01):001, and PUBDB-2016-00461, DESY-15-166; arXiv: 1509.00024.
doi: 10.1088/1475-7516/2016/01/001.

S. Bruggisser, F. Riva and A. Urbano.
The last gasp of dark matter effective theory.
Journal of high energy physics, 2016(11):069, and PUBDB-2016-05269, DESY-16-123.
doi: 10.1007/JHEP11(2016)069.

W. Buchmuller et al.
de Sitter Vacua and Supersymmetry Breaking in Six-Dimensional Flux Compactifications.
Physical review / D, 94(2):025025, and PUBDB-2016-03191, DESY-16-022.
doi: 10.1103/PhysRevD.94.025025.

W. Buchmuller et al.
de Sitter Vacua from an Anomalous Gauge Symmetry.
Physical review letters, 116(22):221303, and PUBDB-2016-02426, DESY-16-030.
doi: 10.1103/PhysRevLett.116.221303.

F. Burger et al.
Leading-order hadronic contributions to the electron and tau anomalous magnetic moments.
The European physical journal / C, 76(8):464, and PUBDB-2017-00391, DESY-15-002; HU-EP-15-01; SFB-CPP-14-107; arXiv:1501.05110.
doi: 10.1140/epjc/s10052-016-4307-2.

A. Cagnazzo, V. Schomerus and V. Tlapak.
Spectra of sigma models on semi-symmetric spaces.
Nuclear physics / B, 906:342, and PUBDB-2016-05835, DESY-14-229.
doi: 10.1016/j.nuclphysb.2016.03.010.

C. Caprini et al.
Science with the space-based interferometer eLISA. II: gravitational waves from cosmological phase transitions.
Journal of cosmology and astroparticle physics, 2016(04):001, and PUBDB-2016-02005, DESY-15-246; arXiv:1512.06239.
doi: 10.1088/1475-7516/2016/04/001.

G. Carvalho Dorsch et al.
Hierarchical versus degenerate 2HDM: The LHC run 1 legacy at the onset of run 2.
Physical review / D, 93(11):115033, and PUBDB-2016-02424, DESY-15-240.
doi: 10.1103/PhysRevD.93.115033.

M. Cè, L. Giusti and S. Schaefer.
Domain decomposition, multilevel integration, and exponential noise reduction in lattice QCD.
Physical review / D, 93(9):094507, and PUBDB-2016-02013, DESY-16-007; arXiv:1601.04587.
doi: 10.1103/PhysRevD.93.094507.

M. Cè et al.
The topological susceptibility in the large-N limit of SU(N) Yang–Mills theory.
Physics letters / B, 762:232, and PUBDB-2017-00453, DESY-16-131; arXiv:1607.05939.
doi: 10.1016/j.physletb.2016.09.029.

M. Chala, G. Nardini and I. Sobolev.
Unified explanation for dark matter and electroweak baryogenesis with direct detection and gravitational wave signatures.
Physical review / D, 94(5):055006, and PUBDB-2016-04421, DESY-16-092.
doi: 10.1103/PhysRevD.94.055006.

M. Chala et al.
Deciphering the CP nature of the 750GeV resonance.
Physics letters / B, 760:220, and PUBDB-2016-03322, DESY-16-054.
doi: 10.1016/j.physletb.2016.06.050.

M. Chala et al.
Tricking Landau–Yang: How to obtain the diphoton excess from a vector resonance.
Physics letters / B, 755:145, and PUBDB-2016-01224, DESY-15-256; arXiv:1512.06833.
doi: 10.1016/j.physletb.2016.02.006.

M. Chiesa, N. Greiner and F. Tramontano.
Automation of electroweak corrections for LHC processes.
Journal of physics / G, 43(1):013002, and PUBDB-2016-00456.
doi: 10.1088/0954-3899/43/1/013002.

B. Chokoufe et al.
NLO QCD predictions for off-shell $t\bar{t}$ and $t\bar{t}H$ production and decay at a linear collider.
Journal of high energy physics, 2016(12):075, and PUBDB-2016-06549, DESY-16-140.
doi: 10.1007/JHEP12(2016)075.

K. Cichy, K. Jansen and P. Korcyl.
Non-perturbative running of renormalization constants from correlators in coordinate space using step scaling.
Nuclear physics / B, 913:278, and PUBDB-2017-00294, DESY-16-158; arXiv:1608.02481.
doi: 10.1016/j.nuclphysb.2016.09.015.

M. Cicoli et al.
α' Inflation: moduli stabilisation and observable tensors from higher derivatives.
Journal of high energy physics, 2016(9):26, and PUBDB-2016-04673, DESY-16-103.
doi: 10.1007/JHEP09(2016)026.

R. Contino et al.
On the validity of the effective field theory approach to SM precision tests.
Journal of high energy physics, 2016(7):144, and PUBDB-2016-04412, DESY-16-067; arXiv:1604.06444.
doi: 10.1007/JHEP07(2016)144.

C. Csaki, C. Grojean and J. Terning.
Alternatives to an Elementary Higgs.
Reviews of modern physics, 88(4):045001, and PUBDB-2017-00308, arXiv:1512.00468.
doi: 10.1103/RevModPhys.88.045001.

M. Dalla Brida, S. M. Sint and P. Vilaseca.
The chirally rotated Schrödinger functional: theoretical expectations and perturbative tests.
Journal of high energy physics, 2016(8):102, and PUBDB-2016-03991, DESY-16-040; TCDMATH-16-02.
doi: 10.1007/JHEP08(2016)102.

B. Dasgupta, J. Kopp and P. Schwaller.
Photons, photon jets, and dark photons at 750 GeV and beyond.
The European physical journal / C, 76(5):277, and PUBDB-2016-02425, DESY-16-028.
doi: 10.1140/epjc/s10052-016-4127-4.

M. Dias, J. Frazer and M. C. D. Marsh.
Simple Emergent Power Spectra from Complex Inflationary Physics.
Physical review letters, 117(14):141303, and PUBDB-2016-04413, DESY-16-073.
doi: 10.1103/PhysRevLett.117.141303.

M. Dias et al.
Numerical evaluation of the bispectrum in multiple field inflation—the transport approach with code.
Journal of cosmology and astroparticle physics, 2016(12):033, and PUBDB-2016-06716, DESY-16-171.
doi: 10.1088/1475-7516/2016/12/033.

C. O. Dib et al.
Distinguishing Dirac/Majorana sterile neutrinos at the LHC.
Physical review / D, 94(1):013005, and PUBDB-2016-03325, DESY-16-077.
doi: 10.1103/PhysRevD.94.013005.

M. Diehl.
Introduction to GPDs and TMDs.
The European physical journal / A, 52(6):149, and PUBDB-2016-02423, DESY-15-234.
doi: 10.1140/epja/i2016-16149-3.

M. Diehl, D. Ostermeier and A. Schäfer.
Erratum to: Elements of a theory for multiparton interactions in QCD.
Journal of high energy physics, 2016(3):1, and PUBDB-2017-00316.
doi: 10.1007/JHEP03(2016)001.

M. Diehl et al.
Cancellation of Glauber Gluon Exchange in the Double Drell–Yan Process.
Few-body systems, 57(6):399, and PUBDB-2017-00312.
doi: 10.1007/s00601-016-1094-0.

M. Diehl et al.
Cancellation of Glauber gluon exchange in the double Drell-Yan process.
Journal of high energy physics, 2016(1):76, and PUBDB-2016-00465, DESY-15-187; arXiv:1510.08696.
doi: 10.1007/JHEP01(2016)076.

B. Döbrich et al.
ALPtraum: ALP production in proton beam dump experiments.
Journal of high energy physics, 2016(2):18, and PUBDB-2016-01167, DESY-15-237; arXiv:1512.03069.
doi: 10.1007/JHEP02(2016)018.

F. Domingo and G. Weiglein.
NMSSM interpretations of the observed Higgs signal.
Journal of high energy physics, 2016(4):95, and PUBDB-2016-01916, DESY-15-179.
doi: 10.1007/JHEP04(2016)095.

J. Dragos et al.
Nucleon matrix elements using the variational method in lattice QCD.
Physical review / D, 94(7):074505, and PUBDB-2016-04670, DESY-16-099.
doi: 10.1103/PhysRevD.94.074505.

M. Duerr, P. F. Pérez and J. Smirnov.
Gamma-ray excess and the minimal dark matter model.
Journal of high energy physics, 2016(6):008, and PUBDB-2016-02422, DESY-15-191.
doi: 10.1007/JHEP06(2016)008.

M. Duerr et al.
How to save the WIMP: global analysis of a dark matter model with two s-channel mediators.
Journal of high energy physics, 2016(9):042, and PUBDB-2016-04677, DESY-16-113.
doi: 10.1007/JHEP09(2016)042.

G. Durieux.
CP violation in multibody decays of beauty baryons.
Journal of high energy physics, 2016(10):5, and PUBDB-2016-04687, DESY-16-153.
doi: 10.1007/JHEP10(2016)005.

G. Durieux et al.
Rare Z decays and neutrino flavor universality.
Physical review / D, 93(9):093005, and PUBDB-2016-02010, DESY-15-235.
doi: 10.1103/PhysRevD.93.093005.

M. Ebert et al.
Exploiting jet binning to identify the initial state of high-mass resonances.
Physical review / D, 94(5):051901, and PUBDB-2016-04417, DESY-16-086.
doi: 10.1103/PhysRevD.94.051901.

A. C. Echeverri, B. von Harling and M. Serone.
The effective bootstrap.
Journal of high energy physics, 2016(9):097, and PUBDB-2016-04671, DESY-16-100.
doi: 10.1007/JHEP09(2016)097.

J. Elias-Miro, M. Montull and M. Riembau.
The renormalized Hamiltonian truncation method in the large E_T expansion.
Journal of high energy physics, 1604(4):144, and PUBDB-2017-00321, arXiv:1512.05746.
doi: 10.1007/JHEP04(2016)144.

J. R. Espinosa, M. Garny and T. Konstandin.
Interplay of infrared divergences and gauge dependence of the effective potential.
Physical review / D, 94(5):055026, and PUBDB-2016-04686, DESY-16-144.
doi: 10.1103/PhysRevD.94.055026.

M. Fairbairn et al.
Constraints on Z' models from LHC dijet searches and implications for dark matter.
Journal of high energy physics, 2016(9):18, and PUBDB-2016-04422, DESY-16-093; arXiv:1605.07940.
doi: 10.1007/JHEP09(2016)018.

T. Fischer et al.
Probing axions with the neutrino signal from the next Galactic supernova.
Physical review / D, 94(8):085012, and PUBDB-2016-04423, DESY-16-094.
doi: 10.1103/PhysRevD.94.085012.

N. Fonseca et al.
Large field excursions from a few site relaxion model.
Physical review / D, 94(1):015010, and PUBDB-2016-03318, DESY-16-011.
doi: 10.1103/PhysRevD.94.015010.

E. Frenkel, S. Gukov and J. Teschner.
Surface operators and separation of variables.
Journal of high energy physics, 2016(1):179, and PUBDB-2016-01158, DESY-15-106; arXiv:1506.07508.
doi: 10.1007/JHEP01(2016)179.

A. Gainutdinov and R. I. Nepomechie.
Algebraic Bethe ansatz for the quantum group invariant open XXZ chain at roots of unity.
Nuclear physics / B, 909:796, and PUBDB-2016-06685, 1603.09249.
doi: 10.1016/j.nuclphysb.2016.06.007.

A. Gainutdinov, N. Read and H. Saleur.
Associative algebraic approach to logarithmic CFT in the bulk: the continuum limit of the $\mathfrak{gl}(1|1)$ periodic spin chain, Howe duality and the interchiral algebra.
Communications in mathematical physics, 341(1):35, and PUBDB-2017-00323, arXiv:1207.6334.
doi: 10.1007/s00220-015-2483-9.

M. García Vera and S. Schaefer.
Multilevel algorithm for flow observables in gauge theories.
Physical review / D, 93(7):074502, and PUBDB-2016-02576, DESY-16-016; arXiv:1601.07155.
doi: 10.1103/PhysRevD.93.074502.

M. Giannotti et al.
Cool WISPs for stellar cooling excesses.
Journal of cosmology and astroparticle physics, 2016(05):057, and PUBDB-2016-02031, DESY-15-245; arXiv:1512.08108.
doi: 10.1088/1475-7516/2016/05/057.

A. Grassi, Y. Hatsuda and M. Marino.
Quantization conditions and functional equations in ABJ(M) theories.
Journal of physics / A, 49:29, and PUBDB-2017-00324, DESY-14-182; arXiv:1410.7658.
doi: 10.1088/1751-8113/49/11/115401.

A. Grassi, Y. Hatsuda and M. Mariño.
Topological Strings from Quantum Mechanics.
Annales Henri Poincaré, 17(11):3177, and PUBDB-2016-06100, DESY-14-181.
doi: 10.1007/s00023-016-0479-4.

M. Grazzini et al.
W^+W^- production at the LHC: fiducial cross sections and distributions in NNLO QCD.
Journal of high energy physics, 2016(8):140, and PUBDB-2016-04414, DESY-16-075; arXiv:1605.02716.
doi: 10.1007/JHEP08(2016)140.

M. Grazzini et al.
$W^{\pm}Z$ production at hadron colliders in NNLO QCD.
Physics letters / B, 761:179, and PUBDB-2016-03324, DESY-16-074.
doi: 10.1016/j.physletb.2016.08.017.

N. Greiner, S. Liebler and G. Weiglein.
Interference contributions to gluon initiated heavy Higgs production in the two-Higgs-doublet model.
The European physical journal / C, 76(3):118, and PUBDB-2016-01922, DESY-15-239.
doi: 10.1140/epjc/s10052-016-3965-4.

C. Grojean.
Physics of the Brout–Englert–Higgs boson: Theory.
37th International Conference on High Energy Physics, Valencia (Spain), 2 Jul 2014 - 9 Jul 2014.
Elsevier, Amsterdam [u.a.]
doi: 10.1016/j.nuclphysbps.2015.09.003.

A. G. Grozin et al.
The three-loop cusp anomalous dimension in QCD and its supersymmetric extensions.
Journal of high energy physics, 2016(1):140, and PUBDB-2016-01140, DESY-15-186; IPhT-T15/174; MITP/15-088; arXiv:1510.07803.
doi: 10.1007/JHEP01(2016)140.

T. Hahn et al.
High Precision Prediction for M_h in the MSSM.
Nuclear and particle physics proceedings, 273-275:794, and PUBDB-2016-06729.
doi: 10.1016/j.nuclphysbps.2015.09.122.

U. Haisch, F. Kahlhoefer and T. M. P. Tait.
On mono-W signatures in spin-1 simplified models.
Physics letters / B, 760:207, and PUBDB-2016-02665, DESY-16-042.
doi: 10.1016/j.physletb.2016.06.063.

A. Hebecker, F. Rompineve and A. Westphal.
Axion monodromy and the weak gravity conjecture.
Journal of high energy physics, 2016(4):157, and PUBDB-2016-01923, DESY-15-242.
doi: 10.1007/JHEP04(2016)157.

A. Hebecker et al.
Axion monodromy inflation with warped KK-modes.
Physics letters / B, 754:328, and PUBDB-2016-01168, DESY-15-244.
doi: 10.1016/j.physletb.2016.01.030.

L. Heurtier and D. Teresi.
Dark matter and observable lepton flavor violation.
Physical review / D covering particles, fields, gravitation, and cosmology, 94(12):125022, and PUBDB-2017-00561, DESY-16-127.
doi: 10.1103/PhysRevD.94.125022.

A. H. Hoang, P. Pietrulewicz and D. Samitz.
Variable flavor number scheme for final state jets in DIS.
Physical review / D, 93(3):034034, and PUBDB-2016-01658, DESY-15-098.
doi: 10.1103/PhysRevD.93.034034.

J. Hoff.
Methods for Higgs boson production at N^3LO.
18th International Conference in Quantum Chromodynamics, Montpellier (France), 29 Jun 2015 - 3 Jul 2015.
Elsevier, Amsterdam [u.a.]
doi: 10.1016/j.nuclphysbps.2016.02.046.

W. Hollik.
A new view on vacuum stability in the MSSM.
Journal of high energy physics, 2016(8):126, and PUBDB-2016-04678, DESY-16-114.
doi: 10.1007/JHEP08(2016)126.

W. Hollik.
Charge and color breaking constraints in the Minimal Supersymmetric Standard Model associated with the bottom Yukawa coupling.
Physics letters / B, 752:7, and PUBDB-2017-00334, TTP15-033; arXiv:1508.07201.
doi: 10.1016/j.physletb.2015.11.028.

R. Horsley et al.
Isospin splittings of meson and baryon masses from three-flavor lattice QCD + QED.
Journal of physics / G, 43(10):10LT02, and PUBDB-2016-04692, DESY-15-153.
doi: 10.1088/0954-3899/43/10/10LT02.

R. Horsley et al.
QED effects in the pseudoscalar meson sector.
Journal of high energy physics, 2016(4):93, and PUBDB-2016-01915, DESY-15-158.
doi: 10.1007/JHEP04(2016)093.

S. J. Huber et al.
Detectable gravitational waves from very strong phase transitions in the general NMSSM.
Journal of cosmology and astroparticle physics, 2016(03):036, and PUBDB-2016-01539, DESY-15-247.
doi: 10.1088/1475-7516/2016/03/036.

E. Huffman et al.
Real-time evolution of strongly coupled fermions driven by dissipation.
Annals of physics, 372:309, and PUBDB-2016-04071.
doi: 10.1016/j.aop.2016.05.019.

M. Isachenkov, V. Mitev and E. Pomoni.
Toda 3-Point Functions From Topological Strings II.
Journal of high energy physics, 1608:066, and PUBDB-2017-00341, DESY-14-236; HU-MATHEMATIK-35-2014; HU-EP-14-57; arXiv:1412.3395.
doi: 10.1007/JHEP08(2016)066.

M. Isachenkov and V. Schomerus.
Superintegrability of d-Dimensional Conformal Blocks.
Physical review letters, 117(7):071602, and PUBDB-2016-03319, DESY-16-026.
doi: 10.1103/PhysRevLett.117.071602.

F. Kahlhoefer et al.
Implications of unitarity and gauge invariance for simplified dark matter models.
Journal of high energy physics, 2016(2):16, and PUBDB-2016-01161, DESY-15-182; arXiv:1510.02110.
doi: 10.1007/JHEP02(2016)016.

R. Kashaev, F. Luo and G. Vartanov.
A TQFT of Turaev–Viro Type on Shaped Triangulations.
Annales Henri Poincaré, 17(5):1109, and PUBDB-2016-03856, DESY-12-195.
doi: 10.1007/s00023-015-0427-8.

H. Kastrup.
Wigner functions for the pair angle and orbital angular momentum.
Physical review / A covering atomic, molecular, and optical physics and quantum information, 94(6):062113, and PUBDB-2017-00361.
doi: 10.1103/PhysRevA.94.062113.

M. Kawasaki, F. Takahashi and M. Yamada.
Suppressing the QCD axion abundance by hidden monopoles.
Physics letters / B, 753:677, and PUBDB-2016-00480, DESY-15-216.
doi: 10.1016/j.physletb.2015.12.075.

S. V. Ketov and T. Terada.
Single-superfield helical-phase inflation.
Physics letters / B, 752:108, and PUBDB-2015-05436, DESY-15-163.
doi: 10.1016/j.physletb.2015.11.039.

W. Kilian et al.
Resonances at the LHC beyond the Higgs boson: The scalar/tensor case.
Physical review / D, 93(3):036004, and PUBDB-2016-01162, DESY-15-183.
doi: 10.1103/PhysRevD.93.036004.

J. S. Kim et al.
A resonance without resonance: Scrutinizing the diphoton excess at 750 GeV.
Physics letters / B, 755:403, and PUBDB-2016-02008, DESY-15-255.
doi: 10.1016/j.physletb.2016.02.041.

D. W. Kolodrubetz et al.
Factorization for jet radius logarithms in jet mass spectra at the LHC.
Journal of high energy physics, 2016(12):54, and PUBDB-2016-06546, DESY-16-080.
doi: 10.1007/JHEP12(2016)054.

A. Kurz et al.
Electron contribution to the muon anomalous magnetic moment at four loops.
Physical review / D, 93(5):053017, and PUBDB-2016-05589, DESY-16-018; HU-EP-16-02; TTP16-004.
doi: 10.1103/PhysRevD.93.053017.

C.-I. Lazaroiu, E.-M. Babalic and I. Coman-Lohi.
Geometric algebra techniques in flux compactifications.
Advances in high energy physics, 2016:7292534, and PUBDB-2017-00367, arXiv:1212.6766.
doi: 10.1155/2016/7292534.

M. Lemos and P. Liendo.
Bootstrapping N = 2 chiral correlators.
Journal of high energy physics, 2016(1):25, and PUBDB-2016-00237, DESY-15-184; arXiv:1510.03866.
doi: 10.1007/JHEP01(2016)025.

M. Lemos and P. Liendo.
$\mathcal{N}$ = 2 central charge bounds from 2d chiral algebras.
Journal of high energy physics, 2016(4):004, and PUBDB-2016-01920, DESY-15-230.
doi: 10.1007/JHEP04(2016)004.

S. Liebler, G. Moortgat-Pick and A. Papanastasiou.
Probing the top-quark width through ratios of resonance contributions of $e^+e^- \to W^+W^-b\bar{b}$.
Journal of high energy physics, 2016(3):99, and PUBDB-2016-01661, DESY-15-169; arXiv:1511.02350.
doi: 10.1007/JHEP03(2016)099.

S. Liebler, S. Profumo and T. Stefaniak.
Light stop mass limits from Higgs rate measurements in the MSSM: is MSSM electroweak baryogenesis still alive after all?
Journal of high energy physics, 2016(4):143, and PUBDB-2016-02002, DESY-16-001; arXiv:1512.09172.
doi: 10.1007/JHEP04(2016)143.

P. Liendo, I. Ramírez and J. Seo.
Stress-tensor OPE in N = 2 $\mathcal{N} = 2$ superconformal theories.
Journal of high energy physics, 2016(2):19, and PUBDB-2016-01160, DESY-15-164; arXiv:1509.00033.
doi: 10.1007/JHEP02(2016)019.

X. Lu, S. Shirai and T. Terada.
Testing ATLAS Z+MET excess with LHC Run 2.
Journal of high energy physics, 2016(5):108, and PUBDB-2016-02103, DESY-16-005; arXiv: 1601.05777.
doi: 10.1007/JHEP05(2016)108.

T. Luthe et al.
Towards the five-loop Beta function for a general gauge group.
Journal of high energy physics, 2016(7):127, and PUBDB-2016-05582, TTP16-025; IPPP-16-57; DESY-16-117;arXiv:1606.08662.
doi: 10.1007/JHEP07(2016)127.

P. Marquard et al.
$\overline{MS}$-on-shell quark mass relation up to four loops in QCD and a general SU(N) gauge group.
Physical review / D, 94(7):074025, and PUBDB-2016-05584, DESY-16-106; TTP16-023; arXiv:1606.06754.
doi: 10.1103/PhysRevD.94.074025.

O. Matsedonskyi, G. Panico and A. Wulzer.
Top partners searches and composite Higgs models.
Journal of high energy physics, 2016(4):3, and PUBDB-2016-02004, DESY-15-243; arXiv:1512.04356.
doi: 10.1007/JHEP04(2016)003.

A. Mazumdar, S. Qutub and K. i. Saikawa.
Nonthermal axion dark radiation and constraints.
Physical review / D, 94(6):065030, and PUBDB-2016-04684, DESY-16-139.
doi: 10.1103/PhysRevD.94.065030.

A. Mazumdar et al.
Possible resolution of the domain wall problem in the NMSSM.
Physical review / D, 93(2):025002, and PUBDB-2016-00466, DESY-15-207.
doi: 10.1103/PhysRevD.93.025002.

E. McDonough and M. Scalisi.
Inflation from nilpotent Kähler corrections.
Journal of cosmology and astroparticle physics, 2016(11):028, and PUBDB-2016-05270, DESY-16-172.
doi: 10.1088/1475-7516/2016/11/028.

I. Moult et al.
Employing helicity amplitudes for resummation.
Physical review / D, 93(9):094003, and PUBDB-2016-01913, DESY-15-065.
doi: 10.1103/PhysRevD.93.094003.

Z. Nagy and D. E. Soper.
Summing threshold logs in a parton shower.
Journal of high energy physics, 2016(10):19, and PUBDB-2016-04420, DESY-16-091.
doi: 10.1007/JHEP10(2016)019.

K. Nakayama et al.
Structure of Kähler potential for D-term inflationary attractor models.
Journal of high energy physics, 2016(5):067, and PUBDB-2016-02430, DESY-16-043.
doi: 10.1007/JHEP05(2016)067.

S. G. Nibbelin and F. Ruehle.
Line bundle embeddings for heterotic theories.
Journal of high energy physics, 2016(4):186, and PUBDB-2016-02007, DESY-15-251; arXiv:1601.00676.
doi: 10.1007/JHEP04(2016)186.

Particle Data Collaboration.
Review of Particle Physics.
Chinese physics / C, 40(10):100001, and PUBDB-2016-04859.
doi: 10.1088/1674-1137/40/10/100001.

C. Peset, A. Pineda and M. Stahlhofen.
Potential NRQCD for unequal masses and the B_c spectrum at N^3LO.
Journal of high energy physics, 2016(5):17, and PUBDB-2016-01919, DESY-15-223.
doi: 10.1007/JHEP05(2016)017.

P. Pietrulewicz, F. J. Tackmann and W. J. Waalewijn.
Factorization and resummation for generic hierarchies between Jets.
Journal of high energy physics, 2016(8):2, and PUBDB-2016-03316, DESY-15-129.
doi: 10.1007/JHEP08(2016)002.

L. C. Price et al.
Designing and testing inflationary models with Bayesian networks.
Journal of cosmology and astroparticle physics, 2016(02):049, and PUBDB-2016-01166, DESY-15-199; arXiv:1511.00029.
doi: 10.1088/1475-7516/2016/02/049.

J. Reuter, B. Chokoufe and T. Ohl.
Making extreme computations possible with virtual machines.
Journal of physics / Conference Series, 762:012071, and PUBDB-2016-05678, DESY-16-034.
doi: 10.1088/1742-6596/762/1/012071.

J. Reuter et al.
Automation of NLO processes and decays and POWHEG matching in WHIZARD.
Journal of physics / Conference Series, 762:012059, and PUBDB-2016-06543, DESY-16-033.
doi: 10.1088/1742-6596/762/1/012059.

A. Ringwald and K. i. Saikawa.
Axion dark matter in the post-inflationary Peccei-Quinn symmetry breaking scenario.
Physical review / D, D93(8):085031, and PUBDB-2016-01891, DESY-15-250; arXiv:1512.06436.
doi: 10.1103/PhysRevD.93.085031.

D. Roest, M. Scalisi and P. Werkman.
Moduli backreaction on inflationary attractors.
Physical review / D covering particles, fields, gravitation, and cosmology, 94(12):123503, and PUBDB-2016-06554, DESY-16-143.
doi: 10.1103/PhysRevD.94.123503.

G. G. Ross, K. Schmidt-Hoberg and F. Staub.
On the MSSM Higgsino mass and fine tuning.
Physics letters / B, 759:110, and PUBDB-2016-02431, DESY-16-062.
doi: 10.1016/j.physletb.2016.05.053.

M. Schlaffer, M. Spannowsky and A. Weiler.
Searching for supersymmetry scalelessly.
The European physical journal / C, 76(8):457, and PUBDB-2016-03317, DESY-15-252.
doi: 10.1140/epjc/s10052-016-4299-y.

M. Shirasaki et al.
Cosmological constraints on dark matter annihilation and decay: Cross-correlation analysis of the extragalactic γ-ray background and cosmic shear.
Physical review / D, 94(6):063522, and PUBDB-2016-04676, DESY-16-112.
doi: 10.1103/PhysRevD.94.063522.

F. Staub et al.
Higgs mass predictions of public NMSSM spectrum generators.
Computer physics communications, 202:113, and PUBDB-2016-01660, DESY-15-122.
doi: 10.1016/j.cpc.2016.01.005.

F. Staub et al.
Precision tools and models to narrow in on the 750 GeV diphoton resonance.
The European physical journal / C, 76(9):516, and PUBDB-2016-04409, DESY-16-025.
doi: 10.1140/epjc/s10052-016-4349-5.

F. J. Tackmann, W. J. Waalewijn and L. Zeune.
Impact of jet veto resummation on slepton searches.
Journal of high energy physics, 2016(7):119, and PUBDB-2016-03320, DESY-16-044.
doi: 10.1007/JHEP07(2016)119.

F. Takahashi and M. Yamada.
Spontaneous baryogenesis from asymmetric inflaton.
Physics letters / B, 756:216, and PUBDB-2016-01662, DESY-15-194; TU-1009; IPMU-15-0188; arXiv:1510.07822.
doi: 10.1016/j.physletb.2016.03.020.

M. Yamada.
Affleck-Dine baryogenesis just after inflation.
Physical review / D, 93(8):083516, and PUBDB-2016-01917, DESY-15-215.
doi: 10.1103/PhysRevD.93.083516.

M. Yamada.
Affleck–Dine leptogenesis and its backreaction to inflaton dynamics.
Physics letters / B, 754:208, and PUBDB-2016-01165, DESY-15-195.
doi: 10.1016/j.physletb.2015.12.080.

M. Yamada, T. T. Yanagida and K. Yonekura.
Cosmologically Safe QCD Axion without Fine-Tuning.
Physical review letters, 116(5):051801, and PUBDB-2016-01163, DESY-15-189.
doi: 10.1103/PhysRevLett.116.051801.

Ph.D. Thesis

N. Aghaei.
Quantization of super Teichmüller spaces.
Universität Hamburg, Hamburg, 2016.

A. Behring.
Three-loop QCD corrections from massive quarks to deep-inelastic structure functions and operator matrix elements.
TU Dortmund, 2016.

B. Broy.
Inflation and Effective Shift Symmetries.
Universität Hamburg, Hamburg, 2016.

D. Ciupke.
Higher-Derivative Supergravity and String Cosmology.
University of Hamburg, 2016.

P. Drechsel.
Precise Predictions for Higgs Physics in the Next-to-Minimal Supersymmetric Standard Model (NMSSM).
Universität Hamburg, Hamburg, 2016.

M. Isachenkov.
Conformal Field Theory and Functions of Hypergeometric Type.
Universität Hamburg, Hamburg, 2016.

B. Kostrzewa.
Maximally Twisted Mass Lattice QCD at the physical pion mass.
Humboldt Universität Berlin, 2016.

A. Kurz.
Leptonische und hadronische Korrekturen zum anomalen magnetischen Moment vom Muon und Elektron.
Karlsruher Institut für Technologie, 2016.

L. Sagunski.
On Soft Limits of Large-Scale Structure Correlation Functions.
Universität Hamburg, Hamburg, 2016.

C. Wiese.
Investigating New Lattice Approaches to theMomentum and Spin Structure of the Nucleon.
Humboldt Universität Berlin, 2016.

ZEUS

Published

H. Abramowicz, A. Caldwell and B. Foster.
Particle Physics after the Higgs.
Annalen der Physik, 528(1-2):16, and PUBDB-2016-06155.
doi: 10.1002/andp.201670017.

I. Abt et al.
Combined electroweak and QCD fit to HERA data.
Physical review / D, 94(5):052007, and PUBDB-2016-03907, DESY-16-063; arXiv:1604.05083.
doi: 10.1103/PhysRevD.94.052007.

I. Abt et al.
Study of HERA ep data at low Q^2 and low x_{Bj} and the need for higher-twist corrections to standard perturbative QCD fits.
Physical review / D, 94(3):034032, and PUBDB-2016-04400, DESY-16-064; arXiv:1604.02299.
doi: 10.1103/PhysRevD.94.034032.

V. Bertone et al.
A determination of $m_c(m_c)$ from HERA data using a matched heavy-flavor scheme.
Journal of high energy physics, 2016(8):050, and PUBDB-2016-03580, OUTP-16-10P; DESY-16-078; arXiv:1605.01946.
doi: 10.1007/JHEP08(2016)050.

M. Wing.
Final combined deep inelastic scattering cross sections at HERA.
3. Excited QCD 2016, Lisbon (Portugal), 6 Mar 2016 - 12 Mar 2016.
Inst. of Physics, Jagellonian Univ., Cracow.
doi: 10.5506/APhysPolBSupp.9.485.

ZEUS Collaboration.
Combined QCD and electroweak analysis of HERA data.
Physical review / D, 93(9):092002, and PUBDB-2016-01901, DESY-16-039; arXiv:1603.09628.
doi: 10.1103/PhysRevD.93.092002.

ZEUS Collaboration.
Limits on the effective quark radius from inclusive ep scattering at HERA.
Physics letters / B, 757:468, and PUBDB-2016-01900, DESY-16-035; arXiv:1604.01280.
doi: 10.1016/j.physletb.2016.04.007.

ZEUS Collaboration.
Measurement of the cross-section ratio $\sigma_{\psi(2S)}/\sigma_{J/\psi(1S)}$ in deep inelastic exclusive ep scattering at HERA.
Nuclear physics / B, 909:934, and PUBDB-2016-02770, DESY-16-008; arXiv:1606.08652.
doi: 10.1016/j.nuclphysb.2016.06.010.

ZEUS Collaboration.
Production of exclusive dijets in diffractive deep inelastic scattering at HERA.
The European physical journal / C, 76(1):16, and PUBDB-2016-00753, DESY-15-070; arXiv:1505.05783.
doi: 10.1140/epjc/s10052-015-3849-z.

ZEUS Collaboration.
Search for a narrow baryonic state decaying to pK_S^0 and $\bar{p}K_S^0$ in deep inelastic scattering at HERA.
Physics letters / B, 759:446, and PUBDB-2016-02537, DESY-16-065; arXiv:1604.02220.
doi: 10.1016/j.physletb.2016.06.001.

Ph.D. Thesis

A. Gizhko.
Measurement of beauty quark mass at HERA and impact on Higgs production in association with beauty quarks at LHC.
Universität Hamburg, Hamburg, 2016.

Photographs and graphics

ATLAS experiment @ CERN
Belle / Belle II experiment @ KEK
CERN
CMS experiment @ CERN
CTA
Dahm Architekten & Ingenieure, Berlin
DESY
DFZ Architekten / DESY
IAXO project @ CERN
KEK
SFB 676/Schaaf
SLAC
Stiftung Jugend forscht e. V.

Lars Berg, Münster
Gesine Born, Berlin
John Deven
Manfred Fleischer, DESY
Nina Laskowski
Marta Mayer, DESY
Heiner Müller-Elsner, Hamburg
Dirk Nölle, DESY
Kirsten Sachs, DESY
Jann Wilken, Hamburg
Barbara Warmbein, DESY

The figures were reproduced by permission of authors or journals.

Acknowledgement

We would like to thank all authors and everyone who helped in the creation of this annual report.

Imprint

Publishing and contact
Deutsches Elektronen-Synchrotron DESY
A Research Centre of the Helmholtz Association

Hamburg location:
Notkestr. 85, 22607 Hamburg, Germany
Tel.: +49 40 8998-0, Fax: +49 40 8998-3282
desyinfo@desy.de

Zeuthen location:
Platanenallee 6, 15738 Zeuthen, Germany
Tel.: +49 33762 7-70, Fax: +49 33762 7-7413
desyinfo.zeuthen@desy.de

www.desy.de
ISBN: 978-3-945931-11-0
doi: 10.3204/PUBDB-2017-01404

Editing
Ilka Flegel, Manfred Fleischer, Thomas Konstandin

Layout
Sabine Kuhls-Dawideit

Production
Britta Liebaug

Printing
EHS Druck GmbH, Schenefeld

Editorial deadline
15 January 2017

Editorial note
The authors of the individual scientific contributions published in this report are fully responsible for the contents.

Reproduction including extracts is permitted subject to crediting the source.
This report is neither for sale nor may be resold.

Deutsches Elektronen-Synchrotron
A Research Centre of the Helmholtz Association

The Helmholtz Association is a community of 18 scientific-technical and biological-medical research centres. These centres have been commissioned with pursuing long-term research goals on behalf of the state and society. The Association strives to gain insights and knowledge so that it can help to preserve and improve the foundations of human life. It does this by identifying and working on the grand challenges faced by society, science and industry. Helmholtz Centres perform top-class research in strategic programmes in six core fields: Energy, Earth and Environment, Health, Key Technologies, Structure of Matter, Aeronautics, Space and Transport.

www.helmholtz.de